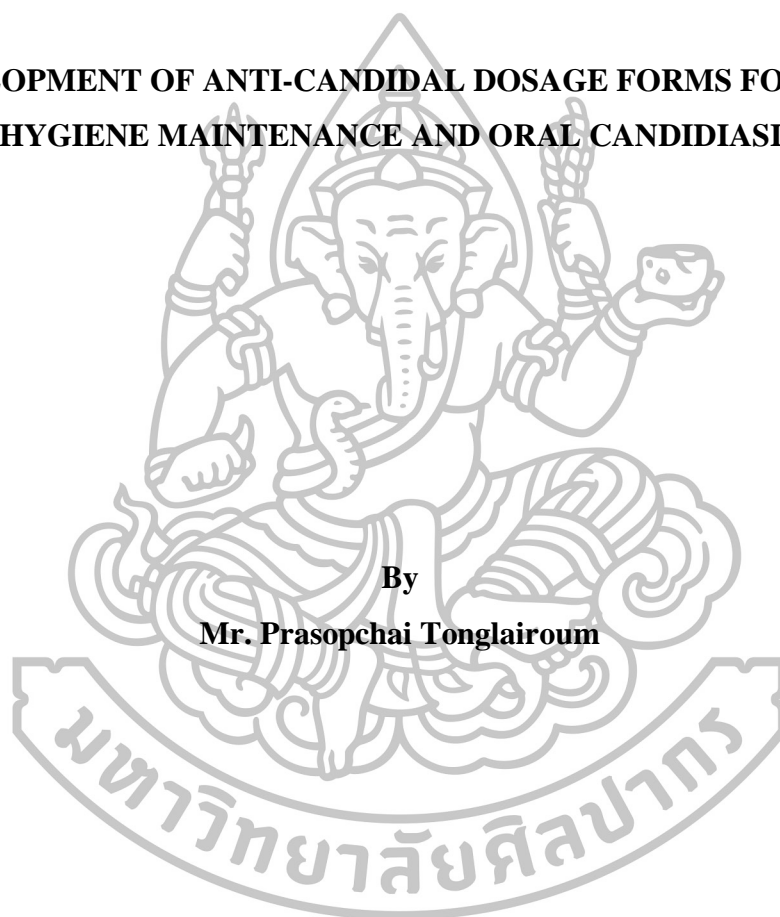




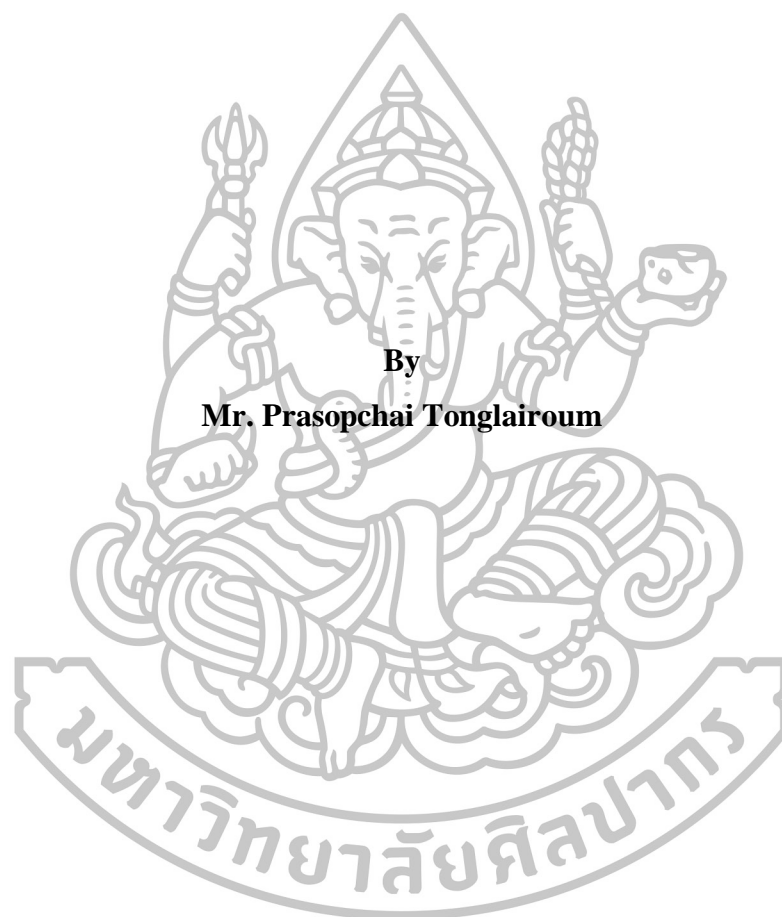
**DEVELOPMENT OF ANTI-CANDIDAL DOSAGE FORMS FOR ORAL
HYGIENE MAINTENANCE AND ORAL CANDIDIASIS**



**By
Mr. Prasopchai Tonglairoum**

**A Thesis Submitted in Partial Fulfillment of the Requirements for the Degree
Doctor of Philosophy Program in Pharmaceutical Technology
Graduate School, Silpakorn University
Academic Year 2016
Copyright of Graduate School, Silpakorn University**

**DEVELOPMENT OF ANTI-CANDIDAL DOSAGE FORMS FOR ORAL
HYGIENE MAINTENANCE AND ORAL CANDIDIASIS**



**By
Mr. Prasopchai Tonglairoum**

**A Thesis Submitted in Partial Fulfillment of the Requirements for the Degree
Doctor of Philosophy Program in Pharmaceutical Technology
Graduate School, Silpakorn University
Academic Year 2016
Copyright of Graduate School, Silpakorn University**

การพัฒนาเภสัชภัณฑ์ต้านแคนดิดาสำหรับรักษาอนามัยช่องปากและโรคราแคนดิดาในช่องปาก



วิทยานิพนธ์นี้เป็นส่วนหนึ่งของการศึกษาตามหลักสูตรปริญญาวิทยาศาสตรดุษฎีบัณฑิต

สาขาวิชาเทคโนโลยีเภสัชกรรม

บัณฑิตวิทยาลัย มหาวิทยาลัยศิลปากร

ปีการศึกษา 2559

ลิขสิทธิ์ของบัณฑิตวิทยาลัย มหาวิทยาลัยศิลปากร

The Graduate School, Silpakorn University has approved and accredited the thesis title of “Development of anti-candidal dosage forms for oral hygiene maintenance and oral candidiasis” submitted by Mr. Prasopchai Tonglairoum as a partial fulfillment of the requirements for the degree of Doctor of Philosophy in Pharmaceutical Technology.

.....
(Associate Professor Panjai Tantatsanawong, Ph.D.)

Dean of Graduate School

...../...../.....

The Thesis Advisors

1. Associate Professor Praneet Opanasopit, Ph.D.
2. Associate Professor Theerasak Rojanarata, Ph.D.
3. Associate Professor Ruchadaporn Kaomongkolgit, Ph.D.

The Thesis Examination Committee

..... Chairman

(Associate Professor Tanasait Ngawhirunpat, Ph.D.)

...../...../.....

..... Member

(Assistant Professor Warisada Sila-on, Ph.D.)

...../...../.....

..... Member

(Associate Professor Praneet Opanasopit, Ph.D.)

...../...../.....

..... Member

(Associate Professor Theerasak Rojanarata, Ph.D.)

...../...../.....

..... Member

(Associate Professor Ruchadaporn Kaomongkolgit, Ph.D.)

...../...../.....

55354801 : MAJOR : PHARMACEUTICAL TECHNOLOGY

KEY WORDS : NANOFIBERS / ELECTROSPINNING / DRUG DELIVERY / CHITOSAN /
POLY(VINYL PYRROLIDONE) / CYCLODEXTRIN / CLOTRIMAZOLE /
CANDIDA / ORAL CANDIDIASIS

PRASOPCHAI TONGLAIROUM : DEVELOPMENT OF ANTI-CANDIDAL DOSAGE
FORMS FOR ORAL HYGIENE MAINTENANCE AND ORAL CANDIDIASIS. THESIS ADVISORS
: ASSOC. PROF. PRANEET OPANASOPIT, Ph.D. ASSOC. PROF. THEERASAK ROJANARATA,
Ph.D. AND ASSOC. PROF. RUCHADAPORN KAOMONGKOLGIT, Ph.D. 188 pp.

In this study, various formulations of electrospun nanofiber mats containing herbal oil or clotrimazole (CZ) were developed for oral hygiene maintenance and treatment of oral candidiasis. To obtain the formulations for oral hygiene maintenance, the herbal oil (betel oil and clove oil) and chitosan (CS) derivatives were screened for anticandidal activity, anticandidal adhesion on acrylic resins and antibiofilm activity. Betel oil and clove oil demonstrated superior antifungal activity and were selected for blending into nanofibers. The herbal oil loaded nanofibers were fabricated by electrospinning technique using polyvinyl pyrrolidone (PVP) as a fiber forming polymer and hydroxypropyl- β -cyclodextrin (HP β CD) to entrap the oil and increase its solubility of. The nanofibers were characterized using numerous techniques. The herbal oils could be released from the mats in a very fast manner and inhibit the growth of candida cells within only few minutes after contact. Besides the natural compounds, CZ which is poorly soluble and commonly used as a topical agent for oral candidiasis was selected for the incorporation into nanofibers. CZ has poor aqueous solubility that might affect its antimycotic activity. To enhance the solubility, various methods were employed to improve the solubility of CZ including complexation with cyclodextrins (CDs), solid dispersion and the use of lipid based system. Fast-dissolving CZ composite nanofibers were firstly developed with the purpose to improve the dissolution of CZ and increase patient compliance. The solubility of CZ and phase solubility of CZ were studied before the optimal cyclodextrin concentration was selected to form complex with CZ. Afterwards, PVP/HP β CD blended nanofiber mats containing CZ were electrospun and characterized. The fiber diameters in the mats were in the nanometer range. The differential scanning calorimeter (DSC) and X-ray Powder Diffractometer (XRPD) revealed a molecular dispersion of amorphous CZ in the nanofiber mats. A fast dissolved and rapid antifungal activity of CZ from the nanofibers mat was achieved. For lipid based system, CZ-loaded microemulsion-containing nanofiber mats were developed. CZ microemulsion is a promising formulation to improve CZ solubility. CS and polyvinyl alcohol (PVA) were chosen as polymers for the incorporation of CZ microemulsions. The nanofibers were prepared using electrospinning. The microemulsion was composed of oleic acid (OA), Tween 80 (T80), and a co-surfactant. The nanofibers were characterized using diverse techniques. The drug release from the fiber mats could be prolonged. In comparison with CZ lozenges, the nanofiber mats exhibited more rapid killing activity. Moreover, the nanofiber mats demonstrated desirable mucoadhesive properties and were safe for 2 h of application. Finally, CZ-composite sandwich nanofibers were fabricated by electrospinning. The CZ-loaded PVP/HP β CD fiber was coated with thiolated chitosan (CS-SH)/PVA to increase the mucoadhesive properties and to achieve a sustained release of the drug from the nanofibers. The initial fast release of CZ followed by sustained release was accomplished. The sandwich nanofiber mats exhibited desirable mucoadhesive properties both *in vitro* and *in vivo*. The *in vivo* release revealed that CZ contained in the sandwich mats could be slowly and constantly released to the saliva at the favourable concentration. The stability study indicated that all the nanofiber mats were stable after being kept under a long-term condition. The nanofiber mats have the potential to be promising candidates for oral candidiasis applications.

Program of Pharmaceutical Technology

Graduate School, Silpakorn University

Student's signature

Academic Year 2016

Thesis Advisors' signature 1..... 2..... 3.....

คำสำคัญ : เส้นใยนาโน / อิเล็กโตรสปินนิง / การนำส่งยา / โคลโคซาน / พอลิไวนิลไพโรลิโดน / ไฮโดรเจล / โครโตรมาโซล / แคนดิดา / โรคราในช่องปาก

ประสพชัย ทองไหลรวม : การพัฒนาเภสัชภัณฑ์ด้านแคนดิดาสำหรับรักษาอนามัยช่องปากและโรคราแคนดิดาในช่องปาก. อาจารย์ที่ปรึกษาวิทยานิพนธ์ : ญ.รศ.ดร.ปรัตน์ โอปะระโสภิต ภ.รศ.ดร.ธีรศักดิ์ โรจนราชา และ รศ.ทญ.ดร.รัชดาภรณ์ เฝ้ามงคลกิจ. 188 หน้า.

ในการศึกษานี้พัฒนาเส้นใยนาโนอิเล็กโตรสปิน ซึ่งมีน้ำมันจากสมุนไพรหรือด้วยโครโตรมาโซล (CZ) เป็นส่วนประกอบหลายตัวรับ สำหรับการรักษานามัยช่องปากและโรคติดเชื้อราในช่องปาก ในการพัฒนาตัวรับสำหรับรักษานามัยช่องปาก น้ำมันจากสมุนไพร (น้ำมันพลู และ น้ำมันกานพลู) และสารอนุพันธ์จากโคลโคซาน ได้ถูกทดสอบฤทธิ์ต้านเชื้อราแคนดิดา ฤทธิ์ด้านการเกาะติดของเชื้อราแคนดิดาบนแผ่นอะคริลิก พบว่าน้ำมันพลูและน้ำมันกานพลูมีฤทธิ์ต้านเชื้อราที่เหนือกว่าสารอื่น จึงถูกเลือกเพื่อบรรจุในแผ่นเส้นใยนาโน แผ่นเส้นใยนาโนบรรจุน้ำมันจากสมุนไพรถูกเตรียมขึ้นโดยวิธีอิเล็กโตรสปินนิง โดยใช้พอลิไวนิลไพโรลิโดน (PVP) เป็นพอลิเมอร์ก่อเส้นใยและใช้ไฮดรอกซีโพลพิวรีดีไฮโดรเจน (HPβCD) สำหรับกักเก็บและเพิ่มการละลายของน้ำมันสมุนไพร เส้นใยนาโนที่เตรียมได้ถูกประเมินด้วยเทคนิคต่างๆ พบว่าน้ำมันสมุนไพรสามารถถูกปลดปล่อยจากแผ่นเส้นใยอย่างรวดเร็วและสามารถยับยั้งการเจริญของเชื้อราแคนดิดาภายในสองถึงสามนาที่หลังการสัมผัส นอกจากนี้สารจากธรรมชาติแล้ว CZ ซึ่งมีสมบัติละลายน้ำยากและมักใช้เป็นยาในรูปแบบเฉพาะสำหรับการรักษาเชื้อราในช่องปาก ได้ถูกเลือกเพื่อบรรจุลงในแผ่นเส้นใยนาโน CZ มีการละลายน้ำยากซึ่งอาจส่งผลกระทบต่อฤทธิ์ต้านเชื้อรา ดังนั้นหลายวิธีได้ถูกใช้เพื่อเพิ่มค่าการละลายของ CZ ได้แก่ การเกิดสารประกอบเชิงซ้อนกับไฮโดรเจล การใช้เทคนิคอิเล็กโตรสปินนิง และการใช้ระบบที่มีไขมันเป็นองค์ประกอบ แผ่นเส้นใยนาโนชนิดละลายเร็วที่มี CZ เป็นองค์ประกอบได้ถูกเตรียมขึ้นเป็นครั้งแรกโดยมีจุดประสงค์เพื่อปรับปรุงการละลายของ CZ และเพิ่มความร่วมมือในการใช้ยาของผู้ป่วย ค่าการละลายของ CZ และวิฤภาคการละลายของ CZ ได้ถูกศึกษาขึ้นก่อนที่ความเข้มข้นที่เหมาะสมของไฮโดรเจลจะถูกละลายเพื่อเกิดสารประกอบเชิงซ้อนกับ CZ จากนั้นแผ่นเส้นใยนาโน PVP/HPβCD ได้ถูกเตรียมขึ้นและทดสอบ พบว่าขนาดเส้นผ่านศูนย์กลางของเส้นใยอยู่ในช่วงขนาดนาโน ผลจากดิฟเฟอเรนเชียล สแกนนิ่ง แคลอริมิเตอร์ (DSC) และ เอกซเรย์ฟลักซ์ดิฟแฟรคโตมิเตอร์ (XRPD) แสดงให้เห็นถึงการกระจายตัวของโมเลกุลของ CZ รูปผลึกฐานในแผ่นเส้นใยนาโน แผ่นเส้นใยนาโนมีการละลายที่รวดเร็วและมีฤทธิ์ต้านเชื้อราที่รวดเร็ว สำหรับระบบที่มีไขมันเป็นองค์ประกอบ แผ่นเส้นใยนาโนบรรจุ CZ ไมโครอิมัลชันได้ถูกพัฒนาขึ้น CZ ไมโครอิมัลชันเป็นคำรับที่คาดว่าช่วยเพิ่มการละลายของ CZ โคลโคซาน (CS) และพอลิไวนิลแอลกอฮอล์ (PVA) ได้ถูกเลือกเป็นพอลิเมอร์สำหรับบรรจุ CZ ไมโครอิมัลชัน แผ่นเส้นใยนาโนถูกเตรียมขึ้นด้วยอิเล็กโตรสปินนิง ไมโครอิมัลชันประกอบด้วย โอลิอิก แอซิด (OA) ทวิน 80 (T80) และสารลดแรงตึงผิวร่วม แผ่นเส้นใยนาโนที่เตรียมได้ถูกทดสอบโดยหลายเทคนิค แผ่นเส้นใยสามารถควบคุมการปลดปล่อยยาให้ยาวนาน เมื่อเปรียบเทียบกับยาเม็ดอม CZ แผ่นเส้นใยนาโนมีฤทธิ์ฆ่าเชื้อที่เร็วกว่า นอกจากนี้แผ่นเส้นใยนาโนมีสมบัติการยึดติดเชื่อมเมือกที่ดีและมีความปลอดภัยในช่วง 2 ชั่วโมงของการใช้ เพื่อปรับปรุงสมบัติการยึดติดเชื่อมเมือก แผ่นเส้นใยนาโนแบบแซนวิชบรรจุ CZ ได้ถูกเตรียมขึ้นโดยอิเล็กโตรสปินนิง แผ่นเส้นใยนาโน PVP/HPβCD ได้ถูกเคลือบด้วยโคลโคซานซิสเทอีน (CS-SH)/PVA เพื่อเพิ่มสมบัติการยึดติดเชื่อมเมือกและเพื่อให้มีการปลดปล่อยยาของยาจากเส้นใยนาโน CZ ถูกปลดปล่อยอย่างรวดเร็วในช่วงแรกตามด้วยการปลดปล่อยแบบเนิ่นเส้นใยนาโนแบบแซนวิชมีสมบัติการยึดติดเชื่อมเมือกที่ดีทั้งการทดสอบภายนอกร่างและภายในร่าง จากกรทดสอบการปลดปล่อยยาในร่าง CZ ถูกปลดปล่อยจากแผ่นเส้นใยนาโนแบบแซนวิชอย่างช้าๆและต่อเนื่องโดยมีความเข้มข้นที่เหมาะสม การศึกษาความคงตัวแสดงให้เห็นว่าแผ่นเส้นใยนาโนทุกตัวรับมีความคงตัวหลังจากเก็บที่สภาวะการศึกษาระยะยาว แผ่นเส้นใยนาโนที่เตรียมได้มีศักยภาพที่จะเป็นตัวเลือกหนึ่งสำหรับการประยุกต์ใช้ในการรักษาการติดเชื้อราในช่องปาก

ACKNOWLEDGEMENTS

I would like to express my sincere appreciation to everyone who have involved in the success of my research project. Firstly, I would like to express my sincere gratitude to my thesis advisor, Assoc. Prof. Dr. Praneet Opanasopit for her marvelous guidance, encouragement, patience, motivation and immense knowledge. She always offers me a great opportunity to gain more life and research experience in various ways. I also would like to express gratitude to my thesis co-advisors, Assoc. Prof. Dr. Theerasak Rojanarata, and Assoc. Prof. Dr. Ruchadaporn Kaomongkolgit for their guidance, helpful support, and insightful comment throughout my thesis. My sincere thanks also go to Ms. Areerut Sripattanaporn, Ms. Kusuma Jamdee and Ms. Niratcha Chaisomboon for their assistance and technical guidance.

I am grateful to Prof. Vitaliy Khutoryanskiy and Dr. Ruairi Brannigan for offering me a great opportunity to do research and broaden my research knowledge concerning the synthesis of mucoadhesive nanomaterials at the University of Reading, United Kingdom. They conveyed the excellent ideas, warm encouragement and guidance, and helped me with technical research skills.

In addition, I must express my profound gratitude to the Commission of Higher Education (Thailand), the Thailand Research Funds through the Golden Jubilee Ph.D. Program (Grant No.PHD/0092/2554) and the graduate school of Silpakorn University for financial support. The Silpakorn University Research and Development Institute and Faculty of Dentistry, Naresuan University for facility support. I also would like to pass my genuine thanks to all my friends and members of the Pharmaceutical Development of Green Innovation Group (PDGIG) for their companionship and generous support.

Finally, I would like to show my greatest appreciation to my parents and my family for their kind-heartedness, understanding, encouragement, and having in confidence in me.

TABLE OF CONTENTS

	Page
English Abstract.....	ix
Thai Abstract.....	v
Acknowledgements.....	vi
List of Tables.....	viii
List of Figures.....	xviii
List of Abbreviations.....	xxvi
Chapter	
1 Introduction.....	1
2 Literature Reviews.....	7
3 Materials and Methods.....	35
4 Results and Discussion.....	53
5 Conclusions.....	111
References.....	114
Appendix.....	130
Biography	184

LIST OF TABLES

Table	Page
2.1 Topical antifungal agents used in the treatment of oral candidiasis....	11
2.2 systemic antifungal agents used in the treatment of oral candidiasis...	12
2.3 Plant extracts that exhibit anticandida activity.....	15
2.4 Advantages and disadvantages of nanofiber fabricating methods.....	16
2.5 Different polymers used in electrospinning and their applications.....	22
2.6 Examples of solubility and dissolution improvement using CD.....	25
2.7 The characteristics and solubility of CDs.....	30
4.1 MIC and MFC values of CS derivatives, betel oil and clove oil.....	55
4.2 The mechanical properties and loading capacity (%) of pure PVP/HP β CD nanofiber mats and betel oil and clove oil loaded nanofiber mats. Each value represents the mean \pm standard deviation from three independent experiments.....	59
4.3 Solubility of CZ in various solvents. Each value represents the mean \pm S.D. from three independent experiments.....	67
4.4 Solution parameters before electrospinning of spinning solution containing various ratios of mixture solvent and different amounts of CZ. Each value represents the mean \pm standard deviation from three independent experiments.....	69
4.5 The entrapment efficiency (%) and loading capacity (mg/mg) of CZ in PVP/HP β CD nanofiber mats. Each value represents the mean \pm standard deviation from three independent experiments	74
4.6 Wetting of the nanofiber mats containing 0-20% CZ.....	75
4.7 Disintegration of the nanofiber mats containing 0-20% CZ.....	76
4.8 Particle size and zeta potential of F1, F2 and F3 microemulsions with and without 25% w/w CZ. The data are expressed as mean \pm standard deviation from three independent experiments.....	84

Table	Page
4.9 The mechanical properties, <i>ex vivo</i> mucoadhesive properties, entrapment efficiency (%) and loading capacity (%) of pure CS-EDTA/PVA nanofibers and different formulations (F1-F3) of CZ-loaded microemulsion-containing nanofibers. Each value represents the mean \pm standard deviation from three independent experiments.....	90
4.10 The mechanical properties, <i>ex vivo</i> mucoadhesive properties, entrapment efficiency (%) and loading capacity (%) of CS/PVA or CS-SH/PVA coated PVP/HP β CD/CZ nanofibers. Each value represents the mean \pm standard deviation from independent experiments.....	98
4.11 The <i>in vivo</i> mucoadhesion time of CS /PVA-coated PVP/HP β CD nanofiber mats and CS-SH/PVA-coated PVP/HP β CD nanofiber mats. Each value represents the mean \pm standard deviation.....	104
B.1 Anti-adhesion activities of CS-acetate (CS-A), CS-mandelate (CS-M), CS-EDTA, N-cinnamyl CS (CS-CIN), betel oil (Betel) and clove oil (Clove) against <i>Candida albicans</i> . Chlorhexidine gluconate (CHX) and phosphate buffer saline (PBS) was used as positive control and negative control, respectively.....	135
B.2 Anti-biofilm activities of CS-acetate (CS-A), CS-mandelate (CS-M), CS-EDTA, N-cinnamyl CS (CS-CIN), betel oil (Betel) and clove oil (Clove) against <i>Candida albicans</i>	135
B.3 Fiber diameters of the PVP/HP β CD nanofibers with varied amounts of HP β CD.....	136
B.4 Fiber diameters of the 30% clove oil loaded PVP/HP β CD nanofibers and the 30% betel oil loaded PVP/HP β CD nanofibers.....	137

Table	Page
B.5 Mechanical properties of the blank PVP/HP β CD nanofibers, clove oil loaded PVP/HP β CD nanofibers and the betel oil loaded PVP/HP β CD nanofibers.....	138
B.6 <i>Ex-vivo</i> mucoadhesion forces of the blank PVP/HP β CD nanofibers, 30 % clove oil loaded PVP/HP β CD nanofibers and the 30% betel oil loaded PVP/HP β CD nanofibers.....	138
B.7 The loading capacity (%) of clove oil in PVP/HP β CD nanofiber mats	139
B.8 The loading capacity (%) of betel oil in PVP/HP β CD nanofiber mats	139
B.9 Cumulative release (%) of betel oil from the PVP/HP β CD nanofiber mats containing 30% betel oil.....	139
B.10 Cumulative release (%) of clove oil from the PVP/HP β CD nanofiber mats containing 30% clove oil.....	139
B.11 Viable cells of <i>C. albicans</i> (CFU/ml) at different treatment time points for the control.....	140
B.12 Viable cells of <i>C. albicans</i> (CFU/ml) at different treatment time points after being treated with 30% betel oil loaded PVP/HP β CD nanofibers.....	140
B.13 Viable cells of <i>C. albicans</i> (CFU/ml) at different treatment time points after being treated with 30% clove oil loaded PVP/HP β CD nanofibers.....	140
B.14 Viable cells of <i>C. albicans</i> (CFU/ml) at different treatment time points after being treated with CZ lozenges (equivalent to CZ 1 mg/mL).....	141
B.15 The percentage cell viability of HGF cells after being incubated with various concentrations of extraction medium of the blank PVP/HP β CD nanofibers for 2 h compared with the control.....	141
B.16 The percentage cell viability of HGF cells after being incubated with various concentrations of extraction medium of the 30% betel oil loaded PVP/HP β CD nanofibers for 2 h compared with the control.....	141

Table	Page
B.17 The percentage cell viability of HGF cells after being incubated with the various concentrations of extraction medium of the 30% clove oil loaded PVP/HP β CD nanofibers for 2 h compared with the control.....	142
B.18 The percentage cell viability of HGF cells after being incubated with various concentrations of extraction medium of the blank PVP/HP β CD nanofibers for 24 h compared with the control....	142
B.19 The percentage cell viability of HGF cells after being incubated with various concentrations of extraction medium of the 30% betel oil loaded PVP/HP β CD nanofibers for 24 h compared with the control.....	143
B.20 The percentage cell viability of HGF cells after being incubated with various concentrations of extraction medium of the 30% clove oil loaded PVP/HP β CD nanofibers for 24 h compared with the control.....	143
C.1 Solubility of CZ in various solvents and solvent systems.....	145
C.2 Phase solubility of CZ/HP β CD in water, and the solvent system of EtOH: H ₂ O: BzOH at the volume ratio of 70: 20: 10.....	145
C.3 Conductivity of the PVP/HP β CD spinning solutions with different solvent ratios and CZ concentrations.....	146
C.4 Viscosity of the PVP/HP β CD spinning solutions with different solvent ratios and CZ concentrations.....	146
C.5 Surface tension of the PVP/HP β CD spinning solutions with different solvent ratios and CZ concentrations.....	146
C.6 Fiber diameters of PVP/HP β CD nanofibers electrospun from the polymer solutions in various solvent systems and different amount of CZ.....	147
C.7 The entrapment efficiency (%) of CZ in PVP/HP β CD nanofiber mats	148
C.8 The loading capacity (%) of CZ in PVP/HP β CD nanofiber mats.....	148

Table	Page
C.9 Cumulative release (%) of CZ from the PVP/HP β CD nanofiber mats containing 5% CZ.....	148
C.10 Cumulative release (%) of CZ from the PVP/HP β CD nanofiber mats containing 10% CZ.....	149
C.11 Cumulative release (%) of CZ from the PVP/HP β CD nanofiber mats containing 15% CZ.....	149
C.12 Cumulative release (%) of CZ from the PVP/HP β CD nanofiber mats containing 20% CZ.....	149
C.13 Cumulative release (%) of CZ from CZ powder.....	150
C.14 Cumulative release (%) of CZ from CZ lozenges.....	150
C.15 Viable cells of <i>C. albicans</i> (CFU/ml) at different treatment times (control).....	150
C.16 Viable cells of <i>C. albicans</i> (CFU/ml) at different treatment times after being treated with the blank PVP/HP β CD nanofibers containing (0% CZ loaded).....	151
C.17 Viable cells of <i>C. albicans</i> (CFU/ml) at different treatment times after being treated with the 5% CZ loaded PVP/HP β CD nanofibers.....	151
C.18 Viable cells of <i>C. albicans</i> (CFU/ml) at different treatment times after being treated with the 10% CZ loaded PVP/HP β CD nanofibers.....	151
C.19 Viable cells of <i>C. albicans</i> (CFU/ml) at different treatment times after being treated with the 15% CZ loaded PVP/HP β CD nanofibers.....	152
C.20 Viable cells of <i>C. albicans</i> (CFU/ml) at different treatment times after being treated with the 20% CZ loaded PVP/HP β CD nanofibers.....	152
C.21 Viable cells of <i>C. albicans</i> (CFU/ml) at different treatment times after being treated with the 20% CZ loaded PVP/HP β CD nanofibers (equivalent to CZ 1 mg/mL in the tested solution)...	152

Table	Page
C.22 Viable cells of <i>C. albicans</i> (CFU/ml) at different treatment time points after being treated with CZ powder (equivalent to CZ 1 mg/mL in the tested solution).....	153
C.23 Viable cells of <i>C. albicans</i> (CFU/ml) at different treatment time points after being treated with CZ lozenges (equivalent to CZ 1 mg/mL in the tested solution).....	153
C.24 The percentage cell viability of HGF cells after being incubated with CZ (0.1-100 µg/mL) for 2 h.....	153
C.25 The percentage cell viability of HGF cells after being incubated with CZ (0.1-100 µg/mL) for 24 h.....	154
C.26 The percentage cell viability of HGF cells after being incubated with various CZ loaded nanofibers for 2 and 24 h compared with the control.....	154
C.27 The percentage cell viability of HGF cells after being incubated with CZ powder and CZ lozenges for 2 and 24 h compared with the control.....	154
C.28 The percentage cell viability of HGF cells derived from three different patients after being incubated with various CZ loaded nanofibers for 2 h compared with the control.....	155
D.1 Components of the microemulsion formulations.....	157
D.2 CZ solubility in different microemulsion formulations.....	157
D.3 Particle size of the microemulsion formulations: F1, F2 and F3, with and without CZ.....	157
D.4 Zeta potential of the microemulsion formulations: F1, F2 and F3, with and without CZ at pH 4.....	158
D.5 Zeta potential of the microemulsion formulations: F1, F2 and F3, with and without CZ at pH 7.....	158
D.6 Zeta potential of the microemulsion formulations: F1, F2 and F3, with and without CZ at pH 9.....	159
D.7 Conductivity of the microemulsion-containing spinning solutions.....	159

Table	Page
D.8 pH of the microemulsion-containing spinning solutions.....	159
D.9 Viscosity of the microemulsion-containing spinning solutions.....	160
D.10 Fiber diameters of the CZ-microemulsion incorporated nanofibers....	160
D.11 The tensile strength (MPa) of blank CS-EDTA/PVA nanofibers and the CZ-microemulsion incorporated nanofibers.....	160
D.12 The <i>ex vivo</i> mucoadhesive properties of blank CS-EDTA/PVA nanofibers and the CZ-microemulsion incorporated nanofibers.	160
D.13 The entrapment efficiency of CZ in the CZ-microemulsion incorporated nanofibers.....	161
D.14 The loading capacity of CZ in the CZ-microemulsion incorporated nanofibers.....	161
D.15 Cumulative release (%) of CZ from CZ lozenges.....	161
D.16 Cumulative release (%) of CZ from the CZ-microemulsion incorporated nanofibers (F1).....	162
D.17 Cumulative release (%) of CZ from the CZ-microemulsion incorporated nanofibers (F2).....	162
D.18 Cumulative release (%) of CZ from the CZ-microemulsion incorporated nanofibers (F3).....	162
D.19 Viable cells of <i>C. albicans</i> (CFU/ml) at different treatment times after being treated with the CZ lozenges.....	163
D.20 Viable cells of <i>C. albicans</i> (CFU/ml) at different treatment time after being being treated with the CZ-microemulsion incorporated nanofibers (F1).....	163
D.21 Viable cells of <i>C. albicans</i> (CFU/ml) at different treatment times after being treated with the CZ-microemulsion incorporated nanofibers (F2).....	163
D.22 Viable cells of <i>C. albicans</i> (CFU/ml) at different treatment times after being treated with the CZ-microemulsion incorporated nanofibers (F3).....	164

Table	Page
D.23 The percentage cell viability of HGF cells after being incubated with CZ the CZ-microemulsion incorporated nanofibers for 2 h compared with the control.....	164
D.24 The percentage cell viability of HGF cells after being incubated with CZ the CZ-microemulsion incorporated nanofibers for 24 h compared with the control.....	165
E.1 Fiber diameters of PVP/HP β CD nanofibers, CS/PVA nanofibers and CS-SH/PVA nanofibers.....	167
E.2 The mechanical properties of CS/PVA coated PVP/HP β CD sandwich nanofibers at 3 h coated times.....	168
E.3 The mechanical properties of CS-SH/PVA coated PVP/HP β CD sandwich nanofibers at 3 h coated times.....	168
E.4 The mechanical properties of CS/PVA coated 20% CZ loaded PVP/HP β CD sandwich nanofibers at 3 h coated times.....	168
E.5 The mechanical properties of CS-SH/PVA coated 20% CZ loaded PVP/HP β CD sandwich nanofibers at 3 h coated times.....	169
E.6 The mechanical properties of CS/PVA coated 20% CZ loaded PVP/HP β CD sandwich nanofibers at 6 h coated times.....	169
E.7 The mechanical properties of CS-SH/PVA coated 20% CZ loaded PVP/HP β CD sandwich nanofibers at 6 h coated times.....	169
E.8 Mucoadhesive properties of CS/PVA coated PVP/HP β CD sandwich nanofibers and CS/PVA coated PVP/HP β CD sandwich nanofibers with/without CZ at 3 h and 6 h coated times.....	170
E.9 The entrapment efficiency (%) of CZ in CS/PVA coated PVP/HP β CD sandwich nanofibers and CS/PVA coated PVP/HP β CD sandwich nanofibers.....	171
E.10 The loading capacity (%) of CZ in CS/PVA coated PVP/HP β CD sandwich nanofibers and CS/PVA coated PVP/HP β CD sandwich nanofibers.....	171

Table	Page
E.11 Cumulative release (%) of CZ from the CS/PVA coated PVP/HP β CD/CZ sandwich nanofibers (3 h coated time).....	172
E.12 Cumulative release (%) of CZ from the CS/PVA coated PVP/HP β CD/CZ sandwich nanofibers (6 h coated time).....	172
E.13 Cumulative release (%) of CZ from the CS-SH/PVA coated PVP/HP β CD/CZ sandwich nanofibers (3 h coated time).....	172
E.14 Cumulative release (%) of CZ from the CS-SH/PVA coated PVP/HP β CD/CZ sandwich nanofibers (6 h coated time).....	173
E.15 Viable cells of <i>C. albicans</i> (CFU/ml) at different treatment times (control).....	173
E.16 Viable cells of <i>C. albicans</i> (CFU/ml) at different treatment times after being treated with the CS-SH/PVA coated PVP/HP β CD/CZ sandwich nanofibers (3 h coated time).....	173
E.17 Viable cells of <i>C. albicans</i> (CFU/ml) at different treatment times after being treated with the CS-SH/PVA coated PVP/HP β CD/CZ sandwich nanofibers (6 h coated time).....	174
E.18 Viable cells of <i>C. albicans</i> (CFU/ml) at different treatment times after being treated with the CS /PVA coated PVP/HP β CD/CZ sandwich nanofibers (3 h coated time).....	174
E.19 Viable cells of <i>C. albicans</i> (CFU/ml) at different treatment times after being treated with the CS/PVA coated PVP/HP β CD/CZ sandwich nanofibers (6 h coated time).....	174
E.20 Viable cells of <i>C. albicans</i> (CFU/ml) at different treatment times after being treated with CZ lozenges.....	175
E.21 The percentage cell viability of HGF cells after being incubated with various sandwich nanofibers for 2 and 24 h compared with the control.....	175
E.22 The percentage cell viability of the HGF cells derived from three different patients after being incubated with various sandwich nanofibers for 24 h compared with the control.....	176

Table	Page
E.23 CZ concentration at different time points in the saliva of seven different subjects after application of the CS-SH/PVA coated PVP/HP β CD/CZ sandwich nanofibers (6 h coated time).....	177
F.1 Fiber diameters (nm) of the fast dissolving CZ loaded PVP/HP β CD nanofibers after being kept under long-term condition and accelerated condition for 1 and 3 months.....	179
F.2 Fiber diameters (nm) of the CZ-microemulsion-containing nanofibers after being kept under long-term condition and accelerated condition for 1 and 3 months.....	180
F.3 Fiber diameters (nm) of the CS-SH/PVA coated 20% CZ loaded PVP/HP β CD sandwich nanofibers after being kept under long-term condition and accelerated condition for 1 and 3 months.....	181
F.4 The percentage of the remaining CZ content in the fast dissolving CZ loaded PVP/HP β CD nanofibers after being kept under long-term condition and accelerated condition for 1 and 3 months.....	182
F.5 The percentage of the remaining CZ content in the CZ-microemulsion-containing nanofibers after being kept under long-term condition and accelerated condition for 1 and 3 months.....	182
F.6 The percentage of the remaining CZ content in the CS-SH/PVA coated 20% CZ loaded PVP/HP β CD sandwich nanofibers after being kept under long-term condition and accelerated condition for 1 and 3 months.....	183

LIST OF FIGURES

Figure		Page
2.1	Schematic of the basic production process of nanofibers by drawing process.....	17
2.2	Schematic illustration of nanofibers made by template synthesis.....	17
2.3	Schematic diagram of the electrospinning process.....	18
2.4	Structures of microemulsion devided by the dispersion of water phrase and oil phrase in the system.....	27
2.5	The pseudo ternary phase diagram construction for obtaining the concentration range of components for the existing range of microemulsions.....	28
2.6	β -cyclodextrin (β -CD) structure.....	29
2.7	Schematic representation of the formation of inclusion complexes. A: drug molecule; B: cyclodextrin (CD) molecule; C: CD cavity; D: water molecules; E: drug-CD complex.....	31
2.8	Molecular structure of HP β CD.....	37
2.9	Molecular structure of CZ.....	33
4.1	Anti-adhesion activities of CS-acetate (CS-A), CS-mandelate (CS-M), CS-EDTA, N-cinnamyl CS (CS-CIN), betel oil (Betel) and clove oil (Clove) against <i>C. albicans</i> . Chlorhexidine gluconate (CHX) and phosphate buffer saline (PBS) was used as positive control and negative control, respectively. *statistically different from the negative control. **statistically different from the positive control.....	56
4.2	Anti-biofilm activities of clove oil (Clove), betel oil (Betel), CS-EDTA, CS-acetate (CS-A), CS-mandelate (CS-M) and N-cinnamyl CS (CS-CIN) against <i>C. albicans</i>	57

Figure	Page
4.3 SEM images of 8% PVP nanofiber mats with different amounts of HPβCD a) 90 mM, b) 110 mM, c) 130 mM d) 150 mM e) 170 mM and f) 190 mM.....	58
4.4 Loading capacity of (■) betel oil loaded nanofiber mats and (□) clove oil loaded nanofiber mats containing 20, 30 and 40% of the oils loaded.....	59
4.5 SEM images of a) 8% PVP/150 mM HPβCD nanofiber mats b) 8% PVP/150 mM HPβCD nanofiber mats loaded with 30% betel oil c) 8% PVP/150 mM HPβCD nanofiber mats loaded with 30% clove oil.....	60
4.6 FT-IR spectra of blank PVP/HPβCD nanofiber mats, pure betel oil, pure clove oil and the herbal oil loaded nanofiber mats.....	61
4.7 DSC thermograms of (a) pure betel oil, (b) pure clove oil, (c) blank PVP/HPβCD nanofibers, (d) betel oil loaded PVP/HPβCD nanofibers and (e) clove oil loaded PVP/HPβCD nanofibers.....	62
4.8 Release profile of (△) betel oil and (□) clove oil from the PVP/HPβCD nanofiber mats. The data are expressed as mean ± standard deviation from three independent experiments.....	63
4.9 Time-kill plots of <i>C. albicans</i> ATCC 90028 versus the treatment time: (◇) control, (△) 30 % betel oil loaded nanofiber mats and (□) 30 % clove oil loaded nanofiber mats. The data are expressed as mean ± standard deviation from three independent experiments. * Statistically significant (P<0.05) from control. ** Statistically significant (P<0.05) from clove oil loaded nanofiber mats.....	64
4.10 In vitro cytotoxicity of (□) blank nanofiber mats, (■) clove oil loaded nanofiber mats, and (■) betel oil loaded nanofiber mats against HGF cells after incubation for a) 2 h and b) 24 h. * Statistically significant (P<0.05) from control.....	66

Figure	Page
4.11 Phase solubility diagram for CZ and CDs system at 37°C; a) in aqueous solution, b) in solvent system of EtOH:H ₂ O:BzOH with a volume ratio of 70:20:10.....	68
4.12 The SEM image (1,000x) and diameter distribution of the PVP/HPβCD nanofiber mats electrospun from EtOH:H ₂ O:BzOH solvent system ratio of 70:20:10 with a different CZ loading amount; a) 5, b) 10, c) 15 and d) 20% wt CZ to polymer.....	70
4.13 FT-IR spectra of the pure CZ powder and PVP/HPβCD nanofiber mats with different amounts of CZ (0, 5, 10, 15, 20% wt CZ to polymer).....	71
4.14 DSC thermogram of the pure CZ powder and PVP/HPβCD nanofiber mats with different amounts of CZ (0, 5, 10, 15, 20% wt CZ to polymer).....	72
4.15 X-ray diffraction pattern of the pure CZ powder and PVP/HPβCD nanofiber mats with different amounts of CZ (0, 5, 10, 15, 20% wt CZ to polymer).....	73
4.16 Release profiles of CZ from CZ-loaded PVP/HPβCD nanofiber mats with different amounts of CZ: (□) 5%, (◻) 10 %, (◻) 15 % and (×) 20 % to polymer, from CZ powder (●) and from CZ lozenges (◻). The data are expressed as mean ± standard deviation from three independent experiments.....	77
4.17 Time kill plot of <i>C. albicans</i> (CFU/ml) versus the treatment time for (□) the control and the 5 mg of CZ-loaded PVP/HPβCD nanofiber mats with different amounts of CZ: (○) 0 %, (◆) 5%, (■) 10 %, (▲) 15 % and (●) 20 % to polymer. The data are expressed as mean ± standard deviation from three independent experiments. * Statistically significant difference (P<0.05) from control, ** Statistically significant difference between from plain nanofiber mats (0% CZ).....	79

Figure	Page
4.18 Time kill plot of <i>C. albicans</i> and (CFU/ml) versus the treatment time: (□) the control, (◆) 20% CZ-loaded PVP/HPβCD nanofiber mats equivalent to CZ 1 mg/ml, (▲) CZ powder equivalent to CZ 1 mg/ml and (■) CZ lozenges equivalent to CZ 1 mg/ml. The data are expressed as mean ± standard deviation from three independent experiments. * Statistically significant (P<0.05) from control, ** Statistically significant between nanofiber mats and CZ lozenges and *** Statistically significant between nanofiber mats and CZ powder.....	80
4.19 The percentage cell viability in HGF cells of CZ solution at CZ concentrations from 0.01 to 100 µg/ml after incubation at pH 7.4 for (◆) 2 h and (■) 24 h in the HGF cells.....	81
4.20 The percentage cell viability in HGF cells of a) CZ loaded PVP/HPβCD nanofiber mats at different initial amounts of CZ (0, 5, 10, 15 and 20% wt CZ to polymer) and CZ lozenges incubated at (□) 2 h and (■) 24 h b) CZ loaded PVP/HPβCD nanofiber mats at different initial amounts of CZ in HGF cells derived from 3 patients: (■) patient #1, (▣) patient #2 and (▢) patient # 3. Each value represents the mean ± standard deviation of five wells. * Statistically significant (P<0.05) from control group.....	82
4.21 Pseudo-ternary phase diagrams of water, oil (OA) and surfactant mixture (surfactant: cosurfactant at the weight ratio of 3:1; a) T80: BzOH b) T80: IPA and c) T80: EtOH (the black area represents microemulsion region).....	83
4.22 SEM images of a) a pure CS-EDTA/PVA nanofiber, b) CZ-loaded microemulsion (F1)-containing nanofiber, c) CZ-loaded microemulsion (F2)-containing nanofiber and d) CZ-loaded microemulsion (F3)-containing nanofiber.....	85

Figure	Page
4.23 FT-IR spectra of a pure CS-EDTA/PVA nanofiber and different formulations (F1-F3) of CZ-loaded microemulsion-containing nanofibers.....	86
4.24 DSC thermograms of a pure CS-EDTA/PVA nanofiber and different formulations (F1-F3) of CZ-loaded microemulsion-containing nanofibers.....	88
4.25 X-ray diffractograms of a pure CS-EDTA/PVA nanofiber and different formulations (F1-F3) of CZ-loaded microemulsion-containing nanofibers.....	89
4.26 Release profiles of CZ from (◆) CZ lozenges, and CZ-loaded microemulsion-containing nanofibers prepared from (■) F1, (▲) F2 and (●) F3 microemulsions. The data are expressed as mean ± standard deviation from three independent experiments.....	91
4.27 Time kill curves for <i>C. albicans</i> treated with the (■) F1, (▲) F2 and (●) F3 formulations of CZ-loaded microemulsion-containing nanofibers; (◆) CZ lozenges and (x) control. The data are expressed as mean ± standard deviation from three independent experiments. *statistically significant (P<0.05) vs. control; **statistically significant difference between nanofiber mats and CZ lozenges.....	92
4.28 The percentage of viable HGF cells after treatment for (■) 2 and (□) 24 h with different formulations (F1-F3) of CZ-loaded microemulsion-containing nanofibers. Each value represents the mean ± standard deviation of five wells. *Statistically significant (P<0.05) vs. control group.....	94

Figure	Page
4.29 The SEM image (3,000x) and the morphology of the a) PVP/HPβCD nanofibers b) CS/PVA nanofibers c) CS-SH/PVA nanofibers and the cross-sectional SEM image (100X) of d) CS-SH/PVA coated PVP/HPβCD nanofibers (at 3h coated time) e) CS-SH/PVA coated PVP/HPβCD nanofibers (at 6h coated time) f) CS-SH/PVA coated PVP/HPβCD nanofibers (at 6h coated time; 200x).....	95
4.30 FT-IR spectra of CZ powder, CS/PVA coated PVP/HPβCD and CS SH/PVA coated PVP/HPβCD nanofibers with and without 20% CZ.....	96
4.31 X-ray diffractogram of the CZ powder and CS-SH/PVA coated PVP/HPβCD nanofibers with and without 20% CZ.....	97
4.32 Release profiles of CZ from CS/PVA coated PVP/HPβCD/CZ nanofibers (□) 3h coated time and (○) 6h coated time, from CS-SH/PVA coated PVP/HPβCD/CZ nanofibers (◇) 3h and (△) 6h coated time), from (●) CZ lozenges. The data are expressed as mean ± standard deviation from three independent experiments.....	100
4.33 Time kill plot against <i>C. albicans</i> of (a) CS/PVA coated PVP/HPβCD/CZ nanofibers: (□) 3h coated time and (○) 6h coated time, b) CS-SH/PVA coated PVP/HPβCD/CZ nanofibers: (◇) 3h and (△) 6h coated time) as compared to (X) the control and CZ lozenges. The data are expressed as mean ± standard deviation from three independent experiments. * Statistically significant difference (P<0.05) from control, **Statistically significant difference from CZ lozenges.....	101

Figure	Page
4.34 (a) The percentage cell viability in HGF cells of CS/PVA or CS-SH/PVA coated PVP/HPβCD with and without 20 % CZ nanofibers at 3h and 6h coated time and incubating for (▣) 2 h and (▤) 24 h (b) incubating for 24 h in HGF cells derived from 3 patients: (▥) patient #1, (▦) patient #2 and (▧) patient # 3. Each value represents the mean ± standard deviation of five wells. * Statistically significant (P<0.05) from control group.....	103
4.35 The in vivo release of CZ from the CS-SH/PVA-coated PVP/HPβCD nanofiber mat in human volunteers. The release is presented as CZ concentration in saliva at different time points: a) average value from seven subjects b) the value from each subject.....	105
4.36 CZ-remaining percentage after the CZ loaded nanofiber mats were kept at a) long-term condition (25 ± 2 °C and 60 ± 5 %RH) and b) accelerated condition ((40 ± 2 °C and 75 ± 5 %RH) for 0, 1 and 3 months.....	107
4.37 SEM images (7000x) and diameters of the fast-dissolving CZ loaded nanofiber mats after keeping under long term condition (upper panel) and accelerated condition (lower panel) for 0, 1 and 3 months.....	108
4.38 SEM images (3000x) and diameters of the CZ-microemulsion loaded nanofiber mats after keeping under long term condition (upper panel) and accelerated condition (lower panel) for 0, 1 and 3 months.....	109
4.39 SEM images (3000x) and diameters of the CZ-incorporated mucoadhesive sandwich nanofibers after keeping under long term condition (upper panel) and accelerated condition (lower panel) for 0, 1 and 3 months.....	110
A.1 Calibration curve of clove oil.....	132

A.2	Calibration curve of betel oil.....	132
A.3	Calibration curve of CZ.....	133



LIST OF ABBREVIATIONS

®	Registered trademark
%	Percent
% w/v	Percent weight by volume
% EE	Percent entrapment efficiency
°C	Degree Celsius
Γ	Gamma
μg	Microgram
μL	Microliter
μm	Micrometer
μs	Microsiemens
ANOVA	Analysis of variance
ATCC	American type culture collection
BzOH	Benzyl alcohol
CDS	Candida-induced denture stomatitis
CDs	Cyclodextrins
cfu	Colony-forming unit
CHX	Chlorhexidine
CLSI	Clinical and laboratory standards institute
cP	Centipoise
CS	Chitosan
CS-SH	Thiolated chitosan
CO ₂	Carbon Dioxide
CZ	Clotrimazole
DMEM	Dulbecco's modified Eagle's medium
DMSO	Dimethyl Sulfoxide
DSC	Differential scanning calorimetry
DTNB	Dithiobis (2-nitrobenzoic acid)
EDAC	1-Ethyl-3-(3-Dimethylaminopropyl) carbodiimide
EDTA	Ethylenediaminetetraacetic acid

e.g.	exempli gratia (Latin); for example,
Eq	Equation
et al.	And others
etc.	et cetera (Latin); and other things/ and so forth
EtOH	Ethanol
FBS	Fetal bovine serum
FT-IR	Fourier transform infrared spectroscopy
H	Hour
HGF	Human gingival fibroblast
H ₂ O	Hydrogen oxide
HPβCD	Hydroxypropyl-β-cyclodextrin
HPLC	High performance liquid chromatography
IC ₅₀	The half maximal inhibitory concentration
ICH	The international conference on harmonisation of technical requirements for registration of pharmaceuticals for human use
IPA	Isopropyl alcohol
KBr	Potassium bromide
KCl	Potassium chloride
kV	Kilovolt
MFC	Minimum fungicidal concentration
mg	Milligram
MIC	Minimum inhibition concentration
min	Minute
mL	Milliter
mm	Millimeter
mM	Millimolar
mN/m	Millinewtons per meter
MPa	Megapascal
MTT	3-(4,5-dimethylthiazol-2-yl)-2,5 diphenyltetrazolium Bromide

MW	Molecular weight
nm	Nanometer
O ₂	Oxygen
OA	Oleic acid
OPC	Oropharyngeal candidiasis
PBS	Phosphate buffer solution
PEG	Polyethylene glycol
pH	Potentia hydrogenii (latin); power of hydrogen
PVA	Polyvinyl alcohol
PVP	Polyvinyl pyrrolidone
RH	Relative Humidity
rpm	Round per minute
SD	Standard deviation
SDA	Sabouraud dextrose Agar
SDB	Sabouraud dextrose broth
SEM	Scanning electron microscopy
Smix	The wight ratio of surfactant to co surfactant
T80	Tween 80
USP	United States Pharmacopoeia
UV	Ultraviolet
V	Volume
XTT	(2,3-Bis-(2-Methoxy-4-Nitro-5-Sulfophenyl)-2H-Tetrazolium-5-Carboxanilide)

CHAPTER 1

INTRODUCTION

1.1 Statement and significance of the research problem

As the gateway to the body, the mouth is challenged by a constant barrage of invaders such as bacteria, viruses, parasites, fungi. Thus, infectious diseases predominate among the ills that can compromise oral health. In adults, the resident oral microflora remains relatively stable and to some extent in harmonious balance with the host. This stability or microbial homeostasis is not a passive response to the environment, but is the result of a dynamic balance being achieved from numerous interactions between different microbial species and host microbial-interactions. The composition of the oral microflora varies at different surfaces within the mouth because of the respective physical and biological properties of each site. These properties include the presence of receptors for microbial adhesion, the redox potential of the site, and the provision of essential nutrients (Marsch et al., 1992). The imbalance of the condition of oral cavity and oral microflora can cause oral infection. Maintaining good oral hygiene is essential to protect oral cavity from being infected. Only few products are available to be used for reducing the microbial on denture and for maintaining oral hygiene.

There are many factors associated with the infection of oral cavity such as defect in immune system, malnutrition, xerostomia and denture wearing. Placement of a prosthesis in the oral cavity results in profound alterations of the environmental conditions as the prosthesis becomes colonized with oral microorganisms and cuts off the underlying mucosa from the mechanical cleansing effect of the tongue and the free flow of saliva. These conditions resulted in overgrowth of oral organisms. One of the organisms that often cause infection in oral cavity is *Candida* spp. (Iacopino and Wathen et al., 1992; Pereira-Cenci et al., 2008)

Candida spp. is a causal agent of opportunistic infections in patients with both local and systemic risk factors, especially in individuals with human immunodeficiency virus (HIV) and immunocompromised patients

(Taweechaisupapong et al, 2005; Cannon et al., 1995). Incidences of globally oropharyngeal infection by *Candida* spp., oropharyngeal candidiasis (OPC), have been raising. *Candida albicans* is generally the main cause of infection (Arendorf, T. and Walker, 1980; Williams and Lewis, 2011). The clinical symptoms of oropharyngeal candidiasis comprise odd sensations, altered taste, and altered smell, affecting the patient's quality of life (Reichart et al., 2000; Kaomongkolgit et al, 2009). *Candida*-induced denture stomatitis (CDS) is one form of oral candidiasis. Acrylic dentures are an important predisposing factor for CDS as they are usually ill-fitting and, with sub-optimal hygiene, can act as reservoirs of infection (Ellepola and Samaranayake, 1998). CDS is observed as an inflammatory candidal lesion of the oral mucosa, occurring particularly under complete or partial removable dentures and it affects up to 65% of denture wearers (Pereira et al., 2013). The ability of *Candida* spp. to adhere to acrylic surfaces is believed to be prominent in the pathogenesis of CDS because adhesion is seemingly the beginning process in the colonization and following infection of host mucosa by *Candida*.

A myriad of effective antifungal drugs may be used either topically or systemically to treat OPC and CDS, but the most efficient treatment are classical polyenes, and azole group antimycotics which are classified into imidazoles and triazoles (Pallasch, 2002; Samaranayake et al., 2002). The azoles are becoming more and more popular in OPC and CDS therapy. Among the azole, CZ is more popular for the topical treatment of oral candidiasis. CZ is a wide spectrum triazole-based antifungal agent. CZ inhibits the enzyme cytochrome P450 14 α -demethylase, which is essential to fungal cell membrane synthesis. CZ has antimycotic activity against *Candida* spp., *Cryptococcus* spp., dermatophytes and *Aspergillus* spp. (Paradkar et al., 2015). However, the poor aqueous solubility of CZ (0.49 μ g/ml) (Hoogerheide and Wyka et al., 1982) may affect its antimycotic activity. Thus, increasing the solubility of CZ is necessary to improve its antimycotic activity. CDs are cyclic oligosaccharides composed of 1, 4-linked glucopyranoside units that can form inclusion complexes with a broad range of drug molecules. These inclusion complexes have altered physicochemical properties from the individual drug molecules (Del Valle, 2004). Complexation of poorly soluble

drugs with CDs can improve the dissolution and stability of the drugs (Albers and Muller, 1995; Bandi et al., 2004). Moreover, a lipid-based system is another option to enhance the solubility of CZ. Lipid-based formulations have attracted great deal of attention to improve the oral bioavailability of poorly water soluble drugs. In fact, the most favored approach is to incorporate lipophilic drugs into inert lipid vehicles such as oils, surfactant dispersions, microemulsions, self-emulsifying formulations, self microemulsifying formulations, and liposomes (Borhade et al., 2012; Pavelic et al., 2005). This could lead to increased solubilization with concomitant modification of their pharmacokinetic profiles, leading to increase in therapeutic efficacy. Microemulsions have been widely studied to enhance the bioavailability of the poorly soluble drugs. They offer a cost-effective approach in such cases. This can be attributed to their unique solubilization properties and thermodynamic stability which has drawn attention for their use as novel vehicles for drug delivery.

Natural products are in considerable demand as traditional curative, since they are distinguished to have minimal side effect on humans. Some natural products may be used to reduce organisms in the mouth or on denture and prevent infection. CS has attracted great interest because of its unique and marvelous properties, for example, biocompatibility (Rinaudo, 2006), biodegradability (VandeVord et al., 2002), and antimicrobial activity (Rabea et al., 2003). Therefore, CS has an assortment of current and potential applications in various fields, for instance, biotechnology, pharmaceuticals, waste water treatment, and food science (Mao et al., 2007; Ramnani and Sabharwal, 2006; Chien et al., 2007). The antimicrobial activity of CS against a variety of bacteria and fungi is well known for its poly-cationic nature (Fujimoto et al., 2006). However, this activity is limited to acidic conditions due to its poor solubility above pH 6.5. Recent studies have focused on the preparation of CS derivatives to increase the solubility and may result in increasing antimicrobial activity (Kim et al, 1997; Sajomsang et al, 2009; Badawy et al., 2013). Also, Piper betle L. is a tropical creeper plant belonging to the pepper family. It is popular as an antiseptic that is commonly applied on wounds and lesions for its healing effects (Keat et al., 2010). The extract of P. betle leaves has been reported to possess anti-oxidative (Choudhury, 2002), anti-inflammatory, antibacterial and antifungal

activities (Nalina and Rahim, 2007; Fathilah et al., 2009). Likewise, clove oil is an essential oil extracted from *Syzygium aromaticum*. It has been empirically used as antimicrobial agents, but the spectrum of activity and mechanisms of action remain unknown. Although only limited consistent data exists about activity toward human fungal pathogens, clove oil has shown outstanding antifungal activity against yeasts, dermatophyte fungi and *Aspergillus* strains, which could anticipate therapeutic benefits, primarily on diseases involving mucosae, skin and respiratory tract (Himratul-Aznita et al., 2011; Cavaleiro, 2006).

In OPC and CDS therapy, topical treatments are becoming considerably popular due to greater patient compliance and reduced side effects (Pallasch, 2002; Mason et al., 2012). Topical dosage forms for oral candidiasis are administered via suspensions, mouth rinses, gels and troches (Akpan and Morgan, 2002; Ellepola and Samaranayake, 2009). However, salivary clearance of the drug can rapidly decrease the drug level in the affected area. An ideal dosage forms for the treatment of oral candidiasis should provide sustained drug release and produce an antifungal effect for a prolonged period of time. These characteristics are achievable if the drug delivery system demonstrates sustained release, and mucoadhesive properties (Collins et al., 2011; Gajra et al., 2014).

Recently, nanofiber-based scaffolds have been popular. These materials demonstrate prominent characteristics such as low density, high porosity, large specific surface areas, very small pore sizes and so on. Nanofibers have been applied in many areas (tissue engineering, drug delivery systems, wound dressing, filtration, etc.) (Kang et al., 2004; Li et al., 2002). Electrospun nanofibers offer great flexibility in the selection of materials or drugs for drug delivery applications. Moreover, electrospun nanofibers exhibit astounding features such as high loading capacity, high encapsulation efficiency, they provide coincident delivery of various compounds, and are cost effective (Van Roey et al., 2004).

This study proposed to investigate the antifungal activity, anti-adhesion activity and antibiofilm activity against *Candida albicans* (*C. albicans*) of CS and CS derivatives and two herbal oils for oral hygiene maintenance. The herbal oil, betel oil and clove oil, which exhibited potent antifungal activity against oral candida were

selected to incorporate into nanofibers by complexation with CDs and fabrication using electrospinning process. With the propose of oral candidiasis treatment, three different types of nanofibers, including fast dissolving patches, microemulsion incorporated patches and mucoadhesive sandwich patches, were prepared. Different techniques, for example electrospinning, complexation with cyclodextrin or using lipid based system, were employed to improve the dissolution of CZ from the electrospun nanofiber mats. The fast dissolving CZ-incorporated nanofiber mats were fabricated using HP β CD functionalized PVP to form the polymeric filaments by electrospinning process. The solvent system ethanol: water: benzyl alcohol (EtOH:H₂O:BzOH) with a 70:20:10 ratio was optimal for the electrospinning. Phase solubility studies of CZ-CDs complex were studied in water and the solvent system. Various amounts of CZ were loaded into the nanofiber mats. The nanofiber mats were investigated for physicochemical properties, wetting time and disintegration time, drug release, antifungal activity, timekill analysis and cytotoxicity. To sustain the release of the drug and increase the retention time at the site of application, CZ-composite sandwich nanofibers were prepared using electrospinning. The CZ-loaded PVP/HP β CD fiber was coated with CS-SH/PVA to increase the mucoadhesive properties and to achieve a sustained release of the drug from the nanofibers. The nanofibers were characterized using scanning electron microscopy (SEM), Fourier transform infrared (FT-IR) spectroscopy and X-ray diffractometry (XRD). The nanofibers mechanical and mucoadhesive properties, drug release, antifungal activity and cytotoxicity was also assessed. Lipid base system was also employed to increase the solubility and dissolution of CZ form delivery system. In this work, CZ-loaded microemulsion-containing nanofiber mats were developed as an alternative for oral candidiasis applications. The microemulsion was composed of O, T80, and a co-surfactant such as BzOH, EtOH or isopropyl alcohol (IPA). The nanofiber mats were obtained by electrospinning a blended solution of a CZ-loaded microemulsion and a mixed polymer solution of 2% w/v CS and 10% w/v PVA at the weight ratio of 30:70. The nanofiber mats were characterized using various analytical techniques. The entrapment efficiency, drug release, antifungal activity and cytotoxicity were investigated. The *in vivo* mucoadhesion time and drug release evaluation of the

selected nanofiber formulation were performed in healthy human volunteers. The optimal formulations were evaluated for the stability according to ICH guideline under normal and accelerated conditions.

1.2 Objective of this research

1.2.1 To investigate the antifungal activity, anti-adhesion activity and antibiofilm activity against *C. albicans* of CS and CS derivatives and two herbal oils for oral hygiene maintenance.

1.2.2 To fabricate nanofiber mats containing CZ for oral candidiasis treatment using electrospinning process.

1.2.3 To evaluate the drug content, drug release, mucoadhesive properties, cytotoxicity, *in vivo* mucoadhesion and *in vivo* release studies of the CZ-loaded nanofiber mats.

1.3 The research of hypothesis

1.3.1 The CS derivatives and herbal oils exhibit good antifungal activity, anti-adhesion, antibiofilm activity against *C. albicans* and can be applied for oral hygiene maintenance.

1.3.2 The CZ-loaded nanofiber mats present good characteristics and demonstrate better or equivalent antifungal activity against *C. albicans* as compared to commercial CZ lozenges and can be used for the treatment of oral candidiasis.

CHAPTER 2

LITERATURE REVIEW

- 2.1 Oral candidiasis
 - 2.1.1 Definition and etiology
 - 2.1.2 Management and treatment of oral candidiasis
 - 2.1.2.1 Topical antifungal agents
 - 2.1.2.2 Systemic antifungal agents
- 2.2 Herbal product
- 2.3 Herbal medicine for oral hygiene and fungal infection
- 2.4 Nanofibers
 - 2.4.1 Nanofiber fabrication
 - 2.4.1.1 Drawing
 - 2.4.1.2 Template synthesis
 - 2.4.1.3 Phase separation
 - 2.4.1.4 Self assembly
 - 2.4.1.5 Electrospinning
 - 2.4.2 Electrospun nanofibers
 - 2.4.2.1 Electrospun nanofiber preparation
 - 2.4.2.2 Parameter affecting the nanofiber properties
 - 2.4.2.3 Polymers used in Electrospinning
 - 2.4.2.4 Application of electrospun nanofibers
- 2.5 Drug dissolution improvement of poorly soluble drugs
 - 2.5.1 Improvement of drug dissolution by electrospinning process
 - 2.5.2 Improvement of drug dissolution by complexation with cyclodextrin
 - 2.5.3 Improvement of drug dissolution using lipid based system
- 2.6 Microemulsion
 - 2.6.1 Microemulsion structure
 - 2.6.2 Pseudoternary phase diagram

- 2.6.3 Microemulsion preparation
- 2.7 Cyclodextrin
 - 2.7.1 Formation of inclusion complex
 - 2.7.2 Hydroxypropyl- β -cyclodextrin
- 2.8 Clotrimazole



2.1 Oral candidiasis

2.1.1 Definition and etiology

Candidiasis of the mouth, also known as oral candidiasis, is an opportunistic fungal infection that occurs when there is an overgrowth of *Candida spp.* The alteration of the environment in oral cavity leads to the conversion of *Candida* from the harmless commensal existence to a pathogenic state. The causes of such changes are the predisposing factors for *Candida* infection and most often these relate to a weakening of host immune defences (Williams and Lewis, 2011). Oral candidiasis is extremely common with individuals with human immunodeficiency virus (HIV) and immunocompromised patients. Moreover, it is also generally diagnosed among the elderly people, particularly in those who wear dentures with poor denture and oral hygiene. The most important fungal pathogens responsible for this disease are *C. albicans*. However, the other species such as *C. tropicalis*, *C. glabrata*, *C. pseudotropicalis*, *C. guillierimondii*, *C. krusei*, *C. lusitaniae*, *C. parapsilosis*, and *C. stellatoidea* also can be found. Among these candida species, *C. albicans*, *C. glabrata*, and *C. tropicalis* correspond to more than 80% of isolates from clinical isolation. The incidence of oral candidiasis has been reported to be 45% in neonates, 45%–65% of healthy children, 30%–45% of healthy adults, 50%–65% of denture wearers, 90% in patients with acute leukaemia undergoing chemotherapy, and 95% of HIV infected patients (Akpan and Morgan, 2002). The clinical symptoms of oropharyngeal candidiasis can be odd sensations, altered taste, and altered smell, affecting the patient's quality of life (Tonglairoum et al., 2014)

2.1.2 Management and treatment of oral candidiasis

Oral hygiene and topical antifungal treatment are usually adequate for uncomplicated oral candidiasis. An important approach of oral candidiasis treatment is the eradication of any underlying causes or predisposing risk factors (McCullough and Savage, 2005). For example, oral and dental hygiene should be controlled with periodic oral examination in patients with oral candidiasis. Oral hygiene comprises cleaning the teeth, buccal cavity, tongue, and dentures. Dentures should be removed at night and submerged in a disinfectant solution such as chlorhexidine solution. Denture

hygiene should also be assessed and checked for proper fitting (Akpan and Morgan, 2002; Garcia-Cuesta et al., 2014; Millsop and Fazel, 2016). In addition, the type of Candida infection should be determined together with the use of appropriate antifungal drugs.

However, sometimes, it is not possible to eradicate the underlying cause, and good oral hygiene alone may not be sufficient. In addition, some cases of oral candidiasis may result in severe oral discomfort or affect quality of life. In these case treatments with antifungal drugs, including topical and systemic antifungal agents, are required. For uncomplicated oral candidiasis, topical antifungal therapy may be adequate and is recommended as a first line treatment due to lower adverse effect. The systemic adverse effects and drug interactions that occur with the systemic drugs do not occur with topical drugs. (Samaranayake et al., 2009; Pappas et al., 2015; Millsop and Fazel, 2016). Systemic antifungal treatment is used in patients with oral candidiasis who exhibit less response or resistance to topical medications and those at high risk of developing systemic infections (Epstein and Polsky, 1998).

2.1.2.1 Topical antifungal agents

The antifungal agents that are used as a topical treatment for oral candidiasis are summarized in Table 2.1. There are various medications and dosage forms that have been used for the uncomplicated treatment.

1. Gentian violet

Gentian violet is a topical fungicidal agent that has been reported to exhibit antistaphylococcal properties. Gentian violet is recommended to use by applying 1.5 mL of 0.5% solution two times a day (Nyst et al., 1992). The possible side effects, could be skin irritation, oral ulcers, and purple staining of the skin and clothing (Balabanova et al., 2003).

2. Polyene antifungals

Polyene antifungal including nystatin and amphotericin B have been used for the treatment of oral candidiasis. The mechanism of action of polyene antifungals is binding to sterols in the cell membrane of fungi, and altering cell membrane permeability (Ellepola and Samaranayake, 2000). Polyene binding to ergosterol which is an important sterol that controls asymmetry and fluidity of the cell

membrane and is needed for membrane-bound enzymes to appropriately function. The binding induces leakage of cytoplasmic contents leading to fungal cell death.

Table 2.1 Topical antifungal agents used in the treatment of oral candidiasis.

Antifungal agents	Dosage form	Dosage and frequency
Gentian violet	Solution	1.5 mL of 0.5% solution twice daily
Nystatin	Cream, Ointment	Apply 3 to 4 times daily
	Suspension	100 U, 4 times daily
	Lozenge	100,000 U; a maximum of 5 times daily for 7-14 days
Amphotericin B	Cream, Ointment, Lotion	3 to 4 times daily for a maximum of 14 days
	Suspension	100 mg/mL, apply 4 times a day
Miconazole	Cream, ointment	2%, twice daily for 2-3 weeks
	Gel	2% gel, 3 to 4 times daily for 2-3 weeks
	Lacquer	1 g, applied once weekly to dentures for 3 weeks
Ketoconazole	Cream	2% cream; 2 to 3 times daily for 14-28 days
Clotrimazole	Cream	1% cream; 2 to 3 times daily for 3-4 weeks
	Solution	1% solution; 3 to 4 times daily for 2-3 weeks
	Troche	10 mg troche; 5 times daily for 2 weeks

Source: Millsop, JW and Fazely N. "Oral candidiasis." **Clinics in Dermatology** 34, 4: 487-494.

The use of polyenes is limited because they exhibit poorly absorption through the gastrointestinal tract. Hence, the principle means of application for polyene antimicrotics is topical application in form of lozenges, oral rinse, pastille and oral suspension.

3. Imidazoles

Imidazole antimycotics demonstrate fungistatic properties by inhibiting ergosterol synthesis in the fungal plasma membrane. The mechanism of action is by inhibiting the enzyme lanosterol demethylase that is a cytochrome P-450

3-A dependent enzyme involved in the synthesis of ergosterol. Subsequent depletion of ergosterol in the fungal cell results in inhibition of fungal growth and impairment of membrane permeability (Anibal et al., 2010; Niimi et al., 2010). They are available in form of gel, cream, ointment, lacquer.

2.1.2.2. Systemic antifungal agents

The treatment of oral candidiasis using systemic antifungals is appropriate in patients, intolerant of or refractory to topical treatment and those at high risk of developing systemic infections (Epstein et al, 1998). Table 2.2 displayed the list of antifungal agents for systemic therapy of oral candidiasis.

Table 2.2 systemic antifungal agents used in the treatment of oral candidiasis.

Antifungal agents	Dosage form	Dosage and frequency
Ketoconazole	Tablet	200 mg daily or twice daily for 2 weeks
Fluconazole	Capsule	loading dose of 250 mg then 50-200 mg daily for 7-14 days
Itraconazole	Capsule	100-200 mg daily for 14 days
Posaconazole	Suspension	100 mg twice daily on day 1, then 100 mg daily for 13 days
Caspofungin	Injection	loading dose 70 mg, then 50 mg daily
Amphotericin B	Injection	3-5 mg/kg daily

Source: Millsop, JW and Fazely N. "Oral candidiasis." **Clinics in Dermatology** 34, 4: 487-494.

Pappas, P. G., et al. (2015). "Clinical Practice Guideline for the Management of Candidiasis: 2016 Update by the Infectious Diseases Society of America." **Clinical Infectious Diseases**. published online December 16, 2015 doi:10.1093/cid/civ933

Azole group antimicotic is usually used for as systemic antifungal to treat moderate to severe oral fungal infection. According to the clinical practice guideline for the management of candidiasis: 2016, oral fluconazole, 100–200 mg daily, for 7–14 days is recommended for moderate to severe disease. For fluconazole-

refractory disease, itraconazole solution 200 mg once daily or posaconazole suspension 400 mg twice daily for 3 days then 400 mg daily for up to 28 days are recommended (Pappas et al., 2015). However, there is a major concern with these agents, especially with fluconazole which has been reported about the growing number of resistance, mainly in patients requiring longterm or recurrent therapy. In order to prevent and cope with the increasing prevalence of more resistant strains of *C. albicans*, strategies must be developed. Besides azo group antifungal agent, intravenous amphotericin B is also used with an excellent record in the treatment of systemic mycoses and refractory oropharyngeal candidiasis. Nevertheless, its routine use for OPC is limited by its toxicity (Epstein et al., 1998).

2.2 Herbal product

The use of natural drugs from the plants are increasing attractiveness due to several advantages such as having less side-effects, better patient acceptance, being relatively less expensive and acceptable due to a long history of use (Tabassum et al., 2014). Since ancient times, the plant kingdom has provided a variety of compounds that exhibit therapeutic effect, such as analgesics, anti-inflammatories, etc. Recently, antimicrobial properties of plant extracts have been reported with increasing frequency from different parts of the world (Cowan, 1999). For instance, the South American population use plant extracts obtained from traditional medicinal plants as medicine for many infectious diseases. Numerous research studies from different parts of the world have verified that extracts from medicinal plants could possess anti-microbial, anti-inflammatory, analgesic, smooth muscle relaxant, anti-tyrosinase, mosquito repellent, a carminative, a mild laxative, anti-oxidative activities, etc. (Pithayanukul et al., 2007; Kumar et al, 2011; Farzaei et al., 2013). Some natural products have been considered to play an important role as an alternative to synthetic chemicals in clinical treatment (Casaroto et al., 2010). A wide variety of plants extracts have been reported to have antifungal activity against *C. albicans* (Rosato et al., 2008). The World Health Organization (WHO) estimates that plant extracts or their active constituents are used as folk medicine in traditional therapies of 80% of the world's population.

2.3 Herbal medicine for the oral hygiene and oral fungal infection

A number of herbal products have been used in folklore remedies for the treatment of fungal infection. Recently, a variety of herbal products are encouraged for oral and dental uses as alternative to standard commercial products. Some herbal compounds have effective antimicrobial effects, and many herbal components such as chamomile, clove oil, echinacea, eucalyptus, ginger, etc. are included in herbal oral products (Sabzghabae et al., 2011). Various research works revealed that essential oils of some medicinal plants exhibited antibacterial, antifungal and insecticidal properties (Burt, 2004) and the essential oils have been used for treatment of serious skin diseases and superficial mycoses (Harris, 2002). Moreover, many plant extracts have shown to have therapeutic values with respect to oral diseases such as ginger, lemongrass, garlic, clove, mango, neem, etc. (Bakri and Douglas, 2005; Prashant et al, 2007; Ficker et al, 2003; Giriraju and Yunus, 2013). In addition, a wide variety of plant extracts have been reported to have antifungal activity against *C. albicans* (Sawaya et al, 2002; Casaroto and Lara, 2010). Examples of the plant extracts that exhibit anticandida activity are listed in Table 2.3.

2.4 Nanofibers

In recent times, various nanoscale materials have attracted much attention especially nanoparticles and nanofibers. Nanofibers are fibers with a diameter of 100 nm or less (Ramakrishna et al, 2012). They exhibit outstanding features, such as low density, high porosity, large specific surface areas and very small pore sizes and superior mechanical properties. Due to these features, the nanofibers have been applied in a wide range of applications (tissue engineering, drug delivery systems, wound dressing, high performance filtration, battery separators, vascular grafts, enzyme immobilization, electrochemical sensing, composite materials, and tissue engineering (Reneker et al., 2000; Smith and Ma, 2004; Ramakrishna et al., 2006).

Table 2.3 Plant extracts that exhibit anticandida activity.

Scientific name	Plant name	Tested sample	Reference
<i>Punica granatum</i> Linn	Pomegranate	Ethanollic extract	Vasconcelos et al,2006
<i>Streblus asper</i> Lour	Shakhotaka	Ethanollic extract	Taweechaisupapong et al, 2005
<i>Azadirachta indica</i>	Neem	Aqueous extract	Polaquini et al, 2006
<i>Vitis nifera</i>	Grape vine	Ethanollic extract	Han, 2007
<i>Maleleuca alternifolia</i>	Tea tree	Essential oil	Catalán et al, 2008
<i>Cuminum cyminum</i>	Cumin	Essential oil	Naeini et al, 2014
<i>Salvadora persica</i>	Miswak	Alcoholic extract	Naeini et al, 2014
<i>Allium sativum</i>	Galic	Aqueous extract	Shuford et al, 2005
<i>Quercus infectoria</i>	Aleppo oak	Methanol extract	Baharuddin et al, 2015
<i>Cassia Spectabilis</i>	Senna	Methanol extract	Torey and Sasidharah, 2011
<i>Morinda citrifolia</i>	Noni	Juice extract	Barani K et al, 2014
<i>Thymus pulgioides</i>	Lemon thyme	Essential oil	Pinto et al, 2006
<i>Syzygium aromaticum</i>	Clove	Essential oil	Pinto et al, 2009
<i>Piper betle</i>	Betel	Essential oil	Nordin, 2014
<i>Cymbopogon citratus</i>	Lemon grass	Essential oil	Silva et al, 2008
<i>Gacinia mangostana</i> Linn.	Mangosteen	Alpha-mangostin	Kaomongkolgit et al, 2009

2.4.1 Nanofiber fabrication

Polymeric nanofibers can be fabricated using various techniques such as drawing, template synthesis, phase separation, self-assembly and electrospinning. The details of the advantages and disadvantages of these processing methods are summarized in Table 2.4.

Table 2.4 Advantages and disadvantages of nanofiber fabricating methods.

Technique	Advantage	Disadvantage
Drawing	- Require minimum equipment	- Discontinuous process - Fiber diameter cannot be controlled - Cannot be scaled up
Template synthesis	- Fibers of different diameters can be easily achieved by using different templates	- Cannot be scaled up
Phase separation	- Require minimum equipment - Process can directly fabricate a nanofiber matrix - Batch-to-batch consistency is achieved easily	- Limited to specific polymers - Fiber diameter cannot be controlled - Cannot be scaled up
Self-assembly	- Good for obtaining smaller nanofibers.	- Complex process - Fiber diameter cannot be controlled - Cannot be scaled up
Electrospinning	- Cost effective, can be scaled up - Continuous fibers can be produced	- Jet instability

2.4.1.1 Drawing

Ondarcuhu and Joachim demonstrated the fabrication of nanofibers using citrate molecules through the process of drawing (Ondarcuhu and Joachim, 1998). In this process, a micropipette with a diameter of a few micrometers was dipped into the droplet near the contact line using a micromanipulator. The micropipette was then withdrawn from the liquid at the edge of the drop and moved at a certain rate, resulting in a nanofiber being pulled. The pulled fiber was deposited on the surface by touching it with the end of the micropipette. The drawing of nanofibers was repeated several times on every droplet. The illustration of the basic production process of nanofibers by drawing process is presented in Figure 2.1.

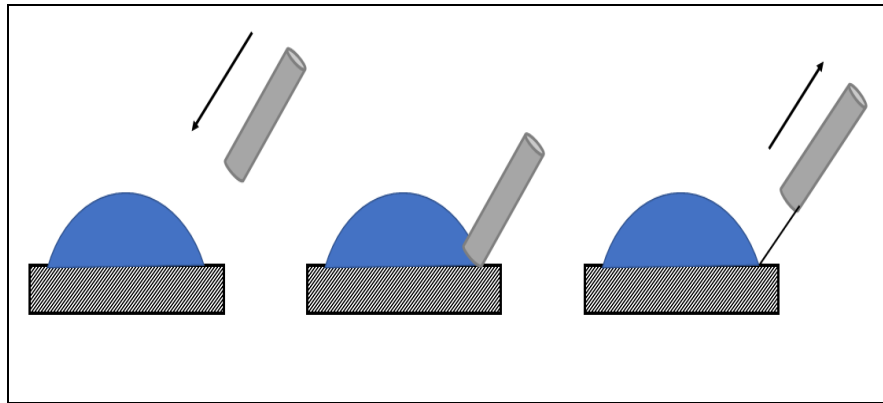


Figure 2.1. Schematic of the basic production process of nanofibers by drawing process.

Source: Ondarçuhu, T. and C. Joachim. "Drawing a single nanofibre over hundreds of microns." *Europhysics Letters* 42, 2: 215.

2.4.1.2 Template synthesis

Template synthesis uses a nanoporous membrane as a template to make nanofibers. Feng et al. demonstrated the fabrication of nanofibers using the template as a metal oxide membrane with pores of nano-scale diameter (Feng et al., 2002). Upon the application of water pressure on one side and restrain from the porous membrane lead to extrusion of the polymer which, after contact with a solidifying solution, gives rise to nanofibers whose diameters are determined by the pores. The illustration of template synthesis process is shown in Figure 2.2.

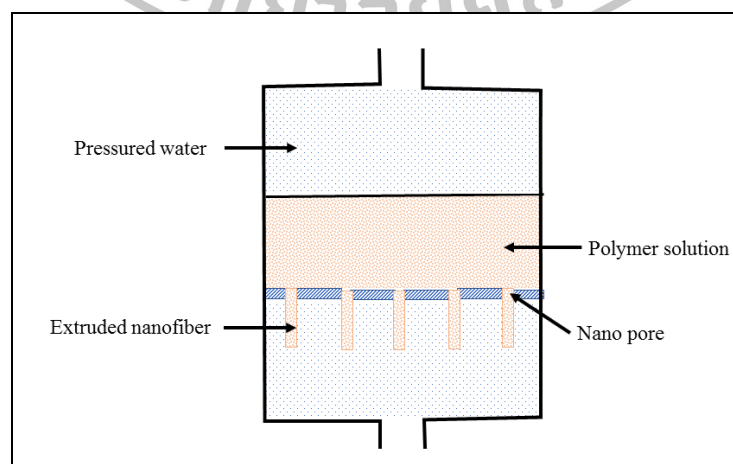


Figure 2.2 Schematic illustration of nanofibers made by template synthesis.

2.4.1.3 Phase separation

In phase separation method, a polymer is firstly mixed with a solvent before undergoing gelation. The main mechanism in this process is the separation of phases due to physical incompatibility. One of the phase - which is that of the solvent - is then extracted, leaving behind the other remaining phase.

2.4.1.4 Self assembly

In general, self-assembly of nanofibers associate with the build-up of nanoscale fibers using smaller molecules as basic building blocks. The main mechanism for a generic self-assembly is the intermolecular forces that bring the smaller units together and the shape of the smaller units of molecules which determine the over shape of the macromolecular nanofibers. the self-assembly is time-consuming in processing continuous polymer nanofibers.

2.4.1.5 Electrospinning

The most common technique used for the fabrication of nanofibers is electrospinning. Electrospinning generates fibers with diameters ranging from nanometer to micrometer. A typical electrospinning setup consists of three main components including a high voltage power supply, a syringe with a metallic needle and a grounded collector as displayed in Figure 2.3.

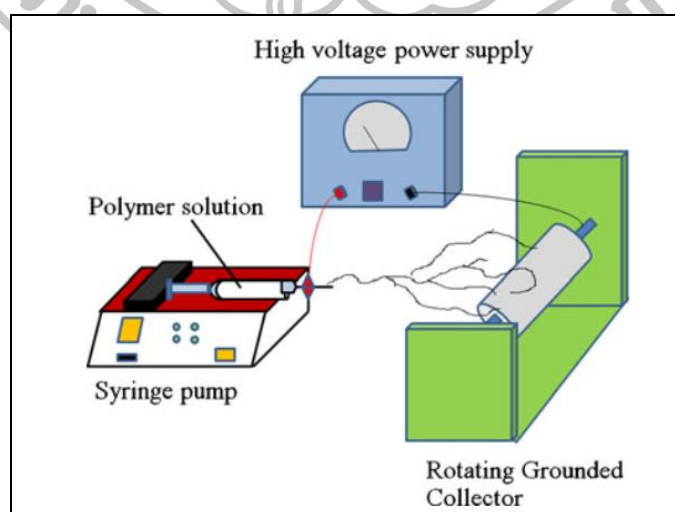


Figure 2.3 Schematic diagram of the electrospinning process.

Source: Tonglairoum, P., et al. "Development and characterization of propranolol selective molecular imprinted polymer composite electrospun nanofiber membrane." **AAPS PharmSciTech** 14, 2: 838-846.

2.4.2 Electrospun nanofibers

2.4.2.1 Electrospun nanofiber preparation

To fabricate electrospun nanofibers, high voltage is applied on solutions or melts and a pendant droplet forms. Once the electrostatic repulsion overcomes the surface tension of the polymer solution, the pendant droplet will deform into a conical droplet known as the Taylor cone (Taylor, 1969) at the tip of the needle. When the electrostatic force is sufficient to overcome the surface tension of the conical droplet, a polymer fiber jet is ejected from the tip of the needle. The interaction between the electric field and the surface tension of the fluid elongates the jet fiber into a long and thin filament and makes it undergo a whipping motion resulting in the evaporation of the solvent. Then, the filament deposits onto a grounded collector, leading to the formation of a uniform fiber. In addition to the polymer solution, molten polymers in high temperature can also be fabricated into nanofibers using electrospinning process by introducing the molten polymer instead of a solution into the capillary. However, the electrospinning process for a polymer melt has to be carried out in a vacuum condition (Larrondo et al., 1981). The capillary tube, the traveling of the charged melt fluid jet, and the metal collecting screen must be encapsulated within a vacuum.

2.4.2.2 Parameters affecting the nanofiber properties

The conversion of polymer solutions into nanofibers through electrospinning can be affected by various parameters. These parameters are usually categorized into three groups including solution parameters (such as solution concentration, viscosity, surface tension, and conductivity), process parameters (such as feed rate, applied voltage, and tip to collector distance), and ambient conditions (such as ambient temperature and humidity) (Yao et al., 2013; Teron et al., 2004).

1. Solution concentration

For the nanofiber fabrication by electrospinning process, it has been observed that at low solution concentration, a mixture of beads and fibers is obtained and after increasing the polymer concentration, the beads morphology changes from spherical to spindle-like and finally form uniform fibers with increased diameters due to the higher viscosity resistance (Deitzel et al., 2001; Ki et al., 2005; Haghi and Akbari, 2007).

2. Solution viscosity

Solution viscosity plays an essential role in the preparation of electrospun nanofibers because it can affect the fiber morphology during spinning of polymeric fibers. It has been discovered that no continuous fiber can be formed at very low viscosity, and the ejection of jets from polymer solution can be problematic with very high viscosity of polymer solution. Therefore, there is a requirement of optimal viscosity for electrospinning (Bhardwaj et al., 2010). Very high viscosity polymer solutions generally display longer stress relaxation times, which might avoid the splitting of the ejected jets during electrospinning. An increase in solution viscosity leads to a larger and more uniform fiber diameter (Deitzel et al., 2001).

3. Solution Surface tension

Surface tension also plays a crucial role in the electrospinning process and nanofiber fabrication. Decreasing the surface tension of a polymer solution, fibers can be produced without beads. Different solvents have different surface tensions. Mostly, a solution with high surface tension may hinder the electrospinning process due to instability of the jets and the generation of sprayed droplets (Hohman et al., 2001). The formation of droplets, beads and fibers counts on the surface tension of solution. A polymer solution with lower surface tension could facilitate the electrospinning process to occur at a lower electric field (Haghi and Akbari., 2007).

4. Solution conductivity

The conductivity of the polymer solution is highly prominent in jet formation. Solution conductivity is mostly controlled by the polymer type, solvent used, and the availability of ionisable salts. It has been noticed that after increasing

electrical conductivity of the solution, a significant decrease in the diameter of the electrospun nanofibers has been observed whereas with low conductivity of the solution, there is insufficient elongation of a jet by electrical force to produce uniform fiber, and beads may also occur (Bhardwaj et al., 2010).

5. Feed rate

The feed rate of the solution is an important factor that manipulates the diameter and morphology of electrospun fibers. As the feed rate of the solution increases, the charge density will decrease. A high charge density may result in the electrospinning jet undergoing secondary bending instabilities, which could lead to the generation of fibers with smaller diameter (Mitchell and Sanders, 2006; Son et al., 2004). Therefore, increasing the feed rate cause an increase in the fibers diameter. This is because the high feed rate of solution could not provide enough time for solvent evaporation (Zuo et al., 2005; Yuan et al., 2004).

6. Applied voltage

The applied voltage is an important element in ultimate electrospun fiber preparation. Increasing the voltage can cause increase in the spinning current that can lead to incidence of beaded morphology, and this structure can reduce the surface area. Increase or decrease in applied voltage can cause change of morphology and structure of fibers (Deitzel et al., 2001). Previous study reports that the increase in voltage leads to increase in fiber length and decrease in fiber size (Megelski et al., 2002).

7. *Tip to Collector Distance.*

The morphology and diameter the of the nanofibers can also be regulated by varying the distance between the tip and the collector. In the electrospinning process, a minimum distance that enables enough time for solvent evaporation before the fibers reach the collector is required. Longer distance has yielded thinner fibers (Hu and Aplett, 2014).

2.4.2.3 Polymers used in electrospinning

A wide range of polymers have been used in electrospinning process and are able to form fine nanofibers within the submicron range and used for various applications. Examples of the polymer used in the nanofiber fabrication using electrospinning and their applications are listed in Table 2.5

Table 2.5 Different polymers used in electrospinning and their applications.

Polymers	Application	Reference
Poly(glycolide) (PGA)	Tissue engineering	Boland et al. (2004)
Poly(lactide-co-glycolide) (PLGA)	Biomedical applications	Zong et al., 2003; Katti et al., 2004)
Poly(ϵ -caprolactone) (PCL)	Bone tissue engineering	Yoshimoto et al. (2003)
Poly(l-lactide) (PLLA)	3D cell substrate	Fertala et al. (2001)
Polyurethane (PU)	Nonwoven tissue template wound healing	Khil et al. (2003)
Poly (ethylene-co-vinyl alcohol) (PEVA)	Nonwoven tissue engineering scaffold	Kenawy et al. (2003)
Polystyrene (PS)	Skin tissue engineering	Sun et al. (2005)
Poly(vinyl alcohol)/cellulose acetate (PVA/CA)	Biomaterials	Ding et al. (2004)
Poly(vinyl alcohol) (PVA)	Wound dressings	Jia et al. (2007)
Silk/chitosan (CS)	Wound dressings	Park et al. (2004)
Chitosan (CS)/PEO	Tissue engineering scaffold, drug delivery, wound healing	Duan et al. (2004)
Collagen/chitosan (CS)	Biomaterials	Chen et al. (2007)

Source: Bhardwaj, N. and S. C. Kundu. "Electrospinning: A fascinating fiber fabrication technique." **Biotechnology Advances** 28, 3: 325-347.

The polymer used can be both natural fibers and synthetic fibers such as poly(glycolide) (PGA), poly(lactide-co-glycolide) (PLGA), poly(ϵ -caprolactone) (PCL), poly(l-lactide) (PLLA), polyurethane (PU), poly(ethylene-co-vinyl alcohol) (PEVA), polystyrene (PS), cellulose acetate, poly (vinyl alcohol) (PVA), silk, chitosan (CS), gelatin, Appropriate electrospinning condition for nanofiber production of each polymer is different and depends on polymer properties.

2.4.2.4 Application of electrospun nanofibers

Electrospun fibers offer numerous advantages such as high surface to volume ratio, very high porosity and enhanced physico-mechanical properties. Furthermore, the electrospun fibers are required in a small quantity, and the electrospinning process itself is a multipurpose, adaptable and handy process which the fibers can be spun into any shape using a wide range of polymers. Electrospun nanofibers have usually been applied in various applications such as tissue engineering scaffolds, wound healing, drug delivery, filtration, as affinity membrane, enzymes immobilization, vascular graft implants, healthcare, biotechnology, environmental engineering, and in various ongoing researches (Reneker et al., 2000; Stitzel et al., 2001; Smith and Ma, 2004).

2.5 Drug dissolution improvement of poorly soluble drugs

In the drug development process, the majority of drugs are highly hydrophobic, exhibiting poor or negligible water solubility. Consequently, the oral absorption of these drugs is often limited by their poor solubility or slow dissolution in the human gastrointestinal media (Amidon et al., 1995). With the purpose of oral absorption enhancement of such poorly water-soluble drugs, various techniques used to increase their dissolution rates, and several formulation strategies have been employed; for example, salt formation (Ware and Lu, 2004), complexation (Thompson, 1997), particle size reduction (Liversidge and Cundy 1995), prodrug (Fleisher et al., 1996), using lipid formulation (Pouton, 2000), and solid dispersions (Serajuddin, 1999).

2.5.1 Improve drug dissolution by electrospinning

It is accepted that the dissolution rate of a drug molecule can be improved by enlarging surface area. Polymer-drug solid dispersions is also an alternative approach for improving dissolution rate (Sareen et al., 2012). Solid dispersions can be defined as the dispersion of one or more active ingredients in an inert carrier or matrix in the solid state (Ignatious et al., 2010). The generally used methods of forming solid dispersions are fusion and solvent methods. For the solvent method, the drug and carrier are dissolved in organic solvents to form a solution.

Then, the solvent is removed using one or a combination of methods, such as solvent evaporation, precipitation by a non-solvent, freeze drying or spray drying. The solid dispersions prepared using both the fusion and solvent methods usually displayed greater dissolution rates than their original crystalline forms (Serajuddin et al., 1999).

Due to a surging interest in nanotechnology, nanofibers have gained more attention owing to their high specific surface area. Nanofiber mats have been applied as drug carriers in the drug delivery system due to their outstanding properties. The nanofibers offer various advantages like high surface area to volume ratio, tunable porosity and the ability to manipulate nanofibers composition in order to get desired properties and function. Due to the extremely high surface area of nanofibers which act as a carrier, the dissolution rate of a particulate drug could be increased. Moreover, the large surface area of the nanofibers lead to fast and efficient solvent evaporation, which provides the limited time for incorporated drug to recrystallize and promote the formation of amorphous dispersions or solid solutions (Verreck et al., 2003). Poorly water soluble drugs are usually incorporated into electrospun nanofibers for improving their dissolution properties. In addition to poorly soluble drugs, the water-soluble drugs can also be spun into the fibers. The release characteristics of the drug-loaded nanofibers can be regulated as rapid, immediate, delayed, or modified dissolution depending on the polymer used.

2.5.2 Improve drug dissolution by complexation with cyclodextrin

CDs are cyclic oligosaccharides consisting of 1,4-linked glucopyranoside units which have ability to form inclusion complexes with a wide ranges of drug molecule leading to an alteration in the physicochemical properties of the complexes (Del Valle, 2003). Complexation of poorly soluble drug with cyclodextrin is a useful method to improve the dissolution and stability of drug (Albers and Muller, 1995). After forming inclusion complexes, major changes in drug properties such as enhanced solubility, physical and chemical stability, and other physicochemical properties, have been reported (Albers and Muller, 1995; Rao and Stella, 2003; Challa et al., 2005). These changes lead to the improvement in biological performance especially solubility enhancement of poorly soluble drugs. CDs could reduce drug crystallinity on complexation or form solid dispersion with poorly soluble

drugs resulting in the increase in apparent drug solubility and dissolution rate (Balata et al., 2011). Methylated CDs with a relatively low molar substitution seem to be the most powerful solubilizers. Sulfobutylether- β -CD was proved to be an outstanding solubilizer for several drugs and was more effective than β -CD but not as effective as Dimethyl- β -CD (Ueda et al., 1998). CDs can also function as release enhancers, for example β -CD enhanced the release rate of poorly soluble naproxen (Bettinetti 2002). Examples of the use of CD for enhancing drug solubility and dissolution are presented in Table 2.6.

Table 2.6 Examples of solubility and dissolution improvement using CD.

CDs	Drugs
β -CD	Nimesulide, Sulfomethiazole, Lorazepam, Ketoprofen, Griseofulvin, Praziquantel, Chlorthalidone, Etodolac, Piroxicam, Itraconazole, Ibuprofen
α -CD	Praziquantel
γ -CD	Praziquantel, Omeprazole, Digoxin
HP- β -CD	Albendazole, Levemopamil HCl, Sulfomethiazole, Ketoprofen, Griseofulvin, Itraconazole, Carbamazepine, Zolpidem, Phenytoin, Rutin
Dimethyl- β -CD	Naproxen, Camptothecin
Sulfobutylether- β -CD	Danazol, Fluasterone, Spiranolactone

Source: Challa, R., et al. "Cyclodextrins in drug delivery: An updated review." *AAPS PharmSciTech* 6, 2: E329-E357.

2.5.3 Improve drug dissolution using lipid based systems

The majority of the newly established drugs are hydrophobic and exhibit poorly water soluble. This could hinder the selection of proper drug delivery system to accomplish sufficient bioavailability of such drugs. Poor water solubility and dissolution rate are limiting factors which affect the absorption rate and bioavailability of the drugs. In order to improve the solubility and dissolution, one of the most popular approaches is the utilization of lipid-based drug delivery systems (Cerpnjak et al., 2013). The utility of solubilizing lipid-based formulations for enhancing the drug solubility and gastrointestinal (GI) absorption of poorly water-

soluble, hydrophobic drugs is well documented in the literature. In the lipid based formulation, a drug is dissolved in a blend of excipients with wide ranges of physicochemical properties ranging from pure triglyceride oils, mono- and diglycerides, and substantial proportion of lipophilic or hydrophilic surfactants and cosolvents (Pouton et al., 2000). In order to obtain better physicochemical stabilities of the lipid based system, a number of efforts have been dedicated for the conversion of liquid lipid systems into solid oral dosage forms. The techniques used include spray drying, lyophilisation, and rotary evaporation. Dry emulsions comprising poorly water-soluble drugs have been formulated which the aqueous phase is removed by spray drying, lyophilisation or rotary evaporation (Christensen et al., 2001; Dollo et al., 2003).

2.6 Microemulsions

Microemulsions are clear, thermodynamically stable, optically isotropic systems. Upon mixing a suitable oil, water, and an amphiphile blend (surfactants either alone or in combination with a cosurfactant), microemulsion can be developed spontaneously with a size range of 5-200 nm (Badawi et al., 2009). Due to their distinctive solubilization properties, Microemulsions have gained growing number of interest as bioavailability enhancers for poorly water soluble active pharmaceutical ingredients (Kawakami et al., 2002). Microemulsions were employed to solubilize drugs and to enhance topical drug availability (Sabale and Vora, 2012).

2.6.1 Microemulsion structure

Microemulsions are dynamic systems wherein the boundary is continuously and spontaneously altering (Lam & Schechter, 1987). Microemulsions can be divided into oil-in-water (o/w), water-in-oil (w/o), and bicontinuous microemulsions. In w/o microemulsion, water droplets are dispersed in the continuous oil phase, while o/w microemulsion is formed when oil droplets are dispersed in the continuous aqueous phase. A bicontinuous microemulsion may be occurred when the quantities of water and oil are equal. The interface of microemulsion is stabilized by a suitable mixture of surfactants and cosurfactants. Various structures can be generated from the mixture of oil, water, and surfactants counting on the ratio of the components

(Spernath and Aserin, 2006). The different structures of microemulsion are illustrated in Figure 2.4.

2.6.2 Pseudo ternary phase diagram

Solubilization and interfacial properties of microemulsions depend on pressure, temperature and nature and concentration of the components (Ashish et al., 2014; Lessner et al., 1983). Thus, determining the phase stability diagram and position of the various structures formed within the component used is very important. The pseudo ternary phase diagram is constructed to find the different zones including microemulsion zone as shown in Figure 2.5.

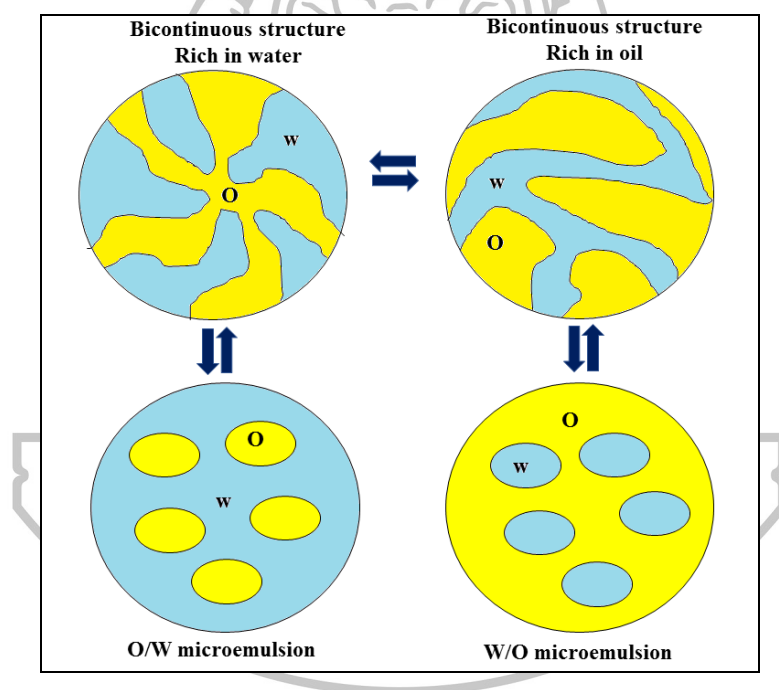


Figure 2.4 Structures of microemulsion divided by the dispersion of water phase and oil phase in the system.

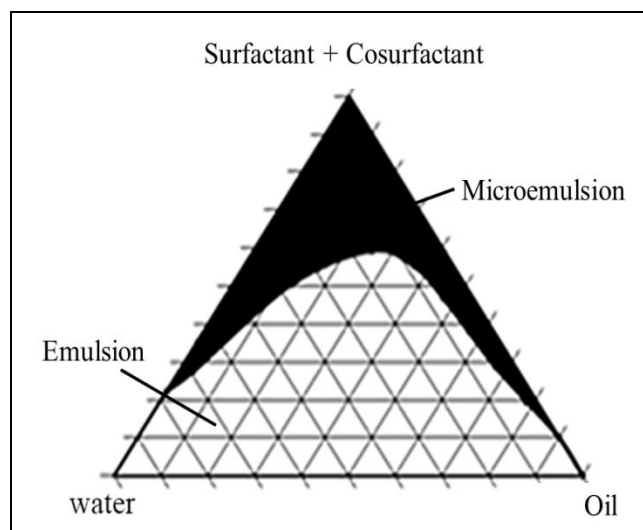


Figure 2.5 The pseudo ternary phase diagram construction for obtaining the concentration range of components for the existing range of microemulsions.

2.6.3 Microemulsion preparation

Microemulsions are usually formulated using the spontaneous emulsification method (phase titration method). Pseudoternary phase diagram is often constructed to find the different zones including microemulsion zone, in which each corner of the diagram represents 100% of the particular component. In this method, the oil phase, surfactant and co-surfactant are mixed at an appropriate ratio before the mixture is titrated dropwise with water to obtain microemulsion.

2.7 Cyclodextrin (CDs)

CDs are cyclic oligosaccharides composed of D-glucopyranoside units (glucose) linked by α -1,4 glycosidic bonds. The CDs of biomedical and pharmaceutical interest are cyclic oligosaccharides made up of six, seven and eight α -(1,4)-linked glycosyl units (α -, β -, and γ -CDs, respectively). CDs are broadly used as "molecular cages" in the pharmaceutical, food and cosmetic industries (Roux et al., 2007). In the pharmaceutical field, they are exploited as complexing agents to improve the aqueous solubility of poorly soluble drugs and to heighten their bioavailability and stability (Loftsson and Duchene, 2007). Moreover, CDs can be

used to reduce gastrointestinal drug irritation, convert liquid drugs into microcrystalline or amorphous powder, and prevent drug–drug and drug–excipient interactions etc. The shape of CDs contains a truncated cone with the lipophilic central cavity and hydrophilic outside surface. Figure 2.6 illustrates the chemical structure and a truncated cone of β CD. As it can be seen from the picture, the cone exterior is composed of hydroxyl groups with the primary hydroxyl groups at the narrow edge and the secondary hydroxyl groups at the wider edge. Skeletal carbons and ethereal oxygens of the glucose residue are located in central cavity (Brewster and Loftsson, 2007).

The most prominent property of CDs is their ability to modify the physicochemical and biological characteristics of drugs. The cavity of CDs can act as a host substance and form interactions molecules using intermolecular forces. The consequential molecular complex is known as inclusion complex or a supramolecular compound (Li et al., 2010). The characteristics of natural CDs and the solubility of CDs in water are displayed in Table 2.7. From the information in the table, β -CD exhibits the lowest solubility, because of the high number of intramolecular hydrogen bonds among secondary hydroxyl groups within the molecule. These interactions make the structure rigid and prevent hydration by water molecules (Szejtli, 1994; Loftsson et al., 2005b).

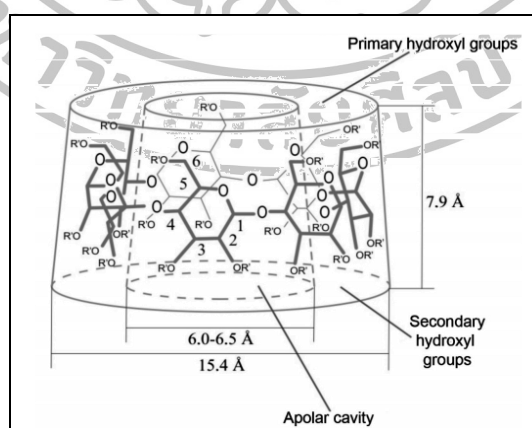


Figure 2.6 β -cyclodextrin (β -CD) structure.

Source: Miranda, J. et al. "Cyclodextrins and ternary complexes: technology to improve solubility of poorly soluble drugs." **Brazilian Journal of Pharmaceutical Sciences** 47, 4: 665-681.

Table 2.7 The characteristics and solubility of CDs.

CDs	Molecular Weight	Cavity diameter (nm)	Solubility (mg/mL)
α -CD	972	0.47-0.53	145
β -CD	1135	0.60-0.66	18.5
γ -CD	1400	0.75-0.83	>600
Hydroxypropyl- β -cyclodextrin (HP β CD)	1460	-	>500
β -cyclodextrin sulfobutyl ether sodium salt (SB β CD)	1312	-	>500
Randomly methylated β -cyclodextrin (RM β CD)	1297	-	232
Hydroxypropyl γ -cyclodextrin (HP γ CD)	1576	-	>500

Source: Vyas, A., S. Saraf and S. Saraf. "Cyclodextrin based novel drug delivery systems." **Journal of Inclusion Phenomena Macrocyclic Chemistry** 62, 1-2: 23-42.

2.7.1 Formation of Inclusion complex

The structure of CDs known as truncated cone allows the inclusion complex of a number of organic molecules in their central cavities. The ability of a cyclodextrin to form an inclusion complex with a guest molecule is a result from two main aspects. The first is the relative size of the cyclodextrin to the size of the guest compound or particular major functional groups within the guest. The size of the guest compound should be appropriate and fit well with the cyclodextrin cavity. The thermodynamic interactions between the different constituents in the the system (cyclodextrin, guest, solvent) is the second important factor. To produce the complex, energetic driving force should be enough to pull the guest into the cyclodextrin. The main driving force of complex formation is the discharge of enthalpy-rich water molecules from the cavity. Then, the water molecules are displaced by more

hydrophobic guest molecules existing in the solution to achieve an apolar–apolar association and decrease of cyclodextrin ring strain resulting in a more stable lower energy state (Szejtli, 1998; Del Valle et al., 2004). This process is dynamically favorable and promote an increase in complex stability, due to the alterations in enthalpy and a decrease in the total energy of the system (Miranda et al., 2011). The illustration of inclusion complex formation is shown in Figure 2.7

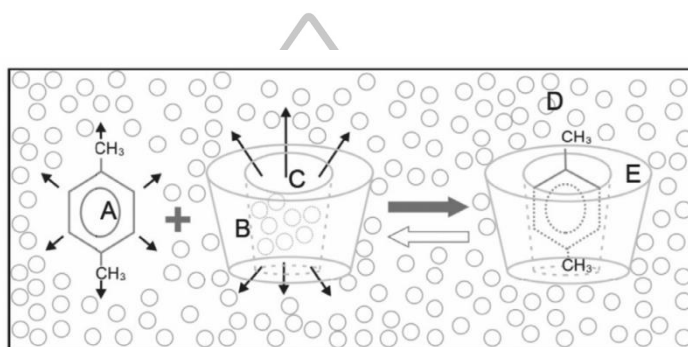


Figure 2.7 Schematic representation of the formation of inclusion complexes. A: drug molecule; B: cyclodextrin (CD) molecule; C: CD cavity; D: water molecules; E: drug-CD complex.

Source: Miranda, J. et al. "Cyclodextrins and ternary complexes: technology to improve solubility of poorly soluble drugs." **Brazilian Journal of Pharmaceutical Sciences** 47, 4: 665-681.

Moreover, additional interactions may also have an important role in the inclusion complexes formation and stabilization, including van der Waals interactions, 3-center, 2-electron bonds (between guest molecule and CD hydroxyl groups), hydrophobic interactions, the release of deformation energy from the macromolecular ring of CDs, and steric effects (Szejtli, 1998; Bibby et al., 2000; Flasiński et al., 2010). The complexes created usually demonstrate better water soluble than the former compound together with more stable in solution form.

2.7.2 Hydroxypropyl- β -cyclodextrin (HP β CD)

Hydroxypropyl- β -cyclodextrin (HP β CD) (hydroxylalkyl derivative of β CD) is an alternative to α -, β - and γ -cyclodextrin, with improved water solubility properties. The molecular structure of HP β CD is presented in Figure 2.8.

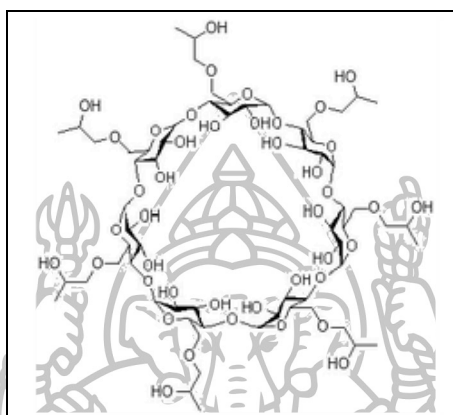


Figure 2.8 Molecular structure of HP β CD.

HP β CD are accepted to use in pharmaceutical field of European and United States pharmacopoeias. The best complexing properties can be achieved with average substitution number of 0.65 per glucose unit (Challa et al., 2005). The rapidly dissociate after parenteral drug administration of the complexes between HP β CD and poorly water soluble drugs, no tissue-irritating effects after intramuscular dosing, and superior oral bioavailability of poorly water-soluble drugs have been reported (Stella and He, 2008). Generally, HP β CD cannot be hydrolyzed by human salivary and pancreatic amylases (Brewster and Loftsson, 2007). In addition, it is considered to be non-toxic at low to moderate oral and intravenous doses because it is not absorbed from the GI tract (Valle, 2004). The clinical studies reported that HP β CD was well tolerated and safe in the majority of patients receiving HP β CD at daily oral doses of 4-8 g for at least 2 weeks (Gould and Scott, 2005). In addition, human experience HP β CD indicates that HP β CD is well tolerated in humans and have no adverse effects on the kidneys or other organs following either oral or intravenous administration (Stella and He, 2008).

2.8 Clotrimazole

Clotrimazole (CZ), a synthetic imidazole derivative, is a broad spectrum antimycotic agent effective against pathogenic dermatophytes, yeasts, and several species of *Candida*, *Tricophyton*, *Microsporum*, *Epidermophyton*, and *Malassezia*. It is primarily used locally in the treatment of vaginal and skin infections due to yeasts and dermatophytes. In addition, it has some in vitro activity against certain Gram-positive bacteria, and at very high concentrations has activity against *Trichomonas* spp (Sawyer et al., 1975). The structure of CZ is shown in Figure 2.9.

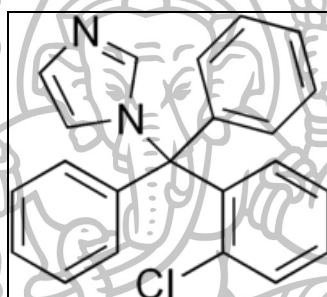


Figure 2.9 Molecular structure of CZ.

The mechanism of action of CZ has been proposed. CZ and other azoles inhibit the synthesis of ergosterol which is an essential constituent of the fungal cytoplasmic membrane in a concentration-dependent fashion, thereby damaging and affecting the permeability of the cell membrane. This results in leakage and loss of fundamental intracellular compounds, and finally lead to cell lysis. Suppression of fungal growth, inhibition of growth and fungicidal activity are the resultant effects of ergosterol depletion at the cellular level (Haller, 1985). CZ is known to be very effective locally and presents no major side effects. CZ is available in several conventional dosage forms such as creams, gels, pessaries, and ovules. However, poor water solubility of CZ (0.49 $\mu\text{g/ml}$) (Hoogerheide and Wyka, 1982) presents a hindrance for its local availability and limits its effective antifungal therapy. Thus, heightening the solubility is required for effective antimycotic activity. There are many formulation approaches to improve CZ solubility, including solid dispersion incorporated gels (Balata et al., 2011), nanospheres (Memişoğlu et al., 2003), solid

lipid nanoparticles (Souto et al., 2004) and hydrogels (Sosnowska and Winnicka, 2013). Some studies have achieved solubilization via the complexation of CZ with cyclodextrin (Prabagar et al., 2007) or by using lipid-based systems such as liposomes (Pavelic et al., 2005), microemulsions (Borhade et al., 2012) and nanoemulsions (Borhade et al., 2012).



CHAPTER 3

MATERIALS AND METHODS

- 3.1 Materials
- 3.2 Equipments
- 3.3 Methods
 - 3.3.1 Investigation of CS, CS derivatives and herbal oils for anti-candidal adhesion on denture acrylic resins
 - 3.3.1.1 Antifungal activity of CS derivatives and herbal oils
 - 3.3.1.1.1 Tested Solutions
 - 3.3.1.1.2 Preparation of CS solutions
 - 3.3.1.1.3 Antifungal susceptibility testing of oral Candidal stains
 - 3.3.1.2 Anti-adhesion assay
 - 3.3.1.2.1 Preparation of acrylic pieces
 - 3.3.1.2.2 Adhesion assay
 - 3.3.1.3 *In vitro* antibiofilm activity
 - 3.3.1.4 Preparation of herbal oil-incorporated nanofiber mats
 - 3.3.1.4.1 Fabrication of blank nanofiber mats
 - 3.3.1.4.2 Fabrication of herbal oil-loaded nanofiber mats
 - 3.3.1.4.3 Scanning electron microscope (SEM)
 - 3.3.1.4.4 Fourier transform infrared spectroscopy (FT-IR)
 - 3.3.1.4.5 Differential scanning calorimetry (DSC)
 - 3.3.1.4.6 Mechanical characterizations
 - 3.3.1.4.7 Determination of the oil content
 - 3.3.1.4.8 *In vitro* release
 - 3.3.1.4.9 Antifungal activity
 - 3.3.1.4.10 *In vitro* cytotoxicity
 - 3.3.2 Fabrication of fast release-CZ loaded nanofiber mats
 - 3.3.2.1 Solubility studies of CZ
 - 3.3.2.2 Phase solubility studies

- 3.3.2.3 Electrospinning of fast release-CZ loaded PVP/HP β CD nanofibers
- 3.3.3 Fabrication of CZ loaded-mucoadhesive nanofiber mats.
 - 3.3.3.1 CZ-microemulsion-containing nanofibers
 - 3.3.3.1.1 Phase diagram construction
 - 3.3.3.1.2 Preparation of CZ-loaded microemulsion systems
 - 3.3.3.1.3 Electrospinning process
 - 3.3.3.2 CZ-incorporated mucoadhesive sandwich nanofibers
 - 3.3.3.2.1 Fabrication of CZ-loaded PVP/HP β CD nanofibers
 - 3.3.3.2.2 Fabrication of CZ-incorporated mucoadhesive sandwich nanofibers
- 3.3.4 Characterizations of nanofiber mats
 - 3.3.4.1 Geometrical characterizations
 - 3.3.4.2 Mechanical characterizations
 - 3.3.4.3 *Ex-vivo* mucoadhesion study
 - 3.3.4.4 CZ content analysis
 - 3.3.4.5 *In vitro* release of CZ
 - 3.3.4.6 Evaluation of wetting time and disintegration time
 - 3.3.4.7 Antifungal activity of the nanofiber mats
 - 3.3.4.7.1 Susceptibility testing of CZ
 - 3.3.4.7.2 Time-kill analysis
 - 3.3.4.8 Cytotoxicity test
 - 3.3.4.9 *In vivo* mucoadhesion time and drug release evaluation
- 3.3.5 Stability test
- 3.3.6 Statistical analysis

3.1 Materials

Clotrimazole (CZ) (Sigma Aldrich[®], St. Louis, MO, USA)

2-hydroxypropyl- β -cyclodextrin (HP β CD) (DXM) (Sigma Aldrich[®], St. Louis, MO, USA)

Polyvinylpyrrolidone (PVP, MW. \sim 1,300,000) (Sigma Aldrich[®], St. Louis, MO, USA)

Chitosan (degree of deacetylation 0.85, MW 110 kDa) (Sigma Aldrich[®], St. Louis, MO, USA)

Ethylenediaminetetraacetic acid (EDTA) (Sigma Aldrich[®], St. Louis, MO, USA)

Polyvinyl alcohol (PVA; degree of polymerization \approx 1600, degree of hydrolysis \approx 97.5–99.5 mol%, average MW = 77,000-82,000 g/mol) (Fluka, Buchs, Switzerland)

Oleic acid (Fluka Chemie AG, Seelze, Germany)

Medium chain triglycerides (Estasan[®] 3580) (Uniqema Asia Pacific, Kuala Lumpur, Malaysia)

Betel oil (Thai China Flavours&Fragrances industry Co., Ltd., Thailand)

Clove oil (Thai China Flavours&Fragrances industry Co., Ltd., Thailand)

All other chemicals and tissue

Sabouraud dextrose broth (Becton, Dickinson and Company, NJ, USA)

Dulbecco's modified Eagle's medium (DMEM) (GIBCO-Invitrogen, NY, USA)

Trypsin-EDTA (GIBCO-Invitrogen, NY, USA)

Dimethyl sulphoxide (DMSO) (Sigma Aldrich[®], St. Louis, MO, USA)

Fetal bovine serum (FBS) (GIBCO[™], Grand Island, NY, USA)

Non-essential amino acid (PAA laboratories, Austria)

1-Ethyl-3-(3-dimethylaminopropyl) carbodiimide hydrochloride (EDAC) (Sigma Aldrich[®], St. Louis, MO, USA)

3-(4,5-Dimethylthiazol-2-yl)-2,5-diphenyl-tetrazolium bromide (MTT) (Sigma Aldrich[®], St. Louis, MO, USA)

4,5'-Dithio-bis-(2-nitrobenzoic acid) (DTNB) (Sigma Aldrich®, St. Louis, MO, USA)

Benzyl alcohol (BzOH) (Sigma Aldrich®, St. Louis, MO, USA)

L-cysteine hydrochloride (Sigma-Aldrich®, St. Louis, MO, USA)

Ethanol (RCI Labscan Limited, Bangkok, Thailand)

Excised porcine buccal mucosa (slaughterhouse in 2015)

Human gingival fibroblast (HGF) (explants of gingival tissue attached to non-carious, freshly extracted third molar, Ethical approval was obtained Naresuan University)

Polyethylene glycol 400 (PEG 400) (Faculty of Pharmacy, Silpakorn University, Nakhon Pathom, Thailand)

Potassium chloride (Ajax Finechem Australia, New Zealand)

Potassium dihydrogen phosphate (Ajax Finechem Australia, New Zealand)

Sodium bicarbonate (BDH AnalaR®, VWR International Ltd. England)

Sodium chloride (Ajax Finechem Australia, New Zealand)

Sodium dihydrogen phosphate (Ajax Finechem Australia, New Zealand)

Sodium hydroxide pellet (Ajax chemicals, New South Wales, Australia)

C. albican ATCC 90028 (Faculty of Dentistry, Naresuan University, Phitsanulok, Thailand)

3.2 Equipments

Analytical balance (Sartorius CP224S and CP3202S; Scientific Promotion Co., Ltd., Bangkok, Thailand)

Automatic Autoclave (Model: LS-2D, Scientific Promotion Co., Ltd., Bangkok, Thailand)

Beaker (Pyrex, USA)

Brookfield viscometer (Model: DV-III ultra, Brookfield Engineering Laboratories, Inc., MA, USA)

CO₂ incubator (Heraeus HERA Cell 240, Heraeus Holding GmbH., Germany)

Conductivity meter (Model: ECTestr11⁺, Eutech Instruments Pte Ltd, Ayer Rajah Crescent, Singapore)

Dialysis bag (CelluSep[®] MWCO (6000-8000), Membrane Filtration Products, USA)

Differential Scanning Calorimeter (Model: Sapphire DSC, Perkin Elmer instrument, MA, USA)

Digital video recorder (Cannon, Japan).

Drop shape analyzer (FTA 100, First Ten Angstroms Inc, Portsmouth, VA, USA)

Drum collector for electrospinning

Fluorescent Inverted Microscope (Model: ECLIPSE TE 2000-U, Nikon, Japan)

Fourier Transform Infrared Spectrophotometer (FT-IR) (Model: Nicolet 4700, Nicolet, USA)

Freeze-dryer (Model: Freezone 2.5, LABCONCO, USA)

Fusion Universal Microplate Analyzer (Model: A153601, Packard Instrument Company, Inc., Illinois, USA)

Genesis10 UV-visible spectrophotometer (Thermo Spectronic, NY, USA)

High voltage power supply (Model: Gamma High Voltage Research, USA)

Hot Air Oven (WTB Binder, Germany)

Incubated shaker (Model: KBLee 1001, Daiki sciences, Bio-Active, Bangkok, Thailand)

Magnetic stirrer (Framo, Germany)

Microcentrifuge tube (Eppendorf[®], Corning Incorporated, NY, USA)

Micropipette 2–20 μ L, 20–200 μ L, 100–1000 μ L, 1–5 mL, and micropipette tip

Microplate (24, 48 Well plate) (Corning Incorporated, NY, USA)

Multipoint pipettor with 8 channels aspiration manifold 20-200 μ L (Bio-Active., Ltd., Bangkok, Thailand)

pH Meter (Horiba compact pH meter B-212, Japan)

Scanning electron microscope (SEM, Camscan Mx2000, England)

Syringe pump (Model: NE-300, New Era Pump Systems Inc., NY, USA)

Texture analyzer (TA.XT plus, Stable Micro Systems, UK)

Tissue culture 96-well plates (Nunc, Denmark)

UV-Vis spectrophotometer (Agilent model 8453 E, Germany)

VertiSep® AQS C18 column (250 mm × 4.6 mm, 5 µm particle size)

Volumetric flask (Pyrex, USA)

Vortex mixer (Model: Labnet, USA)

X-ray powder diffractometer (model Miniflex II, Rigaku Co., Japan)

X-ray powder diffractometer (model Miniflex II, Rigaku Co., Japan)

3.3 Methods

3.3.1 Investigation of CS, CS derivatives and herbal oils for anti-candidal adhesion on denture acrylic resins

3.3.1.1 Antifungal activity of CS derivatives and herbal oils

3.3.1.1.1 Tested Solutions

The CS derivatives including CS-mandelate, CS-EDTA, CS-acetate and N-cinnamyl CS and two herbal oils i.e. betel oil and clove oil were used for antifungal and anti-candidal adhesion tests.

3.3.1.1.2 Preparation of CS solutions

The 2% (w/v) CS-salt solutions were prepared by dissolving 2 g CS with 2 g mandelic acid, 1g EDTA or 0.5% v/v acetic acid in 100 mL PBS (pH 7.4) to obtain CS-mandelate, CS-EDTA, CS-acetate, respectively. The 2% (w/v) N-cinnamyl CS solution was prepared by dissolving N-cinnamyl CS in PBS. All of the solutions were stirred until homogeneous solution were obtained.

3.3.1.1.3 Antifungal susceptibility testing

C. albicans ATCC 90028 was used. Stock culture was maintained on SDA and stored at 4°C during the experimental period. Candida suspension was diluted and spectrophotometrically (Perkin Elmer Lambda 2, Germany) standardized to 1×10^4 CFU/mL. *In vitro* antifungal susceptibility test of the Candida stains to the testing solutions (Chlorhexidine gluconate, CS mandelate, CS acetate, CS-EDTA, N-Cinnamyl CS, Betel oil and Clove oil were investigated. MICs

were determined by a broth microdilution technique in accordance with the guidelines recommended by CLSI (Clinical and Laboratory Standards Institute, 2002) using serial twofold dilutions of the testing solution in SDB medium. Chlorhexidine was used as positive control. Solvent and media controls are used for reference. Briefly, the *Candida* were incubated (10^4 CFU/ml) in 48 well-plates for 24 h at 37 °C and exposed to serial 2-fold dilution in SDB culture medium containing the testing solutions.

3.3.1.2 Anti-adhesion assay

3.3.1.2.1 Preparation of acrylic pieces

Self-polymerizing acrylic powder and monomer liquid were mixed in accordance with the manufacturer's instructions. After 2-3 min, the mixture was placed between two glass slides, 7 x 7 cm². The slides were secured at each end with clips, leaving a uniform distance of 0.4 mm between them. The acrylic was then polymerized at 50 °C for about 30 min. Subsequently, the transparent acrylic sheet formed was stripped from the slides and cut into 5 x 5 mm² pieces, the average thickness being 0.4 mm. The pieces were immersed in distilled water for 2 weeks to leach the excess monomer, then washed in running water for 3 h, sealed and sterilized in petri dishes until ready to use.

3.3.1.2.2 Adhesion assay

The adhesion assay was based on the method of Samaranayake and MacFarlane (Samaranayake and MacFarlane, 1980) with modifications. The acrylic pieces were pretreated with the CS derivative solutions or herbal oils (betel oil or clove oil) at MFC concentration for 30 min at room temperature. After washing with PBS, the acrylic pieces were placed in sterile 48-well plates. Approximately 400 µL of *Candida* suspension was added into the wells and then shaken at 100 rpm for 1 h at 37 °C. PBS and 0.2% chlorhexidine gluconate were used as negative and positive control, respectively. After incubation, the acrylic pieces were removed from the wells and subsequently washed three times by dipping in PBS. The metabolic activities of *Candida* on acrylic were determined using XTT reduction assay.

3.3.1.3 *In vitro* antibiofilm activity

Acrylic resins were individually placed in wells of 48-well microtiter plate. *Candida* cells in SDB medium (10^6 CFU/mL) were added to each well covering the acrylic resin. The plates were incubated at 37 °C for 24 h to allow the formation of biofilm. After incubation, each acrylic resin was washed several times with PBS to remove the unattached cells. Then, the acrylic pieces were soaked with the CS derivative solutions or herbal oils (betel oil or clove oil) for 24 h at 37 °C. The biofilm metabolic activity of *Candida* on acrylic surface after treatment with CS derivative solutions or herbal oils was determined using the 2, 3-bis- (2-methoxy-4-nitro-5-sulphophenyl)-5-[(phenylamino) carbonyl]-2H-tetrazolium hydroxide (XTT) reduction assay

3.3.1.4 Preparation of herbal oil-incorporated nanofiber mats

3.3.1.4.1 Fabrication of blank nanofiber mats

The polymer solutions were prepared by dissolution of PVP in 50:50 volume ratio of ethanol: water mixture at the concentration of 8% (by weight). After which, varied amounts of HP β CD (90-190 mM) were added to the polymer solutions. The polymer solutions were stirred using magnetic stirrer for several hours until homogenous solutions were obtained. The solutions were spun into nanofibers using electrospinning process at room temperature. In this process, the spinning solution was placed in a 5-ml glass syringe connected to a stainless-steel needle with a 0.9 mm inner diameter. The needle was connected to an emitting electrode with a positive polarity of a Gamma High Voltage Research device. The electrospinning process was conducted with a fixed applied voltage of 15 kV, a distance between the tip and the collector of 15 cm, and a feeding rate of 0.4 ml/h. The electrospun nanofibers were collected on an aluminum foil covered the rotating collector.

3.3.1.4.2 Fabrication of herbal oil-loaded nanofiber mats

To fabricate the herbal oil loaded nanofibers, betel oil or clove oil (20-40% weight to polymers) was added to the polymer solution containing 150 mM HP β CD. The mixtures were stirred for 24 h to allow incorporation of the oil into the HP β CD. After which, the mixtures were undergone electrospinning process as

previously mentioned to obtain the herbal oil loaded nanofiber mats. The contents of the oils from the betel oil loaded nanofiber mats and clove oil loaded nanofiber mats were determined to select the suitable quantity to be incorporated.

3.3.2 Fabrication of fast release-CZ loaded nanofiber mats

3.3.2.1 Solubility studies of CZ

The solubility of CZ in various solvents and release medium was determined using a shaken flask method. Excess CZ was added to a plastic microcentrifuge tube containing the selected vehicle and mixed using a vortex mixer. Mixtures were shaken for 24 h in an orbital shaking incubator maintained at 37 °C before being centrifuged at 10000 rpm for 10 min, and filtered through a 0.45 µm syringe driven membrane filter unit. The filtrates were subjected to the determination of dissolved drug using an HPLC with a detector operating at 215 nm and a C18 column with a C18 guard column. The elution was carried out using a solvent system composed of methanol and ammonium carbonate buffer solution (75:25) at 2 ml/min. The assay experiments were performed in triplicate.

3.3.2.2 Phase solubility studies

Phase solubility studies were performed according to the method described by Higuchi and Connors (Higuchi and Connors et al., 1965). Excess CZ was added in an aqueous solution or a solvent system containing EtOH: H₂O: BzOH at a 70:20:10 ratio (by volume) containing increasing amounts of HPβCD (30, 50, 70, 90, and 110, 130 and 150 mM) and the mixtures were agitated on a horizontal movement shaker at 37 °C until equilibrium was reached. After equilibrium, samples were collected and centrifuged, and their CZ content was quantified using HPLC. The experiments were carried out in triplicate.

3.3.2.3 Electrospinning of fast release-CZ loaded PVP/HPβCD nanofibers

EtOH, deionized water and BzOH were used as solvent. To determine the optimal amount of BzOH for the electrospinning process, 8% PVP and appropriate amount of HPβCD were dissolved in EtOH: H₂O: BzOH at the volume

ratios of 70:30:0, 70:25:5 and 70:20:10. After determining the optimal BzOH content, CZ (5%, 10%, 15% and 20%wt to polymer) was added to the mixture and stirred for 12 h at room temperature. The viscosity and conductivity of these mixed solutions were determined using a Brookfield viscometer and a conductivity meter, respectively. The spinning solution was placed in a 5-ml glass syringe connected to a stainless-steel needle with a 0.9 mm inner diameter. The needle was connected to an emitting electrode with a positive polarity of a Gamma High Voltage Research device. The electrospun nanofibers were collected on an aluminum foil covered the rotating collector. The electrospinning process was conducted at 25 °C, with a fixed applied voltage of 15 kV, a 15-cm distance between the tip and the collector, and a feeding rate of 0.3 ml/h. The electrospun nanofibers were collected on aluminum foil covering the rotating collector.

3.3.3 Fabrication of CZ loaded-mucoadhesive nanofiber mats.

3.3.3.1 CZ-microemulsion-containing nanofibers

3.3.3.1.1 Phase diagram construction

Pseudo-ternary phase diagrams were produced to obtain the concentration range of components for the existing range of microemulsions. The microemulsion systems consisted of oil, surfactant and cosurfactant. OA was used as the oil phase, Tween 80 (T80) was used as the surfactant and the cosurfactant was varied. BzOH, EtOH or IPA was used as the cosurfactant in F1, F2 and F3 (formulation), respectively. The weight ratio of surfactant to cosurfactant (S_{mix}) was 3:1. For each pseudo-ternary phase diagram at a specific S_{mix} weight ratio, the mixtures of oil and S_{mix} were prepared at the weight ratios of 10:0, 9:1, 8:2, 7:3, 6:4, 5:5, 6:4, 7:3, 8:2, 9:1 and 0:10. These mixtures were titrated dropwise with water under magnetic stirring. After being equilibrated, the systems were visually characterized. Transparent fluid systems were characterized as microemulsions.

3.3.3.1.2 Preparation of CZ-loaded microemulsion systems

Based on the generated pseudo-ternary phase diagrams, an oil: S_{mix} ratio was selected for the CZ-loaded microemulsion formulations. The selected

variables were the types of cosurfactant (BzOH, EtOH and IPA for F1, F2 and F3, respectively). Oil and S_{mix} were mixed vigorously under magnetic stirring, and CZ (25% w/w to oily phase) was added to this oily phase and mixed. Then, the mixtures were heated at 70°C until the CZ was completely dissolved. Both the physical and chemical stability of CZ in the formulation were determined by visual observation and HPLC analysis. Afterwards, water was incorporated for self-microemulsification. The particle size was determined immediately without dilution whereas zeta potential was determined by diluted with various USP buffer of pH 4, 7 and 9 using a Zetasizer Nano ZS (Malvern Instruments, Malvern, UK). All samples were measured in triplicate at room temperature.

3.3.3.1.3 Electrospinning process

2% w/v CS solution was prepared by dissolving CS and EDTA in distilled water at a weight ratio of 2:1. 10% w/v PVA solution was prepared by dissolving PVA in distilled water at 80 °C, and then the solution was stirred for 4 h. The CS-EDTA solution was mixed with a PVA solution at a weight ratio of 30:70 (Charernsriwilaiwat et al., 2013). The blended polymer solutions were mixed with CZ-loaded microemulsions at appropriate amount. The mixtures were stirred for 12 h at room temperature. The viscosity and conductivity of the mixed solutions were determined using a Brookfield viscometer and a conductivity meter, respectively. The spinning solution was placed in a 5-mL glass syringe connected to a stainless-steel needle with a 0.9 mm inner diameter. The needle was connected to the emitting electrode of positive polarity from a Gamma High Voltage Research device. The electrospinning process was conducted at 25 °C, with a fixed applied voltage of 15 kV, a 15-cm distance between the tip and the collector, and a feeding rate of 0.3 ml/h. The electrospun nanofibers were collected on aluminum foil covering the rotating collector.

3.3.3.2 CZ-incorporated mucoadhesive sandwich nanofibers

3.3.3.2.1 Fabrication of CZ-loaded PVP/HP β CD nanofibers

The CZ-loaded PVP/HP β CD nanofiber mats, used as the inner fiber, were fabricated by electrospinning as previously described. Briefly, 8% PVP

and an appropriate amount of HP β CD were dissolved in EtOH: H₂O: BzOH solvent mixture. CZ (20 wt% to polymer) was added into the mixture and stirred at room temperature for 12 h. The electrospinning process was performed at 25 °C with a fixed applied voltage of 15 kV. The distance between the tip and the collector was 15 cm, and the feeding rate was 0.4 mL/h.

3.3.3.2.2 Fabrication of CZ-incorporated mucoadhesive sandwich nanofibers

20% CZ-loaded PVP/HP β CD nanofibers were used as the inner fiber membrane. The inner fiber membranes were subsequently coated by electrospinning with a 2% CS-SH/EDTA and 10% PVA mixture or a 2% CS/EDTA and 10% PVA mixture (with a weight ratio of 30:70) for 3 h and 6 h, respectively. The electrospinning process was conducted at 25 °C at a fixed applied voltage of 15 kV. The distance between the tip and the collector was 15 cm, and the feeding rate was 0.3 ml/h.

3.3.4 Characterizations of nanofiber mats

3.3.4.1 Geometrical characterizations

The surface morphologies of the nanofiber mats were examined. The samples were attached to aluminium stubs with double side adhesive carbon tape then gold coated with a sputter coater and examined using a scanning electron microscope (Camscan Mx2000, England). The diameters of the nanofiber mats were measured by using image analysis software (JMicroVision V.1.2.7, Switzerland), collect 30 measurements for each sample.

The thermal behavior of the nanofiber mats was determined by differential scanning calorimeter (DSC, Pyris Sapphire DSC, PerkinElmer instrument, USA). Sample (2-4 mg) was placed in an aluminum pan and crimped with its cover to provide hermetically sealed samples. The heating rate was 10 °C/min. All measurements were obtained over 25-250 °C under nitrogen atmosphere.

The powder X-ray pattern of the nanofiber mats was recorded using an X-ray powder diffractometer (model miniflex II, Rigaku Co., Japan). Sample was irradiated with monochromatized CuK α radiation after passing through Nickel filters

and then was analyzed between 5° and 45° (2θ). The voltage and current applied were 30 kV and 15 mA, respectively.

The chemical structures of the fibers were characterized using a Fourier transform infrared spectrophotometer (FT-IR, Nicolet 4700, USA). The fiber samples were ground and pressed into KBr disc before being analyzed by the FT-IR analysis from $400\text{--}4000\text{ cm}^{-1}$

3.3.4.2 Mechanical characterizations

Tensile testing of the nanofiber mats was performed using a texture analyzer by applying a 5-kg load cell equipped with tensile grip holder. All samples were cut into rectangle shapes with dimensions of $25 \times 5\text{ mm}^2$.

3.3.4.3 *Ex vivo* mucoadhesion study

The *ex vivo* mucoadhesion studies of the CZ-incorporated mucoadhesive nanofibers were performed using a texture analyzer device equipped with a 5-kg load cell. The porcine cheek pouch was used as the model surface for bioadhesion testing. After the cheek pouch was excised and trimmed evenly, it was then washed in simulated salivary fluid (2.38 g Na_2HPO_4 , 0.19 g KH_2PO_4 , and 8 g of NaCl per liter of distilled water adjusted with the phosphoric acid to pH 6.8 ± 0.05) and then used immediately. The nanofiber mats were cut into circular shapes with a diameter of 13.7 cm^2 and were fixed to a cylindrical perspex support (diameter 2 cm; length 4 cm; surface area 3.14 cm^2) using double-side adhesive tape. The perspex support was then screwed onto the upper probe of the instrument. During the measurement, 500 μL of simulated salivary fluid was distributed onto the surface of the tissue. The probe was lowered at a speed of 2 mm s^{-1} to come in contact with the tissue at a force of 0.03 N for a contact time of 15 sec.

3.3.4.4 Content analysis

The total amounts of the herbal oil incorporated in the nanofiber mats were quantified in triplicate using UV-visible spectrophotometer (Agilent G1103A UV-Vis Spectrophotometer, Agilent Technologies, USA) at 279 nm. Accurately weighed samples (10 mg) of the fiber mats were dissolved in 1 mL of ethanol and

were continuously shaken in an incubator (Orbital Shaking Incubator Model: SI4) at 150 rpm for 24 h. The experiments were performed in triplicate.

Total CZ content of CZ in the CZ-loaded nanofibers mats was determined in triplicate using HPLC (Agilent Technologies, USA). Briefly, accurately weighed mats were submerged in methanol, and then placed for 24 h, in an incubator with continuous shaking (Orbital Shaking Incubator Model: SI4) at 150 rpm and 37 °C. The sample solutions were then filtered through 0.45 µm-nylon syringe filters prior to HPLC analysis.

The entrapment efficiency (%) and loading capacity (%) were calculated according to equations (1) and (2), respectively:

$$\% \text{ Entrapment efficiency} = \left(\frac{Pt}{Lt} \right) \times 100 \quad (1)$$

where Pt is the amount of herbal oil or CZ embedded in the nanofiber mats and Lt is the theoretical amount of CZ (from the feeding solution) incorporated into the nanofiber mats.

$$\text{Loading capacity} = \left(\frac{Pt}{Mt} \right) \quad (2)$$

where Pt is the amount of herbal oil or CZ embedded in the nanofiber mats and Mt is the weight of nanofiber mats.

3.3.4.5 *In vitro* release of CZ

The *in vitro* release studies of the herbal oil from the herbal oil loaded nanofibers were performed. Briefly, 10 mg of the herbal oil loaded nanofiber mats was placed in a 50-mL bottle containing 20 mL of artificial saliva (pH 6.8) that was incubated at 37°C and shaken at 150 rpm. To determine the amount of the oil released from the fiber mats after a given interval, an aliquot (1.0 ml) of the release medium solution was withdrawn and replaced with the same volume of fresh medium to maintain a constant volume. The amounts of oil in the sample solutions were analyzed by UV-visible spectrophotometer (Agilent G1103A UV-Vis Spectrophotometer, Agilent Technologies, USA). The experiments were conducted in triplicate.

The release characteristics of CZ from the nanofiber mats were investigated in a mixture solvent of 80% artificial saliva (2.38 g Na₂HPO₄, 0.19 g KH₂PO₄, and 8 g of NaCl per liter of distilled water adjusted with phosphoric acid to

a pH of 6.8 ± 0.05) and 20% PEG 400. The CZ incorporated nanofiber mats were placed in the medium that was incubated at $37\text{ }^{\circ}\text{C}$ under shaking at 150 rpm. After a given time, an aliquot of the release medium solution was withdrawn and analyzed by HPLC.

3.3.4.6 Evaluation of wetting time and disintegration time

The wetting time of the fast release-CZ loaded nanofiber mats was evaluated. Briefly, two layers of tissue paper were placed on a Petri dish with a diameter of 10 cm. The nanofiber mats were placed on the paper wetted with artificial saliva (2.38 g Na_2HPO_4 , 0.19 g KH_2PO_4 , and 8 g of NaCl per liter of distilled water adjusted with the phosphoric acid to pH 6.8 ± 0.05 , and the excess saliva was completely drained out. For the disintegration study, artificial saliva was used to evaluate the rate of dissolution of the nanofiber mats. The wetting and disintegration processes were recorded using a digital video recorder (Cannon, Japan).

3.3.4.7 Antifungal activity of the nanofiber mats

3.3.4.7.1 Susceptibility testing of CZ

The antifungal activity of the herbal oils and CZ was determined via susceptibility testing, and the results were expressed as the minimum inhibitory concentration (MIC) and minimum fungicidal concentration (MFC) toward *Candida* cells. A broth microdilution method was undertaken in accordance with the guidelines recommended by the CLSI (Clinical and Laboratory Standards Institute, 2002) using serial two-fold dilutions of the herbal oils and CZ in Sabouraud dextrose medium to determine susceptibility of the *C. albicans* toward the herbal oils and CZ. Briefly, *C. albicans* were incubated (10^4 CFU/ml) in 48-well plates for 24 h at $37\text{ }^{\circ}\text{C}$ before being exposed to serial 2-fold dilutions of the SDB culture medium with the the herbal oils or CZ solution (concentration ranging from 100 to $0.05\text{ }\mu\text{L/ml}$ for the herbal oil and from 200 to $0.4\text{ }\mu\text{g/ml}$ for CZ). The MIC was defined as the lowest concentration at which there is no visible growth by visual inspection. To establish the MFC, aliquots from the first 3 wells without visible growth by visual inspection were removed and inoculated in SDA for 48 h. The MFC value was defined as the lowest

concentration of the test solutions that exhibited no growth. All assays were performed in triplicate.

3.3.4.7.2 Time-kill analysis

The time kill analyses of the herbal oil loaded nanofiber mats were performed using SDB. Ten microliters of the adjusted inoculum suspension (approximately 1×10^6 CFU/ml) was dispensed into a plastic Eppendorf tube containing 1 mL of SDB, providing the starting inoculum of approximately 1×10^4 CFU/ml. The samples of the herbal oil loaded nanofiber mats with varied oil were incubated with *Candida* suspensions under agitation at 37°C. Similarly, the time kill analyses of the CZ loaded nanofiber mats were also determined by incubating the test organism with agitation in SDB medium containing different concentrations of CZ from nanofiber mats or lozenges (10 mg). The samples of nanofiber mats or CZ lozenges were added to a *Candida* suspension. Aliquots of control and CZ-containing media were removed and diluted at appropriate time interval before the surviving colonies were counted (CFU/ml) by spreading each sample onto an SDA agar plate. The plates were incubated for 24 h and the viable colonies were assessed. The kill curves were constructed by plotting the CFU/ml surviving at each time point in the presence and absence of the nanofiber mats or CZ lozenges.

3.3.4.8 Cytotoxicity test

The cytotoxicity of the nanofiber mats was evaluated using an MTT cytotoxicity assay. Human gingival fibroblast cells (HGF) obtained from explants of gingival tissue attached to non-carious, freshly extracted third molars from three patients were used. All patients gave informed consent before tissue collection. The HGF cells were plated in 100 μ l of Dulbecco's modified Eagle's medium (DMEM) supplemented with 10% FBS, 2 mM L-glutamine, 1% non-essential amino acids and 0.1% penicillin-streptomycin before being distributed at 10,000 cells/well in 96-well plates. The cells were grown under a humidified atmosphere (5% CO₂, 95% air, 37 °C) until confluency (typically 24 h). The tested nanofiber mats were sterilized using UV radiation for 1 h before being immersed in a serum-free medium (SFM; containing DMEM, 1% l-glutamine, 1% lactalbumin and 1% antibiotic and

antimycotic formulation) or direct contact with the cells. Then, the cells were re-incubated for 2 h and 24 h. After treatment, the extraction medium or the tested nanofiber mats were removed and subsequently washed with PBS. Finally, the cells were incubated with 100 μ l of an MTT-containing medium (1 mg/ml) for 4 h. The medium was removed, the cells were rinsed with a phosphate buffer (pH 7.4), and the formazan crystals that formed in the living cells were dissolved using 100 μ l DMSO per well. The relative viability (%) was calculated based on the absorbance at 550 nm determined using a microplate reader (Universal Microplate Analyzer, Model AOPUS01 and AI53601, Packard BioScience, CT, USA). The viability of non-treated control cells was arbitrarily defined as 100%.

$$\text{Relative cell viability (\%)} = \frac{[\text{OD550, sample} - \text{OD550, blank}]}{[\text{OD550, control} - \text{OD550, blank}]} \times 100 \quad (3)$$

3.3.4.9 *In vivo* mucoadhesion time and drug release evaluation

In vivo mucoadhesion time and drug release evaluation were performed with six healthy human volunteers. This study was approved by an Investigational Review Board (Human Studies Ethics Committee, Faculty of Pharmacy, Silpakorn University). Each volunteer randomly attached one nanofiber formulation on their buccal mucosa, the time required until the mat detaches from the buccal mucosa was recorded as *in vivo* mucoadhesion time. For the drug release evaluation, each volunteer randomly attached one nanofiber formulation on their buccal mucosa and 0.5-1 ml of saliva of each volunteer was collected at 5, 10, 15, 20, 25, and 30 min. An aliquot of the saliva at each time point was analyzed by HPLC.

3.3.5 Stability test

The stability test of the nanofiber mats was evaluated according to ICH guideline under accelerated condition (40 ± 2 °C and 75 ± 5 %RH) and long term condition (25 ± 2 °C and 60 ± 5 %RH) for 3 months. The morphology, diameter and content of the CZ-loaded nanofiber mats were observed after keeping for 1, and 3 months.

3.3.6 Statistical analysis

All experimental measurements were collected in triplicate. Data were expressed as mean \pm standard deviation (SD). Statistical significance of differences was examined using one-way analysis of variance (ANOVA) (SPSS version 16.0 for Windows (SPSS Inc., USA)).



CHAPTER 4

RESULTS AND DISCUSSION

- 4.1 Investigation of CS, CS derivatives and herbal oils for anti-candidal activity
 - 4.1.1 Antifungal activity of CS derivatives and herbal oils
 - 4.1.2 Anti-adhesion assay
 - 4.1.3 *In vitro* antibiofilm activity
 - 4.1.4 Preparation of herbal oil-incorporated nanofiber mats
 - 4.1.4.1 Fabrication of betel oil or clove oil loaded nanofibers
 - 4.1.4.2 FT-IR analysis
 - 4.1.4.3 Differential scanning calorimetry (DSC)
 - 4.1.4.4 Mechanical properties
 - 4.1.4.5 *In vitro* release
 - 4.1.4.6 Antifungal studies
 - 4.1.4.7 Cytotoxicity studies
- 4.2 Fabrication of fast release-CZ loaded nanofiber mats
 - 4.2.1 Solubility studies of CZ
 - 4.2.2 Phase solubility studies
 - 4.2.3 Electrospinning of fast dissolving-CZ loaded PVP/HP β CD nanofibers
 - 4.2.4 Characterization of PVP/HP β CD nanofiber mats
 - 4.2.4.1 FT-IR analysis
 - 4.2.4.2 Differential scanning calorimetry (DSC)
 - 4.2.4.3 X-ray diffractometry (XPRD)
 - 4.2.5 Drug content and loading capacity
 - 4.2.6 Wetting time and disintegration time
 - 4.2.7 *In vitro* release
 - 4.2.8 Antifungal studies
 - 4.2.9 Cytotoxicity evaluation
- 4.3 Fabrication of CZ loaded-mucoadhesive nanofiber mats.
 - 4.3.1 CZ-microemulsion-containing nanofibers

- 4.3.1.1 Phase diagram construction
- 4.3.1.2 Microemulsion evaluation
- 4.3.1.3 Fabrication of CZ-microemulsion-containing nanofibers
- 4.3.1.4 Characterization of CZ-microemulsion-containing nanofibers
 - 4.3.1.4.1 FT-IR analysis
 - 4.3.1.4.2 Differential scanning calorimetry (DSC)
 - 4.3.1.4.3 X-ray diffractometry (XPRD)
 - 4.3.1.4.4 Mechanical properties and ex vivo mucoadhesion studies
- 4.3.1.5 Drug content and loading capacity
- 4.3.1.6 *In vitro* release
- 4.3.1.7 Antifungal studies
- 4.3.1.8 Cytotoxicity evaluation
- 4.3.2 CZ-incorporated mucoadhesive sandwich nanofibers
 - 4.3.2.1 Morphology of the CZ-loaded sandwich nanofibers
 - 4.3.2.2 FT-IR analysis
 - 4.3.2.3 X-ray diffractometry (XPRD)
 - 4.3.2.4 Mechanical properties
 - 4.3.2.5 *Ex-vivo* mucoadhesion studies
 - 4.3.2.6 Drug content and loading capacity
 - 4.3.2.7 *In vitro* release
 - 4.3.2.8 Antifungal study
 - 4.3.2.9 Cytotoxicity evaluation
 - 4.3.2.10 *In vivo* mucoadhesion time and drug release evaluation
- 4.4 Stability test

4.1 Investigation of CS, CS derivatives and herbal oils for anti-candidal activity

4.1.1 Antifungal activity of CS derivatives and herbal oils

The antifungal activity of CS derivatives (CS-mandelate, CS-EDTA, CS-acetate and N-cinnamyl CS) and herbal oils (betel oil and clove oil) was evaluated against *C. albican* ATCC 90028 using broth microdilution assay, and the results are presented as MIC and MFC values as listed in Table 4.1. It can be seen from the results that CS derivatives exhibited mild anticandidal activity with the high MIC value of 5000 µg/mL except that of N-cinnamyl CS which showed a lower MIC value of 2500 µg/mL presenting the better anticandidal activity. However, the MIC value of N-cinnamyl CS was still too high. On the contrary, the herbal oils (betel oil and clove oil) demonstrated superior antifungal activity with the minimal MIC value. For further development for oral hygiene maintenance or oral candidiasis treatment, betel oil and clove oil appear to be the desirable compounds while the CS derivatives might not be appropriate to be used as an active compound in the formulation.

Table 4.1 MIC and MFC values of CS derivatives, betel oil and clove oil.

Tested compound	MIC	MFC
CS acetate	5,000 µg/mL	5,000 µg/mL
CS-EDTA	5,000 µg/mL	5,000 µg/mL
CS-Mandelate	5,000 µg/mL	10,000 µg/mL
N-cinnamyl CS	2,500 µg/mL	5,000 µg/mL
Betel oil	0.78125 µL/mL	0.78125 µL/mL
Clove oil	0.0488 µL/mL	0.0916 µL/mL

4.1.2 Anti-adhesion assay

The anti-adhesion assay was performed to evaluate the potential of the CS derivatives, betel oil and clove oil to protect the adhesion of the candida cells on the surface of acrylic resins. The results from anti-adhesion experiments are presented in Figure 4.1. All the tested compounds could significantly inhibit the adhesion of candida cell on the acrylic resin as compared to the control. Chlorhexidine which is used as a positive control exhibited the highest inhibition ability due to the prominent antimicrobial activity. The antiadhesion property of clove oil and betel oil seems to be slightly lower than that of chlorhexidine, however, no significant difference was

observed. The CS derivatives demonstrated less anti-adhesion property than chlorhexidine, clove oil and betel oil. This might be due to the inferior antifungal activity of CS derivatives compared with the herbal oil. This finding revealed that the herbal oil (betel oil and clove oil) may be the prospective candidates to be used in the formulation for oral hygiene maintenance.

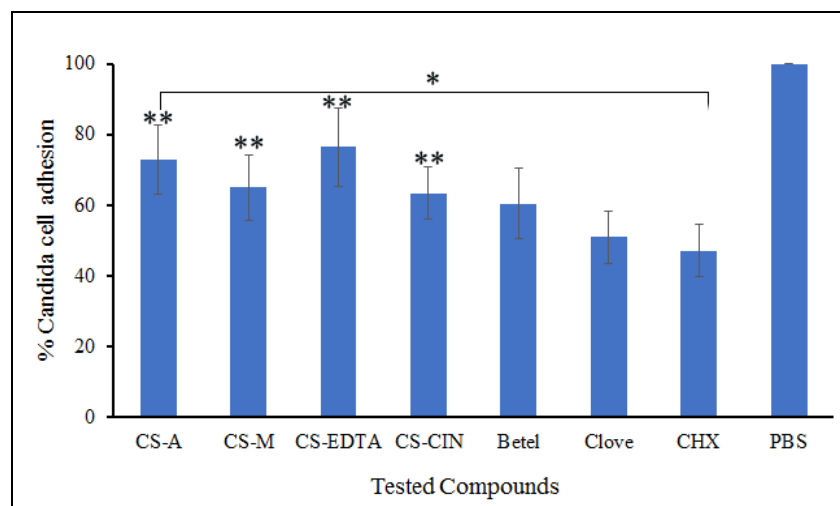


Figure 4.1 Anti-adhesion activities of CS-acetate (CS-A), CS-mandelate (CS-M), CS-EDTA, N-cinnamyl CS (CS-CIN), betel oil (Betel) and clove oil (Clove) against *C. albicans*. Chlorhexidine gluconate (CHX) and phosphate buffer saline (PBS) was used as positive control and negative control, respectively. *statistically different from the negative control. **statistically different from the positive control.

4.1.3 *In vitro* antibiofilm activity

The antibiofilm activity of the CS derivatives and herbal oils was carried out to investigate the ability of the CS derivatives and herbal oils to inhibit the growth and eradicate candida biofilm. In this study, the 24-h biofilm was allowed to form on the acrylic resins before incubating with the CS derivatives or herbal oils for 24 h. The results revealed the favorable antibiofilm activity of the CS derivatives and the herbal oils as shown in Figure 4.2. As expected, the tested compounds at 2xMIC concentration displayed greater antibiofilm activity than those at the lower concentration. Moreover, the antibiofilm activity of the CS derivatives and herbal oils

appeared to be concentration dependent. Although the CS derivatives displayed much higher MIC and MFC values compared with the herbal oils, the antibiofilm activity was comparable to the herbal oils at the fixed concentration of 1/2xMIC, 1xMIC and 2xMIC.

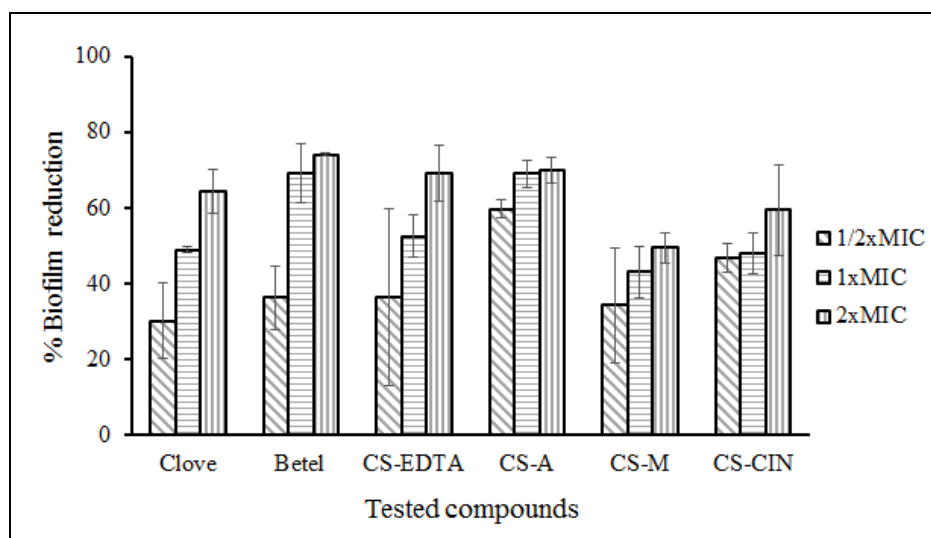


Figure 4.2 Anti-biofilm activities of clove oil (Clove), betel oil (Betel), CS-EDTA, CS-acetate (CS-A), CS-mandelate (CS-M) and N-cinnamyl CS (CS-CIN) against *C. albicans*.

4.1.4 Preparation of herbal oil-incorporated nanofiber mats

As it can be observed from the anticandidal activity of the betel oil and clove oil in the aforementioned experiments, clove oil and betel oil exhibited remarkable antifungal activity against *C. albicans*. Therefore, the herbal oils were selected to be incorporated into nanofibers for oral hygiene maintenance and oral candidiasis application. The incorporation of the herbal oil into the nanofibers could help improve the patient compliance due to more convenient to use. To obtain the nanofibers, the betel oil or clove oil was incorporated into the PVP nanofiber mats using electrospinning process with the assistance of CDs

4.1.4.1 Fabrication of betel oil or clove oil loaded nanofibers

The betel oil or clove oil loaded nanofibers were prepared by electrospinning process with the help of CDs. To fabricate the nanofibers, HP β CD at

various concentrations ranging from 90 to 190 mM was used to determine the optimal concentration for electrospinning. The HP β CD added in to the PVP solution could reduce the hygroscopic property of PVP. In addition, HP β CD could entrap the oil and increase its solubility (Tonglairoum et al., 2014). Figure 4.3 shows the SEM images of the PVP nanofiber mats containing different amount of HP β CD. The nanofiber mats had smooth surface without beads. Increasing the amounts of HP β CD resulted in the increase in diameters of the nanofiber mats. The diameters of the nanofibers containing 90 to 190 mM HP β CD were in range of 394.40 ± 45.17 to 496.07 ± 125.65 nm. The nanofiber mat with 150 mM HP β CD was selected for further investigation because this was the highest amount that can be loaded into the nanofibers with good physical textures.

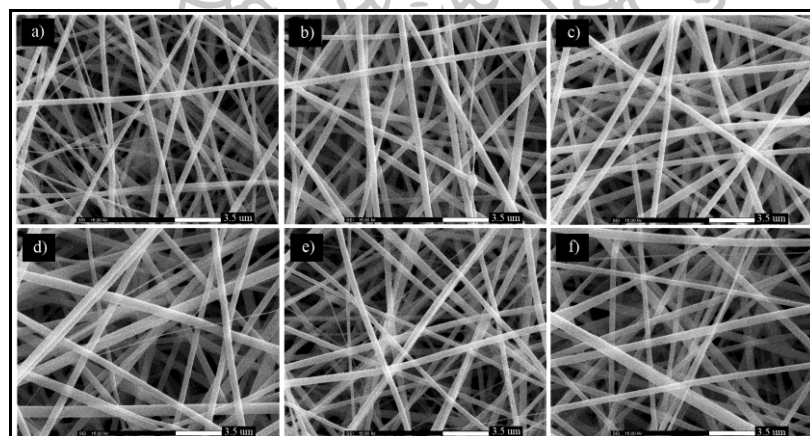


Figure 4.3 SEM images of 8% PVP nanofiber mats with different amounts of HP β CD a) 90 mM, b) 110 mM, c) 130 mM d) 150 mM e) 170 mM and f) 190 mM.

After the appropriate amount of HP β CD to be used was known, the amount of oils was varied from 20-40% weight to polymer. The 8% w/v PVP/150 mM HP β CD mixture solution containing various amounts of betel oil or clove oil (containing 20, 30 and 40% wt to polymer) was prepared and the betel oil or clove oil loaded nanofiber mats were successfully fabricated. The loading capacity of these betel oil or clove oil loaded nanofiber mats was determined and is presented in Figure 4.4. It can be seen from the results that after increasing the amount of oil from 20% to

30%, the loading capacity values increased. However, further increase in the initial amount of the oils from 30% to 40% had no significant effect on the loading capacity. On the other hand, the loading efficiency percentage decreased after increased the initial oil amount especially after the initial oil amount was increased from 30% to 40%. Therefore, the 30% betel oil loaded nanofiber mats and the 30% clove oil loaded nanofiber mats were selected for further investigation.

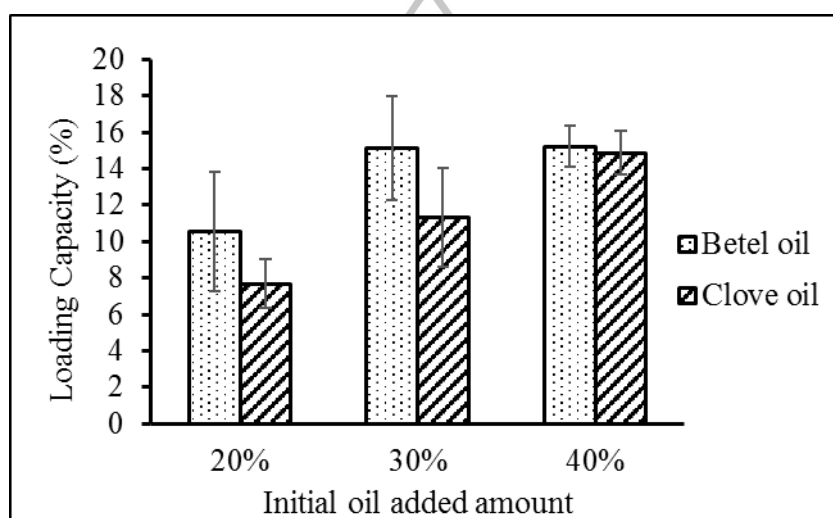


Figure 4.4 Loading capacity of (□) betel oil loaded nanofiber mats and (▨) clove oil loaded nanofiber mats containing 20, 30 and 40% of the oils loaded.

Table 4.2 The mechanical properties and loading capacity (%) of pure PVP/HP β CD nanofiber mats and betel oil and clove oil loaded nanofiber mats. Each value represents the mean \pm standard deviation from three independent experiments.

Nanofiber mats	Young's modulus (MPa)	Loading Efficiency (%)	Loading capacity (%)
PVP/HP β CD nanofiber mats	0.69 \pm 1.12	-	-
30% betel oil loaded mats	3.58 \pm 0.36	50.33 \pm 2.86	15.10 \pm 0.86
30% clove oil loaded mats	1.84 \pm 0.14	37.68 \pm 2.71	11.30 \pm 0.81

The increase in amount of the oil loading from 30% to 40% resulted in the decrease in the amount of betel oil or clove oil entrapped in the nanofiber mats. This may be due to the capacity of nanofiber mats that can carry the oils with the maximum amount at 30%. There were some variations in loading capacity between both oils. The results revealed that 30% betel oil loaded nanofibers showed higher loading capacity than 30% clove oil loaded nanofibers (Table 4.2). This may be due to the difference in composition and properties of these oils (Ferrerres et al., 2014; Rana et al., 2011). Thus, 30% betel oil and 30% clove oil were selected to be incorporated into the nanofiber mats for further investigations.

The SEM images of the blank PVP/HP β CD, 30 % betel oil-loaded and 30 % clove oil-loaded nanofiber mats are illustrated in Figure 4.5. The SEM images revealed the bead-free and smooth fibers without delamination or phase separation of the oils from the nanofiber mats which confirmed the interaction of the oil with the polymer. The addition of the oils into the nanofiber reduced the fiber diameters. The HP β CD added into the polymer solution could entrap the oil into it and help protect the polymer from deliquescent (Tonglairoum et al., 2014). The diameters of the oil-loaded fibers were in the range of 396.56 ± 65.31 to 425.89 ± 82.28 nm.

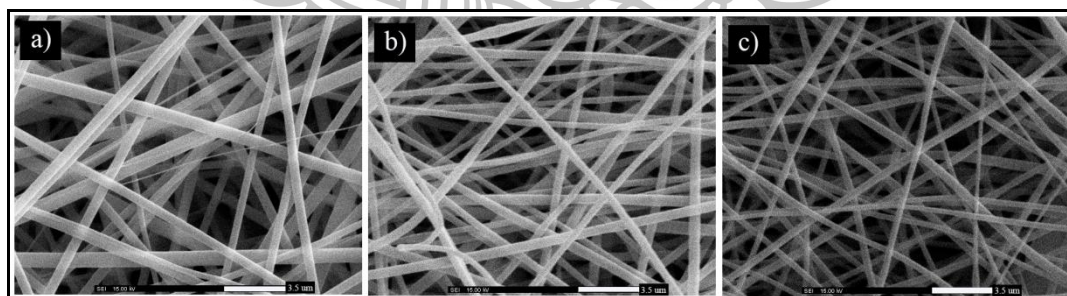


Figure 4.5 SEM images of a) 8% PVP/150 mM HP β CD nanofiber mats b) 8% PVP/150 mM HP β CD nanofiber mats loaded with 30% betel oil c) 8% PVP/150 mM HP β CD nanofiber mats loaded with 30% clove oil.

4.1.4.2 FT-IR analysis

The FTIR spectra of PVP, HP β CD, betel oil, clove oil, PVP/HP β CD nanofiber mats, betel oil loaded nanofiber mats and clove oil loaded nanofiber mats are shown in Figure 4.6. The spectrum of PVP presented the peaks at 3452.2, 2926.5,

1663.4, 1415.7 and 1290.1 cm^{-1} that were attributed to N-H, CH_2 , C=O, C-N stretching vibration and C-H bending, respectively (Basha, 2010). The peaks at 3423.7, 2915.4, 1167.8 and 1083.7 of the HP β CD spectrum corresponded to O-H, C-H, C-H and C-O stretching vibrations, respectively (Al-Zein et al., 2011). The pure PVP/HP β CD nanofiber mats exhibited absorption peaks as observed in the spectra of PVP and HP β CD. The spectrum of betel oil and clove oil exhibited absorption peaks at 3514.0, 3077.1, 2932.3 cm^{-1} that were attributed to O-H, =C-H, and C-H stretching, respectively. The bands at 1602.4 and 1510.8 corresponded to aromatic C=C stretching. The spectrum of betel oil and clove oil loaded nanofiber mats displayed all features of the peaks that were observed in the spectrum of PVP/HP β CD, betel oil and clove oil. It seems to be the evidence for the present of the herbal oil in the nanofiber mats. Especially the bands of aromatic C=C stretching of the betel oil and clove oil spectra that were generally not observed in the spectrum of PVP/HP β CD were found in the spectrum of betel oil and clove oil loaded nanofiber mats.

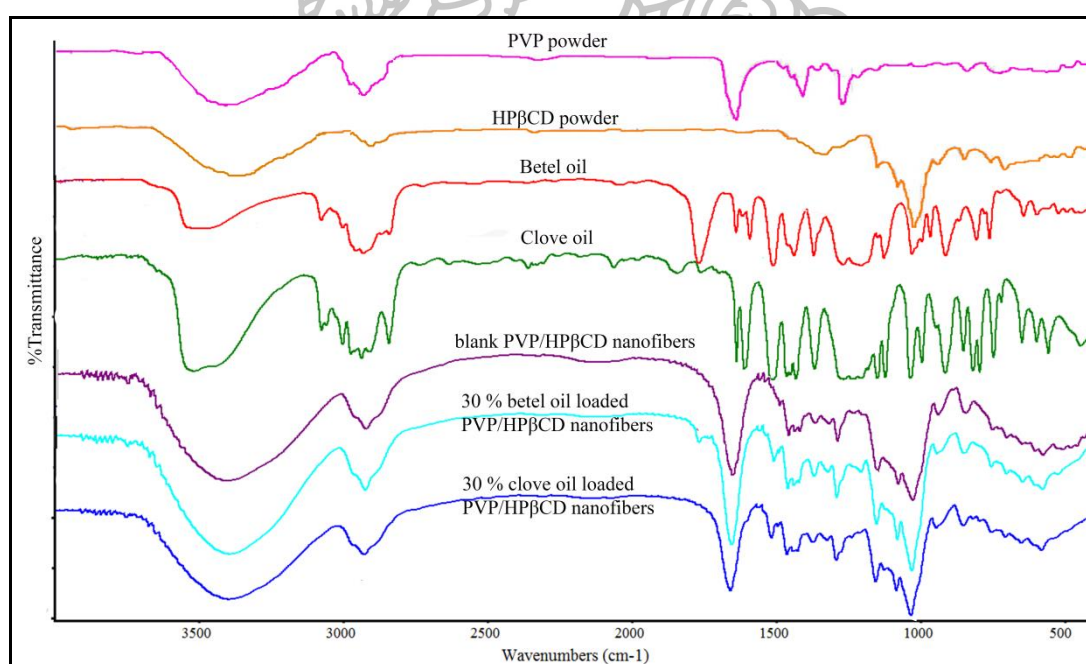


Figure 4.6 FT-IR spectra of blank PVP/HP β CD nanofiber mats, pure betel oil, pure clove oil and the herbal oil loaded nanofiber mats.

4.1.4.3 Differential scanning calorimetry (DSC)

DSC studies were carried out to investigate the thermal behavior of the betel oil and clove oil in the electrospun nanofiber mats, and the thermograms are displayed in Figure 4.7. Pure betel oil and pure clove oil exhibited endothermic peaks related to the process of evaporation at 216.1 and 233.4 °C, respectively. The thermograms of the blank-nanofiber mats and the betel oil or clove oil loaded nanofiber mats were quite similar. This indicated that the incorporation of betel oil and clove oil into the nanofiber mats did not affect the thermal properties of the nanofiber mats.

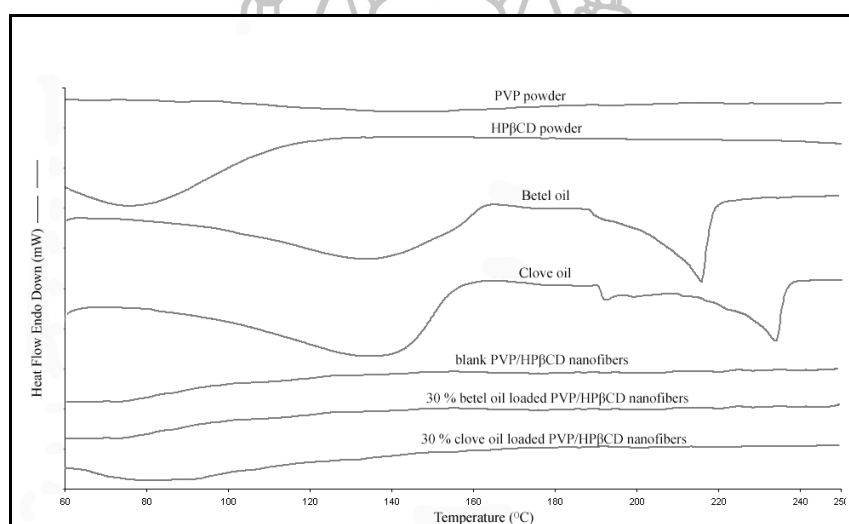


Figure 4.7 DSC thermograms of (a) pure betel oil, (b) pure clove oil, (c) blank PVP/HP β CD nanofibers, (d) betel oil loaded PVP/HP β CD nanofibers and (e) clove oil loaded PVP/HP β CD nanofibers.

4.1.4.4 Mechanical properties

The mechanical properties in terms of Young's modulus of the PVP/HP β CD nanofiber mats with and without the herbal oils loading were determined using a texture analyzer, and the results are displayed in Table 4.2. The Young's modulus values of all tested nanofiber mats were in the range of 0.69-3.58 MPa. Adding the oil into nanofiber did not have negative effect on the tensile strength of the nanofiber mats, but it improved the mechanical properties of the mats. The 30% betel oil loaded nanofiber mats demonstrated the highest value of Young's modulus.

4.1.4.5 *In vitro* release

The release characteristics of the herbal oil loaded nanofiber mats are presented in Figure 4.8. It is clearly observed from the release profiles that both betel oil and clove oil displayed very fast release from the nanofiber mats followed by gradual release. Almost 100% of the betel and clove oil that was incorporated in the nanofiber mats released to the release medium within 1 min. This is due to the very fast dissolving property of PVP polymer. The betel oil loaded nanofiber mats and the clove oil loaded nanofiber mats exhibited quite similar release patterns except that the betel oil loaded nanofiber mats had faster release rate in the initial period. This might be due to the high loading amount of betel oil in the nanofiber mats.

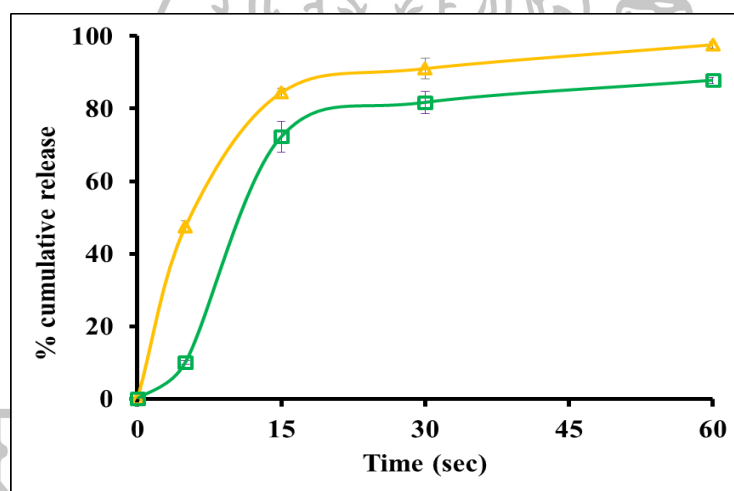


Figure 4.8 Release profile of (Δ) betel oil and (\square) clove oil from the PVP/HP β CD nanofiber mats. The data are expressed as mean \pm standard deviation from three independent experiments.

4.1.4.6 Antifungal studies

The susceptibility testing of betel oil and clove oil was performed using a broth dilution assay to determine MIC and MFC values against *C. albicans* ATCC 90028. Betel oil and clove oil were strongly active against *C. albicans* with MIC values of 0.781 and 0.049 μ g/ml and the MFC values of 0.781 and 0.092 μ g/ml, respectively.

Time-kill analyses were performed to evaluate the antifungal activity of the herbal oil loaded nanofiber mats by determining the exposure time required to kill standardized microbial inoculums. The time-kill plots of nanofiber mats containing betel oil or clove oil and the control sample are displayed in Figure 4.9. As compare to the control sample, the nanofiber mats loaded with betel oil or clove oil could inhibit the growth of candida cell after contact with only few minutes. The betel oil loaded nanofibers started inhibiting the Candida cells since 5 min after contact. The very fast dissolving property of PVP polymer resulted in very fast release of the oils from the nanofiber mats and inhibited the Candida cells. Previous study reported that the rapid wetting/disintegration of the PVP/HP β CD nanofibers leading to free CZ rapidly released from the mats and faster antifungal activity. In addition, the betel oil loaded nanofiber mats exhibited rapid antifungal activity and displayed significantly faster antifungal activity at 30 to 120 min after contact compared to the clove oil loaded nanofiber mats. These results might be due to the greater amount of the betel oil contained in the nanofiber mats with approximately 3 times higher than that of clove oil.

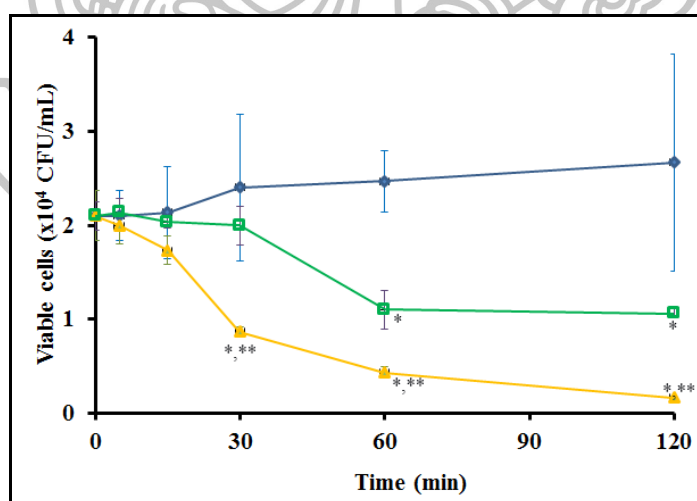


Figure 4.9 Time-kill plots of *C. albicans* ATCC 90028 versus the treatment time: (\diamond) control, (\triangle) 30 % betel oil loaded nanofiber mats and (\square) 30 % clove oil loaded nanofiber mats. The data are expressed as mean \pm standard deviation from three independent experiments. * Statistically

significant ($P < 0.05$) from control. ** Statistically significant ($P < 0.05$) from clove oil loaded nanofiber mats.

4.1.4.7 Cytotoxicity studies

The *in vitro* cytotoxicity of the blank nanofiber mats and herbal oil loaded nanofiber mats were determined using MTT assay. This investigation was performed to evaluate the biocompatibility of the prepared systems and their potential application for oral candidiasis. The cytotoxicity of the prepared systems was assessed at various concentrations (0.0001 mg/mL to 10 mg/mL). The results from the test are illustrated in Figure 4.10. Figure 4.10a and 4.10b show the cell viabilities of the extraction medium from blank nanofiber mats and herbal oil loaded nanofiber mats at the mats concentrations from 0.0001 to 10 mg/ml after incubation at pH 7.4 for 2 h and 24 h, respectively, against the HGF cells. There was a significant decrease in the cell viability when the HGF cells were incubated with high concentration of the herbal oil loaded mats (1-10 mg/ml) compared to the control ($p < 0.05$). This finding might be because the amount of herbal oil was too high and were toxic to fibroblast cells. However, the clove oil loaded nanofiber mats were safe for use at the concentration of 0.0001 to 1 mg/mL for 2 h and at 0.0001 to 0.1 mg/mL for 24 h. On the other hand, the betel oil loaded nanofiber mats exhibit higher toxicity due to the higher oil loading. They were safe for use at the concentration of 0.001 to 0.1 mg/mL for 2 and 24 h. In fact, the nanofiber mats are fast-dissolving and would be contacted with the mouth for only few minutes. This could help reduce the toxicity of the herbal oils against the oral cells.

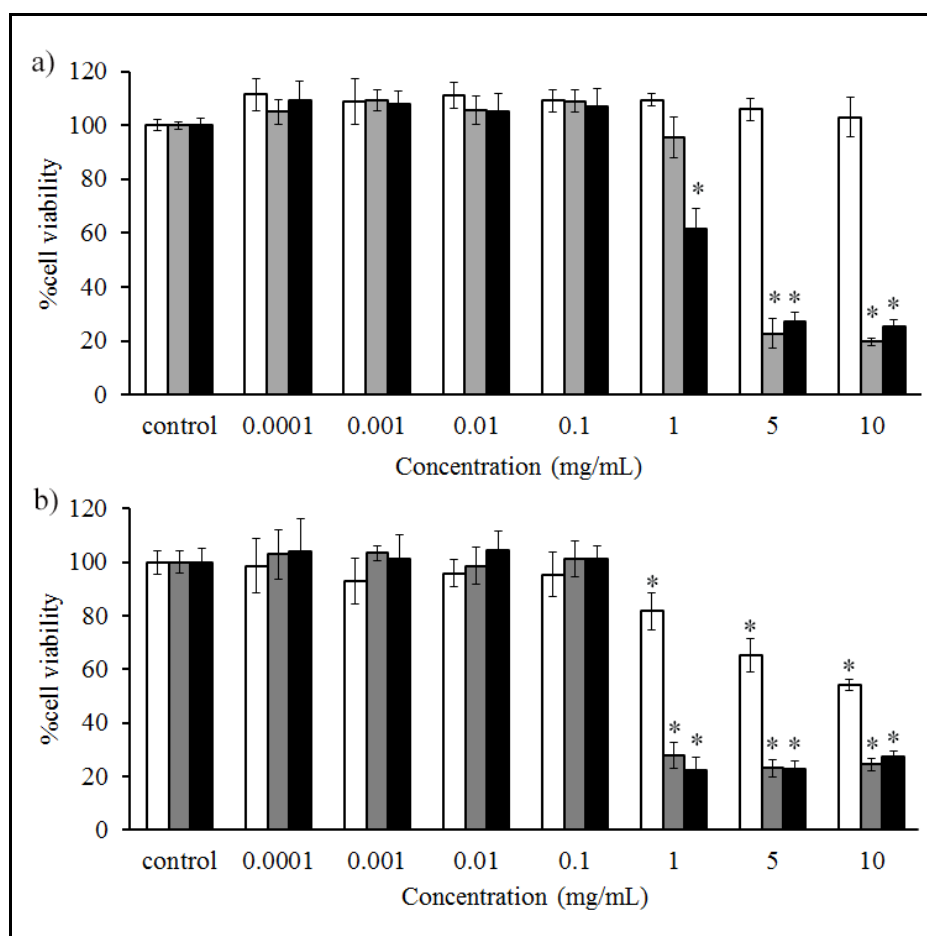


Figure 4.10 *In vitro* cytotoxicity of (□) blank nanofiber mats, (▒) clove oil loaded nanofiber mats, and (■) betel oil loaded nanofiber mats against HGF cells after incubation for a) 2 h and b) 24 h. * Statistically significant ($P < 0.05$) from control.

4.2 Fabrication of fast release-CZ loaded nanofiber mats

4.2.1 CZ Solubility

The solubility of CZ was carried out in H_2O , EtOH, BzOH, a solvent mixture (EtOH: H_2O : BzOH at volume ratio of 70: 20: 10) and a solvent mixture of artificial saliva pH 6.8: PEG 400 with volume ratio of 80:20 as presented in Table 4.3. CZ exhibited very poor solubility in water ($0.40 \pm 0.21 \mu\text{g/ml}$). This result was similar to a previous study revealing that the solubility of CZ in water was $0.49 \mu\text{g/ml}$ (Hoogerheide and Wyka, 1982). CZ appeared to have good solubility in ethanol ($128.15 \pm 12.43 \text{ mg/ml}$) and very good solubility in BzOH ($646.36 \pm 66.12 \text{ mg/ml}$).

Therefore, BzOH and EtOH were chosen as the solvent mixture for electrospinning the CZ-loaded PVP/HP β CD nanofiber mats.

4.2.2 Phase solubility study

The phase solubility study might be a beneficial method for examining inclusion complexation because it enhances the solubility ability and the apparent stability constant of the complexes (Higuchi and Kristiansen, 1980). Therefore, the inclusion complexation of CZ and HP β CD was assessed via phase solubility study. The phase solubility diagram for the CZ and CDs systems in aqueous, and EtOH:H₂O:BzOH (70:20:10 by volume) solvent systems at 37°C are depicted in Figure 4.11. The inclusion complex displayed a different pattern in the aqueous solution (Figure. 4.11a) and EtOH:H₂O:BzOH solvent system (Figure. 4.11b). In the aqueous solution, the solubility of CZ increased linearly with the HP β CD concentration; therefore, it formed an A_L type inclusion complex indicating the complex had a 1:1 ratio. In contrast, the solubility of CZ in the EtOH:H₂O:BzOH (70:20:10) solvent system did not increase linearly as a linear function of HP β CD concentration and thus was identified as a B_s type inclusion complex indicating the formation of a 1:2 complex. CZ was most soluble in the solvent system at 50 mM HP β CD.

Table 4.3 Solubility of CZ in various solvents. Each value represents the mean \pm standard deviation from three independent experiments.

Test solvent	Solubility (mg/ml)
Water	0.000402 \pm 0.00021
Ethanol	128.15 \pm 12.43
Benzyl alcohol	646.36 \pm 66.12
Solvent mixture of EtOH: H ₂ O: BzOH with volume ratio of 70:20:10	265.23 \pm 17.37
Solvent mixture of artificial saliva pH 6.8: PEG 400 with volume ratio of 80:20 (release medium)	0.339 \pm 0.033

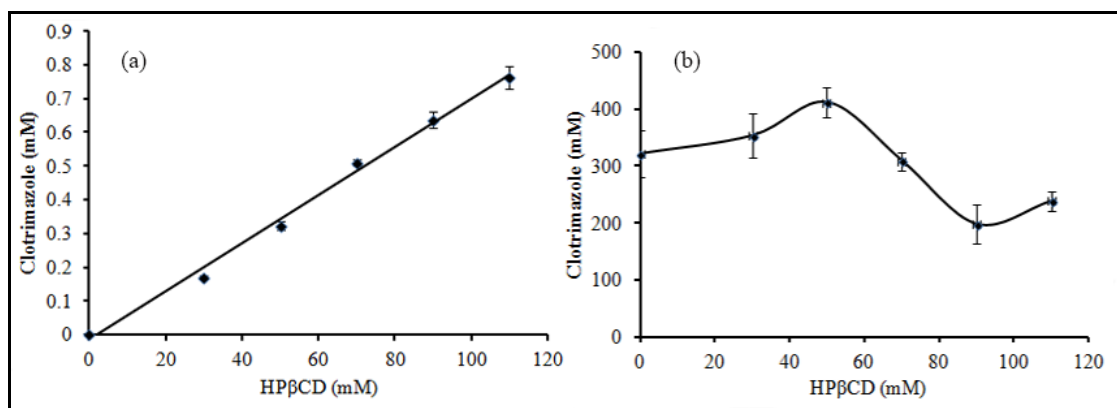


Figure 4.11 Phase solubility diagram for CZ and CDs system at 37°C; a) in aqueous solution, b) in solvent system of EtOH:H₂O:BzOH with a volume ratio of 70:20:10.

4.2.3 Electrospinning of PVP/HPβCD nanofiber mats

The CZ-loaded PVP/HPβCD was electrospun in various EtOH:H₂O:BzOH ratios (70:30:0, 70:25:5 and 70:20:10 v/v). The solution parameters before electrospinning are listed in Table 4.4. The amount of BzOH added to the solution affected the morphology of the nanofiber mats, as illustrated in Figure 4.12. Increasing in the BzOH content in the mixture resulted in a lowered bead-on-string content; in addition, the fiber became more uniform and grew in diameter due to the enhanced viscosity of the solution. These results were in accordance with a previous study revealing that beaded nanofibers were created from an electrospinning solution with a lower viscosity (Shenoy et al., 2005; Uslu et al, 2010). By increasing the BzOH content to 5% v/v, the number of beads was reduced, and the fibers became more uniform; however, the fiber diameter increased due to the dramatical increase in solution viscosity and the decrease in conductivity (Table 4.4). However, the viscosity and conductivity were not significantly different when the BzOH content was increased from 5% to 10% v/v. Therefore, the increase in fiber diameter was not significant. The average fiber diameters of nanofibers that were electrospun from solutions containing 0%, 5% and 10% v/v BzOH content were 471, 663 and 665 nm, respectively. Nevertheless, the fibers became more uniform when BzOH content was increased to 10% because the solvent evaporated more slowly during the

electrospinning process, and more CZ content could be dissolved. When the BzOH content was increased to 15%, the nanofibers could not be formed because the solvent did not evaporate. Therefore, an EtOH:H₂O:BzOH ratio of 70:20:10 was optimal for further experiment. Additionally, electrospinning of PVP/HP β CD solutions containing various CZ content (containing 0, 5, 10, 15 and 20% wt CZ relative to the to polymer) was carried out from EtOH:H₂O:BzOH (70:20:10). By increasing the CZ content, the viscosity and conductivity of the solution were increased but these did not affect the diameter of the nanofiber mats (Figure 4.12). The average diameters of nanofibers electrospun from solutions with 0, 5, 10, 15 and 20% wt CZ relative to the polymer were 665, 663, 667, 657 and 645 nm, respectively. Therefore, large amounts of CZ were incorporated into the nanofiber mats without affecting fiber diameter.

Table 4.4 Solution parameters before electrospinning of spinning solution containing various ratios of mixture solvent and different amount of CZ. Each value represents the mean \pm standard deviation from three independent experiments.

Solvency ratio (EtOH:H ₂ O:BzOH)	CZ content	Viscosity (cP)	Conductivity (μ S)	Surface tension (mN/m)
70:30:00	0%	216.80 \pm 0.69	4.47 \pm 0.75	28.39 \pm 0.74
70:25:05	0%	224.40 \pm 1.04	2.13 \pm 0.42	28.47 \pm 0.68
70:20:10	0%	228.13 \pm 2.37	1.40 \pm 0.26	29.40 \pm 0.25
70:20:10	5%	216.33 \pm 3.65	2.67 \pm 0.15	29.34 \pm 0.10
70:20:10	10%	219.80 \pm 2.62	3.17 \pm 0.31	29.12 \pm 0.14
70:20:10	15%	225.83 \pm 4.08	3.73 \pm 0.32	29.68 \pm 0.17
70:20:10	20%	230.47 \pm 2.15	3.87 \pm 0.12	29.39 \pm 0.17

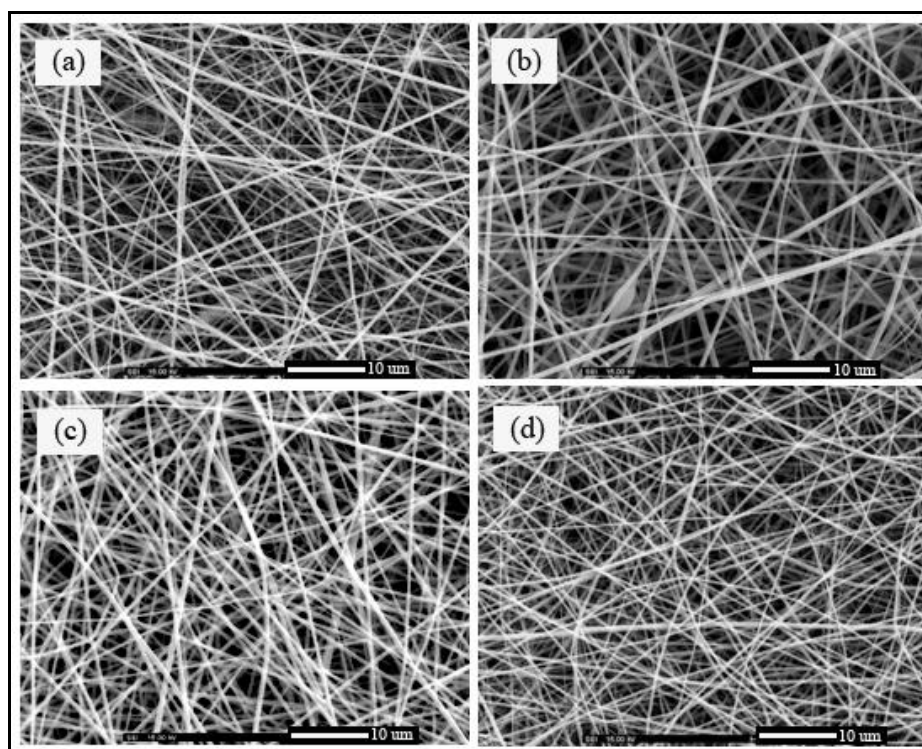


Figure 4.12 The SEM image (1,000x) and diameter distribution of the PVP/HP β CD nanofiber mats electrospun from EtOH:H₂O:BzOH solvent system ratio of 70:20:10 with a different CZ loading amount; a) 5, b) 10, c) 15 and d) 20%wt CZ to polymer.

4.2.4 Characterization of PVP/HP β CD nanofiber mats

4.2.4.1 FT-IR analysis

The FTIR spectra of the CZ powder, the blank nanofiber mats and 5-20% CZ-loaded nanofiber mats are displayed in Figure 4.13. The spectrum of the blank PVP/HP β CD nanofibers mats exhibited absorption peaks at 3380.6, 2941 and 1093.1 cm^{-1} that were attributed to stretching vibrations of NH, OH, CH and CO stretching vibration respectively. The pure CZ powder exhibits dominant absorption peaks at 1586.7, 1490.7, and 1304.9 cm^{-1} that correspond to the benzene ring stretches. The bands at 904.7, 823.68, and 744.59 cm^{-1} are assigned to the C-H stretches. The bands 1081.4 cm^{-1} and 1210.1 cm^{-1} correspond to the chlorobenzene and C-N stretching, respectively. The peaks observed in the CZ powder spectrum

were also observed in spectra of the 5-20% CZ-loaded nanofiber mats. Therefore, CZ was incorporated into the nanofiber mats.

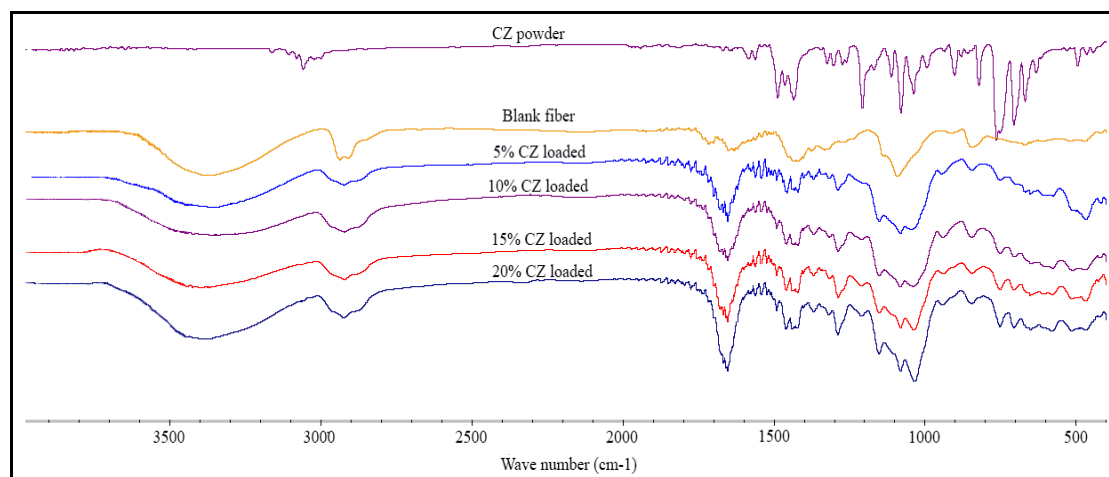


Figure 4.13 FT-IR spectra of the pure CZ powder and PVP/HP β CD nanofiber mats with different amount of CZ (0, 5, 10, 15, 20% wt CZ to polymer).

4.2.4.2 Differential scanning calorimetry (DSC)

DSC studies were undertaken to evaluate the physical state of CZ in the electrospun nanofiber mats, and the thermograms are displayed in Figure 4.14. The thermogram of the CZ powder exhibited an endothermic sharp peak at 145.13 °C due to its melting temperature. A peak in the endothermic curve of the pure nanofiber mat (0% CZ) was also observed at 167.38 °C. The melting points slightly increased to 173.59, 177.12, 178.12 and 186.49 °C when the concentrations of CZ were 5, 10, 15 and 20%, respectively. The melting point of CZ was lower than the melting points of the PVP/HP β CD nanofiber mats, indicating that loading the CZ into the nanofiber mats does not affect their thermal behavior. Moreover, the absence of a detectable crystalline domain at a high CZ content, indicated that CZ was incorporated into PVP/HP β CD nanofiber mats in an amorphous state.

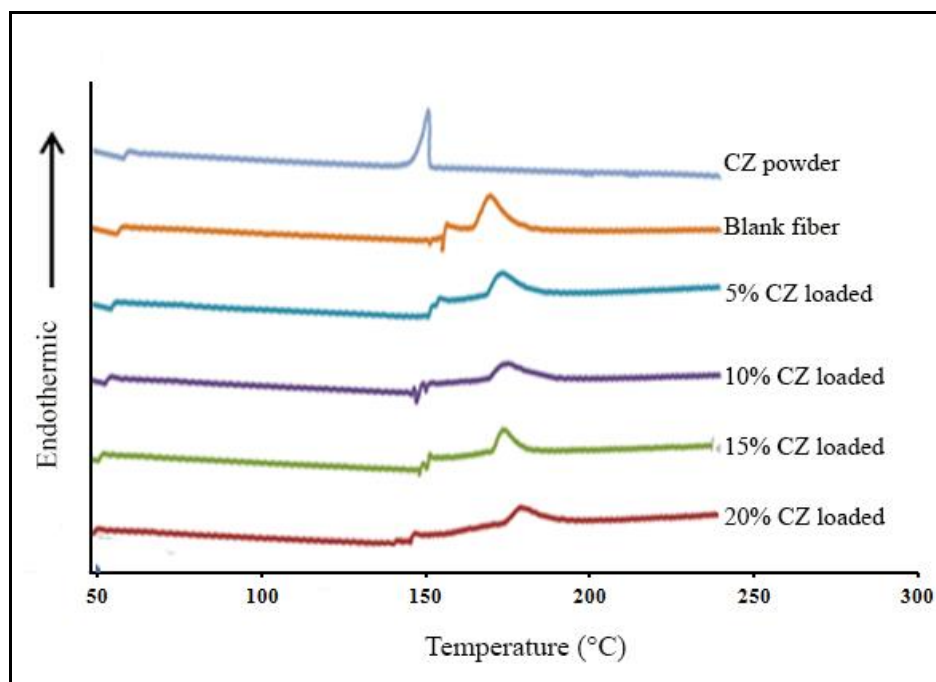


Figure 4.14 DSC thermogram of the pure CZ powder and PVP/HP β CD nanofiber mats with different amount of CZ (0, 5, 10, 15, 20% wt CZ to polymer).

4.2.4.3 X-ray diffractometry (XPRD)

The powder X-ray diffraction patterns of the CZ powder, blank nanofiber mats and 5-20% CZ-loaded nanofiber mats are presented in Figure 4.15. The diffractogram of the CZ powder displayed strong crystalline peaks, indicating its high degree of crystallinity. However, no such peak was found in the diffractograms of the blank or 5-20% CZ-loaded nanofiber mats, indicating that CZ was incorporated into PVP/HP β CD nanofiber mats in an amorphous state.

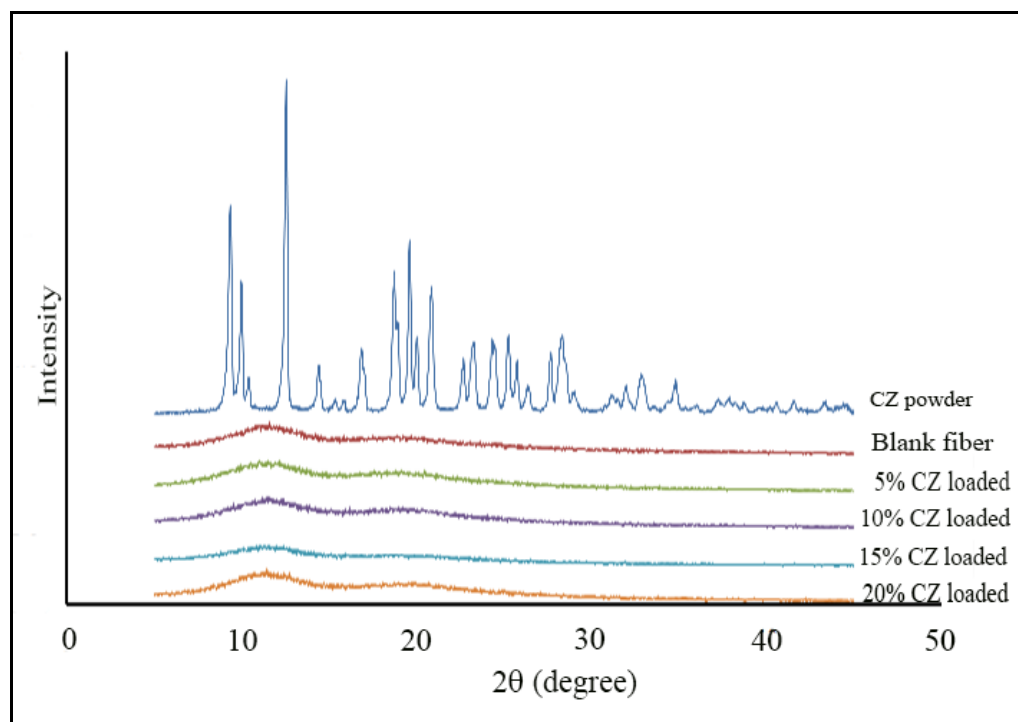


Figure 4.15 X-ray diffraction pattern of the pure CZ powder and PVP/HP β CD nanofiber mats with different amount of CZ (0, 5, 10, 15, 20% wt CZ to polymer).

4.2.5 Drug content and loading capacity

Various amounts of CZ (0, 5, 10, 15, 20 %wt to polymer) were incorporated in PVP/HP β CD nanofiber mats. The entrapment efficiency (% EE) and loading capacity for CZ in the PVP/HP β CD nanofiber mats are listed in Table 4.5. The entrapment efficiency of CZ in the nanofiber mats was 92.60-96.85%, revealing efficient incorporation of CZ into the nanofiber mats. Increasing of the initial amount of CZ caused an overall increase in the amount of CZ entrapped in the nanofiber mats. The loading capacity for CZ in the nanofiber mats increased from 0.046 to 0.161 mg/mg of nanofiber when the initial amount of CZ increased from 5% to 20% wt to polymer.

Table 4.5 The entrapment efficiency (%) and loading capacity (%) of CZ in PVP/HP β CD nanofiber mats. Each value represents the mean \pm standard deviation from three independent experiments.

Amount of CZ in nanofiber mats (% wt to polymer)	Entrapment efficiency (%)	Loading capacity (%)
5%	95.77 \pm 1.43	4.6 \pm 0.70
10%	92.60 \pm 2.52	8.4 \pm 0.22
15%	96.52 \pm 5.26	12.6 \pm 0.69
20%	96.85 \pm 4.51	16.1 \pm 0.75

4.2.6 Wetting time and disintegration time

The wetting time was investigated using a wet tissue paper to mimic the moisture available in the mouth. The 0-20% CZ-loaded nanofiber mats were completely wetted, and lost their original white color within a matter of seconds after absorbing water from the wet paper as displayed in Table 4.6. The wetting time of the nanofiber mats were approximate 3 s. After placing the 0-20% CZ-loaded mats in a glass of artificial saliva, they sank quickly in it, as illustrated in Table 4.7. The mats quickly lost their original white color, and disappeared. The disintegration or dissolution times of the mats containing 0-15% CZ were approximate 1 s. Therefore, electrospun nanofibers possessing extremely high porous structure allowed rapid penetration of saliva into the pores when placed in the oral cavity; thus, they showed rapid wetting and disintegration time which reflected the short time required to release of the drug. However, the mats containing 20% CZ showed different disintegration process. They floated on the surface, lost their original white color, and then disintegrated into small pieces spreading throughout the medium; these reveal that high CZ content affected the dissolution of the mat due to the low solubility of CZ.

Table 4.6 Wetting of the nanofiber mats containing 0-20% CZ.

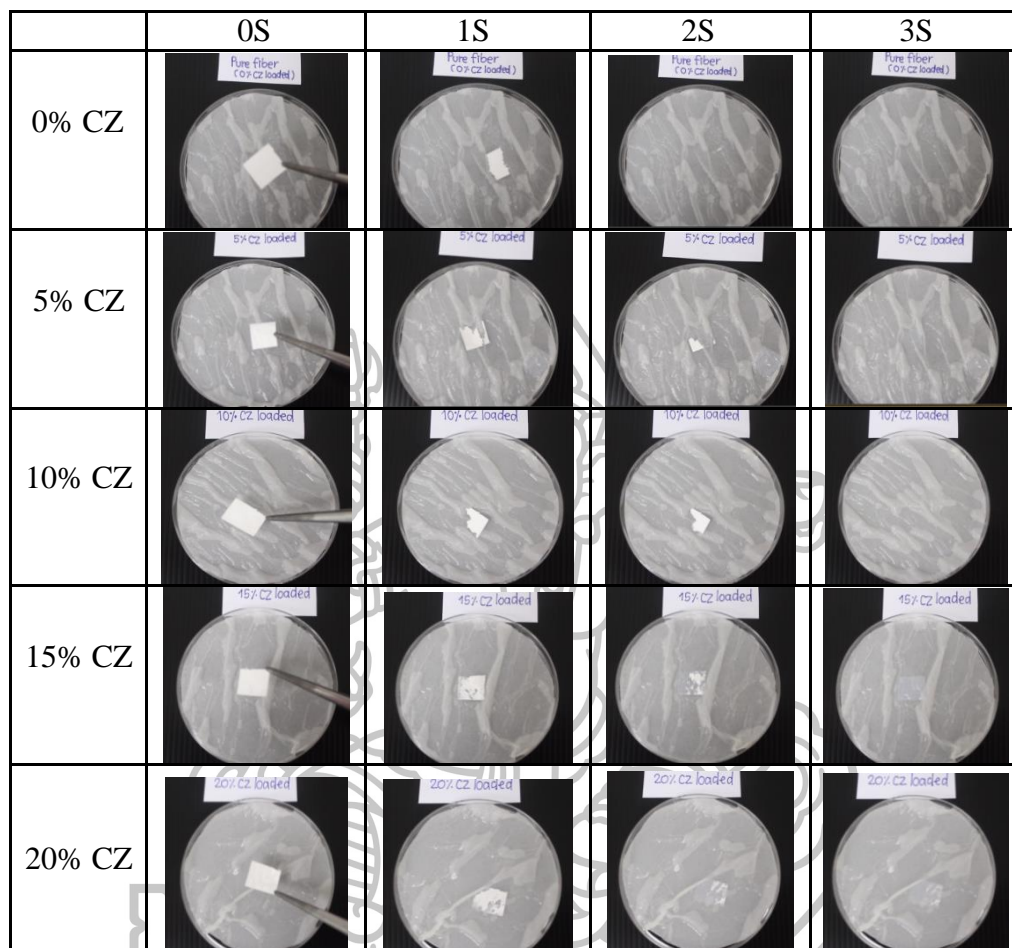
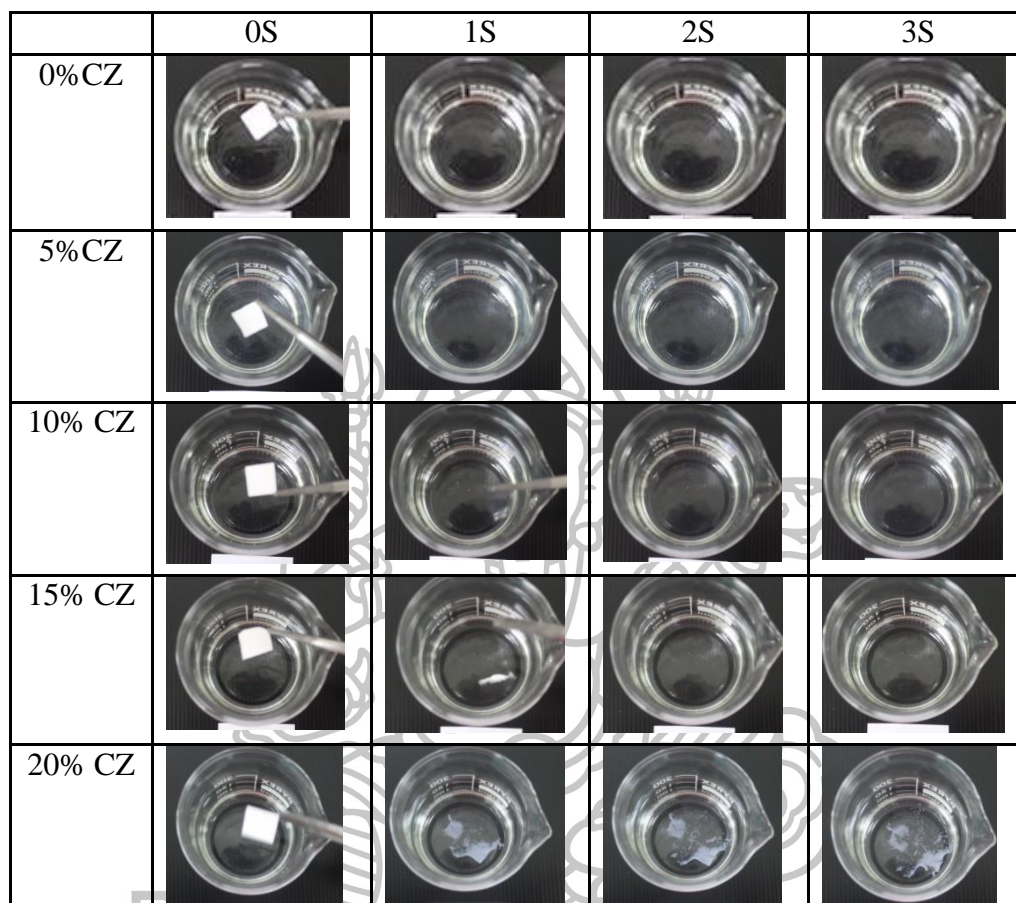


Table 4.7 Disintegration of the nanofiber mats containing 0-20% CZ.



4.2.7 *In vitro* release

The release characteristics of CZ from the CZ-loaded PVP/HP β CD nanofiber mats with different CZ contents, CZ powder and lozenges are shown in Figure 4.16. CZ was rapidly released from the CZ-loaded electrospun nanofiber mats. After 1, 2, 2 and 5 minutes, all of the CZ contained in the 5, 10, 15 and 20% CZ-loaded nanofiber mats were released into the dissolution medium, respectively. On the other hand, the CZ was released from lozenges and powder 23% and 26% in 2h, respectively. The fast release of CZ from the nanofiber mats was caused by the extremely high specific surface area and porosity of the mats, because those characteristics promoted a remarkably fast drug release, and the PVP nanofibers could provide a fast-dissolving hydrophilic environment. Moreover, the electrospinning

process leaves CZ in an amorphous state, facilitating drug dissolution in the medium. In contrast with the lozenges which must take time to disintegrate and subsequently dissolve and CZ powder which hard to dissolve due to high lipophilicity and crystallinity.

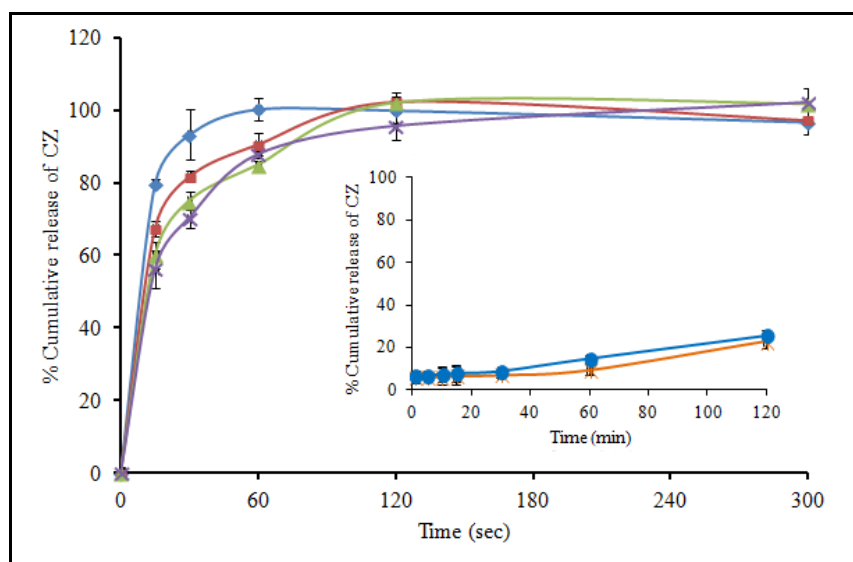


Figure 4.16 Release profiles of CZ from CZ-loaded PVP/HP β CD nanofiber mats with different amounts of CZ: (\blacklozenge) 5%, (\blacksquare) 10%, (\blacktriangle) 15% and (\times) 20% to polymer, from CZ powder (\bullet) and from CZ lozenges ($*$). The data are expressed as mean \pm standard deviation from three independent experiments.

4.2.8 Antifungal study

The MIC and MFC values of CZ were obtained from susceptibility testing using a broth dilution assay. CZ was strongly active against *C. albicans* with MIC and MFC values 12.5 μ g/ml and 25 μ g/ml, respectively. These data agree with a previous report revealing that the MIC and MFC of CZ against *C. albicans* are 10 and 20 μ g/ml (Kaomongkolgit et al., 2009). The antifungal activity of the CZ-loaded nanofiber mats against *C. albicans* was tested by counting the viable cells in a *Candida* suspension after making contact with the nanofiber mats with the suspension. Approximately 10^4 CFU/ml of the strain was exposed to nanofiber mats

with different CZ loadings; furthermore, the CZ-loaded nanofiber mat with a final CZ concentration equivalent to 1mg/ml in the *Candida* suspension was also tested in a time kill assay comparison with the CZ powder and the lozenges at the same concentration of CZ. The CZ-loaded nanofibers could inhibit, killing it, the candida cells within 120 min of contact. In contrast, the pure PVP/HP β CD nanofibers did not hinder the *Candida* growth. The killing abilities of the CZ-loaded nanofiber mats against *Candida* depended on the amount of CZ loaded as displayed in Figure 4.17. 20% CZ-loaded nanofiber mats exhibited significantly faster killing activity than 5% CZ-loaded nanofiber mats at 15, 30 and 60 minutes. Relative to the CZ powder and CZ lozenges, the CZ-loaded nanofibers that have the same final CZ concentration exhibit significantly faster activity against *Candida* than CZ powder and the lozenges at 5 and 15 minutes (Figure 4.18) due to the rapid disintegration of the nanofibers and the amorphous state of the CZ; this amorphous state can dissolve more rapidly and easily than the crystalline state CZ powder; therefore, free CZ rapidly released from the mats caused faster antifungal activity. The CZ lozenges take time to disintegrate and dissolve; therefore, they also display slow antifungal activity. The fast-antifungal activity of the CZ-loaded PVP/HP β CD nanofiber mats makes them promising candidates for topical candidiasis applications (oral, vaginal, skin, etc). For oral candidiasis applications, not only the fast-antifungal activity but also the time period the concentration of drug above the minimum inhibitory concentration (MIC) would be more beneficial than one that only achieves a high CZ concentration for a short period. Therefore, the CZ-loaded mucoadhesive nanofibers were also developed in the next experiments in order to prolong the release of CZ from the nanofiber mats and increase the efficacy of the formulation for oral candidiasis application.

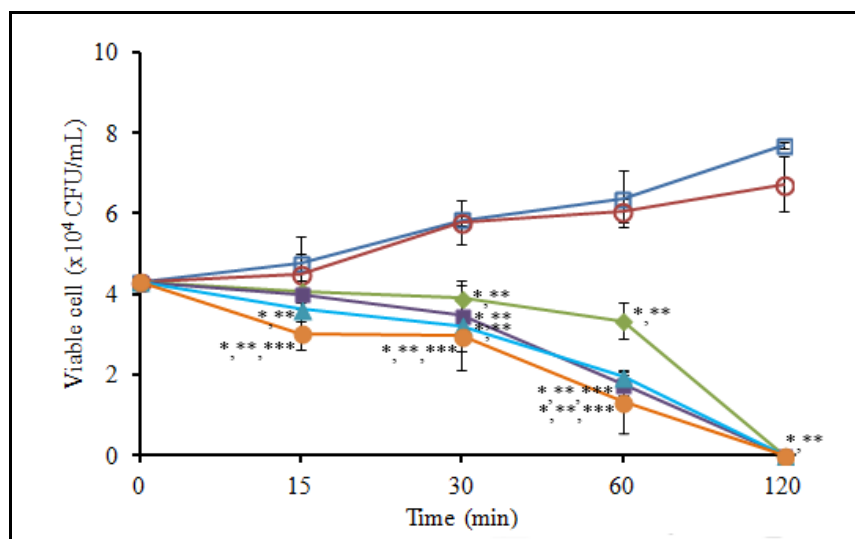


Figure 4.17 Time kill plot of *C. albicans* (CFU/ml) versus the treatment time for (□) the control and the 5 mg of CZ-loaded PVP/HP β CD nanofiber mats with different amounts of CZ: (○) 0 %, (◇) 5%, (■) 10 %, (▲) 15 % and (●) 20 % to polymer. The data are expressed as mean \pm standard deviation from three independent experiments. * Statistically significant difference ($P < 0.05$) from control, ** Statistically significant difference between from plain nanofiber mats (0% CZ), *** Statistically significant from 5% CZ loaded nanofiber mats.

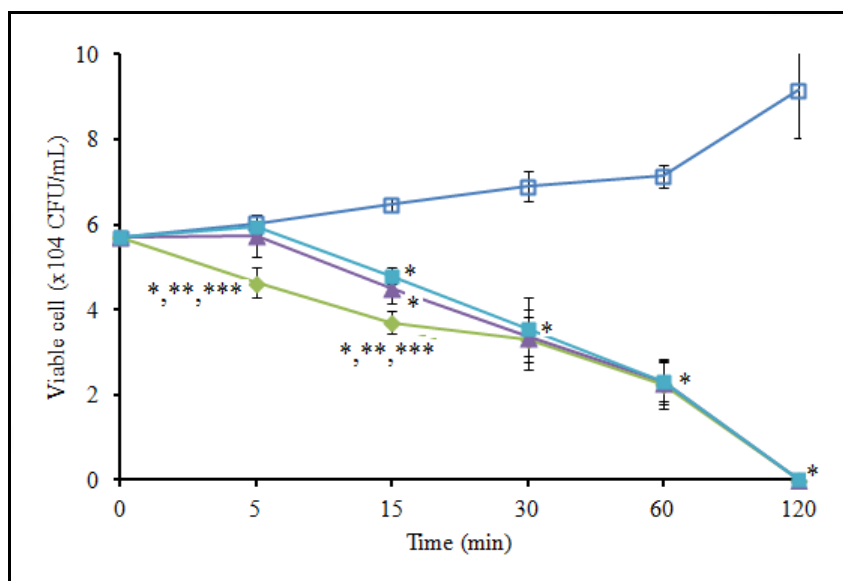


Figure 4.18 Time kill plot of *C. albicans* and (CFU/ml) versus the treatment time: (□) the control, (◆) 20% CZ-loaded PVP/HPβCD nanofiber mats equivalent to CZ 1 mg/ml, (▲) CZ powder equivalent to CZ 1 mg/ml and (■) CZ lozenges equivalent to CZ 1 mg/ml. The data are expressed as mean \pm standard deviation from three independent experiments. * Statistically significant ($P < 0.05$) from control, ** Statistically significant between nanofiber mats and CZ lozenges and *** Statistically significant between nanofiber mats and CZ powder.

4.2.9 Cytotoxicity evaluation

The cytotoxicity of the CZ powder, CZ lozenges and CZ-loaded nanofiber mats was investigated by an MTT assay. Figure 4.19 shows the cell viabilities of CZ powder at CZ concentrations from 0.01 to 100 $\mu\text{g/ml}$ and after incubation at pH 7.4 for 2 h and 24 h in the HGF cells. The results of the CZ powder showed a concentration-dependent cytotoxicity in HGF cells at pH 7.4 when incubated for 2 and 24 h as the IC_{50} was 24.9 and 6.1 $\mu\text{g/ml}$, respectively.

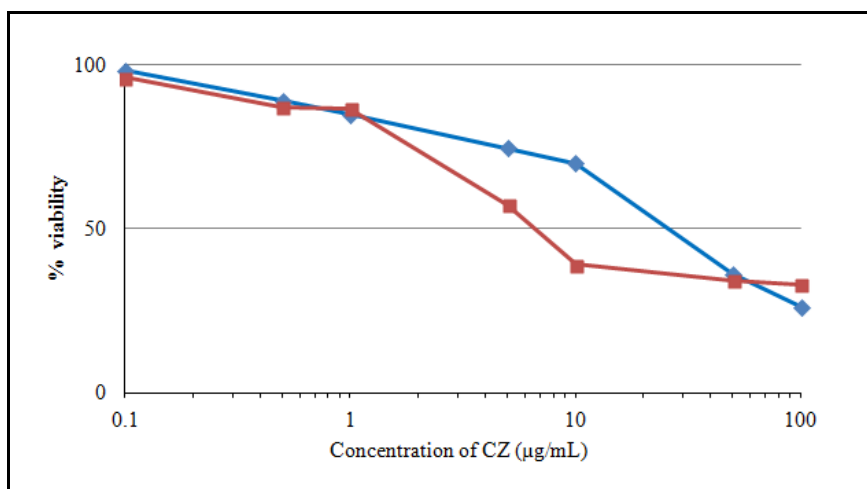


Figure 4.19 The percentage cell viability in HGF cells of CZ solution at CZ concentrations from 0.01 to 100 µg/ml after incubation at pH 7.4 for (◆) 2 h and (■) 24 h in the HGF cells.

The cytotoxicity effect of the extraction medium from CZ lozenges and 0-20% loaded nanofiber mats in HGF cells was evaluated and determined as % viability, as shown in Figure 4.20. For the CZ-loaded nanofiber mats, there was a significant decrease in the cell viability when the HGF cells were incubated with higher CZ loading in the nanofiber mats (15-20%) compared to the control ($p < 0.05$) as illustrated in Figure 4.20a. Cytotoxicity was observed only for a 24-h incubation with the extraction media from the nanofiber mats that contained high levels of CZ (15–20 % wt. to polymer) (Figure 4.20a). This result might be because the amount of CZ was very high and was toxic to fibroblast cells. However, the cytotoxicity of the cell viability was not statistically different in 0–10 % CZ loading in the nanofiber mats. For the CZ lozenges extract medium which has the final CZ concentration equivalent to extraction medium of 20% CZ-loaded nanofiber mats, the cytotoxicity was not significantly different from the extraction medium of 20% CZ-loaded nanofiber mats. Thus, the cytotoxicity may be caused from CZ. After 2-h of incubation with extraction media from the nanofiber mats with different CZ quantity and CZ lozenges, the cell viability remained similar to that of the control cells (cells not treated) at all concentrations. No significant difference in cytotoxicity was observed for CZ-loaded nanofiber mats in HGF cells derived from three different patients, as

presented in Figure 4.20b. The results indicated that CZ-loaded nanofiber mats were safe at the CZ 5–10 % to polymer of the mats for 24 h and all formulations (5-20 %) were safe for 2-h incubation.

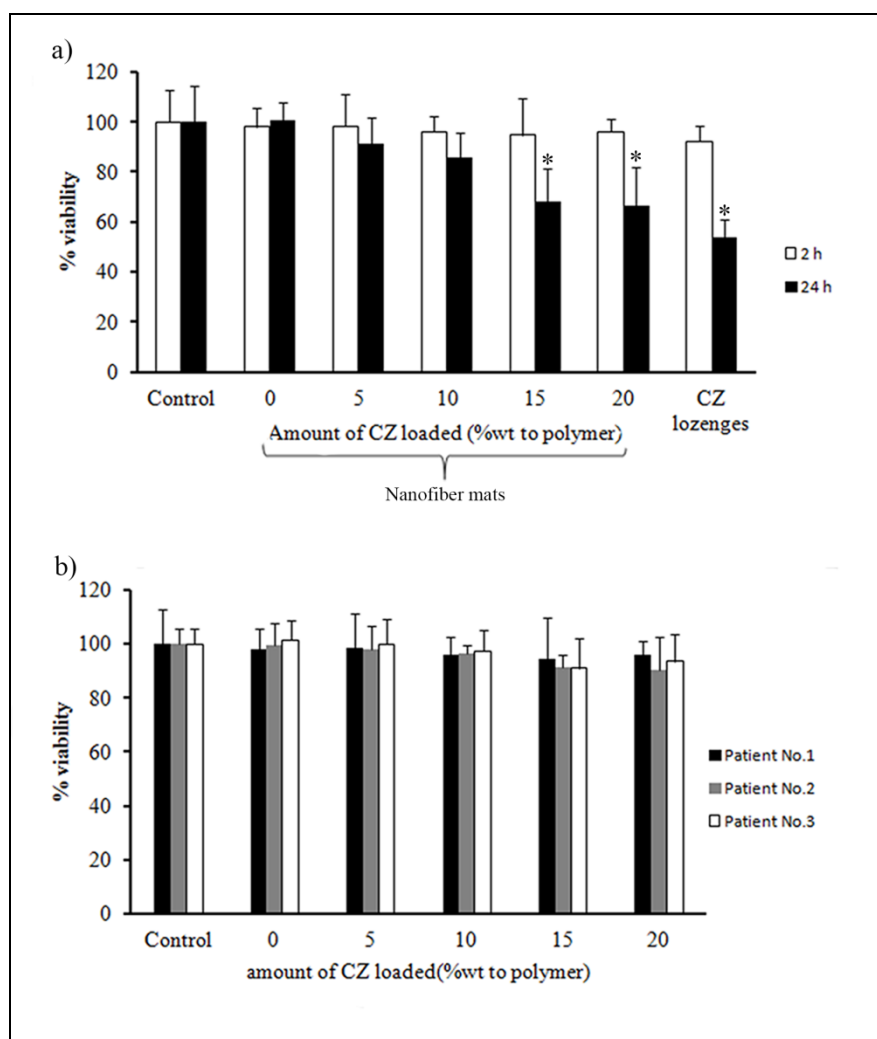


Figure 4.20 The percentage cell viability in HGF cells of a) CZ loaded PVP/HP β CD nanofiber mats at different initial amount of CZ (0, 5, 10, 15 and 20% wt CZ to polymer) and CZ lozenges incubated at (□) 2 h and (■) 24 h b) CZ loaded PVP/HP β CD nanofiber mats at different initial amount of CZ in HGF cells derived from 3 patients: (■) patient #1, (■) patient #2 and (□) patient # 3. Each value represents the mean \pm standard deviation of five wells. * Statistically significant (P < 0.05) from control group.

4.3 Fabrication of CZ loaded-mucoadhesive nanofiber mats.

4.3.1 CZ-microemulsion-containing nanofibers

4.3.1.1 Phase diagram construction

Pseudo-ternary phase diagrams were produced to obtain the concentration range of components for the existing range of microemulsions. After the microemulsion regions in the phase diagram were identified (transparent fluid systems), the appropriate oil, surfactant, cosurfactant and water weight ratios used in the microemulsions were chosen from the constructed phase diagrams (Figure 4.21). The selected percent composition for all the microemulsion systems was 30.32% w/w OA, 9.06% w/w water, 60.62% w/w S_{mix} at a surfactant (T80) to cosurfactant weight ratio of 3:1. The F1, F2 and F3 microemulsion formulations were generated using BzOH, EtOH and IPA, respectively, as the cosurfactant.

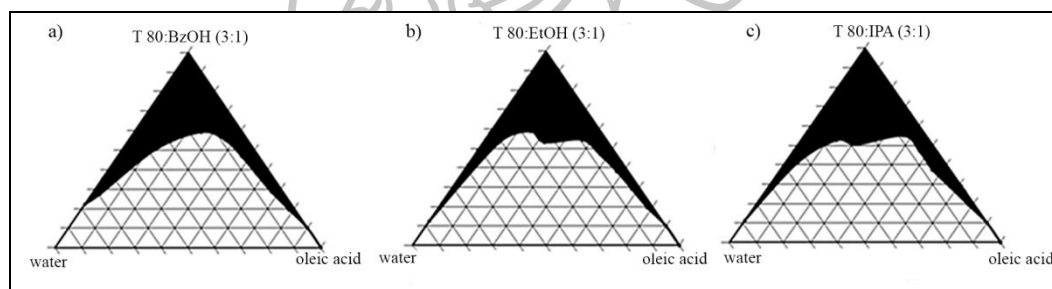


Figure 4.21 Pseudo-ternary phase diagrams of water, oil (OA) and surfactant mixture (surfactant: cosurfactant at the weight ratio of 3:1; a) T80: BzOH b) T80: IPA and c) T80: EtOH (the black area represents microemulsion region).

4.3.1.2 Microemulsion evaluation

Both the physical and chemical stability of CZ in the microemulsion formulation was determined. The color of the CZ-loaded oily phase was not altered, and the recrystallization or precipitation of CZ when stored at room temperature was not found in all formulations by visual observation. Chemical stability due to thermal degradation (heated at 70°C for < 5 min) was another concern. No significant changes in drug content or degradation peaks were observed by the HPLC method (data not shown). These results were in agreement with a previous study, which indicated that

CZ was resistant to thermal degradation (heated at 80°C for 8 h) (Borhade et al, 2012). Three formulations (F1, F2 and F3) of microemulsions with and without CZ were evaluated by measuring the particle size and zeta potential, as listed in Table 4.8. The average particle size and zeta potential of the microemulsions were in the range of 57.80-88.11 nm and -58.73-2.45 mV, respectively. The results revealed that the type of alcohol added to the solution as a cosurfactant did not significantly affect the particle size or zeta potential of the microemulsions. Moreover, the addition of CZ (25% w/w to oil phase) did not significantly affect the particle size the particle size of the microemulsions but did alter the zeta potential. The sharp increase in zeta potential was observed at low pH (pH 4). This outcome confirmed that the increase in zeta potential resulted from the positive charge of CZ molecules that were ionized.

Table 4.8 Particle size and zeta potential of F1, F2 and F3 microemulsions with and without 25% w/w CZ. The data are expressed as mean \pm standard deviation from three independent experiments.

Microemulsions	Particle size (nm)	Zeta potential (mV)		
		pH 4	pH 7	pH 9
F1(O:T80: BzOH)	70.97 \pm 8.09	-25.77 \pm 0.47	-38.13 \pm 2.20	-41.50 \pm 0.70
F2(O:T80: EtOH)	63.38 \pm 13.90	-25.60 \pm 0.36	-40.23 \pm 0.81	-58.73 \pm 0.93
F3(O:T80: IPA)	65.01 \pm 7.44	-26.47 \pm 0.72	-38.57 \pm 0.91	-41.83 \pm 0.32
F1+ 25 % w/w CZ	88.11 \pm 17.48	2.45 \pm 0.14	-17.57 \pm 0.68	-39.47 \pm 0.55
F2+25 % w/w CZ	57.80 \pm 8.23	-3.54 \pm 0.38	-16.87 \pm 0.15	-37.90 \pm 2.02
F3+25 % w/w CZ	64.44 \pm 9.24	3.46 \pm 0.36	-16.73 \pm 0.95	-39.47 \pm 3.04

4.3.1.3 Fabrication of CZ-microemulsion-containing nanofibers

The CZ-loaded microemulsion-containing nanofiber mats were electrospun from a mixture of the CZ-loaded microemulsion (40% wt to polymer) and CS-EDTA/PVA (weight ratio of 30:70) solution. The conductivity of the CS-EDTA/PVA solution was 769.33 \pm 6.03 μ S/mL and that of the CZ-loaded microemulsion (F1, F2 and F3)-containing CS-EDTA/PVA solutions was 770.67 \pm 9.02, 839.33 \pm 8.08 and 892.67 \pm 11.59, respectively. The viscosity of the CS-

EDTA/PVA solution was 358.25 ± 5.29 cP and that of the CZ-loaded microemulsion (F1, F2 and F3)-containing CS-EDTA/PVA solution was 357.72 ± 5.17 , 355.24 ± 3.80 and 356.40 ± 2.10 , respectively. The conductivity of the spinning solutions was increased after the CZ-microemulsion was added due to an excess of CZ loaded in the oily phase, which could be released and ionized in the polymer solution; however, the viscosity of the solution was not altered. After the electrospinning process, the SEM images (Figure 4.22) indicated that bead-free and smooth fibers were generated with CS-EDTA/PVA at a weight ratio of 30/70.

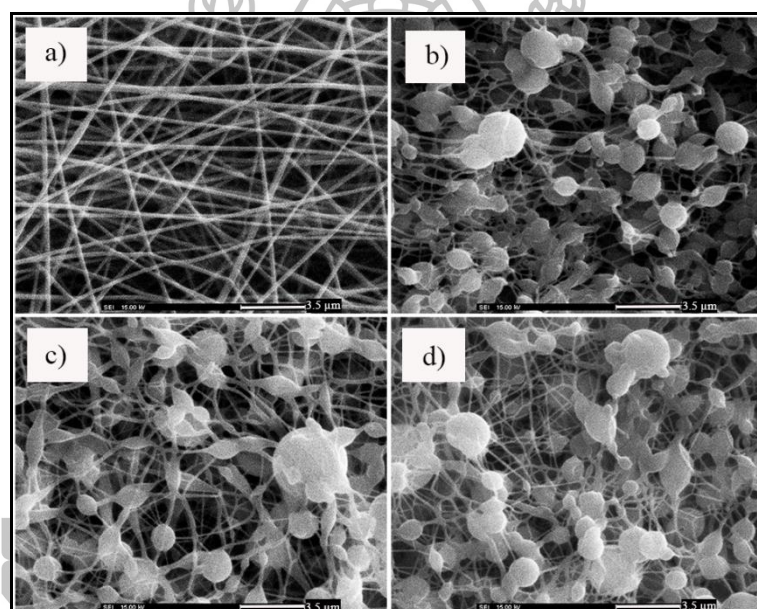


Figure 4.22 SEM images of a) a pure CS-EDTA/PVA nanofiber, b) CZ-loaded microemulsion (F1)-containing nanofiber, c) CZ-loaded microemulsion (F2)-containing nanofiber and d) CZ-loaded microemulsion (F3)-containing nanofiber.

The diameter of the CS-EDTA/PVA nanofibers was 141.75 ± 42.14 nm. However, the nanofibers obtained from the mixture of polymer solution and CZ-loaded microemulsions (F1, F2 and F3) contained globule particles, which might have been the microemulsion particles or polymer beads, that were regularly distributed within the nanofiber mats, and the fiber diameters decreased. The diameters of the fibers were 120.58 ± 25.32 , 125.56 ± 41.93 and 105.91 ± 18.13 nm for the F1, F2 and F3

formulations, respectively. These differences may have been due to the increase in the conductivity of the spinning solution after the addition of the CZ-microemulsion.

The conductivity of the spinning solution affects the tensile force on the fiber in the presence of an electric field and affects fiber diameter. Solutions with high conductivity will possess a greater charge carrying capacity and will be subjected to greater tensile force in the presence of an electric field, resulting in a smaller diameter (Sill and von Recum, 2008). This result is in agreement with previous studies reporting that the average fiber diameter decreases with the increasing conductivity of the solution (Angamma and Jayaram, 2011). Solution conductivity is one of the key parameters in the electrospinning process.

4.3.1.4 Characterization of CZ-microemulsion-containing nanofibers

4.3.1.4.1 FT-IR analysis

The FTIR spectra of the CZ powder, the blank CS-EDTA/PVA nanofiber mats and different formulations of CZ-loaded microemulsion-containing nanofiber mats are presented in Figure 4.23.

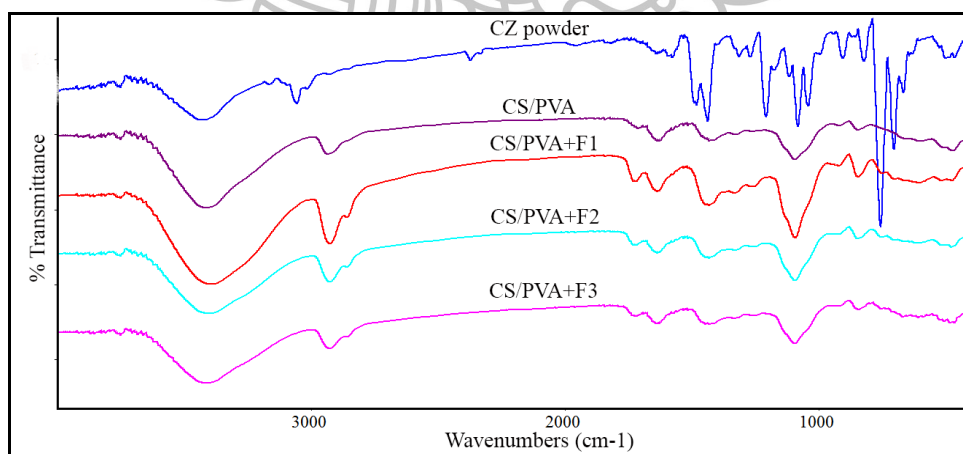


Figure 4.23 FT-IR spectra of a pure CS-EDTA/PVA nanofiber and different formulations (F1-F3) of CZ-loaded microemulsion-containing nanofibers.

The spectrum of the blank nanofiber mats exhibited absorption peaks at 3414, 2937, 1629, 1432 and 1095 cm^{-1} , which were attributed to the ν (O-H), ν_s (CH_2), ν (C=O), δ (CH-O-H) and ν (C-O), respectively. The pure CZ powder exhibited dominant absorption peaks at 1578, 1483, and 1314 cm^{-1} that correspond to benzene ring stretches. The bands at 905, 823, and 756 cm^{-1} were assigned to C-H stretching. The bands at 1083 cm^{-1} and 1208 cm^{-1} correspond to chlorobenzene and C-N stretching, respectively. The peaks observed in the CZ powder spectrum were also observed in spectra of the CZ-loaded microemulsion-containing nanofiber mats with increased intensity. Therefore, CZ-loaded microemulsions were incorporated into the nanofiber mats.

4.3.1.4.2 Differential scanning calorimetry (DSC)

DSC studies were undertaken to evaluate the physical state of CZ in the electrospun nanofiber mats, and the thermograms are displayed in Figure 4.24. The thermogram of the CZ powder exhibited an endothermic sharp peak at 144.13°C due to its melting temperature. The blank CS-EDTA/PVA nanofiber mat exhibited an endothermic curve at 217.83°C. After the incorporation of various formulations of CZ-loaded microemulsions into the nanofiber mats, the absence of a detectable crystalline domain was observed, indicating that CZ was incorporated into the CS-EDTA/PVA nanofiber mats in an amorphous state. Moreover, the melting point of CZ was lower than the melting point of the CS-EDTA/PVA nanofiber mats, indicating that loading of the CZ into the nanofiber mats did not affect their thermal behavior.

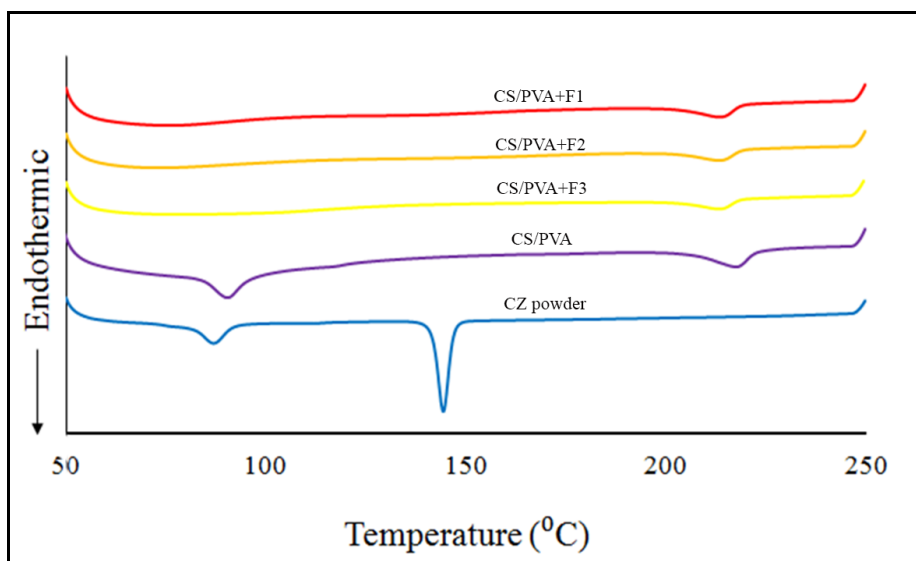


Figure 4.24 DSC thermograms of a pure CS-EDTA/PVA nanofiber and different formulations (F1-F3) of CZ-loaded microemulsion-containing nanofibers.

4.3.1.4.3 X-ray diffractometry (XPRD)

The diffractogram of the CZ powder displayed strong crystalline peaks, indicating its high degree of crystallinity. However, no such peak was found in the diffractograms of the blank or CZ-loaded microemulsion (F1-F3)-containing nanofiber mats (data not shown); these results are in accordance with the DSC-thermogram results, indicating that CZ was incorporated into the nanofiber mats in an amorphous state.

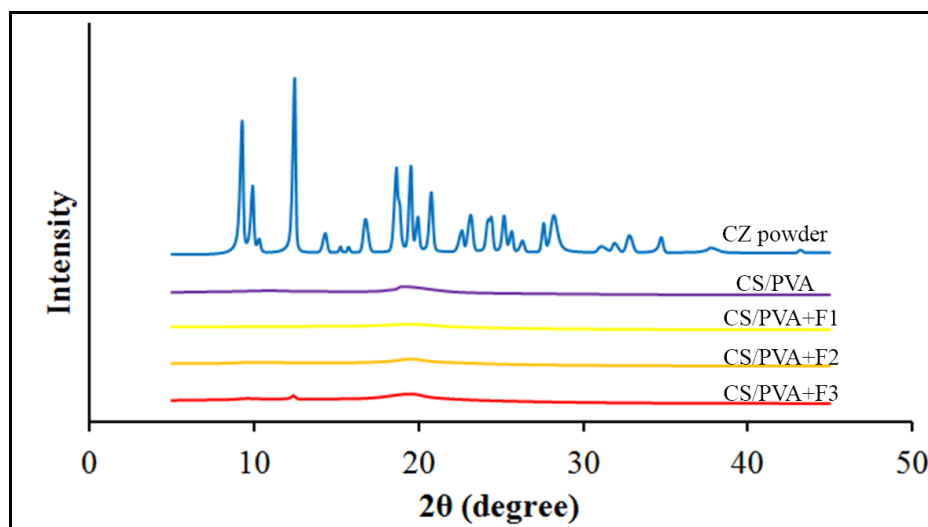


Figure 4.25 X-ray diffractograms of a pure CS-EDTA/PVA nanofiber and different formulations (F1-F3) of CZ-loaded microemulsion-containing nanofibers.

4.3.1.4.4 Mechanical properties and *ex vivo* mucoadhesion studies

The mechanical properties in terms of the tensile strength, strain at the maximum and Young's modulus of the CS-EDTA/PVA nanofiber mats with and without different formulations of CZ-loaded microemulsions were evaluated using a texture analyzer, and the results are presented in Table 4.9. The Young's modulus of all tested nanofiber mats was in the range of 2.8-6.1 MPa. The results demonstrated that the addition of the CZ-loaded microemulsions into the fiber mats exerted little effect on the mechanical properties of the nanofiber mats. The Young's modulus of the mats decreased after the incorporation of the CZ-loaded microemulsions. Moreover, the mucoadhesive strength of the mats also moderately decreased after incorporation of the CZ-loaded microemulsions. The mucoadhesive strength of the mats was in the range of 2.55-6.31 g.

4.3.1.5 Drug content and loading capacity

The total CZ content in the CZ-loaded microemulsion-containing nanofiber mats was determined. The entrapment efficiency (%) and loading capacity

(%) of CZ in the nanofiber mats are listed in Table 4.9. The F3 formulation exhibited the highest entrapment efficiency and loading capacity.

Table 4.9 The mechanical properties, *ex vivo* mucoadhesive properties, entrapment efficiency (%) and loading capacity (%) of pure CS-EDTA/PVA nanofibers and different formulations (F1-F3) of CZ-loaded microemulsion-containing nanofibers. Each value represents the mean \pm standard deviation from three independent experiments.

Nanofiber mats	Young's modulus (MPa)	<i>Ex vivo</i> mucoadhesive strength (g)	Entrapment efficiency (%)	Loading capacity (%)
CS-EDTA/PVA nanofibers	6.1 \pm 1.2	6.31 \pm 0.21	-	-
CS-EDTA/PVA nanofibers+F1	4.8 \pm 0.9	4.29 \pm 0.25	72.86 \pm 2.15	7.56 \pm 0.22
CS-EDTA/PVA nanofibers+F2	4.9 \pm 0.3	2.55 \pm 0.18	72.58 \pm 4.38	7.53 \pm 0.45
CS-EDTA/PVA nanofibers+F3	2.8 \pm 0.6	3.10 \pm 0.14	98.10 \pm 6.95	10.17 \pm 0.72

4.3.1.6 *In vitro* release

The *in vitro* release studies were performed in artificial saliva (pH 6.8) containing 20% PEG-400. The release behavior of CZ from different formulations of the CZ-loaded microemulsion-containing nanofiber mats in comparison with CZ lozenges is presented in Figure 4.26. The results revealed the CZ was released from the different formulations of the CZ-loaded microemulsion-containing nanofiber mats in a burst release manner. In the first 30 min, 46.7%, 33.3%, and 39.2% of the CZ contained in the nanofiber mats of the F1, F2 and F3 formulations, respectively, was released. The percentage of drug release from the fiber mats at 4 h was approximately 74.15, 71.75 and 64.81, respectively. However, the CZ was released in a slower manner after the initial burst release and was sustained for 24 h. Disparate CZ release profiles for the nanofiber mats prepared from different CZ-loaded microemulsions were observed. The nanofiber mats of the F1 formulation exhibited a faster initial release than the F2, F3 and CZ lozenges did. The drug release from the nanofiber

mats of the F1, F2 and F3 formulations was 90.5%, 98.8% and 75.6%, respectively, at 24 h. The release kinetics appeared to follow the Higuchi model; the drug release versus the square root of release time profile yielded a straight line over 60% of the total release process. Higuchi used a pseudo-steady-state approach, which is valid for systems initially containing a large excess of drug (drug loading \gg drug solubility). In this model, the solid drug is assumed to dissolve from the surface layer of the device first; when this layer becomes exhausted of drug, the next layer begins to be depleted by dissolution through the matrix into the external solution (Siepmann and Peppas, 2011).

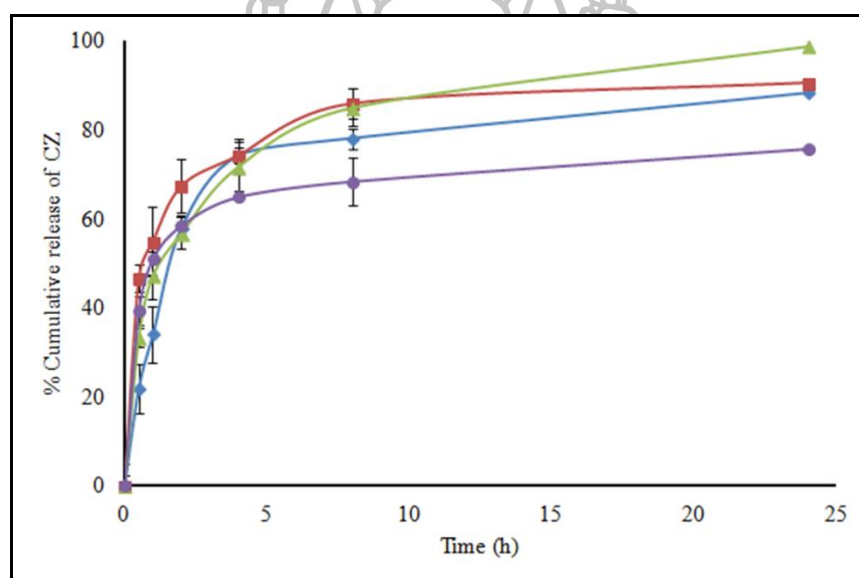


Figure 4.26 Release profiles of CZ from (◆) CZ lozenges, and CZ-loaded microemulsion-containing nanofibers prepared from (■) F1, (▲) F2 and (●) F3 microemulsions. The data are expressed as mean \pm standard deviation from three independent experiments.

4.3.1.7 Antifungal studies

The antifungal activity of the CZ-loaded microemulsion-containing nanofibers was investigated by time-kill analysis to determine the exposure time required to kill standardized microbial inoculums. The time-kill plots of different CZ-loaded microemulsion-containing nanofibers in comparison with CZ lozenges and the

control sample are presented in Figure 4.27. The CZ-loaded microemulsion-containing nanofibers and CZ lozenges inhibited the *Candida* cells within 5 min after contact and killed the *Candida* cells within 1 h. In addition, all formulations of the CZ-loaded microemulsion-containing nanofibers exhibited rapid antifungal activity and displayed significantly faster antifungal activity, compared to the CZ lozenges. These results may be due to the initial rapid release of CZ from the CZ-loaded microemulsion-containing nanofibers in comparison to the CZ lozenges, which require time to disintegrate before CZ dissolution. Moreover, electrospun nanofibers exhibit useful properties, including high porosity, very small pore sizes, large specific surface areas and high surface-to-volume ratios (Matthews et al., 2002; Li and Xia, 2004) resulting in rapid drug released from the mats and rapid antifungal activity.

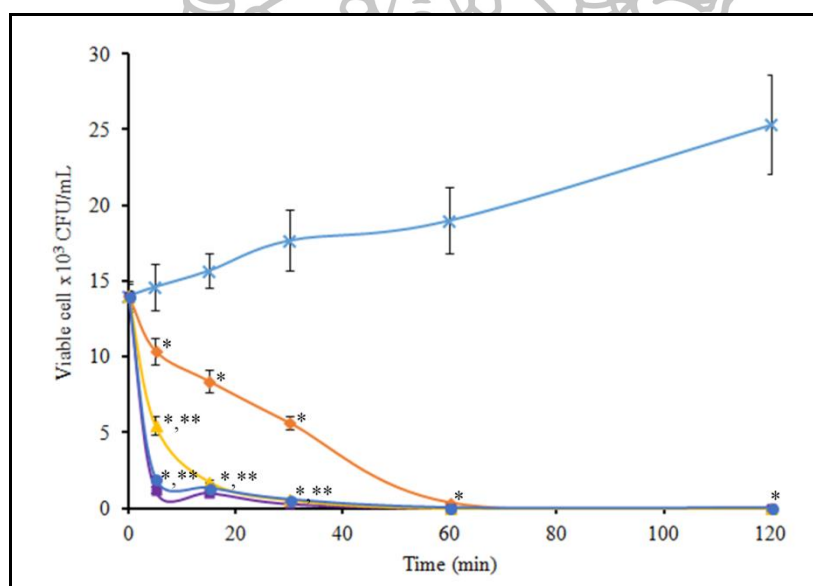


Figure 4.27 Time kill curves for *C. albicans* treated with the (■) F1, (▲) F2 and (●) F3 formulations of CZ-loaded microemulsion-containing nanofibers; (◆) CZ lozenges and (x) control. The data are expressed as mean \pm standard deviation from three independent experiments. *statistically significant ($P < 0.05$) vs. control; **statistically significant difference between nanofiber mats and CZ lozenges.

4.3.1.8 Cytotoxicity evaluation

Cell culture tests were performed to assess the biological compatibility of the nanofibers. The cytotoxicity of the CZ-loaded microemulsion-containing nanofiber mats was investigated after a 2 or 24 h incubation using an MTT assay to determine the % viability, as illustrated in Figure 4.28. A significant decrease in the cell viability (approximately 60% cell viability) was observed when the HGF cells were incubated with CZ-loaded microemulsion-containing nanofibers (F1, F2 and F3) for 24 h, compared to the control (untreated cells) ($p < 0.05$), whereas, after 2 h of incubation with culture media containing nanofiber mats, the cell viability remained similar to that of the control cells for all formulations. These results from the shorter time period (2 h) were in agreement with the time kill studies. Cytotoxicity was observed only for the 24-h incubation with the culture media containing the nanofiber mats. This result may have occurred because a large amount of CZ was loaded into the mats and was toxic to the fibroblast cells. When the incubation time increased, a higher dose of CZ was released, which resulted in a greater amount of CZ coming in contact with the cells. The previous studies mentioned above demonstrated that CZ exhibits concentration-dependent cytotoxicity with HGF cells at pH 7.4 when incubated for 2 and 24 h, with IC_{50} values of 24.9 and 6.1 $\mu\text{g/ml}$, respectively. Moreover, the cytotoxicity of CZ-loaded PVP/HP β CD nanofiber mats was significant increased when the CZ content in the mats increased. In contrast, the blank CS-EDTA/PVA nanofiber mats were also tested, and no significant difference was observed in the cytotoxicity between the blank nanofiber mats and control in previous study (Samprasit et al., 2015). Thus, the cytotoxicity may have resulted from the presence of CZ. The results indicated that all formulations were safe and less cytotoxic for a 2 h incubation. In addition, the cytotoxicity did not differ among the nanofiber mats prepared from the different formulations.

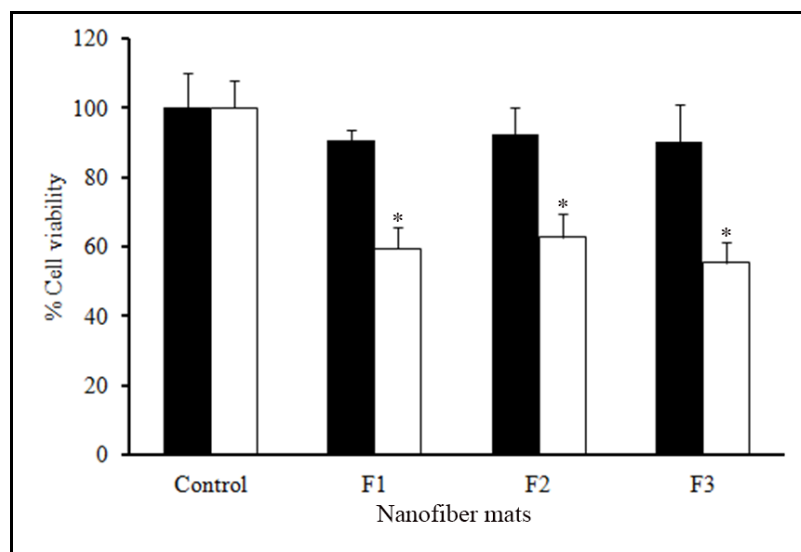


Figure 4.28 The percentage of viable HGF cells after treatment for (■) 2 and (□) 24 h with different formulations (F1-F3) of CZ-loaded microemulsion-containing nanofibers. Each value represents the mean \pm standard deviation of five wells. *Statistically significant ($P < 0.05$) vs. control group.

4.3.2 CZ-incorporated mucoadhesive sandwich nanofibers

4.3.2.1 Morphology of the CZ-loaded sandwich nanofibers

The CZ-loaded sandwich nanofiber mats were designed to improve the solubility of CZ and increase the mucoadhesive properties. CS/PVA-coated PVP/HP β CD/CZ nanofiber mats and CS-SH/PVA-coated PVP/HP β CD/CZ nanofiber mats were prepared using electrospinning. The PVP/HP β CD/CZ nanofiber mats were fabricated and used as the inner layer. The inner fibers were coated with either CS/PVA or CS-SH/PVA for 3 and 6 h on each side to generate the sandwich nanofibers with varying coating thickness. Figure 4.29 shows the SEM images of the as-spun PVP/HP β CD nanofiber mats, CS/PVA nanofiber mats and the sandwich nanofiber mats. The morphology of PVP/HP β CD nanofibers, CS/PVA nanofibers and CS-SH/PVA nanofibers are shown in Figure 4.29a, 4.29b and 4.29c, respectively. Figure 4.29d shows the cross-sectional morphology of the CS/PVA-coated PVP/HP β CD nanofibers at 3 h, and Figure 4.29e and 4.29f present the cross-sectional

morphology of the CS/PVA-coated PVP/HP β CD nanofibers at 6 h (1000x and 100x, respectively). Image analysis revealed that the inner fibers had a mean diameter of (476.7 \pm 64.7) nm, and the coated fibers (CS/PVA and CS-SH/PVA) had a mean diameter of (189.5 \pm 27.5) and (199.9 \pm 29.8) nm, respectively.

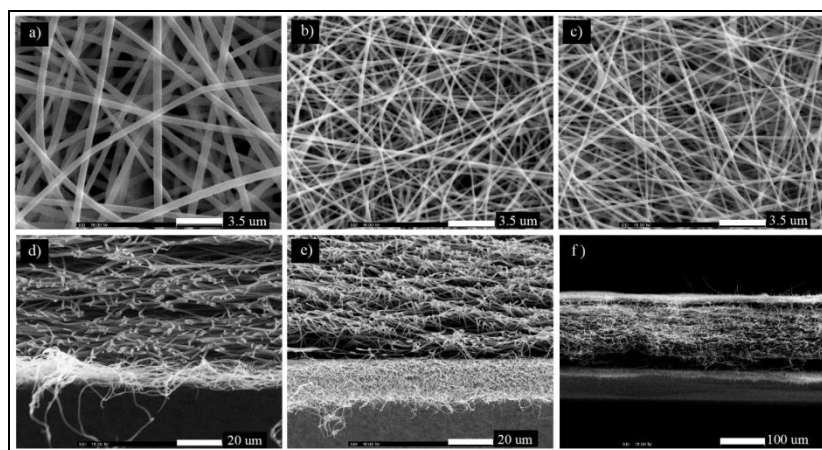


Figure 4.29 The SEM image (3,000x) and the morphology of the a) PVP/HP β CD nanofibers b) CS/PVA nanofibers c) CS-SH/PVA nanofibers and The cross-sectional SEM image (100X) of d) CS-SH/PVA coated PVP/HP β CD nanofibers (at 3h coated time) e) CS-SH/PVA coated PVP/HP β CD nanofibers (at 6h coated time) f) CS-SH/PVA coated PVP/HP β CD nanofibers (at 6h coated time; 200x).

The larger diameter of the PVP/HP β CD fiber measured than the CS/PVA and CS-SH/PVA fiber is a consequence of the higher viscosity and lower conductivity of the PVP/HP β CD spinning solution than those of CS/PVA and CS-SH/PVA spinning solutions (data not shown). The as-spun sandwich nanofibers presented double layers of fibers with a smooth surface and different morphology as presented in Figure 4.29d, 4.29e and 4.29f.

4.3.2.2 FT-IR analysis

The FT-IR spectra of the CZ powder, the CS/PVA-coated PVP/HP β CD nanofibers with/without CZ, and the CS-SH/PVA-coated PVP/HP β CD nanofibers with/without CZ are displayed in Figure 4.30.

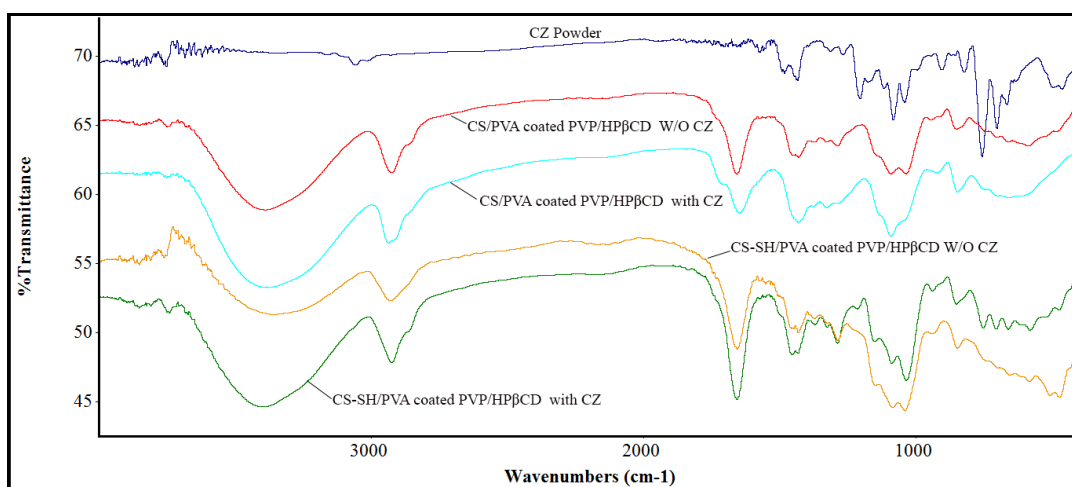


Figure 4.30 FT-IR spectra of CZ powder, CS/PVA coated PVP/HP β CD and CS SH/PVA coated PVP/HP β CD nanofibers with and without 20% CZ.

The spectrum of the blank CS/PVA-coated PVP/HP β CD and the blank CS-SH/PVA-coated PVP/HP β CD nanofiber mats showed a broad -O-H stretching absorption band between 3100 and 3450 cm^{-1} and aliphatic -C-H stretching between 2850 and 3000 cm^{-1} . The major absorption peak between 1020 and 1200 cm^{-1} was attributed to the primary amino groups. The peak at 1632 cm^{-1} correspond to the acetylated amino groups. The peak at 1373 cm^{-1} was assigned to the -C-O stretching of primary alcoholic group (-CH₂-OH). Compared with the CS/PVA-coated PVP/HP β CD, the IR spectrum of the CS-SH/PVA-coated PVP/HP β CD showed the peak at 1291, 1154 and 846 cm^{-1} due to the thiol groups. Moreover, the CS-SH/PVA-coated PVP/HP β CD showed increasing in intensity of the peak at 1632 which was attributed to the overlap of N-H bending and C=O stretching of amide bond occurring after conjugating CS with cysteine. The pure CZ powder exhibited the dominant absorption peaks at 1573.3, 1483.9, and 1315.2 cm^{-1} that correspond to the benzene ring stretches. The peaks at 906.2, 821.6, and 756.3 cm^{-1} were assigned to the C-H stretches. The bands at 1082.0 and 1206.2 cm^{-1} correspond to the chlorobenzene and C-N stretching, respectively. The peaks observed in the CZ powder spectrum especially the peak of chlorobenzene was also observed in spectra of the 20% CZ-loaded sandwich nanofiber mats. Therefore, CZ was incorporated into the nanofiber

mats. However, some functional groups of CZ cannot be observed as some peaks of CZ might overlap with other peaks from functional group of polymers.

4.3.2.3. X-ray diffractometry(XPRD)

The powder X-ray diffraction patterns of the CZ powder, blank CS/PVA-coated PVP/HP β CD nanofibers and CS/PVA-coated PVP/HP β CD/CZ nanofibers are presented in Figure 4.31. Strong crystalline peaks were observed in the diffractogram of the CZ powder. This result indicates the CZ powder has a high degree of crystallinity. However, no such peak was found in the diffractograms of the blank or 20% CZ-loaded nanofiber mats. This indicates that the CZ was incorporated into the PVP/HP β CD nanofiber mats in an amorphous state. The crystalline form of CZ may have changed to the amorphous state during the electrospinning process. Previous studies have reported that the crystallinity of drugs can change to the amorphous state after incorporating into electrospun nanofibers. Yu et al. reported that ibuprofen was present in the amorphous state when loaded into electrospun PVP fibers (Yu et al., 2009)

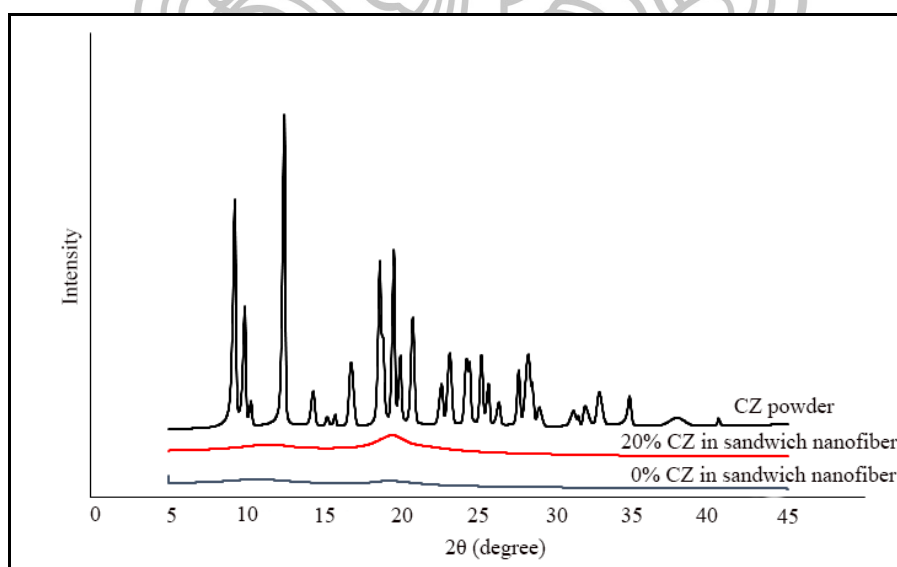


Figure 4.31 X-ray diffractogram of the CZ powder and CS-SH/PVA coated PVP/HP β CD nanofibers with and without 20% CZ.

4.3.2.4. Mechanical properties

The mechanical properties of the sandwich nanofibers were assessed using a texture analyzer in terms of the tensile strength, strain at the maximum load, and Young's modulus. The outcomes are listed in Table 4.10. Young's modulus of the sandwich nanofiber mats was in the range of 2.18 and 3.082 MPa. The CS-SH/PVA-coated PVP/HP β CD nanofiber mats exhibited better mechanical properties than the CS-SH/PVA-coated PVP/HP β CD mats due to the higher flexibility of the CS-SH/PVA nanofibers compared with the CS/PVA nanofibers. The incorporation of CZ into the mats also influenced the mechanical properties of the mats. After the addition of CZ into the mats, the Young's modulus was observed to decrease.

Table 4.10 The mechanical properties, *ex vivo* mucoadhesive properties, entrapment efficiency (%) and loading capacity (%) of CS/PVA or CS-SH/PVA coated PVP/HP β CD/CZ nanofibers. Each value represents the mean \pm standard deviation from independent experiments.

Tested Nanofibers	Young's modulus (MPa) (n=5)	<i>Ex vivo</i> mucoadhesive strength (g) (n=5)	Entrapment efficiency (%) (n=3)	Loading capacity (%) (n=3)
CS/PVA coated PVP/HP β CD (3h coated)	2.569 \pm 0.47	3.5 \pm 0.5	-	-
CS/PVA coated PVP/HP β CD/CZ (3h coated)	2.188 \pm 0.61	3.3 \pm 0.1	85.57 \pm 7.08	17.11 \pm 0.71
CS/PVA coated PVP/HP β CD/CZ (6h coated)	3.048 \pm 0.39	4.3 \pm 0.7	89.54 \pm 7.56	17.91 \pm 0.76
CS-SH/PVA coated PVP/HP β CD (3h coated)	2.795 \pm 0.78	3.7 \pm 0.3	-	-
CS-SH/PVA coated PVP/HP β CD/CZ (3h coated)	2.437 \pm 0.41	3.9 \pm 0.2	92.26 \pm 3.55	18.45 \pm 0.36
CS-SH/PVA coated PVP/HP β CD/CZ (6h coated)	3.082 \pm 0.78	5.4 \pm 0.8	86.40 \pm 4.16	17.28 \pm 0.42

4.3.2.5 Ex-vivo mucoadhesion studies

The *Ex-vivo* mucoadhesion studies were performed to evaluate the ability of the mats to adhere to the mucus within the mouth. The porcine cheek pouch was used as the model surface for bioadhesion testing. The results of mucoadhesion testing are displayed in Table 4.10. All nanofiber mats presented desirable mucoadhesive properties. The mucoadhesive strengths of all nanofiber mats were in the range of 0.33 and 0.54 g. The CS-SH/PVA-coated nanofibers exhibited a higher mucoadhesive strength compared with the CS/PVA-coated nanofibers due to the presence of the thiol groups on the CS-SH. These thiols can then generate the disulfide bond with the mucus. The literature shows that the mucoadhesive properties of thiolated CS are strongly improved compared with unmodified CS (Peh et al., 2000).

4.3.2.6 Drug content and loading capacity

The total content of CZ in the CZ-loaded sandwich nanofiber mats was determined in triplicate using HPLC. The entrapment efficiency (% EE) and loading capacity for CZ in the PVP/HP β CD nanofiber mats are listed in Table 1. The entrapment efficiency of CZ in the nanofiber mats was 85.57-92.26%. This indicates that the incorporation of CZ into the nanofiber mats is very efficient. The loading capacity of CZ in the mats was in range of 17.11-18.45%.

4.3.2.7 *In vitro* release

The release characteristics of CZ from the CS/PVA-coated PVP/HP β CD nanofiber mats, the CS-SH/PVA-coated PVP/HP β CD nanofiber mats and the CZ lozenges are presented in Figure 4.32. It was observed that the releases of CZ from the CZ-loaded CS/PVA-coated PVP/HP β CD nanofiber mats and the CS-SH/PVA-coated PVP/HP β CD nanofiber mats were faster than those from the CZ lozenges. The CZ lozenges take time to disintegrate before the drug is released. This results in a slower initial release rate. The sandwich nanofibers could easily wet and exhibit faster initial release. Moreover, electrospinning can improve the solubility of CZ. The drug is usually distributed on the molecular scale and forced to adopt an amorphous state since the molecules are in random motion in the solution and the electrospinning process is extremely rapid (Kenawy et al, 2009). However, the

sandwich nanofibers coated using a longer coating time resulted in a slower release rate compared with the shorter coating time. The slower release observed at longer coating times may arise due to the longer time for the drug to diffuse through the coated layer and to the greater compression of the coating. No significant difference in the release of CZ from the CS/PVA-coated PVP/HP β CD/CZ nanofiber mats and the CS-SH/PVA-coated PVP/HP β CD/CZ nanofiber mats was observed when coated for the same time.

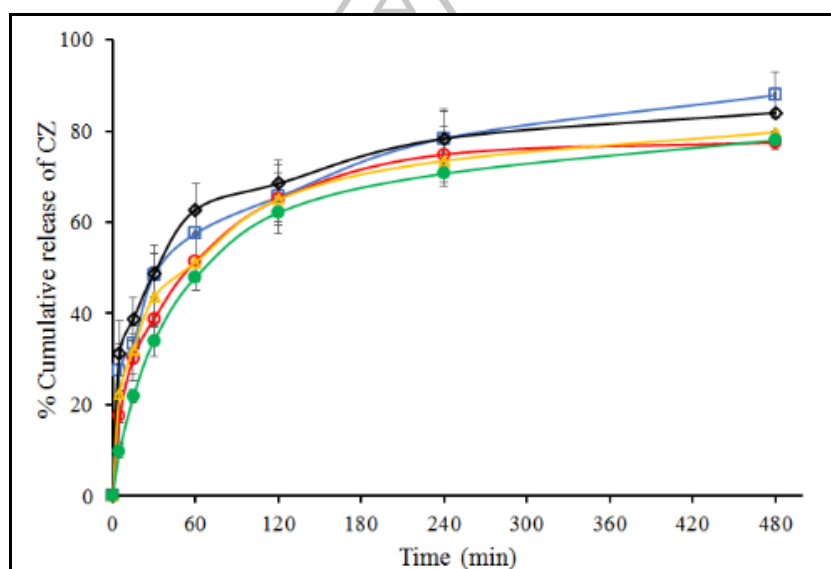


Figure 4.32 Release profiles of CZ from CS/PVA coated PVP/HP β CD/CZ nanofibers (\square) 3h coated time and (\circ) 6h coated time, from CS-SH/PVA coated PVP/HP β CD/CZ nanofibers (\diamond) 3h and (\triangle) 6h coated time), from (\bullet) CZ lozenges. The data are expressed as mean \pm standard deviation from three independent experiments.

4.3.2.8 Antifungal study

The time-kill study was conducted to assess the exposure time required to kill a standardized candida inoculum. The time-kill curves are shown in Figure 4.33.

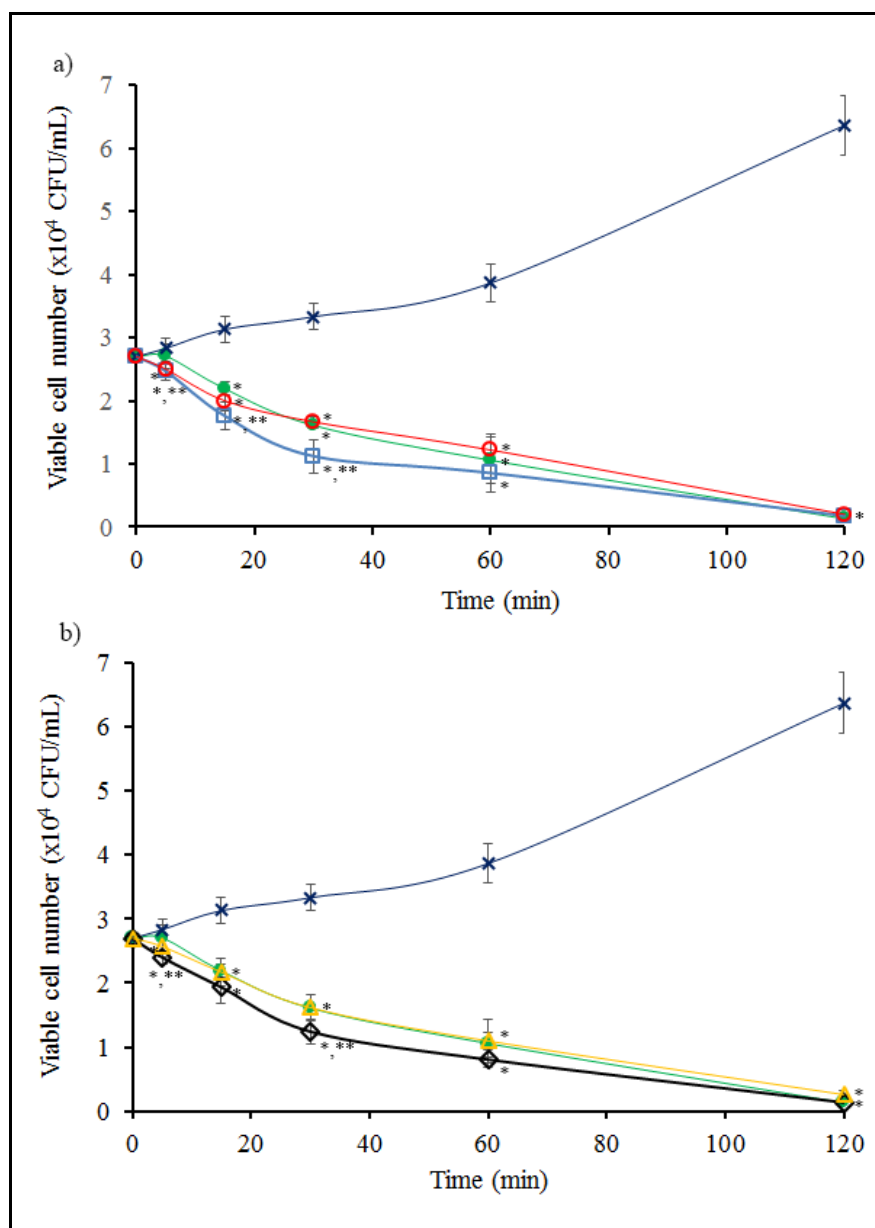


Figure 4.33 Time kill plot against *C. albicans* of (a) CS/PVA coated PVP/HP β CD/CZ nanofibers: (\square) 3h coated time and (\circ) 6h coated time, b) CS-SH/PVA coated PVP/HP β CD/CZ nanofibers: (\triangle) 3h and (\diamond) 6h coated time) as compared to (X) the control and CZ lozenges. The data are expressed as mean \pm standard deviation from three independent experiments. * Statistically significant difference ($P < 0.05$) from control, **Statistically significant difference from CZ lozenges.

The CS/PVA-coated PVP/HP β CD/CZ nanofibers and CS-SH/PVA-coated PVP/HP β CD/CZ nanofibers, coated for 3 h, demonstrated rapid antifungal activity. The coating time had an effect on the CZ release from the mat. Longer coating times resulted in a slower release rate, as well as a lower killing activity of the CZ from the mats. Compared with the commercial CZ lozenges, the 3 h-coated sandwich nanofiber mats (both CS/PVA-coated PVP/HP β CD nanofibers and CS-SH/PVA-coated PVP/HP β CD nanofibers), exhibit significant faster antifungal activity at 5, 15 and 30 min. This may result from the faster initial release of the drug from the nanofiber mats compared with the lozenges. However, the 6 h-coated sandwich nanofiber mats showed no significant difference from the CZ lozenges.

4.3.2.9 Cytotoxicity evaluation

The cytotoxicity of the CZ-loaded sandwich nanofiber mats was evaluated by an MTT assay. The cytotoxicity effect of CS/PVA-coated PVP/HP β CD/CZ nanofiber mats (coated for 3 and 6 h) and CS-SH/PVA-coated PVP/HP β CD/CZ nanofiber mats in HGF cells at 2 and 24 h was assessed and the % viability was determined, as shown in Figure 4.34. Fig. 4.34a represents the cytotoxicity of the sandwich nanofibers at 2 and 24 h. The cytotoxicity of the CS/PVA-coated PVP/HP β CD/CZ and CS-SH/PVA-coated PVP/HP β CD/CZ nanofiber mats was observed only for a 24 h incubation with the nanofiber mats that contained high levels of CZ (20 wt% to polymer) (Figure 4.34a). This result may be because the amount of CZ was very high and was toxic to the fibroblast cells. After a 2 h incubation, no significant difference in the cell viability was observed compared with the control (cells not treated). Moreover, no significant difference in the cytotoxicity was observed for all CZ-loaded sandwich nanofiber mats in HGF cells derived from three different patients, presented in Fig. 4.34b. The results indicate that all formulations were safe for 2 h incubation.

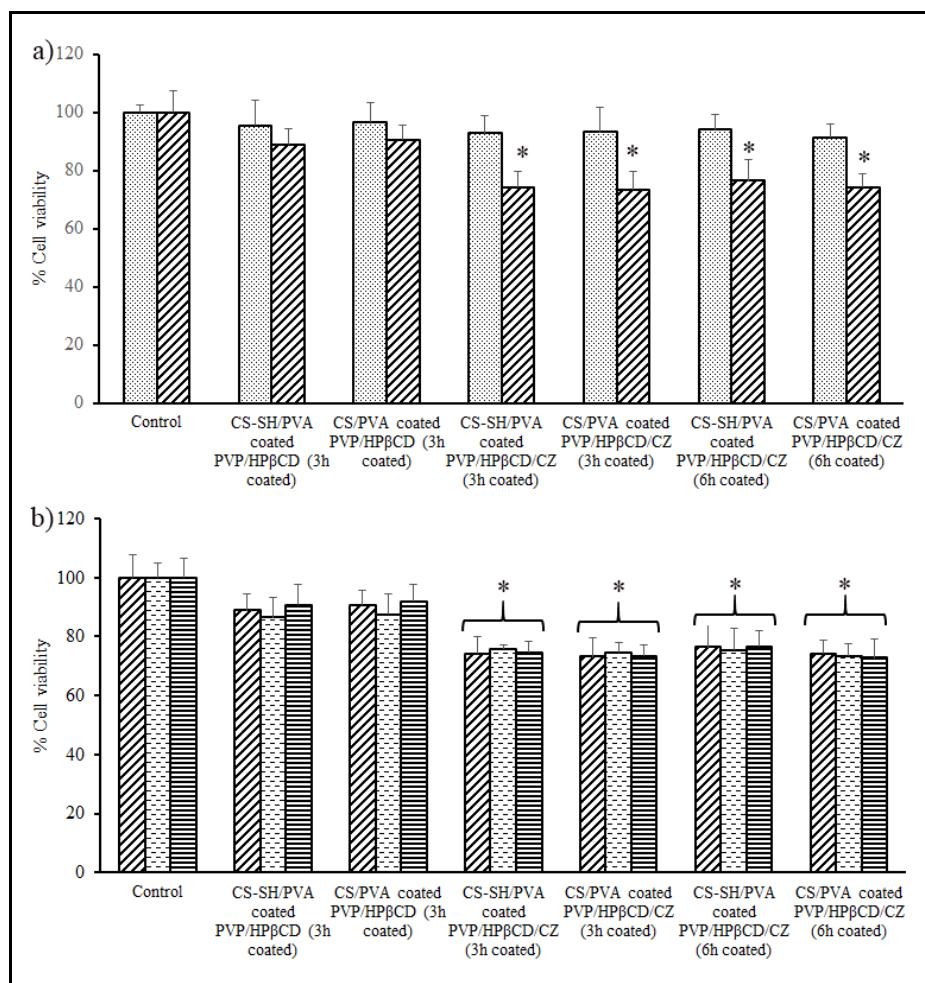


Figure 4.34 (a) The percentage cell viability in HGF cells of CS/PVA or CS-SH/PVA coated PVP/HPβCD with and without 20 % CZ nanofibers at 3h and 6h coated time and incubating for (▣) 2 h and (▤) 24 h (b) incubating for 24 h in HGF cells derived from 3 patients: (▥) patient #1, (▦) patient #2 and (▧) patient # 3. Each value represents the mean ± standard deviation of five wells. * Statistically significant ($P < 0.05$) from control group.

4.3.2.10 *In vivo* mucoadhesion time and drug release evaluation

In vivo mucoadhesion time and drug release evaluation of the CZ loaded-mucoadhesive nanofiber mats were performed in seven healthy human volunteers. The CS-SH/PVA-coated PVP/HPβCD nanofiber mats were selected for this *in vivo* investigation due to the desirable mucoadhesive properties. In this study,

the volunteer randomly attached one nanofiber formulation either CS-SH/PVA-coated PVP/HP β CD nanofiber mats or CS/PVA-coated PVP/HP β CD nanofiber mats on their buccal mucosa, the time required until the mat detach from the buccal mucosa was recorded as *in vivo* mucoadhesion time, and the results are presented in Table 4.11. The results indicate that CS-SH/PVA-coated PVP/HP β CD nanofiber mats (6 h coated) exhibited better mucoadhesive properties as compared with the CS/PVA-coated PVP/HP β CD nanofiber mats. These results are in accordance with the *in vitro* mucoadhesive study which showed that the force for the detachment of the CS-SH/PVA-coated PVP/HP β CD nanofiber mats from the porcine mucosa was greater than that of the CS/PVA-coated PVP/HP β CD nanofiber mats. This is due to the presence of the thiol groups on the thiolated CS that can generate the disulfide bond with the mucus.

Table 4.11 The *in vivo* mucoadhesion time of CS /PVA-coated PVP/HP β CD nanofiber mats and CS-SH/PVA-coated PVP/HP β CD nanofiber mats. Each value represents the mean \pm standard deviation.

Nanofiber formulation	<i>In vivo</i> mucoadhesion time (min)
CS/PVA-coated PVP/HP β CD nanofiber mats (6 h coated)	2.19 \pm 1.78
CS-SH/PVA-coated PVP/HP β CD nanofiber mats (6 h coated)	9.47 \pm 2.36

The *in vivo* release of CZ in healthy human volunteers was also performed to verify the ability of the selected nanofiber mats to release CZ in the mouth of human volunteers. Due to the favorable mucoadhesion time of the CS-SH/PVA-coated PVP/HP β CD nanofiber mat, this nanofiber mat was selected for the *in vivo* release study. In this experiment, the volunteers attached one nanofiber mat on their buccal mucosa and the saliva of each volunteer was collected and analyzed. The release characteristics of CZ from the CS-SH/PVA-coated PVP/HP β CD nanofiber

mats *in vivo* are displayed in Figure 4.35. The release is presented as CZ concentration in saliva at different time points.

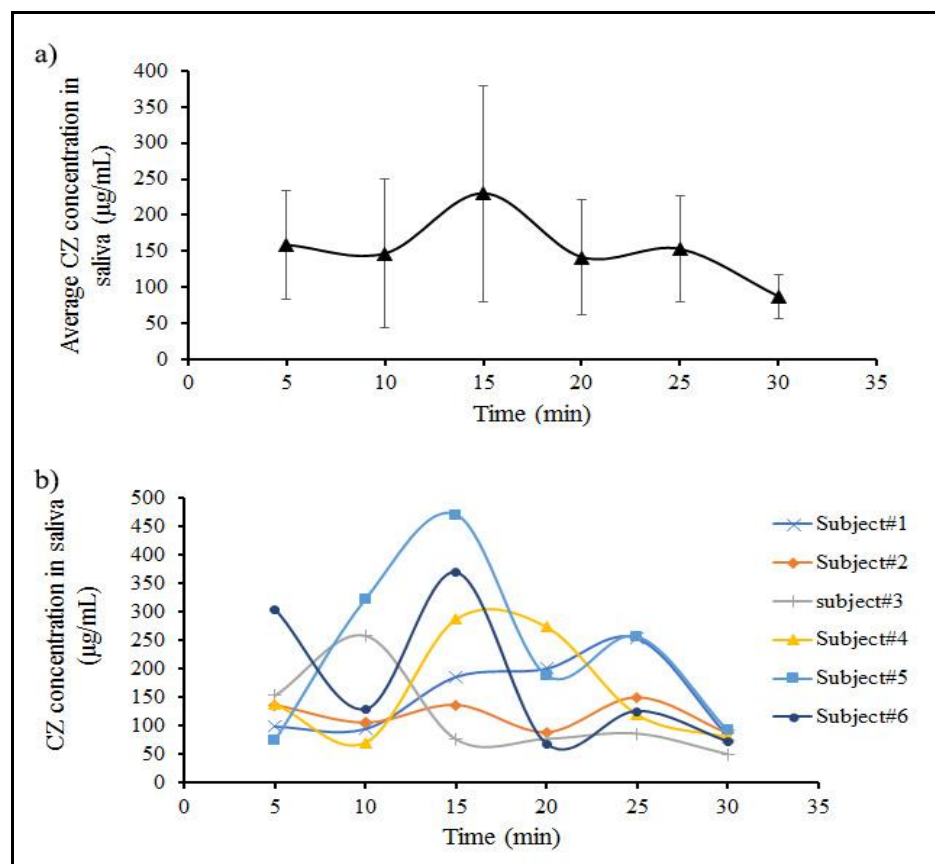


Figure 4.35 The *in vivo* release of CZ from the CS-SH/PVA-coated PVP/HP β CD nanofiber mat in human volunteers. The release is presented as CZ concentration in saliva at different time points: a) average value from seven subjects b) the value from each subject.

As it can be seen from the results, the CZ contained in the nanofiber mats slowly and constantly release to the saliva. The nanofiber mats were able to maintain the release of CZ for more than 30 min. The maximum CZ concentration (229.95 $\mu\text{g/mL}$) in the saliva was observed at 15 min after administration of the nanofiber mats. There were some variations in different subjects (Figure 4.35b) due to the different conditions in the mouth of each subject. As mentioned above, for oral candidiasis applications, not only the fast-antifungal activity but also the time period the concentration of drug above the minimum inhibitory concentration (MIC) would

be more beneficial than one that only achieves a high CZ concentration for a short period. Therefore, the CZ loaded CS-SH/PVA-coated PVP/HP β CD nanofiber mats may be an excellent candidate for the oral hygiene maintenance and oral candidiasis treatment.

4.4 Stability test

To investigate the stability of CZ incorporated in the nanofiber and the nanofiber mats. The CZ-loaded fast-dissolving PVP/HP β CD nanofiber mats, CZ-microemulsion-containing nanofiber mats, and CZ-incorporated mucoadhesive sandwich nanofiber mats were kept under accelerated condition (40 ± 2 °C and 75 ± 5 %RH) and long term condition (25 ± 2 °C and 60 ± 5 %RH) for 3 months, and the % CZ remaining at 0, 1 and 3 month was determined. Figure 4.36 shows the % remaining of the CZ in the fast dissolving nanofiber mats, CZ-microemulsion loaded nanofiber mats and mucoadhesive sandwich nanofiber mats at 0, 1 and 3 month. After the mats were kept at long-term condition for 1 and 3 months, the % CZ remaining in all nanofiber formulations in the nanofibers was observed to be similar to the quantity of CZ at beginning of the study (Figure 4.36a). On the other hand, after the mats were kept at accelerated condition for 1 and 3 months, the CZ contained in the mats appear to be decreased (Figure 4.36b). However, the decrease was not significant after keeping for 3 months. From these findings, it can be assumed that the CZ contained in all the nanofiber formulations was chemically stable for 3 months under long term and accelerated conditions.

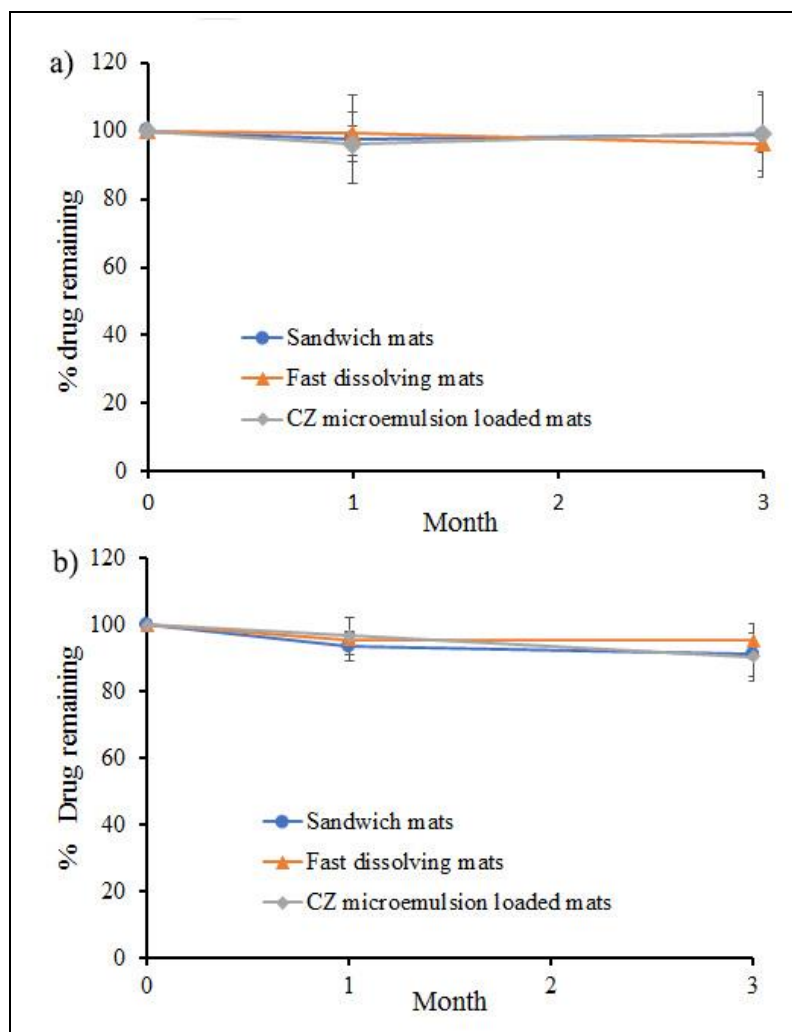


Figure 4.36 CZ-remaining percentage after the CZ loaded nanofiber mats were kept at a) long-term condition (25 ± 2 °C and 60 ± 5 %RH) and b) accelerated condition (40 ± 2 °C and 75 ± 5 %RH) for 0, 1 and 3 months.

After the nanofibers were kept under long-term condition their appearances were not changed. However, when the nanofibers were kept at higher temperature and humidity (accelerated condition), the color changes from white to pale yellow and the fibers became hardened (data not shown). The SEM morphologies of fast-dissolving CZ loaded nanofiber mats after keeping under long term condition and accelerated condition (lower panel) for 0, 1 and 3 months are presented in Figure 4.37. The fiber diameters of the nanofiber mats after keeping under the accelerated condition were altered. The fibers become smaller after 3

months. This may be due to the high temperature which could facilitate the loss of water from the nanofibers to the free space in the container. These results suggested that the lower temperature and humidity of long term conditions were preferred condition for keeping the nanofibers in a long term.

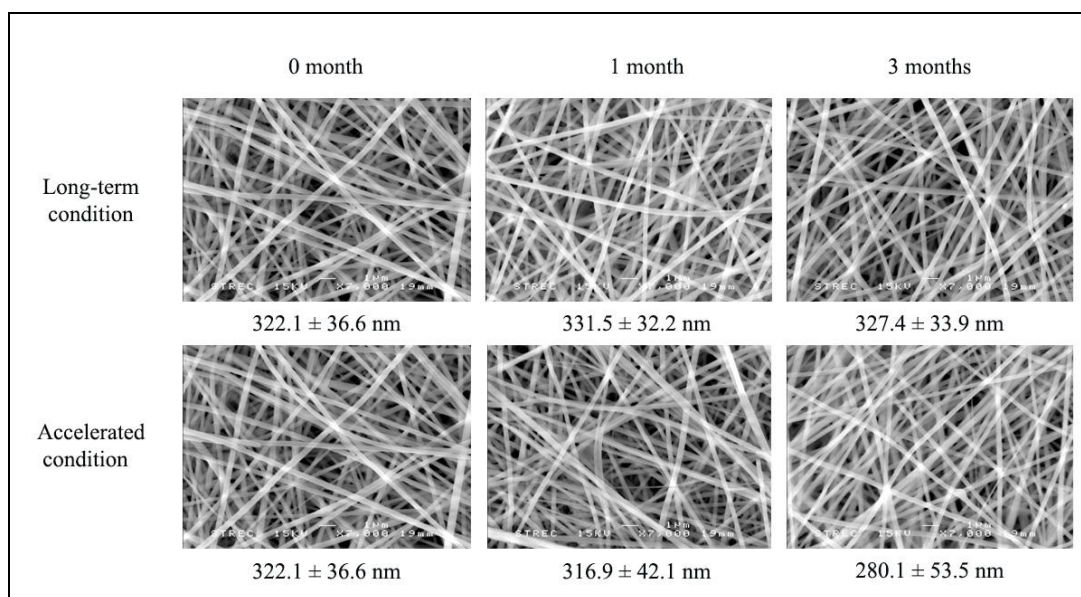


Figure 4.37 SEM images (7000x) and diameter of the fast-dissolving CZ loaded nanofiber mats after being kept under long term condition (upper panel) and accelerated condition (lower panel) for 0, 1 and 3 months.

The stability of the CZ micoremsion incorporated nanofibers is displayed in Figure 4.38. The SEM images show that the lipid contained in the nanofibers could fuse together after keeping the nanofibers for a long period. Although, the average nanofibers diameter of the stored fibers was slightly different from the initial size after keeping the fiber at lower temperature and humidity (long-term condition), little change has been observed from the appearance of the fibers and the lipid. On the other hand, after keeping at higher temperature and humidity (accelerated condition), the lipids were melted and covered on the surface of the fibers. This was because this temperature is higher than the melting point of the lipid used in the formulation. These results suggest that these nanofibers should be kept at low temperature and humidity.

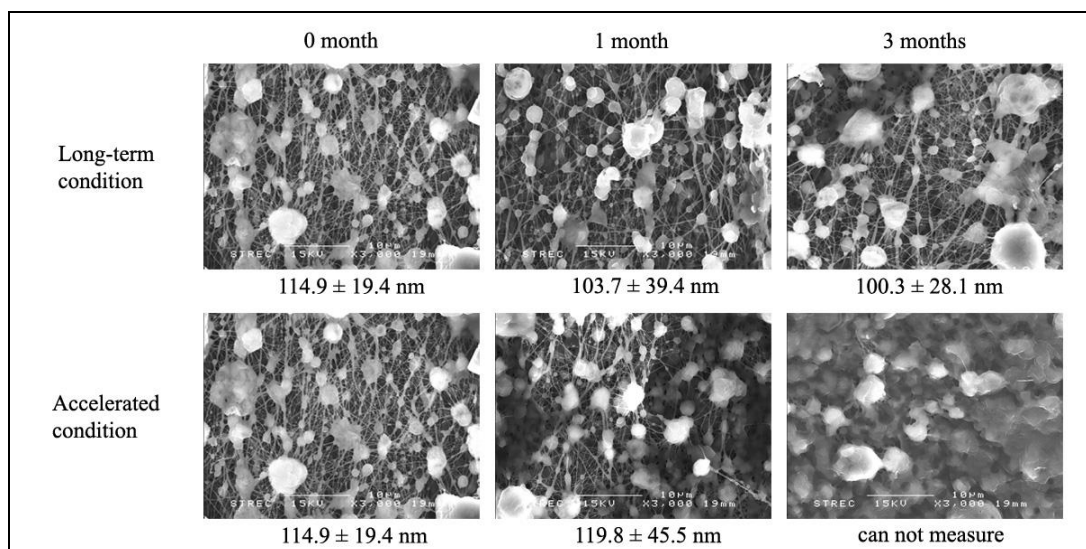


Figure 4.38 SEM images (3000x) and diameter of the CZ-microemulsion loaded nanofiber mats after keeping under long term condition (upper panel) and accelerated condition (lower panel) for 0, 1 and 3 months.

Figure 4.39 reveals the SEM images of the CZ-incorporated mucoadhesive sandwich nanofibers after being kept under long term condition and accelerated condition for 0, 1 and 3 months. The fiber diameters and the morphology of the nanofibers were not significantly changed after keeping at lower temperature and humidity (long-term condition). Nevertheless, the high temperature and humidity of the accelerated condition caused the change of the fibers. The fibers became flatten after being kept for 1 and 3 months. This may be due to the loss of water content from the fibers because of the high temperature. In addition, the fiber mats were observed to be dry and hardened. Moreover, the color of the fibers changed from white to pale yellow after keeping for 3 months. These findings suggest that the lower temperature and humidity of long term conditions were favorable condition for the storage of the nanofibers.

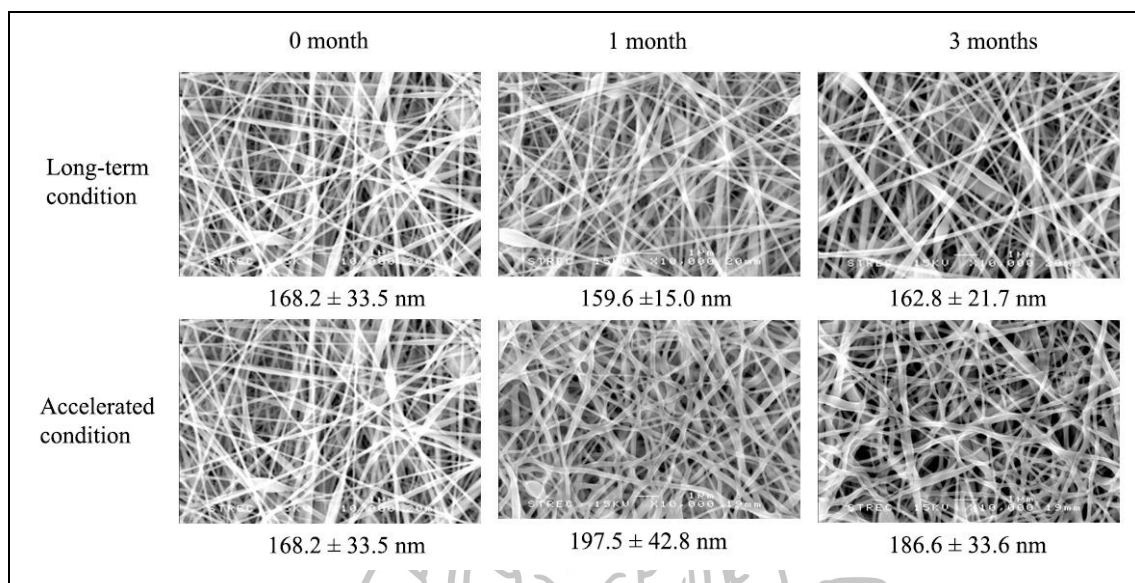
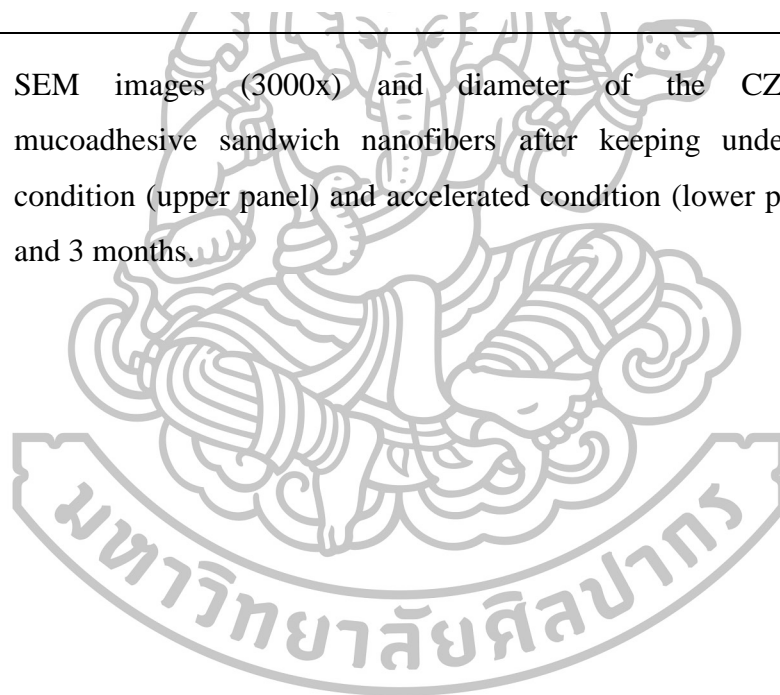


Figure 4.39 SEM images (3000x) and diameter of the CZ-incorporated mucoadhesive sandwich nanofibers after keeping under long term condition (upper panel) and accelerated condition (lower panel) for 0, 1 and 3 months.



CHAPTER 5

CONCLUSIONS

5.1 Development of herbal oil loaded nanofiber mats

With the purpose to attain the formulation for oral hygiene maintenance, betel oil, clove oil and CS derivatives were screened for anticandidal activity, anticandidal adhesion on acrylic resins and antibiofilm activity. Betel oil and clove oil exhibited superior antifungal activity and were selected for incorporating into nanofibers. The herbal oil loaded nanofibers were fabricated by electrospinning technique using PVP as a fiber forming polymer with the aid of HP β CD. Adding the HP β CD helped reduce the hygroscopic property of PVP. In addition, HP β CD could entrap the oil and increase the solubility of the oil. The nanofibers were characterized using numerous techniques including scanning electron microscopy (SEM), Fourier transform infrared spectroscopy (FT-IR), differential scanning calorimetry (DSC) and mechanical testing. The release characteristic, antifungal activity and cytotoxicity were also investigated. Bead-free and smooth fibers without delamination or phase separation of the oils from the nanofiber mats which confirmed the interaction of the oil with the polymer could be obtained. The 30% betel oil loaded nanofiber mats and the 30% clove oil loaded nanofiber mats demonstrated the highest loading capacity. The DSC and FT-IR results confirmed the present of the oil in the nanofiber mats. Both betel oil and clove oil displayed very fast release from the nanofiber mats followed by gradual release and inhibited the growth of candida cells within only few minutes after contact. These nanofiber mats may be beneficial for oral hygiene maintenance or may be a promising candidate as an alternative for oral candidiasis.

5.2 Development of fast-dissolving CZ composite nanofibers

Fast-dissolving CZ composite nanofibers were firstly developed with the purpose to improve the solubility and dissolution of CZ together with to increase

patient compliance. The solubility of CZ in various solvents, and phase solubility of CZ with the present of HP β CD at different concentrations in aqueous and solvent mixture were studied before the optimal CDs concentration was selected to form complex with CZ. In the aqueous solution, the solubility of CZ increased linearly with the HP β CD concentration. PVP/HP β CD blended nanofiber mats containing CZ were electrospun and characterized. The fiber diameters in the mats were in the nanometer range. The DSC and XRPD revealed a molecular dispersion of amorphous CZ in the nanofiber mats. The nanofibers showed rapid wetting and disintegration time which reflected that a short time was required to release of the drug. A fast dissolved and rapid antifungal activity of CZ from the nanofiber mats was achieved.

5.3 Development of CZ-loaded microemulsion-containing nanofiber mats

CZ-loaded microemulsion-containing nanofiber mats were developed. CZ microemulsion is a promising formulation to improve CZ solubility. CS and PVP were chosen as polymers for the incorporation of CZ microemulsion. The microemulsion was composed of OA, T80, and a co-surfactant. The appropriate oil, surfactant, cosurfactant and water weight ratios used in the microemulsions were chosen from the constructed phase diagrams. The selected percent composition for all the microemulsion systems was 30.32% w/w OA, 9.06% w/w water, 60.62% w/w S_{mix} at a surfactant (T80) to cosurfactant weight ratio of 3:1. The nanofibers were prepared using electrospinning and characterized using diverse techniques. The CZ was released in a slower manner after the initial burst release and was then sustained for 24 h. In comparison with CZ lozenges, the nanofiber mats exhibited more rapid killing activity. Moreover, the nanofiber mats demonstrated desirable mucoadhesive properties and were safe for 2 h.

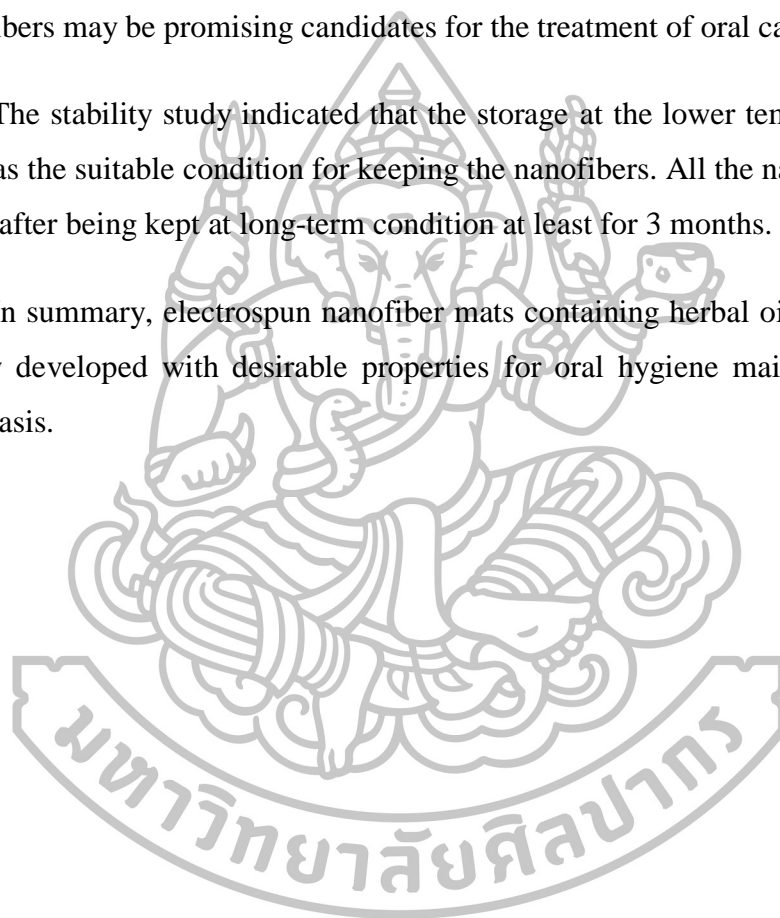
5.4 Development CZ-composite sandwich nanofibers

CZ-composite sandwich nanofibers were prepared by electrospinning technique. The CZ-loaded PVP/HP β CD fiber was coated with CS/PVA or CS-SH/PVA at different coating time to increase the mucoadhesive properties and to achieve a sustained release of the drug from the nanofibers. The CS-SH/PVA-coated

nanofibers exhibited a higher mucoadhesive strength compared with the CS/PVA-coated nanofibers due to the presence of the thiol groups on the CS-SH. The initial fast release of CZ followed by sustained release was accomplished. The sandwich nanofiber mats exhibited desirable mucoadhesive properties both *in vitro* and *in vivo*. The *in vivo* release revealed the CZ contained in the sandwich mats could be slowly and constantly released to the saliva with the favorable concentration. Therefore, these nanofibers may be promising candidates for the treatment of oral candidiasis.

The stability study indicated that the storage at the lower temperature and humidity was the suitable condition for keeping the nanofibers. All the nanofiber mats were stable after being kept at long-term condition at least for 3 months.

In summary, electrospun nanofiber mats containing herbal oil or CZ were successfully developed with desirable properties for oral hygiene maintenance and oral candidiasis.



REFERENCES

- Akpan, A. and R. Morgan. (2002). "Oral candidiasis. " **Postgraduate Medical Journal** 78, 922: 455-459.
- Albers, E. and B. W. Muller (1995). "Cyclodextrin derivatives in pharmaceuticals." **Critical reviews in therapeutic drug carrier systems** 12, 4: 311-337.
- Al-Zein, H., et al. (2011). "Designing an extended release waxy matrix tablet containing nicardipine–hydroxy propyl β cyclodextrin complex." **Saudi Pharmaceutical Journal** 19(4): 245-253.
- Amidon, G. L., et al. (1995). "A theoretical basis for a biopharmaceutic drug classification: the correlation of in vitro drug product dissolution and in vivo bioavailability." **Pharmaceutical Research** 12, 3: 413-420.
- Angamma, C.J. and S.H. Jayaram (2011). "Analysis of the Effects of Solution Conductivity on Electrospinning Process and Fiber Morphology." **IEEE Transactions on Industry Applications** 47: 1109-1117.
- Anibal, P. C., et al. (2010). "Conventional and alternative antifungal therapies to oral candidiasis." **Brazilian Journal of Microbiology** 41, 4: 824-831.
- Arendorf, T. M. and D. M. Walker (1980). "The prevalence and intra-oral distribution of *Candida albicans* in man." **Archives of oral biology** 25, 1: 1-10.
- Ashish, D., et al. (2014). "A short review on microemulsion and its application in extraction of vegetable oil." **International Journal of Research in Engineering and Technology** 3, 9: 147-158
- Badawi, A. A., et al. (2009). "Preparation and Evaluation of Microemulsion Systems Containing Salicylic Acid." **AAPS PharmSciTech** 10, 4: 1081-1084.
- Badawy, M. E. and E. I. Rabea (2013). "Synthesis and structure-activity relationship of N-(cinnamyl) chitosan analogs as antimicrobial agents." **International journal of biological macromolecules** 57: 185-192.
- Bakri, I. M. and C. W. Douglas (2005). "Inhibitory effect of garlic extract on oral bacteria." **Archives of oral biology** 50, 7: 645-651.
- Balabanova, M., et al. (2003). "Dyes in dermatology." **Clinical Dermatology** 21, 1: 2-6.

- Balata, G., et al. (2011). "Improvement of Solubility and Dissolution Properties of Clotrimazole by Solid Dispersions and Inclusion Complexes." **Indian Journal of Pharmaceutical Sciences** 73, 5: 517-526.
- Balata, G., et al. (2011). "Improvement of Solubility and Dissolution Properties of Clotrimazole by Solid Dispersions and Inclusion Complexes." **Indian Journal of Pharmaceutical Sciences** 73, 5: 517-526.
- Bandi, N., et al. (2004). "Preparation of budesonide- and indomethacin-hydroxypropyl-beta-cyclodextrin (HPBCD) complexes using a single-step, organic-solvent-free supercritical fluid process." **European journal of pharmaceutical sciences** 23, 2: 159-168.
- Basha, M. A.-F. (2010). "Magnetic and optical studies on polyvinylpyrrolidone thin films doped with rare earth metal salts." **Polymer Journal** 42(9): 728-734.
- Bettinetti, G., et al. (2002). "Interaction of naproxen with noncrystalline acetyl beta- and acetyl gamma-cyclodextrins in the solid and liquid state." **European journal of pharmaceutical sciences** 15, 1: 21-29.
- Bhardwaj, N. and S. C. Kundu (2010). "Electrospinning: A fascinating fiber fabrication technique." **Biotechnology Advances** 28(3): 325-347.
- Bibby, D. C., et al. (2000). "Mechanisms by which cyclodextrins modify drug release from polymeric drug delivery systems." *International journal of pharmaceutics* 197, 1-2: 1-11.
- Boland, E. D., et al. (2004). "Utilizing acid pretreatment and electrospinning to improve biocompatibility of poly(glycolic acid) for tissue engineering." **Journal of biomedical materials research Part B, Applied biomaterials**. 71, 1: 144-152.
- Borhade, V., et al. (2012). "Clotrimazole nanoemulsion for malaria chemotherapy. Part I: preformulation studies, formulation design and physicochemical evaluation." **International journal of pharmaceutics** 431,1-2: 138-148.
- Brewster, M. E., and T. Loftsson. (2007). "Cyclodextrins as pharmaceutical solubilizers". **Advanced Drug Delivery Reviews** 59, 7: 645–666.
- Brewster, M. E., et al. (1992). "Effect of various cyclodextrins on solution stability and dissolution rate of doxorubicin hydrochloride." **International journal of pharmaceutics** 79, 1: 289-299.

- Burt, S. (2004). "Essential oils: their antibacterial properties and potential applications in foods—a review." **International Journal of Food Microbiology** 94, 3: 223-253.
- Cannon, R. D., et al. (1995). "Oral Candida: clearance, colonization, or candidiasis?" **Journal of dental research** 74(5): 1152-1161.
- Casaroto, A. R. and V. S. Lara (2010). "Phytomedicines for Candida-associated denture stomatitis." **Fitoterapia** 81, 5: 323-328.
- Cavaleiro, C., et al. (2006). "Antifungal activity of Juniperus essential oils against dermatophyte, Aspergillus and Candida strains." **Journal of applied microbiology** 100, 6: 1333-1338.
- Cerpnjak, K., et al. (2013). "Lipid-based systems as a promising approach for enhancing the bioavailability of poorly water-soluble drugs." **Acta pharmaceutica** 63, 4: 427-445.
- Challa, R. et al. (2005). "Cyclodextrins in drug delivery: An updated review." **AAPS PharmSciTech** 6, 2: E329–E357.
- Challa, R., et al. (2005). "Cyclodextrins in drug delivery: An updated review." **AAPS PharmSciTech** 6, 2: E329-E357.
- Charernsriwilaiwat, N., et al. (2013). "Electrospun chitosan-based nanofiber mats loaded with Garcinia mangostana extracts." **International journal of pharmaceutics** 452(1-2): 333-343.
- Chen, Z., et al. (2007). "Electrospinning of collagen–chitosan complex." **Materials Letters** 61, 16: 3490-3494.
- Chien, P.-J., et al. (2007). "Effects of edible chitosan coating on quality and shelf life of sliced mango fruit." **Journal of Food Engineering** 78, 1: 225-229.
- Choudhary, D. and R. K. Kale (2002). "Antioxidant and non-toxic properties of Piper betle leaf extract: in vitro and in vivo studies." **Phytotherapy research** 16, 5: 461-466.
- Christensen, K. L., et al. (2001). "Preparation of redispersible dry emulsions by spray drying." **International journal of pharmaceutics** 212, 2: 187-194.
- Collins, C. D., et al. (2011). "Management of oropharyngeal candidiasis with localized oral miconazole therapy: efficacy, safety, and patient acceptability." **Patient Prefer Adherence** 5: 369-374.

- Cowan, M. M. (1999). "Plant products as antimicrobial agents." **Clinical microbiology reviews**. 12, 4: 564-582.
- Deitzel, J. M., et al. (2001). "The effect of processing variables on the morphology of electrospun nanofibers and textiles." **Polymer** 42, 1: 261-272.
- Del Valle, E. M. M. (2004). "Cyclodextrins and their uses: a review." **Process Biochemistry** 39, 9: 1033-1046.
- Ding, B., et al. (2004). "Fabrication of blend biodegradable nanofibrous nonwoven mats via multi-jet electrospinning." **Polymer** 45, 6: 1895-1902.
- Dollo, G., et al. (2003). "Spray-dried redispersible oil-in-water emulsion to improve oral bioavailability of poorly soluble drugs." **European Journal of Pharmaceutical Sciences** 19, 4: 273-280.
- Duan, B., et al. (2004). "Electrospinning of chitosan solutions in acetic acid with poly(ethylene oxide)." **Journal of Biomaterials Science, Polymer Edition** 15(6): 797-811.
- Ellepol, A. N. and L. P. Samaranayake (1998). "Adhesion of oral *Candida albicans* isolates to denture acrylic following limited exposure to antifungal agents." **Archives of oral biology** 43, 12: 999-1007.
- Ellepol, A. N. and L. P. Samaranayake (2000). "Oral candidal infections and antimycotics." **Critical reviews in oral biology and medicine** 11, 2: 172-198.
- Epstein, J. B. and B. Polsky (1998). "Oropharyngeal candidiasis: a review of its clinical spectrum and current therapies." **Clinical therapeutics** 20, 1: 40-57.
- Farzaei, M. H., et al. (2013). "Parsley: a review of ethnopharmacology, phytochemistry and biological activities." **Journal of traditional Chinese medicine** 33, 6: 815-826.
- Fathilah, A. R., et al. (2009). "Bacteriostatic effect of Piper betle and Psidium guajava extracts on dental plaque bacteria." **Pakistan journal of biological sciences** 12(6): 518-521.
- Feng, L., et al. (2002). "Super-hydrophobic surface of aligned polyacrylonitrile nanofibers." **Angewandte Chemie (International ed in English)** 41, 7: 1221-1223.

- Ferreres, F., et al. (2014). "Piper betle leaves: profiling phenolic compounds by HPLC/DAD-ESI/MS(n) and anti-cholinesterase activity." **Phytochemical analysis** 25(5): 453-460.
- Fertala, A., et al. (2001). "Mapping critical sites in collagen II for rational design of gene-engineered proteins for cell-supporting materials." **Journal of Biomedical Materials Research** 57, 1: 48-58.
- Ficker, C. E., et al. (2003). "Inhibition of human pathogenic fungi by members of Zingiberaceae used by the Kenyah (Indonesian Borneo)." **Journal of ethnopharmacology** 85, 2-3: 289-293.
- Flasinski, M., et al. (2010). "X-ray grazing incidence diffraction and Langmuir monolayer studies of the interaction of beta-cyclodextrin with model lipid membranes." **Journal of Colloid and Interface Science** 348, 2: 511-521.
- Fleisher, D., et al. (1996). "Improved oral drug delivery: solubility limitations overcome by the use of prodrugs." **Advanced Drug Delivery Reviews** 19, 2: 115-130.
- Fujimoto, T., et al. (2006). "Antibacterial effects of chitosan solution against Legionella pneumophila, Escherichia coli, and Staphylococcus aureus." **International Journal of Food Microbiology** 112, 2: 96-101.
- Gajra, B., et al. (2014). "Mucoadhesive Hydrogel Films of Econazole Nitrate: Formulation and Optimization Using Factorial Design." **Journal of Drug Delivery** 2014: 1-14.
- Garcia-Cuesta, C., et al. (2014). "Current treatment of oral candidiasis: A literature review." **Journal of Clinical and Experimental Dentistry** 6, 5: e576-e582.
- Giriraju, A. and G. Y. Yunus (2013). "Assessment of antimicrobial potential of 10% ginger extract against Streptococcus mutans, Candida albicans, and Enterococcus faecalis: an in vitro study." **Indian journal of dental research** 24, 4: 397-400.
- Gould, S., and R. C. Scott. (2005). "2-Hydroxypropyl- β -cyclodextrin (HP- β -CD): A toxicology review." **Food and Chemical Toxicology** 43, 10: 1451-1459.

- Haghi, A. K. and M. Akbari (2007). "Trends in electrospinning of natural nanofibers." **physica status solidi (a)** 204, 6: 1830-1834.
- Haller, I. (1985). "Mode of action of clotrimazole: implications for therapy." **American journal of obstetrics and gynecology** 152, 7 : 939-944.
- Harris, R. (2002). "Progress with superficial mycoses using essential oils." **International Journal of Aromatherapy** 12, 2: 83-91.
- Higuchi, T. and H. Kristiansen (1970). "Binding specificity between small organic solutes in aqueous solution: classification of some solutes into two groups according to binding tendencies." **Journal of Pharmaceutical Sciences** (11): 1601-1608.
- Higuchi, T., and K. A. Connors (1965). "Phase solubility techniques". **Advances in Analytical Chemistry and Instrumentation** 4: 117–212.
- Himratul-Aznita, W.H., N. Mohd-Al-Faisal and A.R. Fathilah. (2011). "Determination of the percentage inhibition of diameter growth (PIDG) of Piper betle crude aqueous extract against oral Candida species." **Journal of Medicinal Plants Research** 5, 6: 878–884.
- Hohman, M.M., et al. (2001). "Electrospinning and electrically forced jets. I. Stability theory." **Physics of Fluids** 13, 8: 2201–2220.
- Hoogerheide, J.G. & Wyka, B.E. (1982). **Clotrimazole**. Analytical Profiles of Drug Substances. Edited by F. Klaus. New York: Academic Press.
- Hu, A. and A. Apblett. (2014). "**Nanotechnology for water treatment and purification**." Springer, Berlin, Germany.
- Iacopino, A. M., & Wathen, W. F. (1992). "Oral candidal infection and denture stomatitis: a comprehensive review." **Journal of the American Dental Association**, 123, 1: 46-51.
- Ignatious, F., et al. (2010). "Electrospun Nanofibers in Oral Drug Delivery." **Pharmaceutical Research** 27, 4: 576-588.
- Jia, J., et al. (2007). Preparation and characterization of antibacterial silver-containing nanofibers for wound dressing applications. **Journal of US-China Medical Science** 4:52–54.

- Kahlweit, M., et al. (1983). "Influence of the properties of the oil and the surfactant on the phase behavior of systems of the type water-oil-nonionic surfactant." **The Journal of Physical Chemistry** 87, 24: 5032-5040.
- Kang, Y. O., et al. (2010). "Chitosan-coated poly(vinyl alcohol) nanofibers for wound dressings." **Journal of biomedical materials research Part B, Applied biomaterials** 92, 2: 568-576.
- Kaomongkolgit, R., et al. (2009). "Antifungal activity of alpha-mangostin against *Candida albicans*." **Journal of Oral Science** 51, 3: 401-406.
- Kaomongkolgit, R., et al. (2009). "Antifungal activity of alpha-mangostin against *Candida albicans*." **Journal of Oral Science** 51(3): 401-406.
- Katti, D. S., et al. (2004). "Bioresorbable nanofiber-based systems for wound healing and drug delivery: optimization of fabrication parameters." **Journal of Biomedical Materials Research Part B, Applied Biomaterials**. 70, 2: 286-296.
- Kawakami, K., et al. (2002). "Microemulsion formulation for enhanced absorption of poorly soluble drugs. II. In vivo study." **Journal of controlled release** 81, 1-2: 75-82.
- Keat, E. C., et al. (2010). "The effect of Piper betel extract on the wound healing process in experimentally induced diabetic rats." **Clinica terapeutica** 161, 2: 117-120.
- Kenawy, E.-R., et al. (2002). "Release of tetracycline hydrochloride from electrospun poly(ethylene-co-vinylacetate), poly(lactic acid), and a blend." **Journal of Controlled Release** 81, 1-2: 57-64.
- Kenawy, E.-R., et al. (2009). "Processing of polymer nanofibers through electrospinning as drug delivery systems." **Materials Chemistry and Physics** 113(1): 296-302.
- Khil, M. S., et al. (2003). "Electrospun nanofibrous polyurethane membrane as wound dressing." **Journal of Biomedical Materials Research Part B, Applied biomaterials** 67, 2: 675-679.
- Ki, C. S., et al. (2005). "Characterization of gelatin nanofiber prepared from gelatin-formic acid solution." **Polymer** 46, 14: 5094-5102.

- Kim, C. H., et al. (1997). "Synthesis of chitosan derivatives with quaternary ammonium salt and their antibacterial activity." **Polymer Bulletin** 38, 4: 387-393.
- Kumar, S., et al. (2011). "Overview for various aspects of the health benefits of Piper longum linn. fruit." **Journal of acupuncture and meridian studies** 4, 2: 134-140.
- Lam, A. C. and R. S. Schechter (1987). "The theory of diffusion in microemulsion." **Journal of Colloid and Interface Science** 120, 1: 56-63.
- Larrondo, L. and R. St. John Manley (1981). "Electrostatic fiber spinning from polymer melts. I. Experimental observations on fiber formation and properties." **Journal of Polymer Science: Polymer Physics Edition** 19, 6: 909-920.
- Li, D. and Y. Xia (2004). "Electrospinning of Nanofibers: Reinventing the Wheel?" **Advanced Materials** 16(14): 1151-1170.
- Li, H., et al. (2010). "Microcalorimetric and spectrographic studies on host-guest interactions of α -, β -, γ - and M β -cyclodextrin with resveratrol." **Thermochimica Acta** 510, 1-2: 168-172.
- Li, W. J., et al. (2002). "Electrospun nanofibrous structure: a novel scaffold for tissue engineering." **Journal of biomedical materials research** 60, 4: 613-621.
- Liu, L., et al. (2010). "Phase behavior of TXs/toluene/water microemulsion systems for solubilization absorption of toluene." **Journal of Environmental Sciences** 22, 2: 271-276.
- Liversidge, G. G. and K. C. Cundy (1995). "Particle size reduction for improvement of oral bioavailability of hydrophobic drugs: I. Absolute oral bioavailability of nanocrystalline danazol in beagle dogs." **International journal of pharmaceutics** 125, 1: 91-97.
- Loftsson, T. and D. Duchene (2007). "Cyclodextrins and their pharmaceutical applications." **International journal of pharmaceutics** 329, 1-2: 1-11.
- Mao, H. Q., et al. (2001). "Chitosan-DNA nanoparticles as gene carriers: synthesis, characterization and transfection efficiency." **Journal of controlled release** 70, 3: 399-421.

- Marsh, P. D., et al. (1992). "The influence of denture-wearing and age on the oral microflora." **Journal of dental research** 71, 7: 1374-1381.
- Mason, K. L., et al. (2012). "Candida albicans and bacterial microbiota interactions in the cecum during recolonization following broad-spectrum antibiotic therapy." **Infection and immunity** 80, 10: 3371-3380.
- Matthews, J. A., et al. (2002). "Electrospinning of collagen nanofibers." **Biomacromolecules** 3(2): 232-238.
- Megelski, S., et al. (2002). "Micro- and nanostructured surface morphology on electrospun polymer fibers." **Macromolecules** 35, 22: 8456-8466.
- Memisoglu, E., et al. (2003). "Direct formation of nanospheres from amphiphilic beta-cyclodextrin inclusion complexes." **Pharmaceutical research** 20, 1: 117-125.
- Millsop, J. W. and N. Fazel (2016). "Oral candidiasis." **Clinics in dermatology** 34(4): 487-494.
- Miranda, J. et al. (2011). "Cyclodextrins and ternary complexes: technology to improve solubility of poorly soluble drugs." **Brazilian Journal of Pharmaceutical Sciences** 47, 4: 665-681.
- Mitchell, S. B. and J. E. Sanders (2006). "A unique device for controlled electrospinning." **Journal of biomedical materials research Part A** 78(1): 110-120.
- Nalina, T. and Z.H. Rahim (2007). "The crude aqueous extract of Piper betle L. and its antibacterial effect towards Streptococcus mutans." **American Journal of Biochemistry and Biotechnology** 3, 1: 10-15.
- Niimi, M., et al. (2010). "Antifungal drug resistance of oral fungi." **Odontology** 98(1): 15-25.
- Nyst, M. J., et al. (1992). "Gentian violet, ketoconazole and nystatin in oropharyngeal and esophageal candidiasis in Zairian AIDS patients." **Annales de la Societe belge de medecine tropicale** 72, 1: 45-52.
- Ondarçuhu, T. and C. Joachim (1998). "Drawing a single nanofibre over hundreds of microns." **Europhysics Letters** 42, 2: 215.

- Pallasch, T. J. (2002). "Antifungal and antiviral chemotherapy." **Periodontol** 2000 28: 240-255.
- Pappas, P. G., et al. (2015). "Clinical Practice Guideline for the Management of Candidiasis: 2016 Update by the Infectious Diseases Society of America." **Clinical Infectious Diseases**. published online December 16, 2015 doi:10.1093/cid/civ933
- Paradkar, M., et al. (2015). "Formulation and evaluation of clotrimazole transdermal spray." **Drug development and industrial pharmacy** 41, 10: 1718-1725.
- Park, W. H., et al. (2004). "Effect of chitosan on morphology and conformation of electrospun silk fibroin nanofibers." **Polymer** 45, 21: 7151-7157.
- Pavelic, Z., et al. (2005). "Characterisation and in vitro evaluation of bioadhesive liposome gels for local therapy of vaginitis." **International journal of pharmaceutics** 301,1-2: 140-148.
- Pavelic, Z., et al. (2005). "Characterisation and in vitro evaluation of bioadhesive liposome gels for local therapy of vaginitis." **International journal of pharmaceutics** 301, 1-2: 140-148.
- Peh, K., et al. (2000). "Mechanical, bioadhesive strength and biological evaluations of chitosan films for wound dressing." **Journal of pharmacy & pharmaceutical sciences** 3(3): 303-311.
- Pereira, C. A., et al. (2013). "Opportunistic microorganisms in individuals with lesions of denture stomatitis." **Diagnostic microbiology and infectious disease** 76, 4: 419-424.
- Pereira-Cenci, T., et al. (2008). "Development of Candida-associated denture stomatitis: new insights." **Journal of applied oral science** 16, 2: 86-94.
- Pithayanukul, P., et al. (2007). "In vitro antimicrobial activity of Zingiber cassumunar (Plai) oil and a 5% Plai oil gel." **Phytotherapy research** 21, 2: 164-169.
- Pouton, C. W. (2000). "Lipid formulations for oral administration of drugs: non-emulsifying, self-emulsifying and 'self-microemulsifying' drug delivery systems." **European journal of pharmaceutical sciences** 11, 2: S93-98.
- Pouton, C. W. (2000). "Lipid formulations for oral administration of drugs: non-emulsifying, self-emulsifying and 'self-microemulsifying' drug delivery systems." **European journal of pharmaceutical sciences** 11, 2: S93-98.

- Prabagar, B., et al. (2007). "Enhanced bioavailability of poorly water-soluble clotrimazole by inclusion with beta-cyclodextrin." **Archives of pharmacal research** 30, 2: 249-254.
- Prashant, G. M., et al. (2007). "The effect of mango and neem extract on four organisms causing dental caries: Streptococcus mutans, Streptococcus salivarius, Streptococcus mitis, and Streptococcus sanguis: an in vitro study." **Indian journal of dental research** 18, 4: 148-151.
- Rabea, E. I., et al. (2003). "Chitosan as antimicrobial agent: applications and mode of action." **Biomacromolecules** 4, 6: 1457-1465.
- Ramakrishna, S. (2012). Introduction. An Introduction to Electrospinning and Nanofibers, **World Scientific Pub Co Inc**: 1-21.
- Ramakrishna, S., et al. (2006). "Electrospun nanofibers: solving global issues." **Materials Today** 9, 3: 40-50.
- Ramnani, S. P. and S. Sabharwal (2006). "Adsorption behavior of Cr(VI) onto radiation crosslinked chitosan and its possible application for the treatment of wastewater containing Cr(VI)." **Reactive and Functional Polymers** 66, 9: 902-909.
- Rana, I. S., et al. (2011). "Evaluation of antifungal activity in essential oil of the Syzygium aromaticum (L.) by extraction, purification and analysis of its main component eugenol." **Brazilian Journal of Microbiology** 42(4): 1269-1277.
- Rao, V. M. and V. J. Stella (2003). "When can cyclodextrins be considered for solubilization purposes?" **Journal of pharmaceutical sciences** 92, 5: 927-932.
- Reichert, P. A., et al. (2000). "Pathology and clinical correlates in oral candidiasis and its variants: a review." **Oral diseases** 6, 2: 85-91.
- Reneker, D. H., et al. (2000). "Bending instability of electrically charged liquid jets of polymer solutions in electrospinning." **Journal of Applied Physics** 87, 9: 4531-4547.
- Rinaudo, M. (2006). "Chitin and chitosan: Properties and applications." **Progress in Polymer Science** 31, 7: 603-632.

- Rosato, A., et al. (2008). "The inhibition of *Candida* species by selected essential oils and their synergism with amphotericin B." **Phytomedicine** 15, 8: 635-638.
- Roux, M., et al. (2007). "Self-assemblies of amphiphilic cyclodextrins." **European biophysics journal** 36, 8: 861-867.
- Sabale, V. and S. Vora (2012). "Formulation and evaluation of microemulsion-based hydrogel for topical delivery." **International Journal of Pharmaceutical Investigation** 2, 3: 140-149.
- Sabzghabae, A. M., et al. (2011). "Clinical evaluation of the essential oil of *Pelargonium graveolens* for the treatment of denture stomatitis." **Dental Research Journal** 8, 1: S105-S108.
- Sajomsang, W., et al. (2009). "Quaternization of N-aryl chitosan derivatives: synthesis, characterization, and antibacterial activity." **Carbohydrate research** 344, 18: 2502-2511.
- Samaranayake, L. P. and T. W. MacFarlane (1980). "An in-vitro study of the adherence of *Candida albicans* to acrylic surfaces." **Archives of oral biology** 25, 8-9: 603-609.
- Samaranayake, L. P., et al. (2002). "Candidiasis and other fungal diseases of the mouth." **Dermatologic Therapy** 15, 3: 251-269.
- Samaranayake, L. P., et al. (2009). "Oral mucosal fungal infections." **Periodontol** 2000 49, 1: 39-59.
- Samprasit, W., et al. (2015). "Fabrication and In Vitro/In Vivo Performance of Mucoadhesive Electrospun Nanofiber Mats Containing α -Mangostin." **AAPS PharmSciTech** 16(5): 1140-1152.
- Sareen, S., et al. (2012). "Improvement in solubility of poor water-soluble drugs by solid dispersion." **International Journal of Pharmaceutical Investigation** 2, 1: 12-17.
- Sawaya, A. C., et al. (2002). "Comparative study of in vitro methods used to analyse the activity of propolis extracts with different compositions against species of *Candida*." **Letters in applied microbiology** 35, 3: 203-207.
- Sawyer, P. R., et al. (1975). "Clotrimazole: A Review of its Antifungal Activity and Therapeutic Efficacy." **Drugs** 9, 6: 424-447.

- Serajuddin, A. T. (1999). "Solid dispersion of poorly water-soluble drugs: early promises, subsequent problems, and recent breakthroughs." **Journal of pharmaceutical sciences** 88, 10: 1058-1066.
- Shenoy, S. L., et al. (2005). "Role of chain entanglements on fiber formation during electrospinning of polymer solutions: good solvent, non-specific polymer–polymer interaction limit." **Polymer** 46(10): 3372-3384.
- Siepmann, J. and N. A. Peppas (2011). "Higuchi equation: derivation, applications, use and misuse." **International journal of pharmaceutics** 418(1): 6-12.
- Sill, T. J. and H. A. von Recum (2008). "Electrospinning: applications in drug delivery and tissue engineering." *Biomaterials* 29(13): 1989-2006.
- Smith, L. A. and P. X. Ma (2004). "Nano-fibrous scaffolds for tissue engineering." **Colloids and surfaces B, Biointerfaces** 39, 3: 125-131.
- Son, W. K., et al. (2004). "The effects of solution properties and polyelectrolyte on electrospinning of ultrafine poly(ethylene oxide) fibers." **Polymer** 45, 9: 2959-2966.
- Sosnowska, K., and K. Winnicka. (2013). "PAMAM dendrimers affect the in vitro release of clotrimazole from hydrogels irrespective of its molecular state". **African journal of pharmacy and pharmacology** 7, 10:567-573.
- Souto, E. B., et al. (2004). "Development of a controlled release formulation based on SLN and NLC for topical clotrimazole delivery." **International journal of pharmaceutics** 278(1): 71-77.
- Spernath, A. and A. Aserin (2006). "Microemulsions as carriers for drugs and nutraceuticals." **Advances in Colloid and Interface Science** 128–130: 47-64.
- Stella, V. J. and Q. He (2008). "Cyclodextrins." **Toxicologic pathology** 36, 1: 30-42.
- Stitzel, J. D., et al. (2001). "Arterial smooth muscle cell proliferation on a novel biomimicking, biodegradable vascular graft scaffold." **Journal of biomaterials application** 16, 1: 22-33.
- Sun, T., et al. (2005). "Self-organization of skin cells in three-dimensional electrospun polystyrene scaffolds." **Tissue Engineering** 11, 7-8: 1023-1033.
- Szejtli, J. (1998). "Introduction and General Overview of Cyclodextrin Chemistry." **Chemical Reviews** 98, 5: 1743-1754.

- Tabassum, N. and M. Hamdani (2014). "Plants used to treat skin diseases." **Pharmacognosy Reviews** 8, 15: 52-60.
- Taweechaisupapong, S., et al. (2005). "In vitro inhibitory effect of *Streblus asper* leaf-extract on adhesion of *Candida albicans* to human buccal epithelial cells, **Journal of ethnopharmacology** 96, 1-2: 221-226.
- Taylor, G. (1969). "Electrically Driven Jets." **Proceedings of the Royal Society of London**. Series A, Mathematical and Physical Sciences 313, 1515: 453-475.
- Theron, S. A., et al. (2004). "Experimental investigation of the governing parameters in the electrospinning of polymer solutions." **Polymer** 45, 6: 2017-2030.
- Thompson, D. O. (1997). "Cyclodextrins--enabling excipients: their present and future use in pharmaceuticals." **Critical reviews in therapeutic drug carrier systems** 14, 1: 1-104.
- Tonglairoum, P., et al. (2013). "Development and characterization of propranolol selective molecular imprinted polymer composite electrospun nanofiber membrane." **AAPS PharmSciTech** 14, 2: 838-846.
- Tonglairoum, P., et al. (2014). "Encapsulation of plai oil/2-hydroxypropyl-beta-cyclodextrin inclusion complexes in polyvinylpyrrolidone (PVP) electrospun nanofibers for topical application." **Pharmaceutical development and technology** 19(4): 430-437.
- Tonglairoum, P., et al. (2014). "Fast-acting clotrimazole composited PVP/HPbetaCD nanofibers for oral candidiasis application." **Pharmaceutical Research** 31, 8: 1893-1906.
- Ueda, H., et al. (1998). "Evaluation of a sulfobutyl ether beta-cyclodextrin as a solubilizing/stabilizing agent for several drugs." **Drug development and industrial pharmacy** 24, 9: 863-867.
- Uslu, I., et al. (2010). "Preparation and Properties of Electrospun Poly(vinyl alcohol) Blended Hybrid Polymer with Aloe vera and HPMC as Wound Dressing." **Hacettepe Journal of Biology and Chemistry**. 2010; 38(1): 19-25.
- Valle, E. M. Martin Del. (2004). "Cyclodextrins and their uses: A review." **Process Biochemistry** 39, 9: 1033-1046.

- Van Roey, J., et al. (2004). "Comparative efficacy of topical therapy with a slow-release mucoadhesive buccal tablet containing miconazole nitrate versus systemic therapy with ketoconazole in HIV-positive patients with oropharyngeal candidiasis." **Journal of acquired immune deficiency syndromes** 35, 2: 144-150.
- VandeVord, P. J., et al. (2002). "Evaluation of the biocompatibility of a chitosan scaffold in mice." **Journal of biomedical materials research** 59, 3: 585-590.
- Verreck, G., et al. (2003). "Preparation and characterization of nanofibers containing amorphous drug dispersions generated by electrostatic spinning." **Pharmaceutical research** 20, 5: 810-817.
- Vyas, A., S. Saraf and S. Saraf. (2008) "Cyclodextrin based novel drug delivery systems." **Journal of Inclusion Phenomena Macroscopic Chemistry** 62, 1-2: 23-42.
- Ware, E. C. and D. R. Lu (2004). "An automated approach to salt selection for new unique trazodone salts." **Pharmaceutical Research** 21, 1: 177-184.
- Williams, D and M. Lewis (2011). "Pathogenesis and treatment of oral candidosis. " **Journal of Oral Microbiology** 3:10.3402/jom.v3i0.5771. Accessed 18 January 2017. Available from <http://doi.org/10.3402/jom.v3i0.5771>
- Yao, S., et al. (2013). "Effects of ambient relative humidity and solvent properties on the electrospinning of pure hyaluronic acid nanofibers." **Journal of nanoscience and nanotechnology** 13, 7: 4752-4758.
- Yoshimoto, H., et al. (2003). "A biodegradable nanofiber scaffold by electrospinning and its potential for bone tissue engineering." **Biomaterials** 24, 12: 2077-2082.
- Yu, D.-G., et al. (2009). "Ultrafine ibuprofen-loaded polyvinylpyrrolidone fiber mats using electrospinning." **Polymer International** 58(9): 1010-1013.
- Yuan, X., et al. (2004). "Morphology of ultrafine polysulfone fibers prepared by electrospinning." **Polymer International** 53, 11: 1704-1710.
- Zong, X., et al. (2003). "Control of structure, morphology and property in electrospun poly(glycolide-co-lactide) non-woven membranes via post-draw treatments." **Polymer** 44, 17: 4959-4967.

Zuo, W., et al. (2005). "Experimental study on relationship between jet instability and formation of beaded fibers during electrospinning." **Polymer Engineering & Science** 45, 5: 704-709.





APPENDIX



APPENDIX A

มหาวิทยาลัยศิลปากร

1. Standard curve

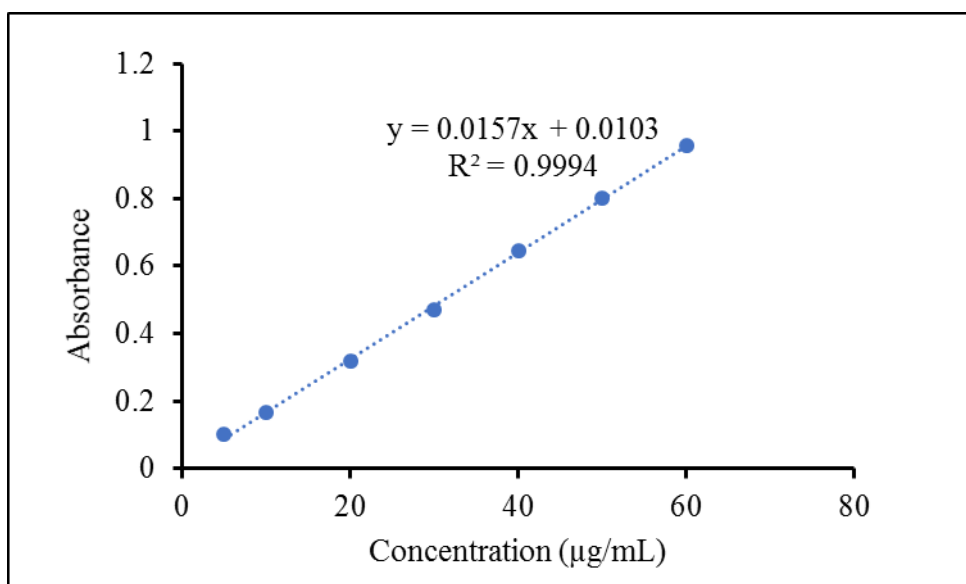


Figure A. 1 Calibration curve of clove oil.

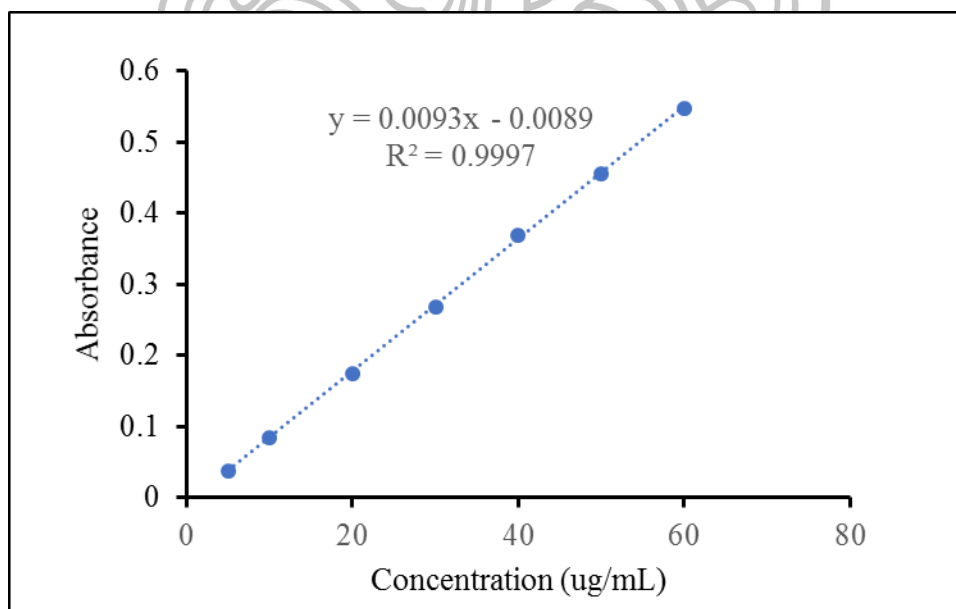


Figure A. 2 Calibration curve of betel oil.

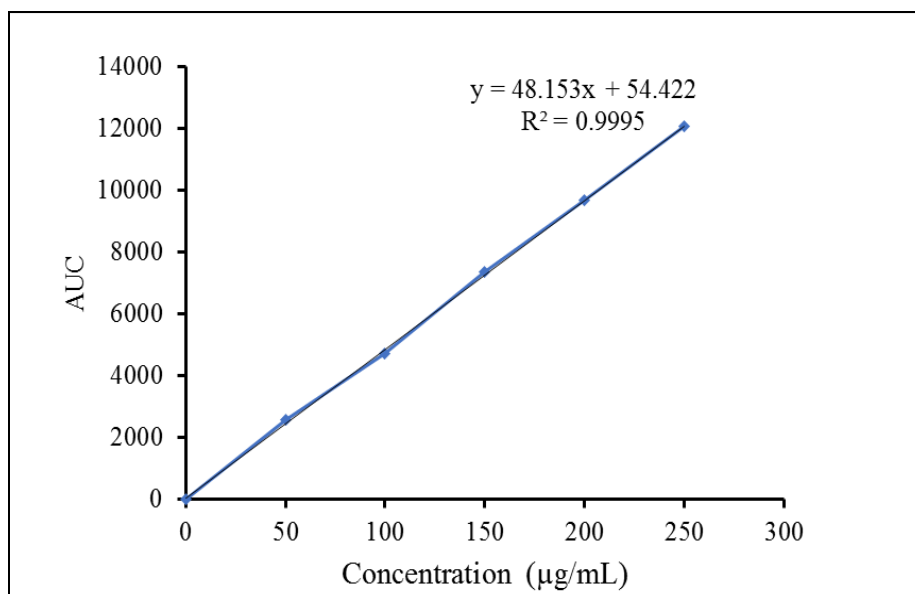


Figure A. 3 Calibration curve of CZ.





APPENDIX B

Antifungal activity of CS and herbal oils

1. Antiadhesion and antibiofilm study

Table B. 1 Anti-adhesion activities of CS-acetate (CS-A), CS-mandelate (CS-M), CS-EDTA, N-cinnamyl CS (CS-CIN), betel oil (Betel) and clove oil (Clove) against *Candida albicans*. Chlorhexidine gluconate (CHX) and phosphate buffer saline (PBS) was used as positive control and negative control, respectively.

Tested compound	adhesion inhibition (%)				
	1	2	3	Mean	SD
CS-Acetate	23.00	18.86	37.36	26.41	9.71
CS-Mandelate	33.10	25.62	43.97	34.23	9.23
CS-EDTA	13.94	19.22	35.06	22.74	10.99
N-cinnamyl CS	37.28	28.11	42.82	36.07	7.43
Betel oil	36.24	30.25	49.71	38.73	9.97
Clove oil	44.25	44.13	56.90	48.43	7.34
CHX	43.90	55.87	57.76	52.51	7.52
PBS	0.00	0.00	0.00	0.00	0.00

Table B. 2 Anti-biofilm activities of CS-acetate (CS-A), CS-mandelate (CS-M), CS-EDTA, N-cinnamyl CS (CS-CIN), betel oil (Betel) and clove oil (Clove) against *Candida albicans*.

Concentration	Clove	Betel	CS-EDTA	CS-A	CS-M	CS-CIN
1/2xMIC	30.10	36.26	36.49	59.65	34.33	46.88
1xMIC	48.94	69.03	52.53	68.98	43.06	47.93
2xMIC	64.34	73.94	69.03	69.90	49.40	59.38

2. Herbal oil load nanofibers

Table B. 3 Fiber diameters of the PVP/HP β CD nanofibers with varied amounts of HP β CD.

No.	Fiber diameter (nm)					
	HP β CD amount					
	90 mM	110 mM	130 mM	150 mM	170 mM	190 mM
1	411.12	351.44	380.17	316.89	713.48	383.60
2	383.60	355.74	441.94	321.56	489.50	482.34
3	411.12	473.01	312.50	420.68	384.89	612.23
4	420.68	414.86	349.39	439.18	359.51	865.83
5	420.68	398.68	450.69	490.52	493.55	662.16
6	451.46	486.72	338.02	321.56	459.11	581.41
7	459.11	498.03	447.43	498.56	477.16	589.06
8	367.72	428.07	441.94	423.04	472.97	575.40
9	420.68	351.44	349.39	557.85	459.11	420.68
10	411.12	428.07	380.17	508.43	492.54	411.12
11	285.53	362.78	391.56	420.68	335.18	459.11
12	359.51	381.82	489.14	536.04	409.91	379.69
13	398.85	432.77	520.10	638.46	482.34	482.34
14	398.85	481.50	468.75	493.55	492.54	465.56
15	341.07	418.50	545.76	451.46	599.93	538.81
16	367.72	338.23	477.01	468.75	468.75	384.89
17	390.02	388.39	455.01	468.75	428.88	352.53
18	348.28	478.33	461.40	550.67	524.79	352.53
19	481.31	424.51	488.14	451.46	578.84	474.02
20	359.51	455.57	441.94	797.69	451.46	448.15
Mean	394.40	417.42	431.52	478.79	478.72	496.07
SD	45.17	50.48	63.47	110.57	84.34	125.65

Table B. 4 Fiber diameters of the 30% clove oil loaded PVP/HP β CD nanofibers and the 30% betel oil loaded PVP/HP β CD nanofibers.

No.	Fiber diameter (nm)	
	30% Clove oil	30% betel oil
1	355.72	359.51
2	393.55	348.28
3	362.77	346.85
4	256.52	324.64
5	414.84	411.12
6	442.01	403.80
7	313.36	472.97
8	342.68	454.75
9	344.15	401.33
10	327.57	411.12
11	424.49	489.50
12	371.05	428.88
13	371.05	550.67
14	413.62	477.16
15	469.77	367.72
16	452.20	448.147265
17	517.94	586.5203904
18	469.77	568.4427687
19	485.66	395.0889577
20	402.46	271.2444904
Mean	396.56	425.89
SD	65.32	82.28

Table B. 5 Mechanical properties of the blank PVP/HP β CD nanofibers, clove oil loaded PVP/HP β CD nanofibers and the betel oil loaded PVP/HP β CD nanofibers.

Nanofibers	Stress (MPa)		Strain (%)		Young's Modulus	
	Mean	SD	Mean	SD	Mean	SD
8% w/v PVP/150mMHP β CD	1.338	0.496	2.059	0.178	0.689	0.1153
20% betel oil loaded 8% w/v PVP/150mMHP β CD	6.298	2.272	1.522	0.337	5.795	0.9235
30% betel oil loaded 8% w/v PVP/150mMHP β CD	1.752	0.61	0.531	0.195	3.58	0.3563
20% clove oil loaded 8% w/v PVP/150mMHP β CD	4.593	0.502	1.423	0.125	4.304	0.287
30% clove oil loaded 8% w/v PVP/150mMHP β CD	1.22	0.133	0.804	0.134	1.838	0.1423

Table B. 6 *Ex-vivo* mucoadhesion forces of the blank PVP/HP β CD nanofibers, 30 % clove oil loaded PVP/HP β CD nanofibers and the 30% betel oil loaded PVP/HP β CD nanofibers.

Nanofibers	Ex-vivo mucoadhesion forces (g)				
	1	2	3	Mean	SD
8% w/v PVP/150mMHP β CD	0.026	0.026	0.025	0.026	0.0006
30% betel oil loaded v PVP/150mMHP β CD	0.033	0.034	0.034	0.034	0.0006
30% clove oil loaded v PVP/150mMHP β CD	0.029	0.027	0.032	0.029	0.0025

Table B. 7 The loading capacity (%) of clove oil in PVP/HP β CD nanofiber mats

Nanofibers (NF)	Loading capacity (%)				
	1	2	3	Mean	SD
20% clove oil loaded NF	7.87	7.38	7.83	7.69	1.36
30% clove oil loaded NF	11.38	12.08	10.46	11.30	2.71
40% clove oil loaded NF	15.10	15.19	14.33	14.87	1.19

Table B. 8 The loading capacity (%) of betel oil in PVP/HP β CD nanofiber mats

Nanofibers (NF)	Loading capacity (%)				
	1	2	3	Mean	SD
20% betel oil loaded NF	11.08	9.81	10.74	10.54	1.36
30% betel oil loaded NF	14.17	15.86	15.27	15.10	2.71
40% betel oil loaded NF	15.10	14.83	15.72	15.22	1.19

Table B. 9 Cumulative release (%) of betel oil from the PVP/HP β CD nanofiber mats containing 30% betel oil.

Time (sec)	Cumulative CZ release (%)				
	1	2	3	Mean	SD
0	0.00	0.00	0.00	0.00	0.00
5	21.62	22.57	24.70	22.96	1.57
15	41.07	41.83	39.44	40.78	1.22
30	45.57	45.70	40.65	43.97	2.88
60	46.51	48.07	46.89	47.16	0.82

Table B. 10 Cumulative release (%) of clove oil from the PVP/HP β CD nanofiber mats containing 30% clove oil.

Time (sec)	Cumulative CZ release (%)				
	1	2	3	Mean	SD
0	0.00	0.00	0.00	0.00	0.00
5	4.52	5.46	5.45	5.14	0.54
15	38.88	39.63	31.86	36.79	4.29
30	43.29	43.42	38.03	41.58	3.07
60	44.17	45.72	44.18	44.69	0.89

Table B. 11 Viable cells of *C. albicans* (CFU/ml) at different treatment times for the control.

Time (min)	Viable cells ($\times 10^4$ CFU/mL)				
	1	2	3	Mean	SD
5	2.30	2.20	1.80	2.10	0.26
15	1.90	2.40	2.00	2.10	0.26
30	1.90	1.80	2.70	2.13	0.49
60	2.80	1.50	2.90	2.40	0.78
120	2.10	2.70	2.60	2.47	0.32

Table B. 12 Viable cells of *C. albicans* (CFU/ml) at different treatment times after being treated with 30% betel oil loaded PVP/HP β CD nanofibers.

Time (min)	Viable cells ($\times 10^4$ CFU/mL)				
	1	2	3	Mean	SD
5	2.30	2.20	1.80	2.10	0.26
15	2.20	2.00	1.80	2.00	0.20
30	1.60	1.70	1.90	1.73	0.15
60	0.80	0.90	0.90	0.87	0.06
120	0.40	0.40	0.50	0.43	0.06

Table B. 13 Viable cells of *C. albicans* (CFU/ml) at different treatment times after being treated with 30% clove oil loaded PVP/HP β CD nanofibers.

Time (min)	Viable cells ($\times 10^4$ CFU/mL)				
	1	2	3	Mean	SD
5	2.00	2.20	1.90	2.03	0.15
15	2.20	2.10	1.90	2.07	0.15
30	1.90	2.00	2.00	1.97	0.06
60	1.70	2.10	2.00	1.93	0.21
120	1.00	0.90	1.30	1.07	0.21

Table B. 14 Viable cells of *C. albicans* (CFU/ml) at different treatment times after being treated with CZ lozenges (equivalent to CZ 1 mg/mL).

Time (min)	Viable cells ($\times 10^4$ CFU/mL)				
	1	2	3	Mean	SD
5	2.25	2.17	2.14	2.19	0.06
15	1.84	1.69	1.77	1.77	0.07
30	1.11	1.18	1.62	1.30	0.28
60	0.69	1.07	0.81	0.86	0.19
120	0.00	0.00	0.00	0.00	0.00

Table B. 15 The percentage cell viability of HGF cells after being incubated with various concentrations of extraction medium of the blank PVP/HP β CD nanofibers for 2 h compared with the control.

Concentration of the extraction medium (mg/mL)	% cell viability	SD
Control	100.00	3.16
0.0001	114.51	6.25
0.001	110.69	10.12
0.01	118.29	4.97
0.1	118.42	7.47
1	113.29	6.04
5	106.72	4.11
10	103.76	7.37

Table B. 16 The percentage cell viability of HGF cells after being incubated with various concentrations of extraction medium of the 30% betel oil loaded PVP/HP β CD nanofibers for 2 h compared with the control.

Concentration of the extraction medium (mg/mL)	% cell viability	SD
Control	100.00	2.75
0.0001	111.59	12.76
0.001	114.08	6.72
0.01	115.25	3.71
0.1	113.24	5.65
1	55.33	5.04
5	18.96	1.59
10	23.26	0.69

Table B. 17 The percentage cell viability of HGF cells after being incubated with various concentrations of extraction medium of the 30% clove oil loaded PVP/HP β CD nanofibers for 2 h compared with the control.

Concentration of the extraction medium (mg/mL)	%cell vialibility	SD
control	100.00	1.38
0.0001	104.94	4.74
0.001	113.36	5.88
0.01	111.63	5.14
0.1	109.01	3.96
1	95.39	10.42
5	16.07	1.46
10	18.68	1.09

Table B. 18 The percentage cell viability of HGF cells after being incubated with various concentrations of extraction medium of the blank PVP/HP β CD nanofibers for 24 h compared with the control.

Concentration of the extraction medium (mg/mL)	%cell vialibility	SD
control	100.00	4.44
0.0001	98.61	10.06
0.001	92.99	8.44
0.01	95.90	5.14
0.1	95.42	8.46
1	81.67	6.88
5	65.26	6.11
10	54.10	2.18

Table B. 19 The percentage cell viability of HGF cells after being incubated with various concentrations of extraction medium of the 30% betel oil loaded PVP/HP β CD nanofibers for 24 h compared with the control.

Concentration of the extraction medium (mg/mL)	%cell viability	SD
control	100.00	5.01
0.0001	104.03	12.29
0.001	101.08	9.05
0.01	104.29	7.26
0.1	101.34	11.65
1	22.49	4.69
5	22.96	2.81
10	27.60	1.81

Table B. 20 The percentage cell viability of HGF cells after incubating with the various concentration of extraction medium of the 30% clove oil loaded PVP/HP β CD nanofibers for 24 h compared with the control.

Concentration of the extraction medium (mg/mL)	%cell viability	SD
control	100.00	4.06
0.0001	102.98	9.18
0.001	103.46	2.81
0.01	98.60	6.97
0.1	101.27	17.84
1	27.89	4.95
5	23.03	3.05
10	24.56	2.36



CZ loaded PVP/HP β CD nanofibers

1. Solubility of CZ

Table C. 1 Solubility of CZ in various solvents and solvent systems.

Tested solvent	Solubility (mg/mL)				
	1	2	3	Mean	SD
Water	0.000598	0.000184	0.000422	0.000402	0.000208
Ethanol	130.9964	114.5411	138.8986	128.1454	12.42648
Benzyl alcohol	693.1347	605.5994	640.3559	646.3636	66.11648
Solvent mixture of EtOH: H ₂ O: BzOH with volume ratio of 70:20:10	259.6715	284.7002	251.3269	265.2328	17.36779
Solvent mixture of artificial saliva pH 6.8: PEG 400 with volume ratio of 80:20 (release medium)	0.35887	0.29806	0.34966	0.33553	0.03277

2. Pharse solubility study

Table C. 2 Pharse solubility of CZ/HP β CD in water, and the solvent system of EtOH: H₂O: BzOH at the volume ratio of 70; 20: 10.

HP β CD (mM)	Solubility (mM)			
	Water		Solvent mixture (EtOH: H ₂ O: BzOH 70:20:10)	
	Mean	SD	Mean	SD
0	0.0011	0.0001	321.24	40.61
30	0.1721	0.0029	353.11	38.80
50	0.3237	0.0140	411.36	26.40
70	0.5111	0.0101	308.67	15.99
90	0.6367	0.0249	197.51	34.14
110	0.7626	0.0324	238.41	17.46

3. Spining solutions

Table C. 3 Conductivity of the PVP/HP β CD spinning solution with different solvent ratios and CZ concentrations.

Solvent ratio (EtOH:H ₂ O:BzOH)	CZ concentration	Conductivity (μ S)				
		1	2	3	Mean	SD
70:30:0	0	5.20	4.50	3.70	4.47	0.75
70:25:5	0	2.00	1.80	2.60	2.13	0.42
70:20:10	0	1.20	1.70	1.30	1.40	0.26
70:20:10	5	2.70	2.50	2.80	2.67	0.15
70:20:10	10	2.90	3.50	3.10	3.17	0.31
70:20:10	20	4.10	3.50	3.60	3.73	0.32

Table C. 4 Viscosity of the PVP/HP β CD spinning solution with different solvent ratios and CZ concentrations.

Solvent ratio (EtOH:H ₂ O:BzOH)	CZ concentration	Viscosity (cP)				
		1	2	3	Mean	SD
70:30:0	0	216.40	217.60	216.40	216.80	0.69
70:25:5	0	223.80	223.80	225.60	224.40	1.04
70:20:10	0	229.40	229.60	225.40	228.13	2.37
70:20:10	5	212.60	216.50	219.90	216.33	3.65
70:20:10	10	219.40	217.40	222.60	219.80	2.62
70:20:10	20	229.60	221.50	226.40	225.83	4.08

Table C. 5 Surface tension of the PVP/HP β CD spinning solution with different solvent ratios and CZ concentrations.

Solvent ratio (EtOH:H ₂ O:BzOH)	CZ concentration	Viscosity (cP)				
		1	2	3	Mean	SD
70:30:0	0	28.61	27.56	29.00	28.39	0.74
70:25:5	0	27.69	28.80	28.92	28.47	0.68
70:20:10	0	29.26	29.26	29.69	29.40	0.25
70:20:10	5	29.46	29.26	29.31	29.34	0.10
70:20:10	10	28.99	29.10	29.26	29.12	0.14
70:20:10	20	29.62	29.54	29.87	29.68	0.17

4. Diameter measurement

Table C.6 Fiber diameters of PVP/HP β CD nanofibers electrospun from the polymer solutions in various solvent systems and different amounts of CZ.

Diameters (nm)							
8% PVP/70 mM HP β CD nanofibers							
Solvent system	70:30:0	70:25:05	70:20:10	70:20:10	70:20:10	70:20:10	70:20:10
CZ content	0%	0%	0%	5%	10%	15%	20%
1	591.08	550.46	414.09	738.13	740.74	506.33	693.69
2	264.34	418.98	667.69	520.03	555.56	632.16	649.27
3	673.93	778.47	667.69	705.07	555.56	495.03	564.05
4	417.96	733.94	667.69	567.57	763.54	495.03	771.06
5	186.92	366.97	523.78	738.13	585.61	566.09	594.94
6	528.68	820.58	414.09	705.07	555.56	739.37	658.40
7	673.93	778.47	763.54	713.48	667.69	716.05	523.04
8	673.93	733.94	667.69	508.43	763.54	582.50	564.05
9	673.93	820.58	414.09	756.76	585.61	823.78	738.13
10	835.91	410.29	414.09	713.48	423.78	885.54	819.82
11	673.93	935.60	925.93	630.63	763.54	700.08	633.78
12	264.34	410.29	585.61	679.21	785.67	749.50	759.38
13	417.96	778.47	740.74	643.12	763.54	700.08	630.63
14	186.92	820.58	828.17	542.49	585.61	358.03	693.69
15	591.08	778.47	785.67	571.06	763.54	664.15	620.03
16	264.34	778.47	585.61	643.12	667.69	661.31	738.13
17	673.93	550.46	585.61	630.63	667.69	819.19	321.56
18	264.34	756.53	763.54	693.69	740.74	614.01	578.38
19	528.68	661.57	828.17	508.43	763.54	686.49	581.41
20	417.96	733.94	828.17	696.55	656.17	739.37	520.03
21	417.96	620.58	828.17	658.40	738.98	664.88	598.27
22	560.75	466.97	740.74	630.63	746.95	661.15	567.57
23	417.96	661.57	794.77	713.48	754.92	657.42	520.03
24	373.83	661.57	803.20	829.47	762.89	653.69	780.05
25	186.92	756.53	411.62	696.55	770.86	649.96	807.60
26	373.83	756.53	620.05	756.76	778.84	646.23	693.69
27	560.75	480.23	828.47	693.69	786.81	642.50	761.99
28	591.08	550.46	736.90	848.43	794.78	638.77	633.78
29	264.34	589.72	445.32	761.99	802.75	635.04	649.27
30	591.08	581.27	553.74	398.85	810.72	631.31	682.13
Mean	471.42	663.27	665.48	663.11	667.75	656.71	644.93
SD	180.93	154.36	155.95	100.07	101.90	129.26	106.36

5. CZ content

Table C. 7 The entrapment efficiency (%) of CZ in PVP/HP β CD nanofiber mats.

Nanofibers (NF)	Loading efficiency (%)				
	1	2	3	Mean	SD
5% CZ loaded NF	97.22	94.36	95.72	95.77	1.43
10% CZ loaded NF	95.15	90.12	92.54	92.60	2.52
15% CZ loaded NF	90.45	99.23	99.87	96.52	5.27
20% CZ loaded NF	100.70	91.90	97.97	96.85	4.51

Table C. 8 The loading capacity (%) of CZ in PVP/HP β CD nanofiber mats.

Nanofibers (NF)	Loading capacity (%)				
	1	2	3	Mean	SD
5% CZ loaded NF	4.63	4.49	4.56	4.56	0.07
10% CZ loaded NF	8.65	8.19	8.41	8.42	0.23
15% CZ loaded NF	11.80	12.94	13.03	12.59	0.69
20% CZ loaded NF	16.78	15.32	16.33	16.14	0.75

6. Release study

Table C. 9 Cumulative release (%) of CZ from the PVP/HP β CD nanofiber mats containing 5% CZ.

Time (sec)	Cumulative CZ release (%)				
	1	2	3	Mean	SD
15	80.60	79.65	78.90	79.72	0.85
30	93.75	91.99	94.26	93.33	1.20
60	103.19	105.40	92.57	100.39	6.86
120	96.64	101.16	102.36	100.05	3.11
300	94.80	94.56	101.13	96.83	3.81
600	93.16	93.63	99.53	95.44	3.56

Table C. 10 Cumulative release (%) of CZ from the PVP/HP β CD nanofiber mats containing 10% CZ.

Time (sec)	Cumulative CZ release (%)				
	1	2	3	Mean	SD
15	68.25	65.49	68.67	67.47	1.73
30	81.52	83.87	79.76	81.72	2.09
60	89.19	90.21	92.41	90.60	1.66
120	99.93	101.30	105.84	102.36	3.08
300	96.47	97.63	97.68	97.26	0.63
600	95.68	96.63	96.43	96.25	0.45

Table C. 11 Cumulative release (%) of CZ from the PVP/HP β CD nanofiber mats containing 15% CZ.

Time (sec)	Cumulative CZ release (%)				
	1	2	3	Mean	SD
15	59.78	59.02	61.35	61.34	1.19
30	74.53	74.88	75.64	74.40	3.55
60	84.54	85.41	84.84	82.11	2.45
120	100.78	102.78	102.41	98.04	1.05
300	100.89	102.60	101.49	95.16	2.85
600	100.61	99.83	100.12	91.88	4.44

Table C. 12 Cumulative release (%) of CZ from the PVP/HP β CD nanofiber mats containing 20% CZ.

Time (sec)	Cumulative CZ release (%)				
	1	2	3	Mean	SD
15	57.17	55.04	56.09	61.34	1.07
30	69.51	69.12	68.86	74.40	5.32
60	82.62	88.08	85.02	82.11	2.74
120	90.15	92.14	91.66	98.04	1.04
300	96.45	96.25	95.19	95.16	3.67
600	89.83	90.12	89.61	91.88	0.26

Table C. 13 Cumulative release (%) of CZ from CZ powder.

Time (min)	Cumulative CZ release (%)				
	1	2	3	Mean	SD
1	6.11	6.00	6.19	6.10	0.85
5	6.12	6.49	6.03	6.22	1.07
10	6.21	6.59	6.43	6.41	3.82
15	6.81	6.76	6.78	6.78	4.10
30	7.17	7.33	7.05	7.18	1.61
60	10.19	9.05	9.31	9.52	2.61
120	23.31	22.04	22.61	22.65	2.80

Table C. 14 Cumulative release (%) of CZ from CZ lozenges.

Time (min)	Cumulative CZ release (%)				
	1	2	3	Mean	SD
1	6.32	6.24	6.65	6.40	2.85
5	6.89	6.90	7.01	6.93	1.31
10	7.32	7.18	7.46	7.32	3.60
15	7.77	7.84	7.80	7.80	4.16
30	9.02	8.60	8.93	8.85	0.98
60	15.11	14.45	14.83	14.80	1.45
120	25.08	25.82	26.18	25.69	2.46

7. Time kill analysis

Table C. 15 Viable cells of *C. albicans* (CFU/ml) at different treatment times (control).

Time (min)	Viable cells ($\times 10^4$ CFU/mL)				
	1	2	3	Mean	SD
15	5.00	4.80	4.50	4.77	0.25
30	5.80	6.10	5.60	5.83	0.25
60	5.80	7.10	6.20	6.37	0.67
120	7.50	7.80	7.80	7.70	0.17

Table C. 16 Viable cells of *C. albicans* (CFU/ml) at different treatment times after being treated with the blank PVP/HP β CD nanofibers containing (0% CZ loaded).

Time (min)	Viable cells ($\times 10^4$ CFU/mL)				
	1	2	3	Mean	SD
15	4.50	3.90	5.10	4.50	0.60
30	5.50	5.80	6.00	5.77	0.25
60	6.80	5.80	5.60	6.07	0.64
120	5.50	7.00	7.70	6.73	1.12

Table C. 17 Viable cells of *C. albicans* (CFU/ml) at different treatment times after being treated with the 5% CZ loaded PVP/HP β CD nanofibers.

Time (min)	Viable cells ($\times 10^4$ CFU/mL)				
	1	2	3	Mean	SD
15	4.20	3.90	4.10	4.07	0.15
30	3.60	4.00	4.10	3.90	0.26
60	3.50	3.00	3.50	3.33	0.29
120	0.00	0.00	0.00	0.00	0.00

Table C. 18 Viable cells of *C. albicans* (CFU/ml) at different treatment times after being treated with the 10% CZ loaded PVP/HP β CD nanofibers.

Time (min)	Viable cells ($\times 10^4$ CFU/mL)				
	1	2	3	Mean	SD
15	4.20	4.00	3.80	4.00	0.20
30	3.30	3.50	3.60	3.47	0.15
60	2.00	1.50	1.80	1.77	0.25
120	0.00	0.00	0.00	0.00	0.00

Table C. 19 Viable cells of *C. albicans* (CFU/ml) at different treatment times after being treated with 15% CZ loaded PVP/HP β CD nanofibers.

Time (min)	Viable cells ($\times 10^4$ CFU/mL)				
	1	2	3	Mean	SD
15	3.50	3.80	3.60	3.60	0.15
30	3.00	3.50	3.20	3.23	0.25
60	2.10	1.80	2.00	1.97	0.15
120	0.00	0.00	0.00	0.00	0.00

Table C. 20 Viable cells of *C. albicans* (CFU/ml) at different treatment times after being treated with the 20% CZ loaded PVP/HP β CD nanofibers.

Time (min)	Viable cells ($\times 10^4$ CFU/mL)				
	1	2	3	Mean	SD
15	3.00	3.40	3.30	3.23	0.21
30	2.60	3.50	2.80	2.97	0.47
60	1.40	1.30	1.30	1.33	0.06
120	0.00	0.00	0.00	0.00	0.00

Table C. 21 Viable cells of *C. albicans* (CFU/ml) at different treatment times after being treated with the 20% CZ loaded PVP/HP β CD nanofibers (equivalent to CZ 1 mg/mL in the tested solution).

Time (min)	Viable cells ($\times 10^4$ CFU/mL)				
	1	2	3	Mean	SD
5	4.40	4.00	4.70	4.37	0.35
15	3.80	3.90	3.40	3.70	0.26
30	2.50	3.90	3.50	3.30	0.72
60	1.62	2.40	2.70	2.24	0.56
120	0.00	0.00	0.00	0.00	0.00

Table C. 22 Viable cells of *C. albicans* (CFU/ml) at different treatment times after being treated with CZ powder (equivalent to CZ 1 mg/mL in the tested solution).

Time (min)	Viable cells ($\times 10^4$ CFU/mL)				
	1	2	3	Mean	SD
5	6.20	5.20	5.80	5.73	0.50
15	4.40	4.90	4.20	4.50	0.36
30	3.80	2.90	3.40	3.37	0.45
60	1.92	2.80	2.20	2.31	0.45
120	0.00	0.00	0.00	0.00	0.00

Table C. 23 Viable cells of *C. albicans* (CFU/ml) at different treatment times after being treated with CZ lozenges (equivalent to CZ 1 mg/mL in the tested solution).

Time (min)	Viable cells ($\times 10^4$ CFU/mL)				
	1	2	3	Mean	SD
5	6.10	5.90	5.80	5.93	0.15
15	5.00	4.60	4.80	4.80	0.20
30	3.00	3.20	4.40	3.53	0.76
60	1.87	2.90	2.20	2.32	0.53
120	0.00	0.00	0.00	0.00	0.00

8. Cytotoxicity

Table C. 24 The percentage cell viability of HGF cells after being incubated with CZ (0.1-100 μ g/mL) for 2 h.

CZ (μ g/mL)	HGF cell viability (%)				
	1	2	3	Mean	SD
0	100.00	100.00	100.00	100.00	0.00
0.1	100.14	94.13	87.48	98.30	6.33
0.5	98.90	76.38	79.22	84.94	12.27
1	85.16	82.00	71.84	74.60	6.96
5	70.74	75.88	67.58	69.97	4.18
10	70.60	68.50	74.59	36.14	3.09
50	30.22	33.25	32.42	26.16	1.57
100	29.12	23.88	23.28	100.00	3.21

Table C. 25 The percentage cell viability of HGF cells after being incubated with CZ (0.1-100 µg/mL) for 24 h.

CZ (µg/mL)	HGF cell viability (%)				
	1	2	3	Mean	SD
0	100.00	100.00	100.00	100.00	1.59
0.1	96.93	96.68	95.90	96.24	2.96
0.5	87.59	84.68	87.98	87.03	4.90
1	91.49	82.66	93.07	86.74	6.62
5	54.39	49.86	55.59	57.53	4.85
10	27.06	36.27	36.35	39.06	4.65
50	28.31	23.41	38.76	34.43	4.37
100	34.59	27.46	36.07	32.93	5.76

Table C. 26 The percentage cell viability of HGF cells after being incubated with various CZ loaded nanofibers for 2 and 24 h compared with the control.

Nanofibers (NF)	HGF cell viability (%)			
	2-h incubation		24-h incubation	
	Mean	SD	Mean	SD
Control	100.00	12.95	100.00	14.44
0% CZ loaded NF	98.01	7.65	100.85	7.10
5% CZ loaded NF	98.42	12.91	91.34	10.13
10% CZ loaded NF	96.19	6.35	85.58	9.86
15% CZ loaded NF	94.65	14.89	67.97	13.18
20% CZ loaded NF	95.98	5.06	66.55	15.27

Table C. 27 The percentage cell viability of HGF cells after being incubated with CZ powder and CZ lozenges for 2 and 24 h compared with the control.

Tested compound	HGF cell viability (%)			
	2-h incubation		24-h incubation	
	Mean	SD	Mean	SD
Control	100.00	0.30	100.00	4.29
CZ powder	98.01	7.65	68.46	10.60
CZ lozenges	92.13	6.32	53.77	7.28

Table C. 28 The percentage cell viability of the HGF cells derived from three different patients after being incubated with various CZ loaded nanofibers for 2 h compared with the control.

Nanofibers (NF)	HGF cell viability (%)					
	Patient#1		Patient#2		Patient#3	
	Mean	SD	Mean	SD	Mean	SD
Control	100.00	12.95	100.00	5.65	100.00	5.65
0% CZ loaded NF	98.01	7.65	99.44	8.33	101.44	7.49
5% CZ loaded NF	98.42	12.91	97.83	8.69	99.77	9.36
10% CZ loaded NF	96.19	6.35	96.28	3.29	97.32	8.03
15% CZ loaded NF	94.65	14.89	91.21	4.51	91.02	11.11
20% CZ loaded NF	95.98	5.06	90.17	12.52	93.60	9.90





APPENDIX D

มหาวิทยาลัยศิลปากร

CZ-microemulsion-containing nanofibers

1. Microemulsion composition

Table D. 1 Components of the microemulsion formulations.

Formulation	Oil phrase	Surfactant	Co-surfactant
F1	OA	T80	BzOH
F2	OA	T80	EtOH
F3	OA	T80	IPA

2. Solubility of CZ in the microemulsion formulations

Table D. 2 CZ solubility in different microemulsion formulations.

Formulation	Solubility (mg/g)				
	1	2	3	Mean	SD
F1	159.65	165.71	168.93	164.76	4.71
F2	135.07	140.30	138.24	137.87	2.63
F3	119.11	114.32	109.98	114.47	4.57

3. Size and charge measurement

Table D. 3 Particle size of the microemulsion formulations: F1, F2 and F3, with and without CZ.

Microemulsions	Particle size (nm)				
	1	2	3	Mean	SD
F1(O: T80: BzOH)	69.75	79.61	3.56	70.97	8.09
F2(O: T80: EtOH)	78.86	51.97	59.30	63.38	13.90
F3(O: T80: IPA)	68.15	70.37	56.51	65.01	7.44
F1+ 25 % w/w CZ	68.33	101.5	94.49	88.11	17.48
F2+25 % w/w CZ	49.06	58.96	65.39	57.80	8.23
F3+25 % w/w CZ	53.84	70.79	68.69	64.44	9.24

Table D. 4 Zeta potential of the microemulsion formulations: F1, F2 and F3, with and without CZ at pH 4.

Microemulsions	Zeta potential (mV)				
	1	2	3	Mean	SD
F1(O: T80: BzOH)	-25.60	-25.40	-26.30	-25.77	0.47
F2(O: T80: EtOH)	-25.90	-25.70	-25.20	-25.60	0.36
F3(O: T80: IPA)	-27.30	-26.00	-26.10	-26.47	0.72
F1+ 25 % w/w CZ	2.62	2.36	2.38	2.45	0.14
F2+25 % w/w CZ	-3.68	-3.10	-3.83	-3.54	0.38
F3+25 % w/w CZ	3.73	3.60	3.05	3.46	0.36

Table D. 5 Zeta potential of the microemulsion formulations: F1, F2 and F3, with and without CZ at pH 7.

Microemulsions	Zeta potential (mV)				
	1	2	3	Mean	SD
F1(O: T80: BzOH)	-35.6	-39.2	-39.6	-38.13	2.20
F2(O: T80: EtOH)	-40.8	-40.6	-39.3	-40.23	0.81
F3(O: T80: IPA)	-37.6	-38.7	-39.4	-38.57	0.91
F1+ 25 % w/w CZ	-17.8	-16.8	-18.1	-17.57	0.68
F2+25 % w/w CZ	-16.7	-17.0	-16.9	-16.87	0.15
F3+25 % w/w CZ	-16.4	-16.0	-17.8	-16.73	0.95

Table D. 6 Zeta potential of the microemulsion formulations: F1, F2 and F3, with and without CZ at pH 9.

Microemulsions	Zeta potential (mV)				
	1	2	3	Mean	SD
F1(O:T80: BzOH)	-42.3	-41	-41.2	-41.50	0.70
F2(O:T80: EtOH)	-58.3	-59.8	-58.1	-58.73	0.93
F3(O:T80: IPA)	-41.6	-42.2	-41.7	-41.83	0.32
F1+ 25 % w/w CZ	-39.5	-40	-38.9	-39.47	0.55
F2+25 % w/w CZ	-35.6	-38.7	-39.4	-37.90	2.02
F3+25 % w/w CZ	-37.1	-42.9	-38.4	-39.47	3.04

4. Spinning solution

Table D. 7 Conductivity of the microemulsion-containing spinning solutions.

Spinning solution	Conductivity (uS)				
	1	2	3	Mean	SD
CS-EDTA/PVA	770	763	775	769.33	6.03
CS-EDTA/PVA +F1+CZ	780	770	762	770.67	9.02
CS-EDTA/PVA +F2+CZ	832	848	838	839.33	8.08
CS-EDTA/PVA +F3+CZ	887	906	885	892.67	11.59

Table D. 8 pH of the microemulsion-containing spinning solutions.

Spinning solution	pH				
	1	2	3	Mean	SD
CS-EDTA/PVA	4.90	4.80	4.90	4.86	0.06
CS-EDTA/PVA +F1+CZ	5.20	5.10	5.00	5.10	0.10
CS-EDTA/PVA +F2+CZ	5.10	5.10	5.10	5.10	0.00
CS-EDTA/PVA +F3+CZ	5.00	5.10	5.10	5.07	0.60

Table D. 9 Viscosity of the microemulsion-containing spinning solutions.

Viscosity	Viscosity (cP)				
	1	2	3	Mean	SD
CS-EDTA/PVA	352.43	362.75	359.57	358.25	5.29
CS-EDTA/PVA +F1+CZ	352.43	357.99	362.75	357.72	5.17
CS-EDTA/PVA +F2+CZ	351.00	356.39	358.34	355.24	3.80
CS-EDTA/PVA +F3+CZ	358.78	355.60	354.81	356.40	2.10

5. Characterization of CZ-microemulsion-containing nanofibers

Table D. 10 Fiber diameters of the CZ-microemulsion incorporated nanofibers.

Nanofibers	Mean	SD
CS-EDTA/PVA	148.06	38.48
CS-EDTA/PVA +F1+CZ	120.58	25.32
CS-EDTA/PVA +F2+CZ	125.56	41.93
CS-EDTA/PVA +F3+CZ	105.91	18.13

Table D. 11 The tensile strength (MPa) of blank CS-EDTA/PVA nanofibers and the CZ-microemulsion incorporated nanofibers.

Nanofibers	Young's modulus (MPa/%)				
	1	2	3	Mean	SD
CS-EDTA/PVA	6.7	4.7	6.8	6.1	1.2
CS-EDTA/PVA +F1+CZ	5.8	3.9	4.6	4.8	0.9
CS-EDTA/PVA +F2+CZ	6.2	2.5	5.9	4.9	0.3
CS-EDTA/PVA +F3+CZ	2.3	2.6	3.4	2.8	0.6

Table D. 12 The *ex vivo* mucoadhesive properties of blank CS-EDTA/PVA nanofibers and the CZ-microemulsion incorporated nanofibers.

Nanofibers	Force (g)				
	1	2	3	Mean	SD
CS-EDTA/PVA	6.46	6.41	6.06	6.31	0.21
CS-EDTA/PVA +F1+CZ	4.29	4.04	4.55	4.29	0.25
CS-EDTA/PVA +F2+CZ	2.66	2.65	2.35	2.55	0.18
CS-EDTA/PVA +F3+CZ	3.18	2.94	3.17	3.10	0.14

Table D.13 The entrapment efficiency of CZ in the CZ-microemulsion incorporated nanofibers.

Nanofibers	Loading efficiency (%)				
	1	2	3	Mean	SD
CS-EDTA/PVA +F1+CZ	74.50	73.64	70.42	72.86	2.15
CS-EDTA/PVA +F2+CZ	68.33	77.07	72.34	72.58	4.38
CS-EDTA/PVA +F3+CZ	100.49	103.53	90.26	98.10	6.95

Table D.14 The loading capacity of CZ in the CZ-microemulsion incorporated nanofibers.

Nanofibers	Loading capacity (%)				
	1	2	3	Mean	SD
CS-EDTA/PVA +F1+CZ	7.45	7.36	7.04	7.29	0.22
CS-EDTA/PVA +F2+CZ	6.83	7.71	7.23	7.26	0.44
CS-EDTA/PVA +F3+CZ	10.05	10.35	9.03	9.81	0.70

6. Release study

Table D. 15 Cumulative release (%) of CZ from CZ lozenges.

Time (h)	Cumulative CZ release (%)				
	1	2	3	Mean	SD
0	0.00	0.00	0.00	0.00	0.00
0.5	19.32	23.11	19.32	21.82	2.19
1	33.99	37.60	33.99	32.84	2.08
2	58.38	59.00	58.38	55.00	0.36
4	70.42	69.36	70.42	68.21	0.61
8	71.64	69.74	71.64	68.46	1.10
24	72.58	77.08	72.58	75.00	2.60

Table D. 16 Cumulative release (%) of CZ from the CZ-microemulsion incorporated nanofibers (F1).

Time (h)	Cumulative CZ release (%)				
	1	2	3	Mean	SD
0	0.00	0.00	0.00	0.00	0.00
0.5	43.26	44.74	43.26	43.75	0.85
1	53.92	52.26	53.92	53.37	0.96
2	60.96	64.40	60.96	62.11	1.99
4	74.19	67.47	74.19	71.95	3.88
8	83.62	86.95	83.62	84.73	1.92
24	88.06	93.81	88.06	89.98	3.32

Table D. 17 Cumulative release (%) of CZ from the CZ-microemulsion incorporated nanofibers (F2).

Time (h)	Cumulative CZ release (%)				
	1	2	3	Mean	SD
0	0.00	0.00	0.00	0.00	0.00
0.5	31.13	34.69	31.13	32.32	2.06
1	46.26	45.84	46.26	46.12	0.24
2	56.39	51.51	56.39	54.76	2.82
4	74.83	67.77	74.83	72.48	4.08
8	89.25	78.11	89.25	85.54	6.43
24	94.19	99.55	94.19	95.98	3.09

Table D. 18 Cumulative release (%) of CZ from the CZ-microemulsion incorporated nanofibers (F3).

Time (h)	Cumulative CZ release (%)				
	1	2	3	Mean	SD
0	0.00	0.00	0.00	0.00	0.00
0.5	39.20	37.42	39.49	38.70	1.12
1	50.86	48.13	49.89	49.63	1.38
2	58.36	56.02	56.41	56.93	1.25
4	64.81	65.51	62.30	64.21	1.69
8	68.28	67.32	68.02	67.87	0.50
24	75.62	75.02	80.88	77.17	3.22

7. Time-kill analysis

Table D. 19 Viable cells of *C. albicans* (CFU/ml) at different treatment time points after being treated with the CZ lozenges.

Time (min)	Viable cells (CFU/mL)				
	1	2	3	Mean	SD
5	10300	10700	10100	10366.7	305.5
15	8000	8400	8700	8366.7	351.2
30	5500	5600	5800	5633.3	152.8
60	320	400	380	366.7	41.6
120	0	0	0	0	0

Table D. 20 Viable cells of *C. albicans* (CFU/ml) at different treatment time points after being treated with the CZ-microemulsion incorporated nanofibers (F1).

Time (min)	Viable cells (CFU/mL)				
	1	2	3	Mean	SD
5	1000	1400	1200	1200.0	200.0
15	800	1200	1100	1033.3	208.2
30	300	0	600	300.0	300.0
60	0	10	20	10.0	10.0
120	0	0	0	0	0

Table D. 21 Viable cells of *C. albicans* (CFU/ml) at different treatment time points after being treated with the CZ-microemulsion incorporated nanofibers (F2).

Time (min)	Viable cells (CFU/mL)				
	1	2	3	Mean	SD
5	5900	5400	5100	5466.7	404.1
15	1500	2100	1700	1766.7	305.5
30	160	900	600	553.3	372.2
60	10	0	0	3.3	5.8
120	0	0	0	0	0

Table D. 22 Viable cells of *C. albicans* (CFU/ml) at different treatment time points after being treated with the CZ-microemulsion incorporated nanofibers (F3).

Time (min)	Viable cells (CFU/mL)				
	1	2	3	Mean	SD
5	1800	2200	1900	1966.7	208.2
15	1400	1100	1500	1333.3	208.2
30	500	800	400	566.7	208.2
60	0	40	20	20.0	20.0
120	10	0	0	3.3	5.8

8. Cytotoxicity

Table D. 23 The percentage cell viability of HGF cells after being incubated with CZ the CZ-microemulsion incorporated nanofibers for 2 h compared with the control.

Replication	HGF cell viability (%)			
	Control	F1	F2	F3
1	112.73	88.42	88.86	92.62
2	108.31	87.98	95.93	91.07
3	91.95	91.51	82.45	98.14
4	96.15	94.83	103.45	72.28
5	90.85	91.29	91.07	97.48
Mean	100.00	90.80	92.35	90.32
SD	9.93	2.77	7.87	10.53

Table D. 24 The percentage cell viability of HGF cells after being incubated with CZ the CZ-microemulsion incorporated nanofibers for 24 h compared with the control.

Replication	HGF cell viability (%)			
	Control	F1	F2	F3
1	85.82	58.24	51.72	48.28
2	98.08	59.77	60.92	45.59
3	111.11	74.33	68.58	76.63
4	109.20	59.00	77.39	59.39
5	95.79	46.36	54.79	47.13
Mean	100.00	59.54	62.68	55.40
SD	10.37	9.93	10.45	13.06





APPENDIX E

CZ-incorporated mucoadhesive sandwich nanofibers

1. Fiber diameter

Table E. 1 Fiber diameters of PVP/HP β CD nanofibers, CS/PVA nanofibers and CS-SH/PVA nanofibers.

No. Nanofibers	Fiber diameter (nm)		
	PVP/HP β CD	CS/PVA	CS-SH/PVA
1	413.22	197.64	160.78
2	443.45	200.10	183.86
3	473.78	237.99	222.96
4	526.53	182.22	254.22
5	525.62	187.50	191.80
6	504.19	182.22	201.90
7	309.72	156.25	199.42
8	431.39	168.29	169.80
9	515.48	197.64	229.55
10	383.11	197.64	157.66
11	464.58	182.22	160.78
12	464.58	227.50	227.38
13	499.41	197.64	211.52
14	510.81	200.10	282.03
15	481.81	197.64	230.14
16	484.79	182.22	157.66
17	598.51	176.78	189.19
18	540.91	168.29	229.55
19	464.58	125.00	183.86
20	443.45	220.97	169.80
21	443.45	182.22	189.19
22	515.10	156.25	165.66
23	464.58	237.99	180.42
24	638.17	182.22	191.80
25	431.39	176.78	191.80
26	447.30	220.97	199.42
27	380.21	237.99	199.42
28	450.82	139.75	211.52
29	524.66	197.64	222.96
30	527.44	168.29	220.72
Mean	476.77	189.53	199.56
SD	64.28	27.51	29.84

2. Mechanical testing

Table E. 2 The mechanical properties of CS/PVA coated PVP/HP β CD sandwich nanofibers at 3 h coated times.

No.	Thickness (μm)			Average	Contact Area (mm^2)	Product Width (mm)	Stress (MPa)	Strain (%)	Y-Modulus (MPa/%)
1	27	22	22	23.67	0.142	0.024	5.8432	2.676	2.721
2	18	25	29	24.00	0.144	0.024	8.8459	4.556	2.763
3	33	36	35	34.67	0.208	0.035	5.6014	3.056	2.371
4	38	37	33	36.00	0.216	0.036	5.5953	4.296	1.828
5	28	21	28	25.67	0.154	0.026	6.5235	2.636	3.252
6	33	31	25	29.67	0.178	0.030	5.7884	2.956	2.478

Table E. 3 The mechanical properties of CS-SH/PVA coated PVP/HP β CD sandwich nanofibers at 3 h coated times.

No.	Thickness (μm)			Average	Contact Area (mm^2)	Product Width (mm)	Stress (MPa)	Strain (%)	Y-Modulus (MPa/%)
1	7	6	3	5.33	0.032	0.005	11.2021	3.036	4.247
2	14	9	14	12.33	0.074	0.012	6.2356	3.376	2.139
3	9	10	5	8.00	0.048	0.008	5.8825	2.536	2.396
4	6	8	10	8.00	0.048	0.008	8.5853	3.476	3.049
5	10	5	6	7.00	0.042	0.007	9.1597	3.696	2.667
6	3	10	15	9.33	0.056	0.009	4.6613	2.836	2.271

Table E. 4 The mechanical properties of CS/PVA coated 20% CZ loaded PVP/HP β CD sandwich nanofibers at 3 h coated times.

No.	Thickness (μm)			Average	Contact Area (mm^2)	Product Width (mm)	Stress (MPa)	Strain (%)	Y-Modulus (MPa/%)
1	33	41	33	35.67	0.214	0.036	6.1790	2.456	2.565
2	44	45	42	43.67	0.262	0.044	5.1200	2.916	2.100
3	52	54	55	53.67	0.322	0.054	3.4520	2.636	1.664
4	28	41	33	34.00	0.204	0.034	6.1000	2.416	3.120
5	44	50	43	45.67	0.274	0.046	2.5500	2.156	1.431
6	41	40	42	41.00	0.246	0.041	5.8030	3.636	2.248

Table E. 5 The mechanical properties of CS-SH/PVA coated 20% CZ loaded PVP/HP β CD sandwich nanofibers at 3 h coated times.

No.	Thickness (μm)			Average	Contact Area (mm^2)	Product Width (mm)	Stress (MPa)	Strain (%)	Y-Modulus (MPa/%)
1	21	24	21	22.00	0.132	0.022	11.4382	4.536	2.522
2	14	15	19	16.00	0.096	0.016	8.1209	5.496	1.478
3	26	16	12	18.00	0.108	0.018	7.9067	3.416	2.315
4	12	16	18	15.33	0.092	0.015	9.1556	3.616	2.532
5	13	15	17	15.00	0.090	0.015	12.5718	5.676	2.215
6	17	14	14	15.00	0.090	0.015	10.6519	4.156	2.563

Table E. 6 The mechanical properties of CS/PVA coated 20% CZ loaded PVP/HP β CD sandwich nanofibers at 6 h coated times.

No.	Thickness (μm)			Average	Contact Area (mm^2)	Product Width (mm)	Stress (MPa)	Strain (%)	Y-Modulus (MPa/%)
1	87	89	90	88.67	0.532	0.089	9.6371	3.116	3.093
2	73	77	90	80.00	0.480	0.080	14.0644	3.616	3.890
3	62	64	61	62.33	0.374	0.062	11.1743	3.636	3.073
4	76	79	76	77.00	0.462	0.077	10.4671	3.256	3.215
5	65	61	67	64.33	0.386	0.064	11.1797	3.756	2.976
6	74	87	83	81.33	0.488	0.081	8.4170	3.076	2.736

Table E. 7 The mechanical properties of CS-SH/PVA coated 20% CZ loaded PVP/HP β CD sandwich nanofibers at 6 h coated times.

No.	Thickness (μm)			Average	Contact Area (mm^2)	Product Width (mm)	Stress (MPa)	Strain (%)	Y-Modulus (MPa/%)
1	15	16	22	17.67	0.106	0.018	10.3700	5.996	1.729
2	20	20	25	21.67	0.130	0.022	9.0413	3.176	2.847
3	22	16	16	18.00	0.108	0.018	8.6201	3.296	2.615
4	13	15	17	15.00	0.090	0.015	12.7498	3.216	3.964
5	13	13	18	14.67	0.088	0.015	11.4097	3.616	3.155
6	13	17	23	17.67	0.106	0.018	12.3473	3.476	3.552

3. Mucoadhesive properties

Table E. 8 Mucoadhesive properties of CS/PVA coated PVP/HP β CD sandwich nanofibers and CS/PVA coated PVP/HP β CD sandwich nanofibers with/without CZ at 3 h and 6 h coated times.

Tested Nanofibers	<i>Ex vivo</i> mucoadhesive strength (g)						
	1	2	3	4	5	Mean	SD
CS/PVA coated PVP/HP β CD (3h coated)	3.7	3.1	3.6	3.7	3.6	3.5	0.5
CS/PVA coated PVP/HP β CD/CZ (3h coated)	3.3	3.2	3.4	3.2	3.4	3.3	0.1
CS/PVA coated PVP/HP β CD/CZ (6h coated)	5.1	3.8	4.5	3.7	4.3	4.3	0.7
CS-SH/PVA coated PVP/HP β CD (3h coated)	4.1	3.8	3.4	3.3	3.8	3.7	0.3
CS-SH/PVA coated PVP/HP β CD/CZ (3h coated)	3.7	4.2	4.0	4.0	3.7	3.9	0.2
CS-SH/PVA coated PVP/HP β CD/CZ (6h coated)	4.5	4.9	6.7	6.0	5.1	5.4	0.8

4. CZ content

Table E. 9 The entrapment efficiency (%) of CZ in CS/PVA coated PVP/HP β CD sandwich nanofibers and CS/PVA coated PVP/HP β CD sandwich nanofibers

Nanofibers (NF)	Loading efficiency (%)				
	1	2	3	Mean	SD
CS/PVA coated PVP/HP β CD/CZ (3h coated)	84.77	89.45	82.50	85.57	7.08
CS/PVA coated PVP/HP β CD/CZ (6h coated)	85.55	90.02	93.06	89.54	7.56
CS-SH/PVA coated PVP/HP β CD/CZ (3h coated)	90.86	91.66	94.26	92.26	3.55
CS-SH/PVA coated PVP/HP β CD/CZ (6h coated)	85.58	88.76	84.85	86.40	4.16

Table E. 10 The loading capacity (%) of CZ in CS/PVA coated PVP/HP β CD sandwich nanofibers and CS/PVA coated PVP/HP β CD sandwich nanofibers

Nanofibers (NF)	Loading capacity (%)				
	1	2	3	Mean	SD
CS/PVA coated PVP/HP β CD/CZ (3h coated)	16.95	17.89	16.50	17.11	0.71
CS/PVA coated PVP/HP β CD/CZ (6h coated)	17.11	18.00	18.61	17.91	0.76
CS-SH/PVA coated PVP/HP β CD/CZ (3h coated)	18.17	18.33	18.85	18.45	0.36
CS-SH/PVA coated PVP/HP β CD/CZ (6h coated)	17.12	17.75	16.97	17.28	0.42

5. Release study

Table E. 11 Cumulative release (%) of CZ from the CS/PVA coated PVP/HP β CD/CZ sandwich nanofibers (3 h coated time).

Time (h)	Cumulative CZ release (%)				
	1	2	3	Mean	SD
0	0.00	0.00	0.00	0.00	0.00
0.15	29.86	24.89	7.06	27.50	5.99
0.25	33.55	33.43	8.42	33.36	4.35
0.5	48.04	48.87	12.13	48.45	4.62
1	57.68	58.36	13.98	56.62	4.91
2	66.53	66.32	15.55	63.80	5.32
4	79.92	79.41	18.32	75.80	5.80
8	87.61	86.84	21.36	89.10	5.13

Table E. 12 Cumulative release (%) of CZ from the CS/PVA coated PVP/HP β CD/CZ sandwich nanofibers (6 h coated time).

Time (h)	Cumulative CZ release (%)				
	1	2	3	Mean	SD
0	0.00	0.00	0.00	0.00	0.00
0.15	16.60	17.22	18.60	17.47	4.80
0.25	30.77	27.91	32.14	30.27	5.57
0.5	40.53	37.51	38.62	38.89	5.14
1	51.31	50.68	52.24	51.41	4.60
2	64.42	68.24	62.44	65.03	6.18
4	74.66	77.45	72.47	74.86	5.83
8	74.04	79.78	78.74	77.52	6.20

Table E. 13 Cumulative release (%) of CZ from the CS-SH/PVA coated PVP/HP β CD/CZ sandwich nanofibers (3 h coated time).

Time (h)	Cumulative CZ release (%)				
	1	2	3	Mean	SD
0	0.00	0.00	0.00	0.00	0.00
0.15	24.74	31.14	38.29	31.39	8.79
0.25	42.38	39.36	34.64	38.80	6.92
0.5	49.79	48.47	48.25	48.84	4.77
1	65.25	59.63	63.42	62.77	6.13
2	68.08	70.85	66.55	68.49	5.69
4	78.03	79.95	77.05	78.34	5.18
8	81.25	87.81	82.96	84.00	6.48

Table E. 14 Cumulative release (%) of CZ from the CS-SH/PVA coated PVP/HP β CD/CZ sandwich nanofibers (6 h coated time).

Time (h)	Cumulative CZ release (%)				
	1	2	3	Mean	SD
0	0.00	0.00	0.00	0.00	0.00
0.15	22.40	23.12	21.87	60.74	4.69
0.25	28.66	33.78	34.05	82.04	6.33
0.5	44.36	44.65	42.04	67.98	5.25
1	52.56	53.87	47.27	85.92	6.63
2	65.38	62.09	67.70	80.99	6.25
4	78.86	70.10	71.48	97.07	7.49
8	80.33	79.13	79.73	60.03	4.63

6. Time-kill analysis

Table E. 15 Viable cells of *C. albicans* (CFU/ml) at different treatment times (control).

Time (min)	Viable cells x(10 ⁴ CFU/mL)				
	1	2	3	Mean	SD
5	3.00	2.70	2.80	2.83	0.15
15	3.20	2.90	3.30	3.13	0.21
30	3.50	3.40	3.10	3.33	0.21
60	3.60	3.80	4.20	3.87	0.31
120	6.20	6.90	6.00	6.37	0.47

Table E. 16 Viable cells of *C. albicans* (CFU/ml) at different treatment times after being treated with the CS-SH/PVA coated PVP/HP β CD/CZ sandwich nanofibers (3 h coated time).

Time (min)	Viable cells x(10 ⁴ CFU/mL)				
	1	2	3	Mean	SD
5	2.30	2.50	2.60	2.47	0.15
15	1.51	1.89	1.88	1.76	0.22
30	1.43	0.95	0.99	1.12	0.27
60	1.17	0.86	0.54	0.86	0.32
120	0.19	0.13	0.21	0.18	0.04

Table E. 17 Viable cells of *C. albicans* (CFU/ml) at different treatment times after being treated with the CS-SH/PVA coated PVP/HP β CD/CZ sandwich nanofibers (6 h coated time).

Time (min)	Viable cells x(10 ⁴ CFU/mL)				
	1	2	3	Mean	SD
5	2.60	2.40	2.50	2.50	0.10
15	2.20	1.90	2.00	2.03	0.15
30	1.74	1.59	1.67	1.67	0.08
60	1.50	1.09	1.07	1.22	0.24
120	0.13	0.23	0.24	0.20	0.06

Table E. 18 Viable cells of *C. albicans* (CFU/ml) at different treatment times after being treated with the CS /PVA coated PVP/HP β CD/CZ sandwich nanofibers (3 h coated time).

Time (min)	Viable cells x(10 ⁴ CFU/mL)				
	1	2	3	Mean	SD
5	2.40	2.30	2.50	2.40	0.10
15	2.20	1.90	1.70	1.93	0.25
30	1.30	1.03	1.40	1.24	0.19
60	0.86	0.77	0.79	0.81	0.05
120	0.11	0.18	0.12	0.14	0.04

Table E. 19 Viable cells of *C. albicans* (CFU/ml) at different treatment times after being treated with the CS/PVA coated PVP/HP β CD/CZ sandwich nanofibers (6 h coated time).

Time (min)	Viable cells x(10 ⁴ CFU/mL)				
	1	2	3	Mean	SD
5	2.60	2.40	2.70	2.57	0.15
15	2.10	2.40	2.00	2.17	0.21
30	1.84	1.56	1.45	1.62	0.20
60	0.97	1.23	1.09	1.10	0.13
120	0.21	0.25	0.32	0.26	0.06

Table E. 20 Viable cells of *C. albicans* (CFU/ml) at different treatment times after being treated with CZ lozenges.

Time (min)	Viable cells x(10 ⁴ CFU/mL)				
	1	2	3	Mean	SD
5	2.90	2.50	2.70	2.70	0.20
15	2.30	2.10	2.16	2.19	0.10
30	1.57	1.67	1.60	1.61	0.05
60	1.48	0.93	0.77	1.06	0.37
120	0.18	0.11	0.09	0.13	0.05

7. Cytotoxicity study

Table E. 21 The percentage cell viability of HGF cells after being incubated with various sandwich nanofibers for 2 and 24 h compared with the control.

Nanofibers (NF)	HGF cell viability (%)			
	2-h incubation		24-h incubation	
	Mean	SD	Mean	SD
Control	100.00	4.15	100.00	3.67
CS-SH/PVA coated PVP/HP β CD	93.51	7.41	81.11	4.24
CS/PVA coated PVP/HP β CD	93.87	5.46	80.63	1.67
CS-SH/PVA coated (3h) PVP/HP β CD with 20% CZ	84.02	1.86	72.09	4.56
CS-SH/PVA coated (6h) PVP/HP β CD with 20% CZ	83.63	2.28	70.94	1.87
CS/PVA coated (3h) PVP/HP β CD with 20% CZ	86.13	4.42	71.34	4.84
CS/PVA coated (6h) PVP/HP β CD with 20% CZ	85.31	3.73	72.54	2.60

Table E. 22 The percentage cell viability of the HGF cells derived from three different patients after being incubated with various sandwich nanofibers for 24 h compared with the control.

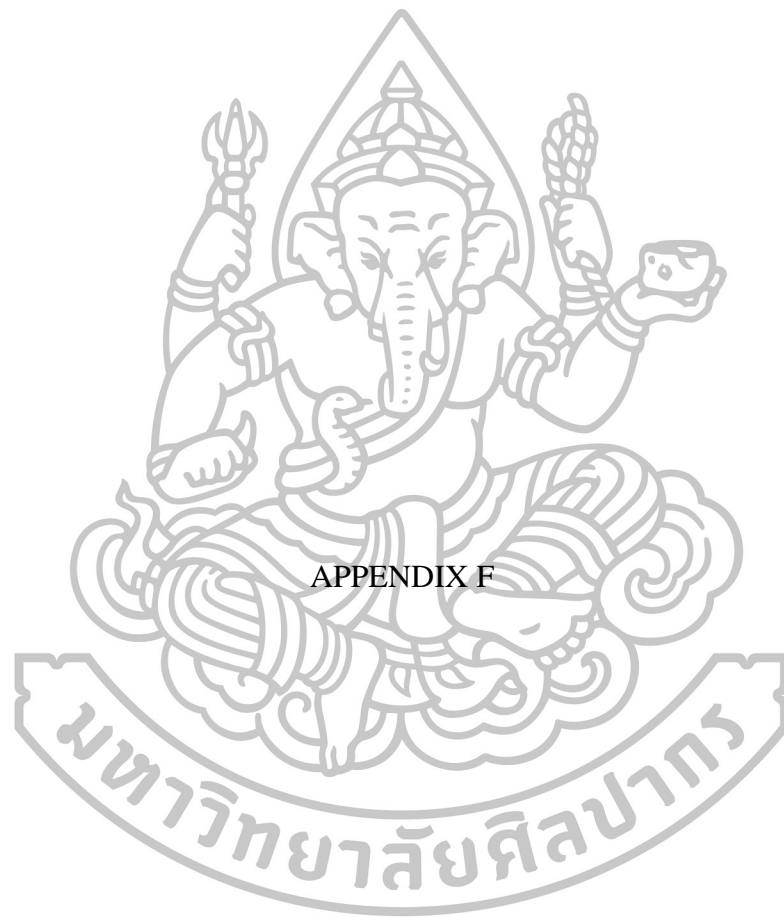
Nanofibers (NF)	HGF cell viability (%)					
	Patient#1		Patient#2		Patient#3	
	Mean	SD	Mean	SD	Mean	SD
Control	100.00	3.67	100.00	1.70	100.00	3.58
CS-SH/PVA coated PVP/HP β CD	81.11	4.24	80.39	2.51	85.35	3.44
CS/PVA coated PVP/HP β CD	80.63	1.67	80.51	3.15	85.87	1.35
CS-SH/PVA coated (3h) PVP/HP β CD with 20% CZ	72.09	4.56	73.11	1.19	69.41	6.90
CS-SH/PVA coated (6h) PVP/HP β CD with 20% CZ	70.94	1.87	74.06	2.32	70.21	5.77
CS/PVA coated (3h) PVP/HP β CD with 20% CZ	71.34	4.84	72.83	6.77	71.23	7.78
CS/PVA coated (6h) PVP/HP β CD with 20% CZ	72.54	2.60	70.94	3.49	73.64	4.82

8. *In vivo* release study

Table E. 23 CZ concentration at different time points in the saliva of seven different subjects after application of the CS-SH/PVA coated PVP/HP β CD/CZ sandwich nanofibers (6 h coated time).

Time (min)	CZ concentration ($\mu\text{g/mL}$)					
	5	10	15	20	25	30
subject 1	98.64	94.74	185.98	200.45	253.54	82.88
subject 2	135.71	105.13	135.80	88.52	148.92	86.70
subject 3	152.77	258.17	75.20	76.27	85.65	49.37
subject 4	137.94	70.53	287.35	273.72	119.60	79.58
subject 5	74.58	322.29	469.81	187.47	256.13	91.37
subject 6	205.91	47.26	87.55	96.47	79.63	148.33
subject 7	302.63	128.01	367.97	67.06	124.93	71.89
average	158.31	146.59	229.95	141.42	152.63	87.16
SD	75.96	103.06	149.94	79.27	73.69	30.27





APPENDIX F

Stability study

Table F. 1 Fiber diameters (nm) of the fast dissolving CZ loaded PVP/HP β CD nanofibers after being kept under long-term condition and accelerated condition for 1 and 3 months.

No.	Fiber diameter (nm)				
	Long-term condition			Accelerated condition	
	initial	1 month	3 months	1 month	3 months
1	349.97	339.75	348.72	380.97	272.73
2	316.34	313.61	305.05	333.15	302.64
3	291.10	317.94	312.12	288.67	234.92
4	359.93	358.81	304.60	272.73	273.60
5	270.62	323.27	362.98	339.75	249.85
6	272.57	329.13	336.96	331.51	206.78
7	285.48	286.89	359.26	391.58	263.04
8	271.72	303.21	332.85	365.98	256.33
9	340.40	367.00	285.95	311.54	295.68
10	301.80	332.74	294.28	370.06	342.45
11	354.94	316.76	228.33	347.50	297.98
12	322.45	340.75	356.25	323.27	351.41
13	300.81	390.62	329.20	288.67	210.70
14	347.32	314.16	308.66	371.44	286.41
15	358.92	337.13	319.25	230.22	321.47
16	367.30	325.69	327.56	370.06	263.56
17	343.01	333.15	300.61	269.83	280.75
18	341.27	284.97	353.98	311.10	269.83
19	401.68	359.20	356.25	249.85	222.53
20	283.97	329.03	319.25	295.68	243.07
21	380.99	330.79	319.67	371.17	235.21
22	284.67	321.47	284.53	327.78	190.80
23	320.70	277.81	343.29	318.05	380.97
24	279.75	391.58	330.42	298.55	225.58
25	315.72	289.73	396.59	280.99	263.04
26	323.78	337.23	316.29	340.75	337.23
27	317.49	282.93	329.20	281.11	353.06
28	374.07	348.68	336.37	272.85	296.26
29	277.50	410.57	319.67	280.99	256.33
30	306.47	349.56	403.64	292.43	418.23
Mean	322.09	331.47	327.39	316.94	280.08
SD	36.56	32.25	33.91	42.08	53.46

Table F. 2 Fiber diameters (nm) of the CZ-microemulsion-containing nanofibers after being kept under long-term condition and accelerated condition for 1 and 3 months.

No.	Fiber diameters				
	Long-term condition			Accelerated condition	
	Initial	1 month	3 months	1 month	3 months
1	145.60	286.93	122.14	257.15	-
2	126.49	160.32	128.58	171.57	-
3	107.70	107.92	100.40	100.40	-
4	120.00	80.16	128.58	152.93	-
5	116.62	107.92	117.09	160.64	-
6	107.70	107.92	108.14	140.56	-
7	116.62	89.62	100.40	141.99	-
8	134.16	100.20	100.40	82.79	-
9	100.00	100.20	100.40	102.39	-
10	100.00	107.92	60.24	127.00	-
11	107.70	100.20	100.40	189.44	-
12	121.66	107.92	89.80	117.09	-
13	120.00	102.18	102.39	56.80	-
14	116.62	100.20	80.32	80.32	-
15	80.00	100.20	117.09	80.32	-
16	100.00	113.36	156.83	80.32	-
17	84.85	89.62	120.48	63.50	-
18	140.00	100.20	89.80	102.39	-
19	121.66	72.26	102.39	100.40	-
20	128.06	60.12	100.40	89.80	-
21	144.22	80.16	82.79	80.32	-
22	107.70	134.43	100.40	89.80	-
23	80.00	89.62	20.08	85.19	-
24	160.00	100.20	161.89	100.40	-
25	140.00	89.62	120.48	134.70	-
26	101.98	102.18	100.40	127.00	-
27	100.00	82.63	60.24	179.60	-
28	100.00	82.63	89.80	146.19	-
29	101.98	72.26	63.50	179.60	-
30	116.62	82.63	82.79	72.40	-
Mean	114.93	103.72	100.29	119.77	-
SD	19.41	39.44	28.07	45.48	-

Table F.3 Fiber diameters (nm) of the CS-SH/PVA coated 20% CZ loaded PVP/HP β CD sandwich nanofibers after being kept under long-term condition and accelerated condition for 1 and 3 months.

No.	Fiber diameters				
	Long-term condition			Accelerated condition	
	initial	1 month	3 month	1 month	3 month
1	109.87	185.06	235.59	223.83	189.06
2	153.06	158.39	163.44	210.93	170.59
3	131.42	146.98	157.32	163.85	162.70
4	119.28	144.69	150.00	219.75	189.06
5	172.79	167.18	164.21	200.97	196.33
6	142.41	134.14	158.15	231.35	192.69
7	139.00	147.41	125.06	277.39	174.20
8	188.77	147.18	161.92	280.76	200.00
9	149.78	176.57	199.42	310.82	225.99
10	210.85	153.39	163.67	156.92	266.79
11	222.30	163.86	140.32	151.71	201.21
12	149.09	174.89	172.19	183.63	227.21
13	198.83	160.02	145.28	204.26	197.74
14	149.89	181.53	181.76	178.53	147.06
15	197.28	152.94	165.57	193.07	139.82
16	196.15	166.07	151.81	146.20	178.03
17	123.36	190.52	130.61	188.32	206.89
18	197.88	155.74	178.15	237.47	179.19
19	181.66	162.70	149.45	140.47	181.59
20	181.66	148.93	144.85	204.68	277.47
21	184.93	133.36	160.70	180.15	156.96
22	219.20	149.74	170.21	161.75	194.83
23	222.30	137.70	151.53	171.99	166.59
24	120.56	161.27	169.45	199.86	200.09
25	160.90	159.41	173.36	218.34	191.61
26	194.66	149.98	149.97	167.26	137.70
27	175.93	183.61	183.67	123.36	176.47
28	116.96	169.42	177.79	160.58	119.98
29	176.31	171.61	132.71	225.73	176.86
30	159.73	152.83	175.03	212.63	171.80
Mean	168.23	159.57	162.77	197.55	186.55
SD	33.53	14.98	21.71	42.86	33.55

Table F. 4 The Percentage of the remaining CZ content in the fast dissolving CZ loaded PVP/HP β CD nanofibers after being kept under long-term condition and accelerated condition for 1 and 3 months.

No.	Long-term condition		Accelerated condition	
	1 month	3 months	1 month	3 months
1	92.87	90.69	92.98	90.36
2	98.90	94.91	96.62	95.94
3	105.90	103.58	97.23	99.87
Mean	99.22	96.39	95.61	95.39
SD	6.52	6.57	2.30	4.78

Table F. 5 The Percentage of the remaining CZ content in the CZ-microemulsion-containing nanofibers after being kept under long-term condition and accelerated condition for 1 and 3 months.

No.	Long-term condition		Accelerated condition	
	1 month	3 months	1 month	3 months
1	92.22	110.50	114.45	98.37
2	102.27	85.08	89.96	84.80
3	94.01	88.05	85.76	88.06
Mean	96.17	94.54	96.72	90.41
SD	5.36	13.90	15.49	7.08

Table F. 6 The Percentage of the remaining CZ content in the CS-SH/PVA coated 20% CZ loaded PVP/HP β CD sandwich nanofibers after being kept under long-term condition and accelerated condition for 1 and 3 months.

No.	Long-term condition		Accelerated condition	
	1 month	3 months	1 month	3 months
1	92.88	96.07	90.24	87.75
2	112.22	112.52	98.14	98.55
3	87.78	88.21	91.76	87.12
Mean	97.63	98.93	93.38	91.14
SD	12.89	12.41	4.19	6.42



BIOGRAPHY

Name	Prasopchai Tonglairoum, Mr
Date of Birth	December 24, 1988
Place of Birth	Suphanburi, Thailand
Nationality/Religion	Thai/Buddhism
E-mail address	tonglairoum_p@su.ac.th; tonglairoum@gmail.com
Education	
2012-2016	Doctor of Philosophy, Ph.D. in Pharmaceutical Technology, Silpakorn University, Thailand
2007-2011	Bachelor of Pharmacy (1 st Class Honours), in Pharmaceutical Technology, Silpakorn University, Thailand
Scholarship	Thailand Research Funds through the golden Jubilee Ph.D. Program (Grant No. PHD/0092/2554) Newton UK-Thailand and Research and Innovation Partnership Fund (Ph.D. Placement)
Research training	
2015-2016	Pharmacy Research Ad Hoc (Development of mucoadhesive nanomaterial for drug delivery) at School of Chemistry, Food and Pharmacy, University of Reading, United Kingdom.

Presentation

Poster

1. Todsapon Nitanan, **Prasopchai Tonglairoum**, Prasert Akkaramongkolporn, Theerasak Rojanarata, Tanasait Ngawhirunpat, Praneet Opanasopit. "Electrospun polystyrene sulfonic acid-co-maleic acid/polyvinyl alcohol blend ion exchange fibers" The 29th Annual Research Conference in Pharmaceutical Sciences, 6-7 December 2012, Chulalongkorn University Bangkok, Thailand.

2. **Prasopchai Tonglairoum**, Tanasait Ngawhirunpat, Theerasak Rojanarata, Ruchadaporn Kaomongkolgit and Praneet Opanasopit. “Preparation and characterization of fast dissolved-clotrimazole composited PVP/HP β CD nanofibers for oral candidiasis application” 15th Asian Chemical Congress, 19-23 August 2013, Sentosa, Singapore.
3. **Prasopchai Tonglairoum**, Tanasait Ngawhirunpat, Theerasak Rojanarata, Ruchadaporn Kaomongkolgit and Praneet Opanasopit. “Fabrication and evaluation of clotrimazole-loaded PVP/HP β CD nanofiber mats for oral candidiasis” The 30th Annual Research Conference in Pharmaceutical Sciences, 10-11 January 2014, Chulalongkorn University Bangkok, Thailand.
4. **Prasopchai Tonglairoum**, Wanchai Sutananta, Theerasak Rojanarata, Tanasait Ngawhirunpat, Praneet Opanasopit: Thermally Crosslinked Chitosan-EDTA/PVA Electrospun Nanofiber Mats: Crosslinking Conditions. PHARMATECH 2014, 3rd International Conference and Exhibition on Pharmaceutical, Nutraceutical and Cosmeceutical Technology. QSNCC - Queen Sirikit National Convention Center. Bangkok, Thailand.
5. **Prasopchai Tonglairoum**, Theerasak Rojanarata, Tanasait Ngawhirunpat, Ruchadaporn Kaomongkolgit, Wanchai Sutananta and Praneet Opanasopit. Fabrication and evaluation of erythrosine-loaded fast dissolving electrospun PVP/HP β CD patches for dental plaque disclosing. 2017 Seoul International Conference on Engineering and Applied Science (SICEAS). February 7-9, 2017 Seoul, South Korea.

Oral

1. **Prasopchai Tonglairoum**, Tanasait Ngawhirunpat, Theerasak Rojanarata, Ruchadaporn Kaomongkolgit and Praneet Opanasopit. “Fabrication of clotrimazole composite polymer-base sandwich nanofiber mats for oral candidiasis application” The 3rd Current Drug Development International Conference, Pavilion Queen's Bay Krabi, Ao Nang Beach, Krabi, Thailand.

2. **Prasopchai Tonglairoum**, Tanasait Ngawhirunpat, Theerasak Rojanarata, and Praneet Opanasopit. “Electrospun polystyrene sulfonic acid-co-maleic acid/polyvinyl alcohol nanofiber mats loaded with lysozyme for wound recuperation” The 7th Annual Northeast Pharmacy Research Conference of 2015, Faculty of Pharmaceutical Sciences, Khon Kaen University, Thailand.
3. **Prasopchai Tonglairoum**, Tanasait Ngawhirunpat, Theerasak Rojanarata, Ruchadaporn Kaomongkolgit and Praneet Opanasopit. Preparation and characterization of herbal oil-encapsulated PVP/ HP β CD nanofiber mats for oral candidiasis. 26th FAPA congress 2016. 9-13 November 2016. Bangkok, Thailand.

Scientific Publication:

1. **Prasopchai Tonglairoum**, Ruairi P Brannigan, Praneet Opanasopit, Vitaliy V Khutoryanskiy. Maleimide-bearing nanogels as novel mucoadhesive materials for drug delivery. *Journal of Materials Chemistry B*. 2016;4(40):6581-7.
2. **Prasopchai Tonglairoum**, Tanasait Ngawhirunpat, Theerasak Rojanarata, Prasert Akkaramongkolporn, Nattawat Nattapulwat and Praneet Opanasopit. The utilization of surface free energy for predicting flowability of filler-lubricant or filler-glidant mixtures. *Indian Journal of Pharmaceutical Sciences*. 2016; 78(6): 942.
3. **Prasopchai Tonglairoum**, Thisirak Woraphatphadung, Tanasait Ngawhirunpat, Theerasak Rojanarata, Prasert Akkaramongkolporn, Warayuth Sajomsang, Praneet Opanasopit: Development and evaluation of N-naphthyl-N,O-succinyl chitosan micelles containing clotrimazole for oral candidiasis treatment. *Pharmaceutical Development and Technology*. 2016 (in press)
4. **Prasopchai Tonglairoum**, Tanasait Ngawhirunpat, Theerasak Rojanarata, Ruchadaporn Kaomongkolgit, Praneet Opanasopit. Fabrication and evaluation of nanostructured herbal oil/hydroxypropyl- β -cyclodextrin/

polyvinylpyrrolidone mats for denture stomatitis prevention and treatment. AAPS PharmSciTech. 2016 (in press).

5. **Prasopchai Tonglairoum**, Wanchai Sutananta, Theerasak Rojanarata, Tanasait Ngawhirunpat, Praneet Opanasopit: Thermally Crosslinked Chitosan-EDTA/PVA Electrospun Nanofiber Mats: Crosslinking Conditions. *Advanced Materials Research*. 2015; 1060:192-195.
6. **Prasopchai Tonglairoum**, Tanasait Ngawhirunpat, Theerasak Rojanarata, Suwanee Panomsuk, Ruchadaporn Kaomongkolgit, Praneet Opanasopit: Fabrication of mucoadhesive chitosan coated polyvinylpyrrolidone/cyclodextrin/clotrimazole sandwich patches for oral candidiasis. *Carbohydrate Polymers*. 2015; 132:173-179.
7. **Prasopchai Tonglairoum**, Tanasait Ngawhirunpat, Theerasak Rojanarata, Praneet Opanasopit: Lysozyme-immobilized electrospun PAMA/PVA and PSSA-MA/PVA ion-exchange nanofiber for wound healing. *Pharmaceutical Development and Technology*. 2015; 20(8):976-983.
8. **Prasopchai Tonglairoum**, Praneet Opanasopit: Effect of Nutrient Formulations on Permeation of Proteins and Lipids through Porcine Intestine in vitro. *Tropical Journal of Pharmaceutical Research*. 2015; 14(7):1161-1166.
9. **Prasopchai Tonglairoum**, Tanasait Ngawhirunpat, Theerasak Rojanarata, Ruchadaporn Kaomongkolgit, Praneet Opanasopit: Fabrication of a novel scaffold of clotrimazole-microemulsion-containing nanofibers using an electrospinning process for oral candidiasis applications. *Colloids and surfaces B: Biointerfaces*. 2014; 126: 18-25.
10. **Prasopchai Tonglairoum**, Tanasait Ngawhirunpat, Theerasak Rojanarata, Ruchadaporn Kaomongkolgit, Praneet Opanasopit: Fast-Acting Clotrimazole Compositated PVP/HP beta CD Nanofibers for Oral Candidiasis Application. *Pharmaceutical Research*. 2014; 31(8): 1893-1906.

11. **Prasopchai Tonglairoum**, Wanita Chaijaroenluk, Theerasak Rojanarata, Tanasait Ngawhirunpat, Prasert Akkaramongkolporn, Praneet Opanasopit: Development and Characterization of Propranolol Selective Molecular Imprinted Polymer Composite Electrospun Nanofiber Membrane. *AAPS PharmSciTech*. 2013; 14(2): 838-846.
12. **Prasopchai Tonglairoum**, Tudduo Chuchote, Tanasait Ngawhirunpat, Theerasak Rojanarata, Praneet Opanasopit: Encapsulation of plai oil/2-hydroxypropyl- β -cyclodextrin inclusion complexes in polyvinylpyrrolidone (PVP) electrospun nanofibers for topical application. *Pharmaceutical Development and Technology*. 2013; 19(4): 430-437.
13. **Prasopchai Tonglairoum**, Tanasait Ngawhirunpat, Theerasak Rojanarata, Ruchadaporn Kaomongkolgit, Praneet Opanasopit. Fabrication and evaluation of clotrimazole-loaded PVP/HP β CD nanofiber mats for oral candidiasis. *Thai Journal of Pharmaceutical Sciences*. 2013; 38 (supplement):255-259.
14. Todsapon Nitanan, **Prasopchai Tonglairoum**, Prasert Akkaramongkolporn, Theerasak Rojanarata, Tanasait Ngawhirunpat, Praneet Opanasopit. Electrospun polystyrene sulfonic acid-co-maleic acid/ polyvinyl alcohol blend ion exchange fibers. *Thai Journal of Pharmaceutical Sciences*. 2012; 36 (Supplement): 112-115.

Thai Article Publication

1. **Prasopchai Tonglairoum** and Praneet Opanasopit. Thiomers: a new generation mucoadhesive polymer for transmucosal drug delivery systems. *Thai Bulletin of Pharmaceutical Sciences (TBPS)*. 2013; 8 (1): 19-27.